SPATIAL AND ENERGETIC ASPECTS OF ELECTRON ENERGY DEPOSITION

By

CHARLES HERBERT JACKMAN

A DISSERTATION PRESENTED TO THE GRADUATE COUNCIL OF
THE UNIVERSITY OF FLORIDA
IN PARTIAL FULFILLMENT OF THE REQUIREMENTS FOR THE
DEGREE OF DOCTOR OF PHILOSOPHY

UNIVERSITY OF FLORIDA

1978

ACKNOWLEDGEMENTS

Dr. A.E.S. Green has helped the author a great deal in his efforts to complete this work. The author sincerely appreciates this guidance. He also wishes to thank Dr. R.H. Garvey and Dr. R.A. Hedinger for their helpful discussion about the dissertation. David Doda, David Killian, E. Whit Ludington, George Sherouse, and Ken Cross were instrumental in providing assistance with computer problems and other dissertation-related work.

Woody Richardson, Marjorie Niblack, and Wesley Bolch were extremely helpful in drafting the figures. The final manuscript was then typed and refined by Adele Koehler. The author is grateful to Adele for her prompt and professional assistance.

The author wishes to thank Joseph Pollack for aiding in editorial matters concerning the dissertation. A thorough reading and criticism of the dissertation by the author's committee (including Dr. A.E.S. Green, Dr. L.R. Peterson, Dr. T.L. Bailey, Dr. S.T. Gottesman, and Dr. G.R. Lebo), Dr. W.L. Chameides, and Dr. A.G. Smith was extremely helpful.

The author is especially grateful to his parents, Rev. and Mrs. H.W. Jackman, and to his sister, Kathi Jouvenat, for their encouragement and support throughout graduate school.

The author gratefully acknowledges financial support from the Department of Physics and Astronomy and the Graduate School of the University of Florida and from NASA grant number NGL-10-005-008.

TABLE OF CONTENTS

Page

Abstract of Dissertation Presented to the Graduate Council
of the University of Florida in Partial Fulfillment of the Requirements
for the Degree of Doctor of Philosophy

SPATIAL AND ENERGETIC ASPECTS OF ELECTRON ENERGY DEPOSITION

By

Charles Herbert Jackman

August, 1978

Chairman: A.E.S. Green
Major Department: Physics and Astronomy

The spatial and energetic aspects of the electron energy degradation into molecular nitrogen gas have been studied by a Monte Carlo method. Perpendicularly monoenergetic incident electrons with energies from 0.1 through 5.0 KeV were injected into the N_2 gas. This Monte Carlo degradation scheme employed previously developed N_2 cross sections with new phenomenological differential elastic and doubly differential ionization cross sections. All these agree quite well with experimental work and are consistent with the higher energy theoretical total cross section fall-off with energy.

Information has been generated concerning the following topics: 1) range values and 3914 Å intensity profiles for the longitudinal and radial directions which can be easily compared with experimental work; 2) a sensitivity study characterizing the influence of the input cross sections on the spatial energy deposition of the electrons; 3) the rate of energy loss by the electrons as they interact with the N_2 gas; and 4) spatial yield spectra for incident electron energies in the range from 0.1 to 5.0 KeV (evaluated between 2 eV and the incident energy) which are analytically characterized for future work on atmospheric problems dealing with incident energetic electrons.

CHAPTER I

INTRODUCTION

Calculating the spatial and energetic aspects of the energy deposition of intermediate energy electrons (with incident energies from 100 to 5000 eV) in the earth's atmosphere is a difficult, yet intriguing, problem. These intermediate energy electrons (hereafter called IEEs) include the highest energy photoelectrons, a large bulk of the auroral electrons, and many secondary electrons produced by solar protons and cosmic rays.

These electrons lose most of their energy through ionization events, electronic excitations, vibrational excitations, and rotational excitations. Elastic collisions reduce the electron energy slightly, but mainly these interactions influence the direction of motion of the electron.

The atmosphere is dominated by the presence of molecular nitrogen up to a height of about 150 kilometers. Even above this altitude (at least up to 300 km), N_2 continues to play a substantial role in the atmospheric processes. For this reason the study of the influence of impinging electrons on molecular nitrogen is the major thrust of this paper.

One aspect of this study is the formulation of a complete cross section (differential and total) set for IEEs impacting on N_2. The very difficult problem of modeling the interactions of the impinging IEEs in

the upper atmosphere is then reduced in complexity. Since N_2 interacts with electrons similar to the way that other atmospheric gases interact with electrons, it follows that differential and total cross section sets for these gases could be assembled in a like manner.

Another aspect of this work is a sensitivity comparison among several of the influences on the electron energy deposition. The spatial energy degradation is vitally linked to the elastic phase function used. Since there are data available on the elastic differential cross sections of N_2 as well as the energy degradation resulting from electron impact on N_2, a comparison illustrating the effects of a variation of the elastic phase function is quite useful. Other influences on the spatial energy deposition, including ionization and excitation differential cross sections and the total elastic cross sections, are also considered in this work.

In order to deal with these spatial and energetic aspects of electron energy degradation, a Monte Carlo (which may be abbreviated MC) calculation is used. The MC technique, depending on how it is used, can be the most accurate energy deposition approach. Use of this MC method at various incident energies helps in the assemblage of the best cross section set for N_2 and provides the easiest way of comparing some of the influences on the spatial energy deposition.

The details of this undertaking are discussed in Chapters II through VIII. A paragraph summary of each chapter is given below.

The second chapter presents a brief review of some of the standard electron energy deposition methods. The continuous slowing down approximation, discrete energy bin, Fokker-Planck equation, two-stream equation of transfer, and the multi-stream equation of transfer are all included

in section II.A. The MC method which was used in this study along with three other MC approaches are briefly described in section II.B.

This MC approach requires knowledge of differential and total cross sections. The third chapter discusses the cross sections that were used for N_2. Section III.A includes the elastic differential and total cross sections. The inelastic differential and total cross sections are next discussed in section III.B. Section III.C, then, considers the total (inelastic plus elastic) cross section of N_2.

In Chapter IV, the MC calculational procedure is considered. A brief discussion of the approach is given in section IV.A. The computer programs and machinery used in this work are discussed in section IV.B with the programs listed in appendices A and B. A detailed discussion of the MC electron energy degradation technique is presented in section IV.C. Finally, the statistical error resulting from the Monte Carlo calculation is given in section IV.D.

The MC three-dimensional intensity plots with comparison to experiment are given in Chapter V. The excitation of the N_2^+ $B^2\ \Sigma_u^+$ state is discussed in section V.A with the concept of range being defined in section V.B. Previous experimental and theoretical work on the 3914 Å emission from N_2^+ is considered in section V.C and section V.D presents some range results and intensity plots in the longitudinal direction from this MC calculation. Section V.E, then, concludes the chapter with a comparison between the MC intensity plots in the radial direction and the experimental data.

The main concern of Chapter VI is a sensitivity study. The effects of the ionization differential cross section on the intensity distributions are considered in section VI.A. Section VI.B, then, discusses the

influence of inelastic differential cross sections on the intensity distribution. A comparison of different elastic phase functions on the electron-N_2 collision profile (no energy loss) is given in section VI.C. Next, the influence of different elastic phase functions on the electron energy deposition is presented in section VI.D. Finally, section VI.E considers the influence of the total elastic cross section on the electron energy deposition.

The energy loss plots and yield spectra from the MC calculations are given in Chapter VII. Section VII.A presents the energy loss plots and section VII.B includes a discussion of the yield spectra.

Chapter VIII concludes this paper with a summary of this work and its impact on the spatial and energetic aspects of the electron energy deposition problem.

CHAPTER II

A SHORT REVIEW OF ENERGY DEPOSITION TECHNIQUES

Several standard energy deposition techniques will be discussed in this chapter. In the first section, II.A, several general ways for treating the degradation of the energy of charged particles will be reviewed briefly. The second section, II.B, includes a brief sketch of four Monte Carlo energy deposition schemes: The MC approach applied in this work and three other MC techniques.

A. Energy Deposition Techniques

Since the turn of the century, researchers have been studying the energy degradation of rapidly moving particles in a medium. Initial work in this area was carried out by Roentgen, Becquerel, Thompson, Bragg, Rutherford, Bohr, and other founders of modern physics.

These pioneers in the energy degradation process were mainly concerned with the medium affecting the particle. In order to solve this complex energy degradation problem, most of the early workers used a local energy deposition approximation. Even today many degradation problems can be solved fairly accurately with this local approximation.

One of the earliest local energy deposition methods is that of the continuous slowing down approximation (hereafter called CSDA) first used by Niels Bohr (1913, 1915). Bethe (1930) expanded on this work and used an approximate theoretical treatment (valid at high energies) to describe the slowing down of particles in a medium.

This work of Bethe (1930) required knowledge of the stopping power, $-\frac{dE}{dx}$ (the rate at which energy E is lost from the impinging particles incident along the x axis). This stopping power is given by

$$-\frac{dE}{dx} = n \underset{i}{\vec{S}} W_i \, \sigma_i \,(E) \qquad (2.1)$$

(see Dalgarno, 1962, p. 624) where the summation $\underset{i}{\vec{S}}$ includes integration over the continuum (thus allowing for energy loss through ionization), W_i is the energy loss for the ith state, and $\sigma_i(E)$ is the cross section for excitation to the ith state at energy E. Knowledge of the stopping power then leads to information about the mean distance traveled by the particle (referred to as the range). This range R(E) of a particle of energy E is simply given by

$$R(E) = \int_0^E \frac{dE}{(-\frac{dE}{dx})} \qquad (2.2)$$

Atmospheric researchers are more interested in the effects that the particles have on the medium rather than the medium affecting the particles. These effects could include both spectral emissions by the constituents and heating of the atmosphere.

Green and Barth (1965) were the first workers to adapt a variation of the CSDA to the problems in aeronomy. In this approach the total energy loss function $L(E) = -(\frac{1}{n}) \frac{dE}{dx}$ is determined by

$$L(E) = \sum_k W_k \sigma_k(E) + \sum_j I_j \sigma_{I_j}(E) + \sum_j \int_0^{(E - I_j)/2} T \frac{d\sigma_{I_j}(E,T)}{dT} \, dT \qquad (2.3)$$

where W_k is the threshold for excitation to the kth state, $\sigma_k(E)$ is the cross section for excitation to the kth state at energy E, I_j is the threshold for ionization and excitation to the jth state, and $\frac{d\sigma_{I_j}(E,T)}{dT}$

is the secondary differential ionization cross section for the creation of a secondary electron of energy, T, from a primary electron of energy E. The loss function with detailed atomic cross sections (hereafter called DACSs) was used to make reasonable estimates of the ultraviolet emissions resulting from an aurora event. In this approach, the excitations $J_k(E)$ of the kth state resulting from an electron of energy E were simply represented as

$$J_k(E) = \int_{W_k}^{E} \frac{\sigma_k(E')}{L(E')} dE' \tag{2.4}$$

Green and Dutta (1967) built on this work and used the Born-Bethe approximations, the Massey-Mohr-Bethe surface, the Bethe sum rule, and a "distorted" oscillator strength to lay the groundwork for extension of the DACS approach to other gases. Jusick, Watson, Peterson, and Green (1967), Stolarski, Dulock, Watson, and Green (1967), and Watson, Dulock, Stolarski, and Green (1967) applied this approach to helium, molecular nitrogen, and molecular oxygen, respectively.

Stolarski and Green (1967) used this CSDA to calculate auroral intensities with these DACSs and Green and Barth (1967) applied this method to the problem of photoelectrons exciting the dayglow. Other atmospheric physicists (namely, Kamiyami, 1967; and Rees, Stewart, and Walker, 1969) started around this same time and also employed a CSDA type approach to that problem of energetic electrons depositing their energy in the atmosphere.

The oldest discrete energy apportionment method is that of Fowler (1922-23) which is directly related to the Spencer and Fano (1954) approach (see Inokuti, Douthat, and Rau, 1975). The Fowler equation is

solved by building on the lower-energy solutions to obtain the higher energy solutions. The Spencer-Fano method introduces the electron at the highest energy and solves the equation at successively lower energies. An approach similar to the Spencer-Fano method was developed by Peterson (1969) and is called the discrete energy bin (hereafter called the DEB) method.

Peterson (1969) pointed out certain differences between the CSDA and the DEB results. In particular, he noted that the DEB method tends to predict higher populations of some excited states than does the CSDA.

In the modification of the DEB method by Jura (1971), Dalgarno and Lejeune (1971), and Cravens, Victor, and Dalgarno (1975), the equilibrium flux or degradation spectrum $f(E,E_0)$ (for incident energy E_0 and electron energy E and in units of # cm^{-2} sec^{-1} eV^{-1}) of Spencer and Fano (1954) is obtained directly. Douthat (1975), in an effort to make the degradation spectra suitable for applications, proposed an approximate method of "scaling." Unfortunately, this method is quite cumbersome and not very accurate. This impelled Garvey, Porter, and Green (1977) to seek an analytic representation of the degradation spectra and, despite its complex nature, they found an analytic expression to represent this spectra for H_2.

The concept of the "yield spectra" $U(E,E_0)$ was first initiated through a modified DEB approach given in Green, Jackman, and Garvey (1977) in an effort to find a quantity with simpler properties than the degradation spectra. By utilizing the product

$$U(E,E_0) = \sigma_T(E)\ f(E,E_0)$$

where $\sigma_T(E)$ is the total inelastic cross section for an electron of energy E, one defines a quantity $U(E,E_0)$ which not only has a simpler

shape than $f(E,E_0)$ but also has approximately the same magnitude for all substances. This yield spectrum can also be represented analytically. It effectively embodies the non-spatial information of the degradation process.

Jackman, Garvey, and Green (1977a), using this modified DEB, elaborated on the differences between the DEB method and the CSDA. The more accurate modified DEB method was found to produce consistently more ions per energy loss while at the same time producing less excitations of some of the low lying states when compared with the CSDA. The CSDA, although inexpensive to use, appears to be ill-suited for calculations requiring an absolute accuracy better than about 20%. Since auroral and dayglow intensities are rarely measured to better than this accuracy, the CSDA has been adequate for most purposes of concern in aeronomy. However, with future improved measurements it should be purposeful to utilize more accurate deposition techniques.

Several recent spatial electron energy deposition studies have been concerned with the spatial aspects of auroral electron energy deposition. Walt, MacDonald, and Francis (1967) employed the Fokker-Planck diffusion equation to give a detailed description of kilovolt auroral electrons. The Fokker-Planck equation, as given in the Strickland, Book, Coffey, and Fedder (1976) paper, is written

$$\mu \frac{\partial\phi(z,E,\mu)}{n(z)\sigma(E)\partial z} = \frac{Q(E)}{2\sigma(E)} \frac{\partial}{\partial\mu} [(1 - \mu^2) \frac{\partial\phi(z,E,\mu)}{\partial\mu}]$$

$$+ \frac{1}{\sigma(E)} \frac{\partial}{\partial E} [L(E)\phi(z,E,\mu)] \qquad (2.5)$$

where $\phi(z,E,\mu)$ is the flux (in units of $cm^{-2}\ sec^{-1}\ eV^{-1}\ sr^{-1}$), z is the distance into the medium along the z axis, E is the electron energy,

and μ is the cosine of the pitch angle associated with the direction of motion of the electron. The symbols n, σ, Q, and L are the number density of the scatterers, the total cross section (both elastic and inelastic), the momentum transfer cross section, and the loss function, respectively.

The momentum transfer cross section, given in terms of the differential elastic cross section, $\frac{d\sigma(E)}{d\Omega}$, is written as

$$Q(E) = \int_0^{2\pi} \int_0^{\pi} \frac{d\sigma(E)}{d\Omega} (1 - \cos\theta)\sin\theta d\theta d\phi \tag{2.6}$$

This Fokker-Planck equation may be thought of as a CSDA approach to the spatial energy degradation problem. Its solution, therefore, is only accurate in the higher energy regime.

Banks, Chappell, and Nagy (1974) were able to calculate the emission as a function of altitude for a model aurora using the Fokker-Planck equation for electrons with energy E > 500 eV along with a two-stream equation of transfer for electrons with energy E ≤ 500 eV. The two-stream equation of transfer solves the transport of electrons in terms of the hemispherical fluxes of two electron streams $\phi^+(E,z)$, the electron flux upward along z, and $\phi^-(E,z)$, the electron flux downward along z. The steady state continuity equations for ϕ^+ and ϕ^- can then be written as

$$\frac{d\phi^+}{dz} = \frac{-1}{\langle\cos\theta\rangle} \sum_k n_k[\sigma_a^k + p_e^k\sigma_e^k]\,\phi^+$$

$$+ \frac{1}{\langle\cos\theta\rangle} \sum_k n_k p_e^k \sigma_e^k \phi^- + \frac{q}{2\langle\cos\theta\rangle} + \frac{q^+}{\langle\cos\theta\rangle} \tag{2.7}$$

and

$$-\frac{d\phi^-}{dz} = -\frac{1}{\langle\cos\theta\rangle}\sum_k n_k[\sigma_a^k + p_e^k\sigma_e^k]\,\phi^-$$

$$+\frac{1}{\langle\cos\theta\rangle}\sum_k n_k p_e^k\sigma_e^k\phi^+ + \frac{q}{2\langle\cos\theta\rangle} + \frac{q^-}{\langle\cos\theta\rangle} \tag{2.8}$$

where

$$\sigma_a^k = \sum_i \sigma_{ai}^k \tag{2.9}$$

$$q^+(E,z) = \sum_k n_k(z) \sum_{\substack{j\\E'>E}} \{p_{aj}^k(E')\sigma_{aj}^k(E'\to E)\phi^-(E,z)$$

$$+ [1 - p_{aj}^k(E')]\sigma_{aj}^k(E'\to E)\phi^+(E',z)\} \tag{2.10}$$

$$q^-(E,z) = \sum_k n_k(z) \sum_{\substack{j\\E'>E}} \{p_{aj}^k(E')\sigma_{aj}^k(E'\to E)\phi^+(E',z)$$

$$+ [1 - p_{aj}^k(E')]\sigma_{aj}^k(E'\to E)\phi^-(E',z)\} \tag{2.11}$$

and z is the distance along a magnetic field line (positive outward); $n_k(z)$ is the kth neutral species number density; $p_e^k(E)$ is the electron backscatter probability for elastic collisions with the kth neutral species; $\sigma_e^k(E)$ is the electron total scattering cross section for the kth neutral species; q(E,z) is the electron production rate in the range E to E+dE due to ionization processes (both electron ionization and photoionization); $q^{\pm}$ is the electron production in the range E to E+dE due to cascading from higher-energy electrons undergoing inelastic collisions; p_{aj}^k is the electron backscatter probability for collisions with the kth neutral species resulting in the jth inelastic process; and σ_{aj}^k is the inelastic cross section for the jth excitation of the kth neutral species.

This approach combined these two methods of electron energy deposition in order to find a reasonable solution to the very difficult auroral energy deposition problem. The Fokker-Planck method is accurate only at large incident energies; therefore, it should only be used at energies above 500 eV. The two-stream equation of transfer approach, on the other hand, is more accurate at energies below 500 eV. This combination then provided a very reasonable solution to the auroral electron spatial deposition problem for a reasonable amount of calculation.

The Fokker-Planck equation and the two-stream equation of transfer may both be derived from the Boltzmann equation or the general equation of transfer. This general equation of transfer, in one of its simpler forms, is written as (from Strickland et al., 1976)

$$\mu \frac{d\phi(z,E,\mu)}{dz} = -n(z)\sigma(E)\phi(z,E,\mu)$$

$$+ n(z)\sigma(E) \int R(\mu',\mu,E',E)\phi(z,E',\mu')dE'd\mu' \tag{2.12}$$

(assuming a steady state condition and no external fields) where

$$R(\mu',\mu,E',E) = \frac{\sum_j \sigma_j(\mu',\mu,E',E)}{\sigma(E)} \tag{2.13}$$

with the sum over all processes. The symbols μ and μ' are the cosines of the pitch angles θ and θ' which are associated with the directions $\vec{n}$ and $\vec{n}'$ given in Figure 2.1.

The first term on the right hand side of Eq. (2.12) represents the scattering out of μ. The $R(\mu',\mu,E',E)$ in the second term is the probability ($eV^{-1}(2\pi sr)^{-1}$) that a collision of an electron of energy E' and direction μ' with some particle will result in an electron of energy E

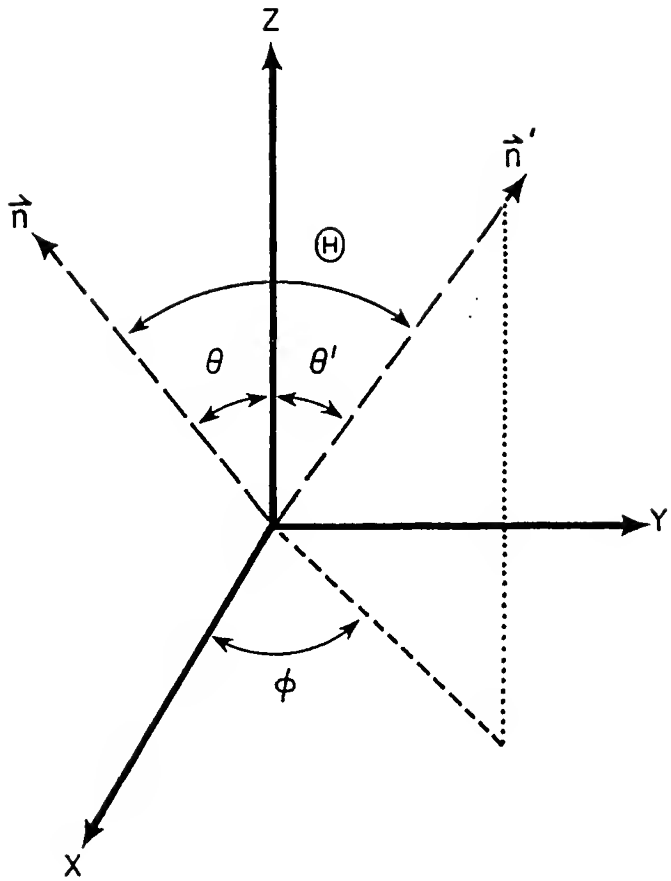

Figure 2.1 The directions denoted by $\vec{n}'$ and $\vec{n}$ are the incident and scattered directions of the electron, respectively.

and direction μ. The integral in Eq. (2.12) is over all possible energies E' and directions of motion μ'.

Strickland et al. (1976) studied the auroral electron scattering and energy loss with a multiangle equation of transfer. Their approach is one of the most accurate yet applied to auroral electrons. This multiangle method of solution is more realistic than the two-stream approach and it is computationally more difficult as well.

The methods discussed above are the "state of the art" approaches (excluding the Monte Carlo methods which are discussed in section II.B) to the IEEs degrading in the atmosphere. Other approaches used by Jasperse (1976, 1977) and Mantas (1975) are mainly concerned with photoelectrons and will not be discussed here.

The Monte Carlo approach can rival any of these electron energy deposition methods in accuracy when used in the proper manner. This stochastic technique for solving the deposition problem will be considered next in section II.B.

B. Monte Carlo Energy Deposition Techniques

Another method of solving the spatial energy deposition problem is the use of the Monte Carlo approach. The MC technique, which is used in this paper, is a stochastic method of degrading an energetic electron. The approach can be one of the most exact methods of electron energy deposition. Briefly, one electron is taken at a time and allowed to degrade in energy collision by collision. This deposition attempts to mimic the randomness of the actual degradation process that occurs in nature.

Many MC schemes have been applied in all areas of physics. Some are more exact and more detailed than others. Since virtually all the MC methods are run on the computer, the most exact approaches cost the most computer time and money. The precision of the technique must be balanced against a finite computer budget.

Three approaches using the MC deposition scheme, that have been applied to electrons impinging on the atmosphere, are discussed below. Brinkmann and Trajmar (1970) applied experimental differential electron impact energy loss data in a MC computation for electrons of 100 eV energy. Because of the large amount of input cross sections in numerical form, only electrons of 100 eV incident energy were degraded with this method.

In the lower electron energy regime (below 25 eV), Cicerone and Bowhill (1970, 1971) used a MC technique to simulate photoelectron diffusion through the atmosphere. This method, which included both elastic and inelastic processes, predicted escape fluxes from the atmosphere.

Berger, Seltzer, and Maeda (1970, 1974) (hereafter called BSM) worked with high energy electrons (with energies from 2 KeV to 2 MeV). They employed a MC approach that has two variations which are pointed out below. They treat inelastic collisions in a continuous slowing down manner. The energy deposited by the electrons along their path is assumed to be equal to the mean loss given by the loss function, L(E), from Rohrlich and Carlson (1954).

The angular deflection resulting from elastic collisions has been evaluated by two separate methods in BSM. One approach employed the multiple scattering distribution of Goudsmit and Saunderson (1940) applied to the screened Rutherford cross section given in BSM. The

other approach involved a sampling of each elastic collision. Application of the BSM technique to a constant density medium and no magnetic field gave good agreement with laboratory experiments (Grün, 1957; and Cohn and Caledonia, 1970).

In this study, a MC method was needed that could be applied to IEEs. The basic equation of transfer is solved with the use of the MC approach. This equation can be rewritten as

$$\mu \frac{dU(\mu,z,E,E_0)}{\sigma_T(E)\, dz} = -n(z)U(\mu,z,E,E_0)$$

$$+ \; n(z) \int_{E}^{E+\Delta E_{Elas}} \int_{-1}^{1} p_e(\mu',\mu,E',E)U(\mu',z,E',E_0)d\mu'dE'$$

$$+ \, n(z) \sum_i \int_{2E+I_i}^{E_0} \int_{-1}^{+1} p_{IONi}(\mu',\mu,E',E)U(\mu',z,E',E_0)d\mu'dE'$$

$$+ \, n(z) \sum_j \int_{W_j}^{E_0} p_{aj}(\mu',\mu,E',E)U(\mu',z,E',E_0)d\mu'dE' \tag{2.14}$$

No external fields are included here and a steady state is assumed. The $U(\mu,z,E,E_0)$ is the "yield spectra" (in eV^{-1} sec^{-1} sr^{-1}) and it is assumed that there is only one neutral scattering species. In this equation $\sigma_T(E)$ is the total cross section (elastic + inelastic)for the species,

$$\Delta E_{Elas} = 2E(1 - \cos\Theta) \frac{M_{electron}}{M_{\substack{neutral\\species}}} \tag{2.15}$$

is the energy loss during an elastic collision, $p_e(\mu',\mu, E',E)$ is the probability during an elastic collision with a neutral specie that an electron with energy E' and direction μ' will result in an electron of

energy E and direction μ, $p_{IONi}(\mu',\mu, E',E)$ is the probability during an ionization collision with a neutral species that an incident electron with energy E' and direction μ' will result in a secondary electron of energy E and direction μ, and $p_{aj}(\mu',\mu,E',E)$ is the probability during an inelastic collision (excitation or ionization) with a neutral specie that an incident electron with energy E' and direction μ' will result in the incident electron being scattered into direction μ with energy E.

Some techniques from each of the other three MC methods were included in this work. Some new approximations and assumptions were made, however, to enhance the accuracy of the computations as well as simplify some of the calculations. These assumptions are discussed in detail in Chapter IV.

In this MC work the information is stored in a collision by collision manner on a magnetic tape. Once all the case histories are generated, then, the tape is scanned and any correlations of interest may be determined. The choice of altitude and energy intervals is specified only during the scanning of the tape. This method allows for greater flexibility in minimizing the statistical uncertainties of the results, while, at the same time retaining good spatial or energy resolution (Porter and Green, 1975).

All the degradation methods mentioned in this chapter require cross sections as input. The cross sections used in this MC work are, therefore, discussed in the next chapter.

CHAPTER III

ELASTIC AND INELASTIC DIFFERENTIAL AND TOTAL CROSS SECTIONS FOR N_2

In this chapter differential and total cross sections for electron impact on N_2 will be discussed. Section III.A reviews the elastic cross sections of N_2 and discusses three models for representation of these properties. In section III.B the inelastic cross sections of N_2 are presented with their relationship to theory and experiment. Section III.C, then, concludes this chapter with a discussion of the total (elastic plus inelastic) cross section for N_2. Any energy degradation technique requires knowledge of these cross sections for a complete evaluation of the energy loss by electrons in a gas.

A. Elastic Differential and Total Cross Sections for N_2

One of the most common differential elastic cross section forms is the screened Rutherford cross section which can be expressed in the form

$$\frac{d\sigma}{d\Omega} = \left[\frac{Z^2e^4}{p^2v^2(1 - \cos\theta + 2\eta)^2}\right] K_{rel}(\theta) \tag{3.1}$$

where $K_{rel}(\theta)$ is the spin-relativistic correction factor.

The familiar Rutherford cross section (unscreened case) which can be derived from classical scattering theory is given by

$$\frac{d\sigma}{d\Omega} = \frac{Z^2e^4}{p^2v^2(1 - \cos\theta)^2} \tag{3.2}$$

where

$$\sin^2 \frac{\theta}{2} = 1 - \cos\theta$$

Here, an electron is elastically scattered by a nucleus of charge Z using the Coulomb potential

$$V(r) = \frac{Ze^2}{r} \qquad (3.3)$$

with r being the distance between the two particles.

Treating scattering in a quantum mechanical approach with the use of the Born approximation and a potential of the form

$$V(r) = \frac{Ze^2}{r} e^{-\gamma r} \qquad (3.4)$$

where γ is a positive but small quantity approaching 0, Eq. (3.2) can again be derived. The Born approximation, using the potential in Eq. (3.4), is only valid in certain angle and energy regimes (Mott and Massey, 1965, pp. 24 and 466). At sufficiently high angles and low energies, the Born approximation fails. The range of validity varies for different substances and for N_2 the Born approximation is probably not accurate at all angles for energies less than 100 eV and at large angles for energies less than 500 eV.

Equation (3.2) does, however, go to infinity when θ approaches 0°. This differential cross section also leads to an infinite value in the total elastic cross section. Both of these results are unreasonable for elastic scattering of electrons by atoms and molecules. The most popular way of correcting this unreal behavior is to add a screening parameter η. Equation (3.1) portrays this resulting form.

Equation (3.1) has a maximum at $\theta = 0°$ and a minimum at $\theta = 180°$. At energies below 200 eV, experimental results indicate a minimum in the elastic differential cross sections at about 90° with a strong forward scattering peak at $\theta = 0°$ and a secondary backward scattering peak at $\theta = 180°$.

In Figure 3.1 experimental data for energies at E = 30 and 70 eV are presented. These data are taken from Shyn, Stolarski, and Carignan (1972) with the small circles denoting 30 eV points and the crosses denoting the 70 eV data.

Later on in this section the screened Rutherford cross section and another analytic model of the differential elastic cross section are compared with experimental data. Before discussing the differential cross section in more detail, first, consider the total elastic cross section.

Several experiments have been performed deriving the total elastic cross sections for N_2. There have also been several theoretical studies on the N_2 elastic total cross sections. Two recent reviews of the data available on this subject are Kieffer (1971) and Wedde (1976).

A plot of all this data would obscure the analytic total cross sections specifically considered in this work. Consequently, only data from Sawada, Ganas, and Green (1974) (theoretical), Shyn, Stolarski, and Carignan (1972) (experimental), and Herrmann, Jost, and Kessler (1976) (experimental) are plotted in Figure 3.2. The sets of data overlap to a degree such that the disagreement in absolute magnitude of the total cross sections is readily apparent.

In view of this disagreement, no experimental or theoretical data are assumed to be absolutely correct and some average of this data is

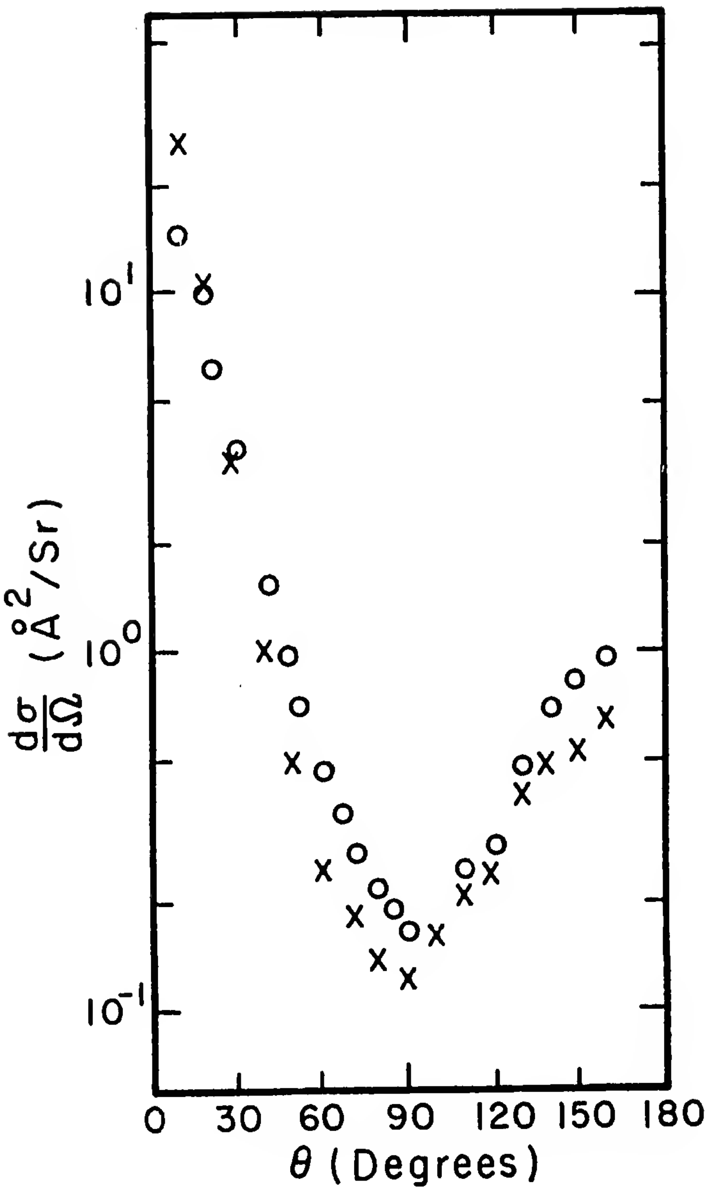

Figure 3.1 N_2 experimental electron impact elastic cross section data from Shyn, Stolarski, and Carignan (1972). o's denote data from E = 30 eV and the x's denote data from E = 70 eV.

Figure 3.2 N_2 electron impact total elastic cross section data from Sawada, Ganas, and Green (1974), x; Shyn, Stolarski, and Carignan (1972), o; Herrmann, Jost, and Kessler (1976), ◆; and Banks, Chappell, and Nagy (1974), ▿. Equation (3.6) is represented by the dash-dot line, Eq. (3.8) by the dashed line, and Eq. (3.9) by the solid line.

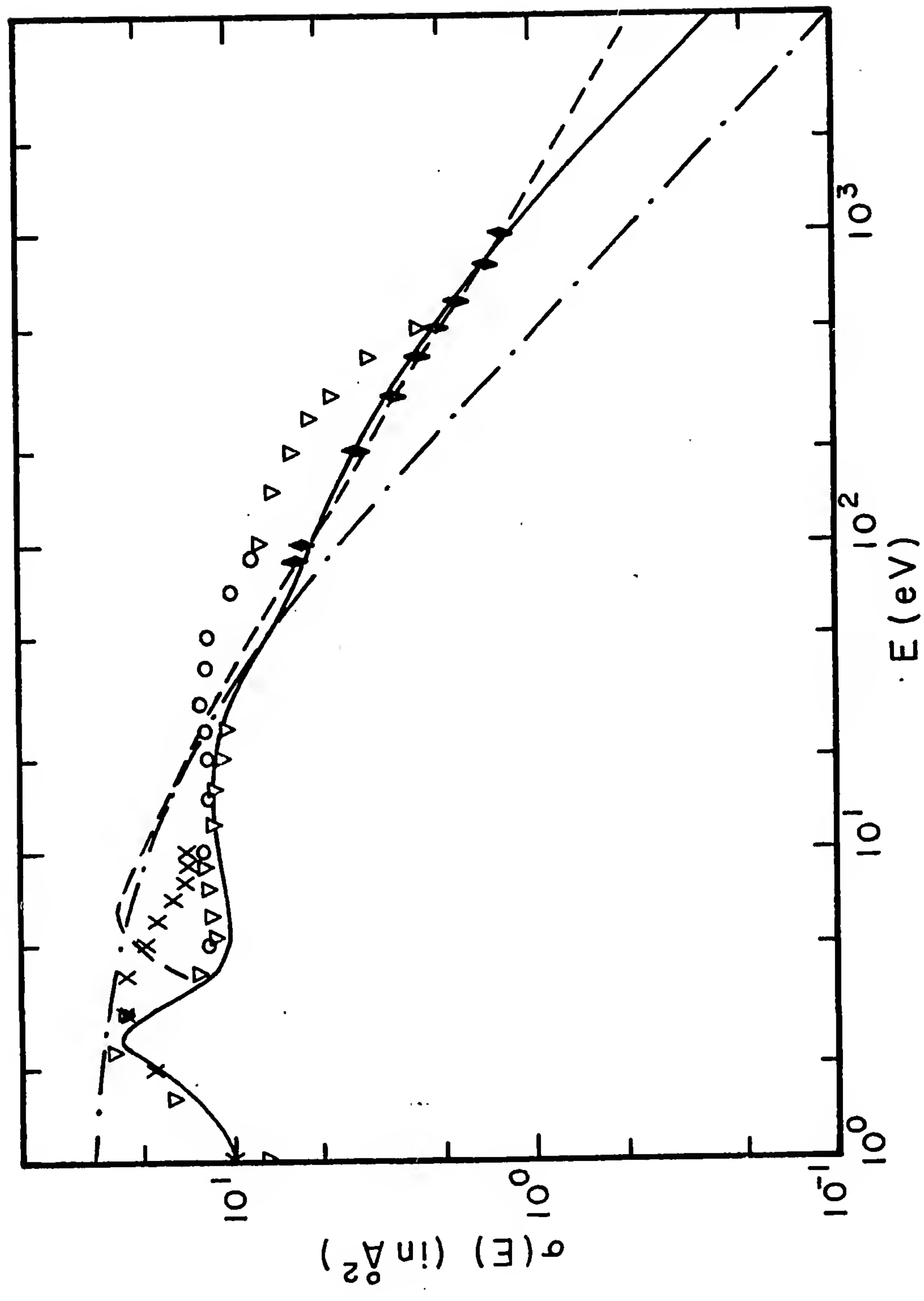

E (eV)
σ(E) (in Å²)
10⁰
10¹
10²
10³
10⁻¹

desirable. An analytic function representing the total elastic cross section is most easily used in a computer program. Consider now an analytic form derived from the differential screened Rutherford cross section.

Knowledge of the differential cross section implies knowledge of the total elastic cross section as they are simply related by

$$\sigma(E) = \int_0^{2\pi}\int_0^{\pi} \frac{d\sigma}{d\Omega} \sin\theta d\theta d\phi \tag{3.5}$$

where ϕ is the azimuthal angle. Substituting Eq. (3.1) into Eq. (3.5), the total elastic cross section, $\sigma_R(E)$, resulting from the screened Rutherford cross section is very simply given as

$$\sigma_R(E) = \frac{Z^2\ 51.8}{E^2} \frac{\pi}{\eta(1 + \eta)} \tag{3.6}$$

If E is given in eV then $\sigma_R(E)$ is in units of 10^{-16} cm^2. The screening parameter

$$\eta = \eta_c \frac{1.70 \times 10^{-5}\ Z^{2/3}}{\tau(\tau + 2)} \tag{3.7}$$

according to the Moliere (1947, 1948) theory. Berger, Seltzer, and Maeda (1970) assumed that η_c was a constant value and decided on $\eta_c = 1$ as its best value. The τ in Eq. (3.7) is the electron energy in units of the electron rest energy so that $\tau = E/mc^2$. In the energy regime of interest ($E \leq 5$ KeV), $\tau << 2$, and $Z = 7$. Noting these observations, Eq. (3.7) can be rewritten as $\eta \approx \frac{16}{E}$.

The total cross section from Eq. (3.6) is plotted in Figure 3.2 as the dash-dot line. A noticeable difference is evident between this model and the experimental values at practically all energies.

Using the form

$$\sigma(E) = \frac{q_0 F[1 - (\frac{W}{E})^{\alpha}]^{\beta}}{E^c\ W} \tag{3.8}$$

implemented first by Green and Barth (1965), where q_0 = 651.3 Å^2 eV^2, the total elastic cross section for N_2 was characterized fairly well in the range from 30 to 1000 eV using the parameters α = 1, β = 0.6, c = 0.64, F = 0.43, and W = 2.66. The $E^{-0.64}$ dependence of Eq. (3.8) at the larger energies is similar to that seen by Wedde and Strand (1974) for N_2. This form does not represent the data as well below 30 eV and, in fact, is not defined below an energy of 2.66 eV.

Porter and Jump (1978) have used a more complex total elastic cross section form which is written as

$$\sigma(E) = T\left\{\frac{E^X}{\eta(\eta + 1)[V^{2+X} + E^{2+X}]} + \frac{F_1 G_1^2}{(E - E_1)^2 + G_1^2} + \frac{F_2 G_2^2}{(E - E_2^2) + G_2^2}\right\} \tag{3.9}$$

Here, $\eta = \frac{U}{E}$

and for N_2:

$T = 2.5 \times 10^{-6}$ cm^2	$F_1 = 7.33$
$U = 1.95 \times 10^{-3}$ eV	$E_1 = 2.47$ eV
$V = 150$ eV	$G_2 = 24.3$ eV
$X = -0.770$	$F_2 = 2.71$
$G_1 = 0.544$ eV	$E_2 = 15.5$ eV

In the large energy limit, the total cross section falls off as 1/E, similar to the screened Rutherford cross section. This form does contain two other terms (the second and third terms) which were introduced

phenomenalogically to describe the low energy shape and Feshbach resonances.

If either Eq. (3.8) or (3.9) is used as the total elastic cross section, the differential elastic cross section must be normalized such that:

$$\int_0^{2\pi}\int_0^{\pi} P(\theta,E)\ \sin\theta d\theta d\phi = 1 \tag{3.10}$$

where $P(\theta,E)$ is the phase function and the differential cross section can be written as

$$\frac{d\sigma}{d\Omega} = \sigma(E)\ P(\theta,E) \tag{3.11}$$

With this in mind consider now three separate phase function forms. The first phase function form is very similar to the screened Rutherford cross section and it is written here as

$$P_{M1}(\theta,E) = \frac{-1}{2\pi[(2 + a(E))^{-1} - a(E)^{-1}][1 - \cos\theta + a(E)]^2} \tag{3.12}$$

This is known as model 1. The parameter "a" acts in a similar manner to the "2η" term in the denominator of the screened Rutherford cross section form and is written

$$a(E) = a_1\left(\frac{E}{1\ \text{eV}}\right)^{a_2}$$

The second phase function form (model 2) includes the forward scattering term of Eq. (3.12) along with a backscattering term and is given as

$$P_{M2}(\theta,E) = \frac{-f(E)}{2\pi[(2 + a(E))^{-1} - a(E)^{-1}][1 - \cos\theta + a(E)]^2}$$

$$- \frac{(1 - f(E))}{2\pi[(2 + c(E))^{-1} - c(E)^{-1}][1 + \cos\theta + c(E)]^2} \qquad (3.13)$$

where

$$f(E) = \frac{(E/f_1)^{f_2}}{(E/f_1)^{f_2} + f_3}$$

$$a(E) = a_1 \left(\frac{E}{1\ \mathrm{eV}}\right)^{a_2}$$

and

$$c(E) = c_1 \left[1 - \left(\frac{c_2}{E}\right)^{c_3}\right]$$

Irvine (1965) was one of the first researchers in scattering problems to use a phase function containing forward and backward scattering terms. He applied a sum of two Henyey-Greenstein functions to the problem of photon scattering by large particles. Porter and Jump (1978) also have used a sum of two terms (one for forward scatter and one for backward scatter). They fitted experimental data at several separate energies with their form. Use of their differential cross section form in a deposition calculation probably would require the use of spline functions or other interpolative techniques.

The third phase function (model 3) is now considered. At small angles the differential cross section shows a near exponential-like fall off. This behavior has been pointed out by several experimenters (see, for example, Shyn, Carignan, and Stolarski, 1972; and Herrmann, Jost, and Kessler, 1976). It was this experimental observation that led to

model 3 which is written as

$$P_{M3}(\theta,E) = \frac{f_1(E)[1 - b^2(E)]e^{-\theta/b(E)}}{2\pi\, b^2(E)[1 + e^{-\pi/b(E)}]}$$

$$- \frac{f_2(E)}{2\pi[(2 + a)^{-1} - a^{-1}][1 - \cos\theta + a]^2}$$

$$- \frac{[1 - f_1(E) - f_2(E)]}{2\pi[(2 + c(E))^{-1} - c(E)^{-1}][1 + \cos\theta + c(E)]^2} \qquad (3.14)$$

where

$$f_1(E) = \frac{(E/f_{11})^{f_{12}}}{[(E/f_{11})^{f_{12}} + f_{13}]}$$

$$f_2'(E) = \frac{(E/f_{21})^{f_{22}}}{[(E/f_{21})^{f_{22}} + f_{23}]}$$

$$f_2(E) = 1 - f_1(E) \qquad \text{for } E > 200 \text{ eV}$$

$$f_2(E) = f_2'(E)[1 - f_1(E)] \qquad \text{for } E \lesssim 200 \text{ eV}$$

$$b(E) = b_1\left(\frac{E}{1\text{ eV}}\right)^{b_2}$$

$$c(E) = c_1\left[1 - \left(\frac{c_2}{E}\right)^{c_3}\right]$$

The parameters used for the rest of this study in Eq. (3.14) are

f_{11} = 100 eV	a = 0.11
f_{12} = 0.84	b_1 = 0.43
f_{13} = 1.92	b_2 = -0.29

$f_{21} = 10$ eV $\qquad c_1 = 1.27$

$f_{22} = 0.51$ $\qquad c_2 = 12$ eV

$f_{23} = 0.87$ $\qquad c_3 = 0.27$

This form is more complex than the other phase function models but it does describe the experimental differential cross section data the most realistically. It includes an exponential term for the near exponential-like forward scattering as well as a backward scattering term for electron energies below 200 eV.

Comparisons of the screened Rutherford and model 3 cross sections are given in Figures 3.3 and 3.4 at the two energies of 30 eV and 1000 eV. Both forms are normalized to the total elastic cross section form of Eq. (3.9). This modified screened Rutherford cross section vastly underestimates the forward scattering from $\theta = 0°$ to $30°$, overestimates the scattering in the range from $\theta = 30°$ to $120°$, and underestimates the scattering at the larger angles with $\theta = 120°$ to $180°$. Model 3 does a fairly reasonable job of representing the differential cross section data at both of these representative energies and the other energies as well.

Although there is not a large amount of energy loss during an elastic collision, there is some. Using classical considerations (see Green and Wyatt, 1965), the energy loss is approximately given by Eq. (2.15). For molecular nitrogen and $\theta = 90°$, the energy loss is about 8×10^{-5} E.

The MC approach, being a stochastic process, uses the concept of probability for scattering within a given angle interval. In order to compare phase functions, the probability for backscatter may be compared.

Figure 3.3 (a and b) N_2 electron impact elastic differential cross sections. The screened Rutherford (dashed line) and the model 3 (solid line) are compared with the experimental data of Shyn et al. (1972), x, and Herrman et al. (1976), o, at the energies of 30 eV (Figure 3.3a) and 1000 eV (Figure 3.3b).

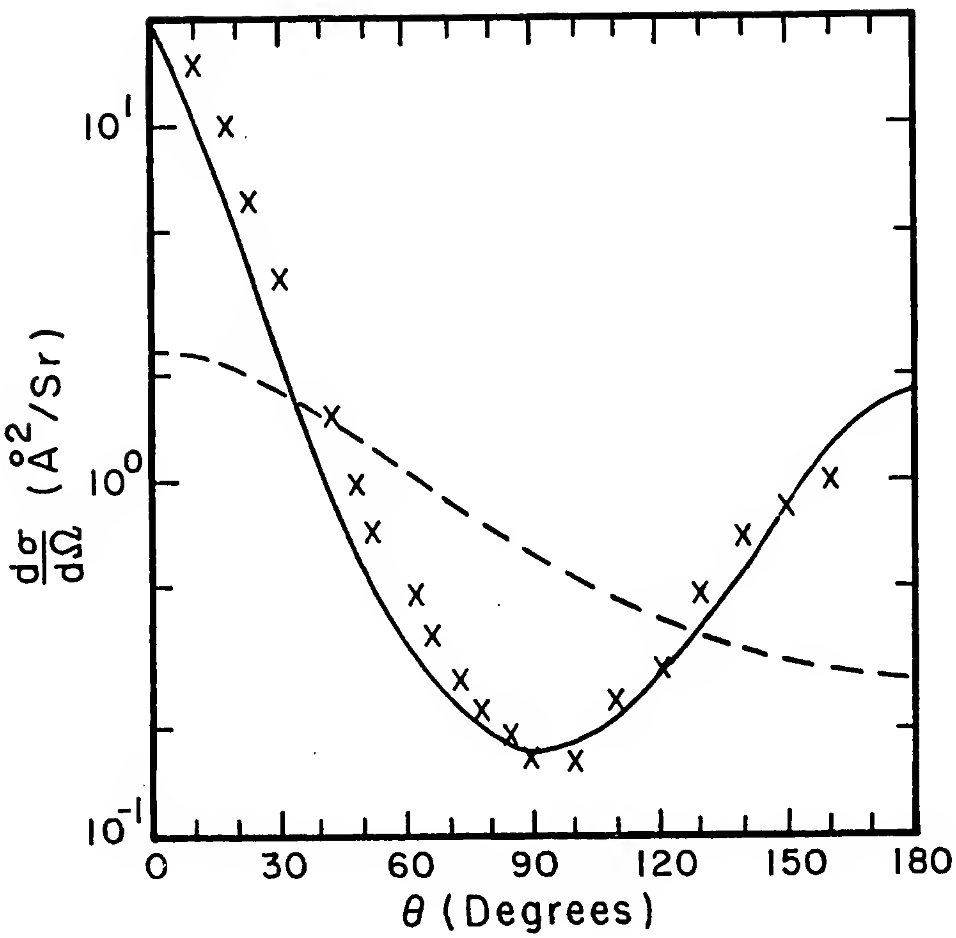
10^1
10^0
10^{-1}
$\frac{d\sigma}{d\Omega}$ ($\mathring{A}^2$/Sr)
0
30
60
90
120
150
180
θ (Degrees)

Figure 3.3a

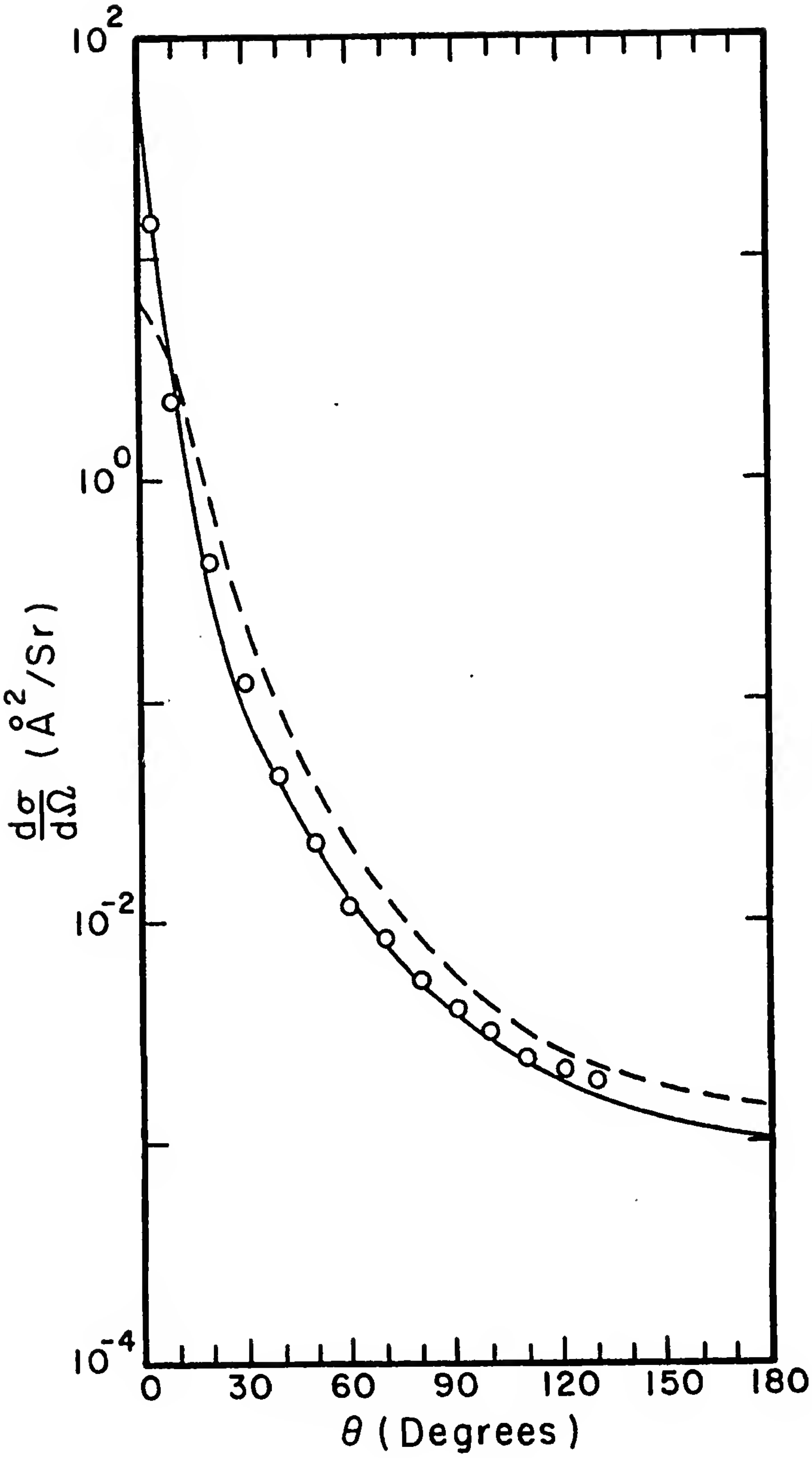
10^2
10^0
10^{-2}
10^{-4}
$\frac{d\sigma}{d\Omega}$ ($\mathring{A}^2$/Sr)
0
30
60
90
120
150
180
θ (Degrees)

Figure 3.3b

Figure 3.4 (a and b) N_2 electron impact elastic differential cross sections between 0° and 20°. The screened Rutherford (dashed line) and the model 3 (solid line) are compared with the experimental data of Shyn et al. (1972), x (the ⊠'s denote extrapolated points), and Herrmann et al. (1976), o, at the energies of 30 eV (Figure 3.3a) and 1000 eV (Figure 3.3b).

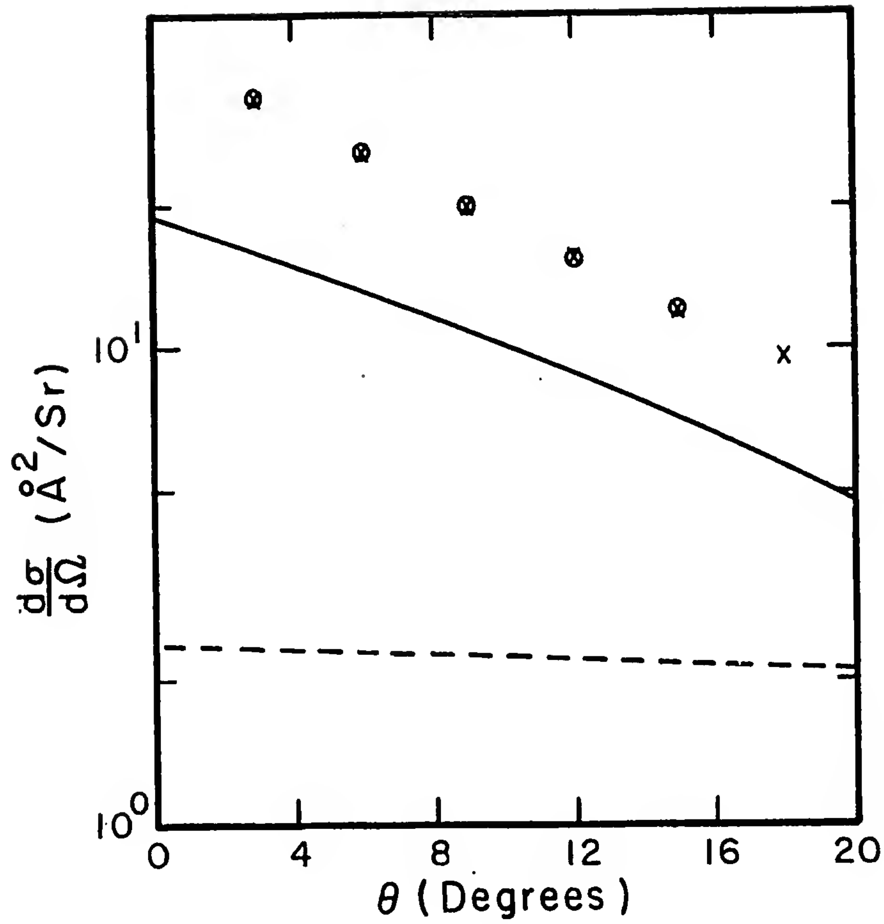

$\frac{d\sigma}{d\Omega}$ ($\mathring{A}^2$/Sr)
10^1
10^0
0
4
8
12
16
20
θ (Degrees)

Figure 3.4a

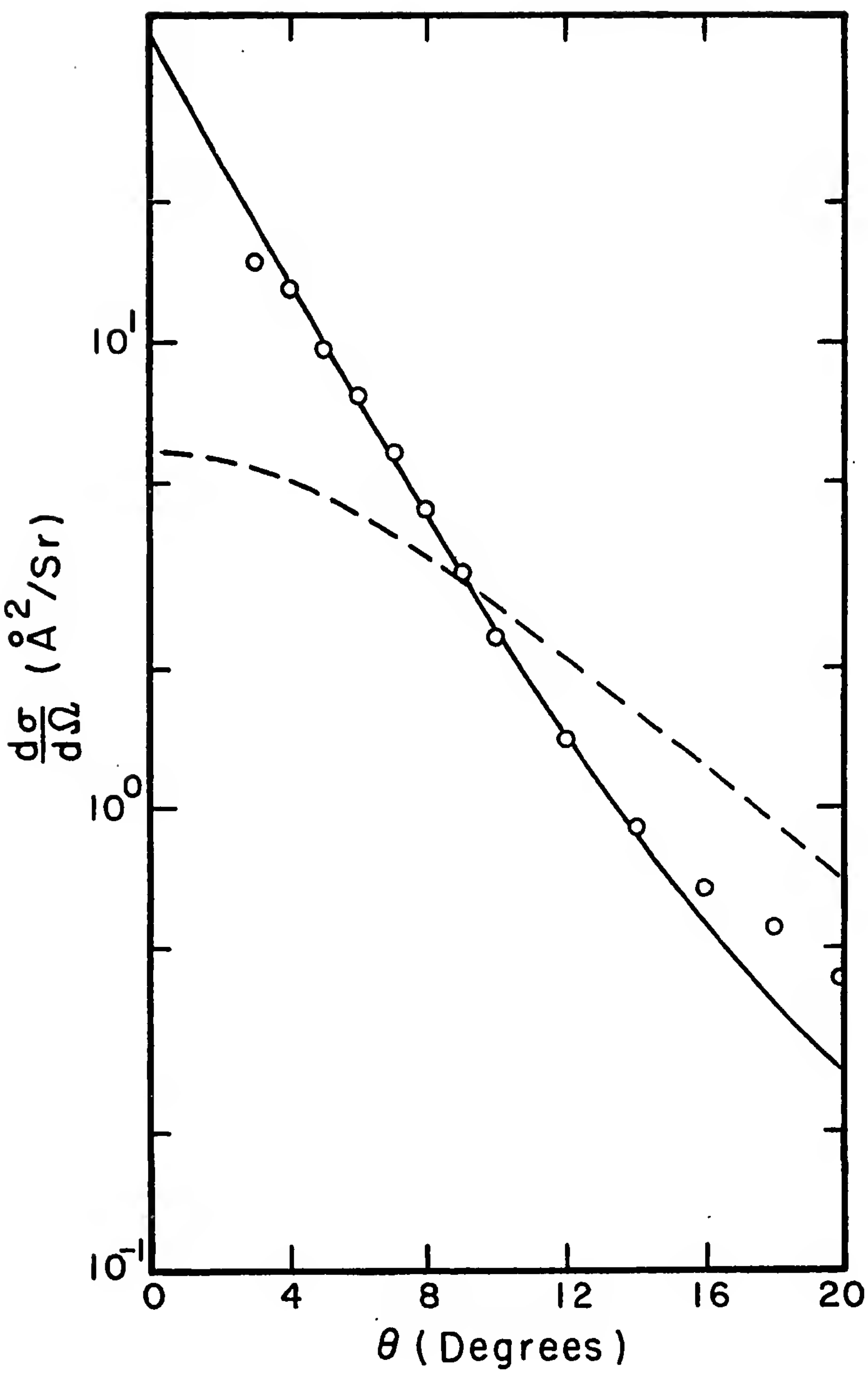
10^1
10^0
10^{-1}
$\frac{d\sigma}{d\Omega}$ ($\mathring{A}^2$/Sr)
0
4
8
12
16
20
θ (Degrees)

Figure 3.4b

This probability, $P_B(E)$, is simply calculated with

$$P_B(E) = \frac{\int_0^{2\pi} \int_{\pi/2}^{\pi} \frac{d\sigma}{d\Omega} \sin\theta d\theta d\phi}{\int_0^{2\pi} \int_0^{\pi} \frac{d\sigma}{d\Omega} \sin\theta d\theta d\phi} \tag{3.15}$$

In Figure 3.5, $P_B(E)$ from the screened Rutherford and model 3 are compared with other theoretical (Wedde and Strand, 1974) and experimental (Shyn et al., 1972) values. Model 3 does have a tendency to estimate less backscatter than the screened Rutherford at the larger energies. (The $P_B(E)$ curves for model 3 and the screened Rutherford do tend to converge at 5 KeV however.) The dominant exponential-like forward scattering is the reason behind this behavior. The discontinuity observed at 200 eV in model 3 values results from the lack of the backscatter characteristic above this energy.

The elastic scattering collisions influence mostly the direction of travel of the electrons. There is some energy loss during an elastic collision (as pointed out above), but this loss is not important for electrons with energies above 2 eV colliding only with N_2 particles.

Inelastic collisions, on the other hand, result in a fairly substantial energy loss with some scattering. Consider now the differential and total cross sections for these inelastic events.

B. Inelastic Differential and Total Cross Sections for N_2

Inelastic collisions are divided into two types: 1) electron excitation and 2) electron ionization. In the excitation process the electron is excited to a higher state which may either be an optically

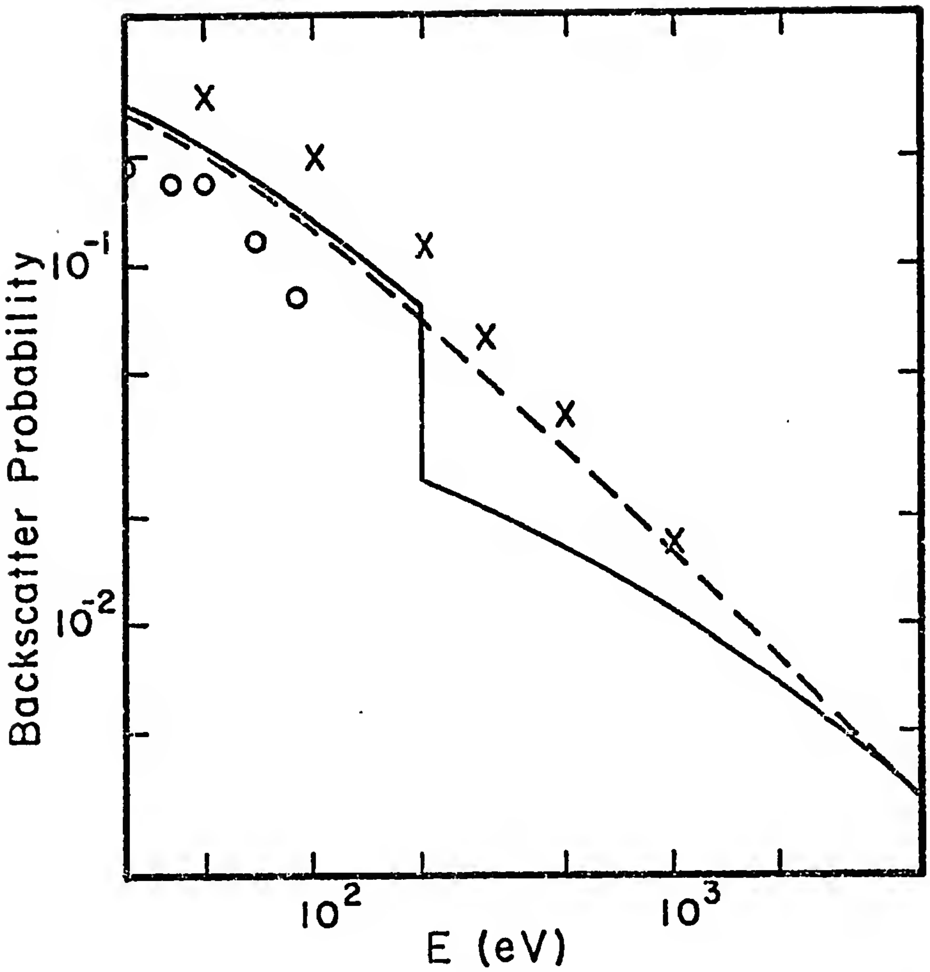

Figure 3.5 Backscatter probabilities for the screened Rutherford (dashed line) and the model 3 (solid line) are compared with Wedde and Strand (1974), x; and Shyn et al. (1972), o.

allowed or an optically forbidden transition. This transition for many molecules leads to a repulsive state which can dissociate the molecule. In N_2, dissociation of the molecule in this manner is virtually non-existant because N_2 is a very stable homonuclear molecule in which both the singlet and triplet states are found to be strongly bound. As a consequence of this, the main process for dissociation is through pre-dissociation of stable electronic terms by repulsive states that are themselves strongly optically forbidden in direct excitation.

Porter, Jackman, and Green (1976) (hereafter called PJG) compiled branching ratios for dissociation of N_2 using several experimental and theoretical papers (see, for example, Winters, 1966; Rapp, Englander-Golden, and Briglia, 1965; Polak, Slovetskii, and Sokolov, 1972; and Mumma and Zipf, 1971). In PJG the efficiencies for the production of atomic nitrogen from proton impact were determined.

This study does not include a calculation of the atomic nitrogen production; however, the PJG branching ratios with the yield spectra, discussed in section VII.B, can be applied to calculate this atomic yield. The excitation events, not resulting in the dissociation of the N_2 molecule, are either electronic or vibrational transitions. Cross sections for these transitions are taken from both PJG and Jackman, Garvey, and Green (hereafter called JGG) (1977b).

In the ionization event an electron is stripped from the molecule and given some kinetic energy. The ionization cross section is a substantial portion of the total inelastic cross section above 50 eV (compare Figures 3.6 and 5.1) and the total amount of energy loss is always $\geq$ the lowest ionization threshold (which is 15.58 eV for N_2). Subsequently, most of the energy loss of the electrons (for energies

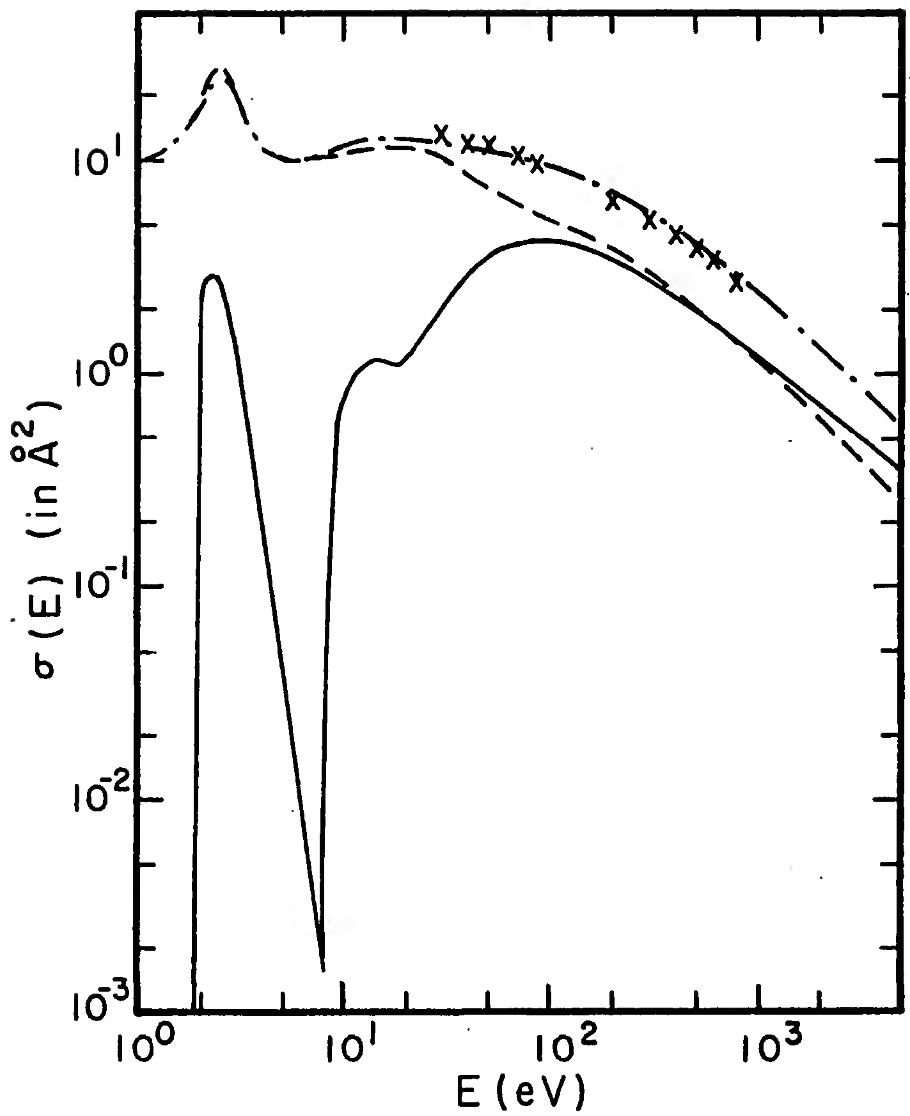

Figure 3.6 N_2 electron impact cross sections. The total inelastic, Eq. (3.16) (solid line), total elastic, Eq. (3.9) (dashed line), total inelastic plus elastic, Eq. (3.16) plus Eq. (3.9) (dash-dot line), and the experimental inelastic plus elastic values (Blaauw et al., 1977), x, are presented here.

> 50 eV) is from the ionization collisions. These ionization cross sections were also taken from PJG and JGG. The total inelastic cross section found by summing these inelastic cross sections was fit with the function

$$\sigma_{TI}(E) = \frac{q_0 F[1 - (\frac{W}{E})^{\alpha}]^{\beta} \ln(\frac{4EC}{W} + e)}{WE} \tag{3.16}$$

This form has the characteristic Born-Bethe ln E/E fall off behavior at the large energies. The parameters $\alpha = 1$, $\beta = 4.81$, $C = 0.36$, $F = 4.52$, and $W = 11$ were found with the use of a nonlinear least square fitting program which fit Eq. (3.16) to the sum of all the inelastic cross sections. From 30 eV up to 5 KeV this form was used for the total inelastic cross section.

Below 30 eV much structure in the total inelastic cross section is evident. At these low energies, the total inelastic cross section can be read numerically into the MC program. This total inelastic cross section is illustrated by the solid line in Figure 3.6.

Consider now the scattering of the two electrons involved in an electron impact ionization collision. In reality, only the incident electron is scattered. The other electron is simply stripped from the molecule and given kinetic energy in a certain direction of travel. Experiments are unable to distinguish between the incident electron and the electron stripped from the molecule. In this paper, the ionization event is assumed to cause scattering of both electrons. The scattering angle of either is then measured with respect to the incident electron's path.

After the collision event the electron with the higher energy is designated the primary electron and the electron with the lower energy

is called the secondary electron. There should be a correlation between the primary and secondary scattering, but this mutual influence is difficult to quantify. The impinging electron ionizes a many body particle, a molecule of nitrogen, thus momentum and energy can be conserved without all the momentum and energy shared by the two resulting electrons. Only recently has work been done on triply differential cross sections for N_2 and this interaction was measured only at one energy E = 100 eV (see Jung, Schubert, Paul, and Ehrhardt, 1975). More experimental and theoretical work needs to be done in this area before any generalization can be made concerning the correlation between the primary and secondary scattering.

The primary and secondary scattering will thus be treated separately in this work. In dealing with the scattering of the primary electron after an ionization collision, a differential ionization cross section form based on the Massey-Mohr-Bethe surface of hydrogen, is used. The form (with a_o, the Bohr radius, and R_e, the Rydberg energy) is

$$\frac{d\sigma}{dTd\Omega} = \frac{4a_o^2R_e}{Wx}\left(1 - \frac{W}{E}\right)^{1/2} F(x) \tag{3.17}$$

where $x = (Ka_o)^2$ is the momentum transfer, W is the energy loss in the collision process which is equal to the ionization potential, I, plus the kinetic energy of the secondary, T, and F(x) is a complex function given in PJG.

Equation (3.17) is very highly forward peaked for small energy losses but becomes less forward peaked as the energy loss becomes significant when compared with the incident energy, E.

The secondary electron is also scattered in the ionization event. Probably the most comprehensive work that exists on secondary doubly

differential cross sections is that of Opal, Beaty, and Peterson (1972). (More recent data by DuBois and Rudd (1978) agrees with their work.) This data indicates a preferred angle range in the scattering process (usually between 45° and 90°) at all primary and secondary energies. A Breit-Wigner form has been chosen to represent the data. Here,

$$\frac{d\sigma}{dT d\Omega} = \frac{S(E,T)C^2}{[C^2 + B(\cos\theta - \cos\theta_o)^2]N_f} \tag{3.18}$$

where

$$B(E) = 0.0448 + \left(\frac{E}{72900\ \mathrm{eV}}\right)^{0.91}$$

$$C(T) = \frac{36.6\ \mathrm{eV}}{(T + 183\ \mathrm{eV})}$$

$$\theta_o(E) = 0.873 + \frac{\theta_A(E)}{(T + \theta_B(E))}$$

$$\theta_A(E) = 20\ \mathrm{eV} + 0.042\ E$$

$$\theta_B(E) = 28\ \mathrm{eV} + 0.066\ E$$

$$N_f = \frac{-2\pi C}{\sqrt{B}} \left\{\tan^{-1}\left[\frac{-\sqrt{B}\ (1 + \cos\theta_o)}{C}\right] - \tan^{-1}\left[\frac{\sqrt{B}\ (1 - \cos\theta_o)}{C}\right]\right\}$$

and

$$S(E,T) = \frac{d\sigma}{dT} = A(E)\Gamma^2(E)/[(T - T_o(E))^2 + \Gamma^2(E)] \tag{3.19}$$

is from Green and Sawada (1972) with

$$A(E) = \sigma_o \frac{5.30}{E} \ln\left[\frac{E}{1.74\ \mathrm{eV}}\right]$$

$$T_o(E) = 4.71\ \mathrm{eV} - \frac{1000\ (\mathrm{eV})^2}{(E + 31.2\ \mathrm{eV})}$$

$\Gamma(E) = 13.8 \text{ eV } E/(E + 15.6 \text{ eV})$

$\sigma_0 = 1 \times 10^{-16} \text{ cm}^2$

Equation (3.18) may seem highly complicated; however, integration over the solid angle is given very simply as Eq. (3.19) which is the singly differential ionization cross section. The total ionization cross section is then

$$\sigma_{ION}(E) = \int_0^{T_M} \frac{d\sigma}{dT}\, dT \tag{3.20}$$

with

$$T_M = \frac{1}{2}(E - I)$$

so that

$$\sigma_{ION}(E) = A\Gamma\{\tan^{-1}[(T_M - T_0)/\Gamma] + \tan^{-1}(T_0/\Gamma)\} \tag{3.21}$$

The fit to Opal, Beaty, and Peterson's (1972) data is given in Figure 3.7 at several primary and secondary energies. The x's represent the experimental data and the solid line represents the analytic expression, Eq. (3.18).

Other inelastic processes include the simple excitation events. The scattering of the incident electron due to the excitation of a particular state has been studied by Silverman and Lassettre (1965), and more recently by Cartwright, Chutjian, Trajmar, and Williams (1977) and Chutjian, Cartwright, and Trajmar (1977).

In order to account for this scattering, the Silverman and Lassettre (1965) generalized oscillator strength data for the 12.85 eV peak (corresponding to the optically allowed b $^1\pi_u$ state) were fit with the use of a phase function similar to model 1. The very sharply forward scattering

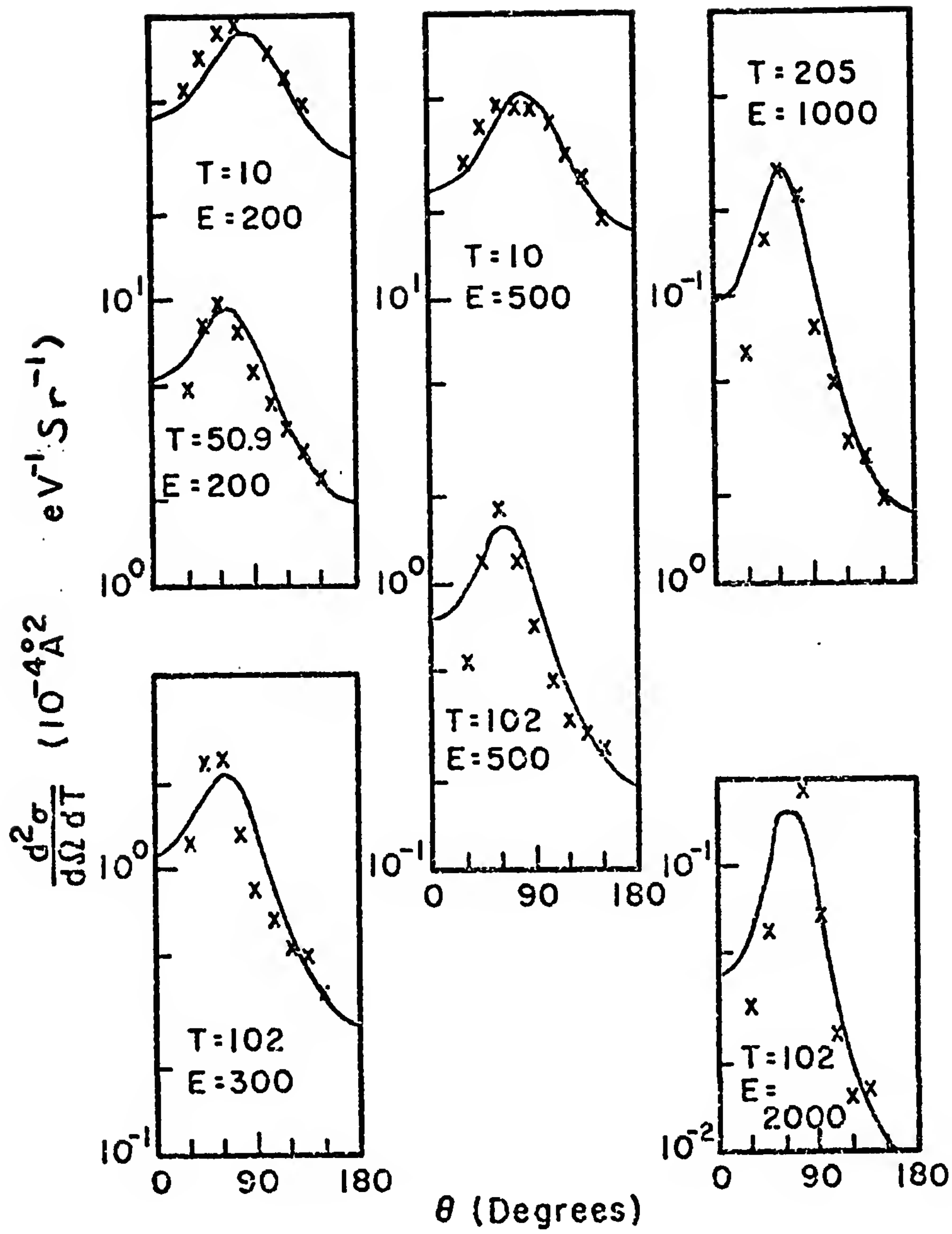

Figure 3.7 N_2 experimental ionization doubly differential cross sections from Opal, Beaty, and Peterson (1972) are represented by x's. The solid line (——) denotes the cross section resulting from the use of Eq. (3.18). The incident electron energy is denoted by E (eV) and the secondary electron energy is denoted by T (eV).

peak indicated in these data was used in a MC calculation. The electron scattering which results using this inelastic scattering approximation in a computation was so small as to be virtually undetectable.

Cartwright et al. (1977) and Chutjian et al. (1977) have studied a more comprehensive list of states and have observed significant electron scattering (especially due to the optically forbidden states) in the range from 10 eV to 60 eV. Characterizing this data in some way appears to be a rather endless task.

Dealing with this type of inelastic scattering is thus still a problem. Above 100 eV the optically allowed excitations are the most important; thus it is safe to conclude that the inelastic scattering events will not affect the energy degradation process. Below 100 eV, as a first approximation, it is assumed in this work that the inelastic excitation events scatter as much as the elastic events. This is probably a reasonable approximation to the very complex inelastic excitation scattering. In section VI.B the effects of this assumption are discussed.

C. Total Cross Section (Elastic Plus Inelastic)

Elastic and inelastic processes have been considered in sections III.A and III.B. Another aspect of the cross sections is the total (elastic plus inelastic) cross section.

Blaauw, de Heer, Wagenaar, and Barends (1977) have recently published experimental data on the total cross section values of N_2. These experimental values are compared with the cross section values from this work in Figure 3.6.

Throughout the energy range the cross sections used in this study compare favorably with those of Blaauw et al. (1977). For an easy reference, the total inelastic and total elastic cross sections are also given in Figure 3.6 as separate curves.

All the major influences on the IEE energy loss and scattering have been accounted for in this chapter. The next chapter presents the MC energy deposition scheme which employs these cross sections.

CHAPTER IV

THE MONTE CARLO METHOD OF ENERGY DEPOSITION BY ELECTRONS IN MOLECULAR NITROGEN

A Monte Carlo calculation is used here for energy degradation by energetic electrons in N_2. This stochastic process is probably the most accurate method for obtaining the energy loss of particles in a medium. The generalizations about electron impact on N_2 that are made through the use of this technique can be applied in other energy deposition approaches to electrons impinging on the atmosphere. (This is true even though the magnetic field is neglected in these MC calculations. The three dimensional yield spectrum $U(E,z,E_0)$ [see Chapter VII] is most useful for applications to the atmosphere and changes in the magnetic field will not affect the yield spectra greatly below altitudes of about 300 km where the gas density is fairly high [see Berger, Seltzer, and Maeda, 1970 and 1974].)

Building on the MC work done in this paper, more exact models of auroral electrons and photoelectrons can be established. In the first section, IV.A, a brief discussion of the MC calculation outlines the general procedure involved in the degradation process. The computer program and machinery used are briefly described in section IV.B. Section IV.C relates in detail the various aspects of the calculation. Finally, section IV.D discusses the statistical error that arises from the use of the MC calculation.

A. Brief Discussion of the Monte Carlo Calculation

In Figure 4.1 a short version of the MC calculation is presented. Briefly, each electron is degraded in a collision by collision manner down to 30 eV. Below 30 eV the electrons are degraded with the use of a multiple scattering distribution. This multiple scattering approach characterizes the resultant coordinates of the electron which goes through several elastic collisions between each inelastic collision.

The incident electron has an energy E_0. To begin with, the running total of the electron energy, E, is set equal to E_0. At the position START, this energy E is checked against a cutoff energy, E_c. If the E is more than E_c, then, first the distance traveled by the electron to the collision is calculated.

Second, the type of collision which occurs is determined. If a collision is elastic then the electron is scattered with the use of a phase function, the appropriate energy ΔE_{Elas} is lost, and the electron goes back up to the START of the degradation process. Whether a collision is inelastic it is determined if the collision is an ionization event or an excitation event. In the excitation process, scattering occurs if the energy E is less than 100 eV, E is reduced by the threshold, W, for excitation of this state, and the electron goes back up to the START of the degradation process.

Ionization collisions are the most complex occurrences to compute. The energy loss, W, by the incident electron is equal to the kinetic energy, T, of the secondary electron produced plus the ionization threshold, I. The primary electron is then scattered and reduced in energy by W. If the secondary electron has a kinetic energy greater than E_c, then,

Figure 4.1 Flowchart of the Monte Carlo degradation of an incident electron of energy E_0.

MONTE CARLO CALCULATION

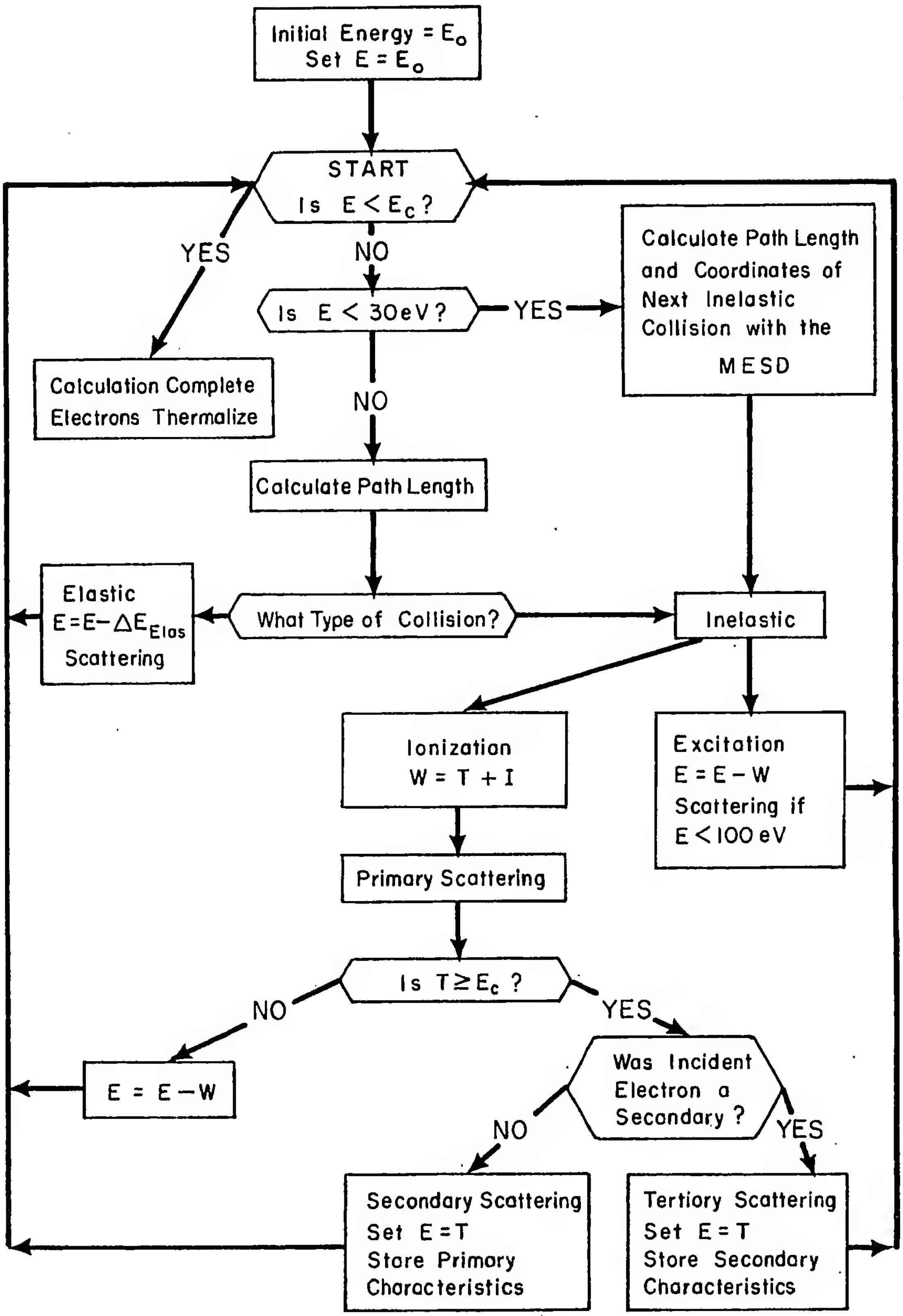

it is scattered and sent back to the START to be degraded further. In the meantime, the primary electron's properties are stored.

If a secondary produces a tertiary electron with a kinetic energy greater than E_c, then that tertiary is completely degraded before any further degradation of the secondary is considered. Like the primary, the secondary electron's properties are stored in the meantime. No other generations were included in this study as their contribution would be, at most, a couple of tenths of a percent of the incident electron's energy.

After the tertiary is entirely degraded below E_c, then the secondary is again sent back to the START to be degraded further. The secondary is next entirely degraded below E_c, and, finally, the primary is again sent back to the START to be further degraded. This whole process may then again repeat itself.

B. Computer Programs and Machinery Used in the Monte Carlo Calculation

In the previous section a brief discussion was given of the electron energy degradation process. A brief discussion will be given below about the MC computer codes and the computing machinery used. The MC computer program employed in this work evolved from an original MC code written by R.T. Brinkmann (see applications in Brinkmann and Trajmar, 1970). This program was revised for use in Heaps and Green (1974), Kutcher and Green (1976), and Riewe and Green (1978). The author has further modified this MC technique for energetic electron impact into N_2 to be used in the energy range from 2 eV to 5 KeV.

This MC technique was applied to several incident electron energies. The vast majority of the MC program runs used the Amdahl 470/175 computer at the Northeast Regional Data Center at the University of Florida. There were, however, several MC runs using the PDP 11/34 of the Aeronomy group of the University of Florida.

It should be noted here that running the same program on both machines at the same energy, E_0 = 1 KeV, showed a factor of 240 difference in the execution time. Thus a program that takes four hours on the PDP 11/34 will take one minute on the Amdahl 470/175. This time advantage plus the ability to store each collision of the electrons on magnetic tape does make the Amdahl 470/175 a more desirable "number-crunching" machine. The PDP 11/34 is only able to produce intensity plots in the longitudinal direction. This mini-computer is thus mainly useful in deriving a range (to be described in the next chapter).

Two programs were used in deriving the MC results. The first program (listed in Appendix A), the modified version of Brinkmann's code, degraded the electrons in energy from their initial E_0 down to the E_c and recorded each collision and its properties on the tape. The second program (listed in Appendix B) coalesces the data from the tape into an array of ordered output. This output contains information for three dimensional intensity plots, energy loss plots, and yield spectra.

C. Detailed Discussion of the Monte Carlo Electron Energy Degradation Technique

Now, a more detailed discussion is given for the MC method of degrading an electron's energy. An electron will start off with an energy of E_0 and coordinates x_0, y_0, z_0, θ_0, and ϕ_0. The symbols x, y,

and z are the Cartesian coordinates of the electron. The polar angle θ is measured with respect to the z-axis and the ϕ denotes the azimuthal angle measured with respect to the x-axis (see Figure 4.2). In this approach, the initial coordinates x_0, y_0, z_0, θ_0, and ϕ_0 were all set equal to zero. The coordinates x_b, y_b, z_b, θ_b, and ϕ_b of the electron before starting on its journey to a collision are, therefore, initially established as $x_b = x_0$, $y_b = y_0$, $z_b = z_0$, $\theta_b = \theta_0$, and $\phi_b = \phi_0$.

The MC approach relies on the random number, R, between 0.0 and 1.0 to aid in the deposition calculation. For each collision several R's are needed and for each R a new property of the collision is gained. In order to explain this MC approach, an accounting of the random numbers and their subsequent usefulness is now made. The multiple elastic scattering distribution used below 30 eV and the lowest energy cutoff 2 eV are also described.

1. First Random Number, R_1

The first random number, R_1, is used to find the path, P_T, traveled by the electron before it collides with a molecule of N_2. Calculation of P_T proceeds in the following manner. The mean free path, λ, is defined as

$$\lambda = \frac{1}{n\sigma_T(E)} \tag{4.1}$$

where n is the density of N_2 molecules in $\#/cm^3$ and $\sigma_T(E)$ is the total (inelastic plus elastic) cross section of N_2 in units of cm^2 at an energy E. The densities used at the various initial input energies are given in Table 4.1.

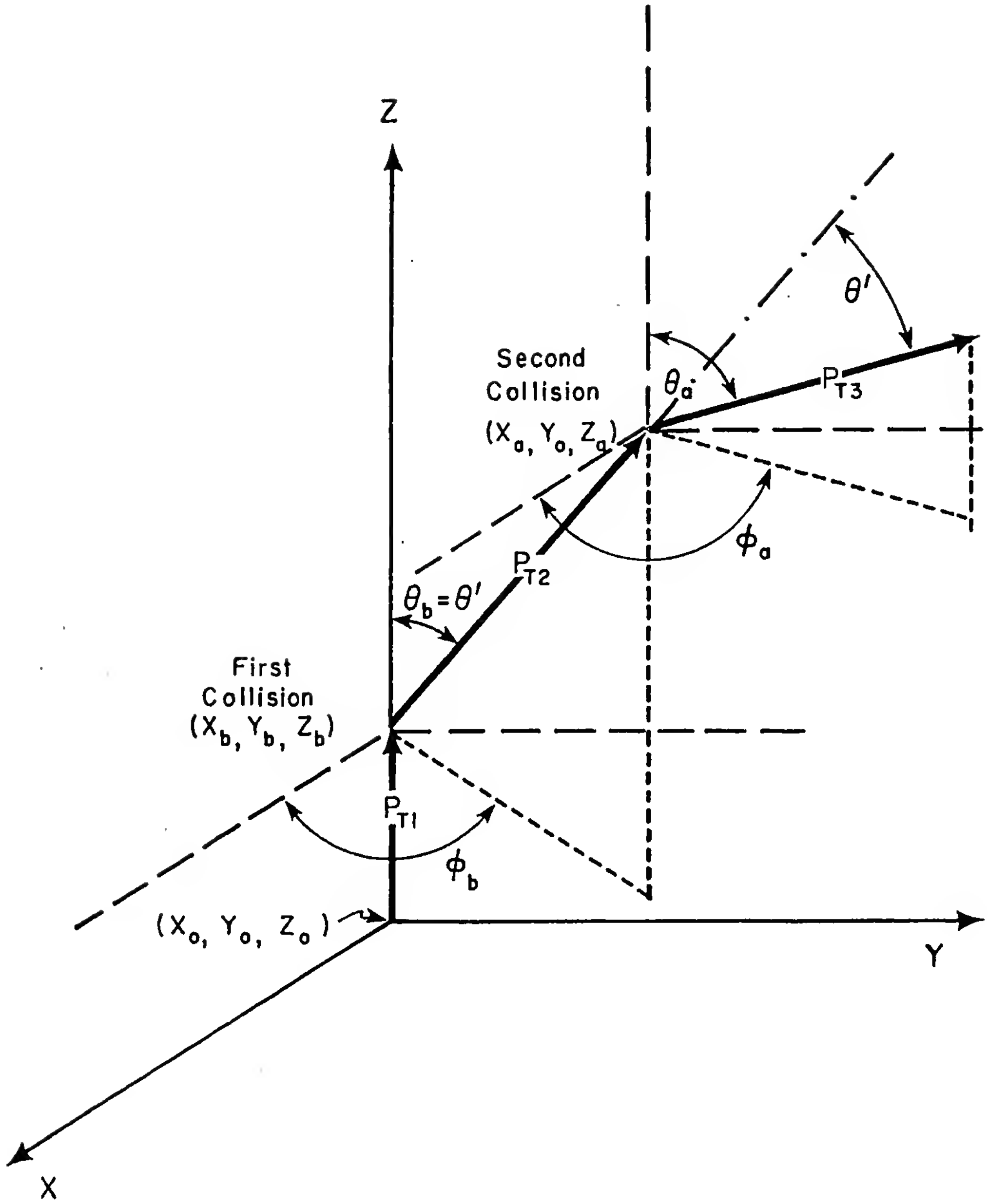

Figure 4.2 Schematic representation of the coordinates and directions of motion of the electron in its travel between collisions with the N_2 molecules.

Table 4.1 The energy E is presented in the first column with the number density n, used in the MC calculation, being given in the second column. (8.0 E+ 14 means 8.0 x 10^{14})

E (KeV)	n (#/cm^3)
0.1	8.0 E+14
0.3	2.0 E+15
1.0	8.2 E+15
2.0	2.8 E+16
5.0	1.2 E+17

All electrons are forced to be degraded in a 30 cm long cylinder; thus an increase in the density is required for an increase in the energy. There are 10 cm allowed in the negative z direction and 20 cm allowed in the positive z direction. The x and y axes extend to infinity. Some electrons actually escape from the cylinder, but the energy lost due to these electrons is only a few tenths of a per cent of the incident electron energy. The path length P_T is then given as

$$P_T = -\lambda \ln(R_1) \tag{4.2}$$

using the relation that

$$R_1 = e^{-P_T/\lambda} \tag{4.3}$$

Figure 4.2 represents a schematic of the electron traveling and colliding with three N_2 molecules. The P_{T1}, P_{T2}, and P_{T3} are the path lengths traveled by the electron between the initial coordinates and the first collision, the first and second collisions, and the second and third collisions, respectively.

The x_a, y_a, and z_a coordinates at this collision can now be found from P_T, x_b, y_b, z_b, θ_b, and ϕ_b using

$$x_a = x_b + P_T \sin\theta_b \cos\phi_b \tag{4.4}$$

$$y_a = y_b + P_T \sin\theta_b \sin\phi_b \tag{4.5}$$

$$z_a = z_b + P_T \cos\theta_b \tag{4.6}$$

In Figure 4.2 the coordinates of the first and second collisions are represented to illustrate how the electron's direction of motion might change during its collisions with N_2. So far emphasis has been only on

the Cartesian coordinates. Now, calculate the azimuthal angle ϕ_a and the polar angle θ_a of the electron after a collision.

2. Second and Third Random Numbers, R_2 and R_3

In actuality the type of collision must be specified before the scattering can be calculated. It is assumed, however, that the type of collision is already known (see subsection IV.C.4). The second, R_2, and third, R_3, random numbers are not chosen if the collision is an excitation event and E is greater than 100 eV. They are chosen for all other collisions.

The R_2 is used to calculate the azimuthal scattering angle, ϕ', of the electron from its direction of motion. The premise is that the azimuthal scattering is isotropic; therefore,

$$\phi' = R_2 \, 2\pi \tag{4.7}$$

(Note that the ϕ' angle is the only angle not represented in Figure 4.2. Inclusion of ϕ' adds too much complication to an already cluttered figure.)

The third random number, R_3, is employed to calculate the polar scattering angle θ' of the electron from its direction of motion. (The angle θ' is represented twice in Figure 4.2: Once as the scattering due to the first collision and once as the scattering due to the second collision.)

For elastic collisions, Eq. (3.1), (3.12), (3.13), or (3.14) are used in determining θ'. In all but one of these phase functions, an analytic expression can be used to determine θ' from the random number, R_3. These analytic expressions are given below.

Using the screened Rutherford differential cross section form (see Eq. (3.1)), it follows that

$$\theta' = \cos^{-1}\left[1 + 2\eta - \frac{2\eta(1+\eta)}{1+\eta-R_3}\right] \tag{4.8}$$

For model 1 (see Eq. (3.12))

$$\theta' = \cos^{-1}\left[\frac{-1}{R_3[(2+a)^{-1} - a^{-1}] + a^{-1}} + 1 + a\right] \tag{4.9}$$

and for model 2 (see Eq. (3.13))

$$\theta' = \cos^{-1}\left[\frac{-B \pm \sqrt{B^2 - 4AC}}{2A}\right] \tag{4.10}$$

with

$$A = R_3 + \frac{f}{a[(2+a)^{-1} - a^{-1}]} - \frac{(1-f)}{(2+c)[(2+c)^{-1} - c^{-1}]}$$

$$B = -A(a-c) + \frac{f}{[(2+a)^{-1} - a^{-1}]} + \frac{(1-f)}{[(2+c)^{-1} - c^{-1}]}$$

and

$$C = -A(1+a)(1+c) + \frac{f(1+c)}{[(2+a)^{-1} - a^{-1}]} - \frac{(1-f)(1+a)}{[(2+c)^{-1} - c^{-1}]}$$

Model 3 (Eq. (3.14)) is not so easy to write in such a convenient form. The equation for primary scattering after an ionization event (Eq. (3.17)) is, also, not easily inverted.

For these two differential cross sections, the following approach is taken. The angular range from 0° to 180° is divided up into angular intervals. A certain probability for scattering at angles less than the end of each angle interval is calculated from the differential cross

section form. The angle θ' is then found through the correct placement of R_3 into an angular segment whose beginning and ending point scattering probabilities bracket R_3.

For this work twenty-four angular segments were chosen. Their end-points are given in Table 4.2. With twenty-four angular intervals, the results from the Monte Carlo calculation came out to be the same as with the use of forty angular intervals. If sixteen or even twenty segments were used, the MC computation gave results that were 5% to 10% different.

The ϕ' and θ' are not the scattering angles from the original coordinate system, but represent the azimuthal and polar scattering of the scattered electron from the direction of travel of the incident electron. In order to calculate ϕ_a and θ_a, the azimuthal and polar angles representing the motion of the electron after the collision, some spherical trigonometry must be used. The following relations hold in this transposition:

$$\cos\phi_a = [\cos\theta_b \cos\phi_b \sin\theta' \cos\phi' - \sin\phi_b \sin\theta' \sin\phi' + \sin\theta_b \cos\phi_b \cos\theta']/\sin\theta_a \tag{4.11}$$

$$\sin\phi_a = [\cos\theta_b \sin\phi_b \sin\theta' \cos\phi' + \cos\phi_b \sin\theta' \sin\phi' + \sin\theta_b \sin\phi_b \cos\theta']/\sin\theta_a \tag{4.12}$$

$$\phi_a' = \cos^{-1}(\cos\phi_a) \tag{4.13}$$

$$\cos\theta_a = \cos\theta_b \cos\theta' - \sin\theta_b \sin\theta' \cos\phi' \tag{4.14}$$

$$\sin\theta_a = \sqrt{1 - \cos^2\theta_a} \tag{4.15}$$

Table 4.2 Twenty-four angle intervals are given here that were used in the Monte Carlo calculation. First column lists the index of the segment and the second and third columns give the beginning and end points for each segment with units of radians (degrees).

Index	Beginning	End
1	0.00 (0.00)	0.01 (0.57)
2	0.01 (0.57)	0.05 (2.87)
3	0.05 (2.87)	0.11 (6.30)
4	0.11 (6.30)	0.20 (11.46)
5	0.20 (11.46)	0.40 (22.92)
6	0.40 (22.92)	0.60 (34.38)
7	0.60 (34.38)	0.80 (45.84)
8	0.80 (45.84)	0.90 (51.57)
9	0.90 (51.57)	1.00 (57.30)
10	1.00 (57.30)	1.10 (63.03)
11	1.10 (63.03)	1.20 (68.75)
12	1.20 (68.75)	1.30 (74.48)
13	1.30 (74.48)	1.40 (80.21)
14	1.40 (80.21)	1.50 (85.94)
15	1.50 (85.94)	1.60 (91.67)
16	1.60 (91.67)	1.80 (103.13)
17	1.80 (103.13)	2.00 (114.59)
18	2.00 (114.59)	2.20 (126.05)
19	2.20 (126.05)	2.40 (137.51)
20	2.40 (137.51)	2.60 (148.97)
21	2.60 (148.97)	2.80 (160.43)
22	2.80 (160.43)	3.00 (171.89)
23	3.00 (171.89)	3.07 (175.90)
24	3.07 (175.90)	3.14 (180.00)

and

$$\theta_a = \cos^{-1}(\cos\theta_a) \tag{4.16}$$

Now the azimuthal angle ϕ_a and the polar angle θ_a have been established for the collision with respect to the fixed coordinate system. These angles are also represented in Figure 4.2. The two angular coordinates ϕ_b and θ_b of the electron before traveling to the next collision are then set as $\phi_b = \phi_a$ and $\theta_b = \theta_a$.

3. Fourth Random Number, R_4

A fourth random number, R_4, is required if a secondary is produced and if that secondary has an energy above the cutoff energy, E_c. This R_4 is chosen to determine the polar angle, θ', of scattering of the secondary. Again, an analytic formula can be employed to define θ'. This equation was derived from Eq. (3.18) and is written as

$$\theta' = \cos^{-1}\left[\frac{C}{\sqrt{B}} \tan\left[R_4\left\{\tan^{-1}\left(\frac{-\sqrt{B}(1+\cos\theta_o)}{C}\right) - \tan^{-1}\left(\frac{\sqrt{B}(1-\cos\theta_o)}{C}\right)\right\} + \tan^{-1}\left(\frac{\sqrt{B}(1-\cos\theta_o)}{C}\right)\right] + \cos\theta_o\right] \tag{4.17}$$

The ϕ' for the secondary is found with the use of Eq. (4.7) and θ_a and ϕ_a result from the use of Eqs. (4.11) through (4.16).

4. Fifth Random Number, R_5

The fifth random number, R_5, determines the type of collision that occurs. Here, the type may be either elastic or inelastic. If the

type is inelastic then the individual excitation or ionization event is found as well.

There are cross sections for thirty-four states of N_2 employing the papers of Jackman, Garvey, and Green (1977) and Porter, Jackman, and Green (1976). Using all these states in the MC calculation would greatly increase the cost. It was therefore decided to reduce these thirty-four states to nine states. Two allowed states, the b $^1\pi_u$ and the b' $^1\Sigma_u^+$, and the six ionization states were kept the same as given in the papers. For the ninth state, all the Rydberg and forbidden states were combined.

Above 200 eV, the forbidden states are contributing only a minuscule amount to the total cross section. Since the other states have roughly the same ln E/E fall-off at high energies, it is assumed that the probabilities for excitation to any of these states will be constant. These probabilities were simply found from the ratio of the cross section of the state in question to the total inelastic cross section at the electron energy of 5 KeV.

In Table 4.3 these states, their probabilities, and thresholds are presented. The probability, p_c, of the composite state is simply

$$p_c = \sum_{i=1}^{m} p_i \tag{4.18}$$

where m = the total number of Rydberg and forbidden states and p_i is the probability for excitation of the ith Rydberg or forbidden state. The average threshold, W_c, for exciting the composite state is found easily with the following equation

$$W_c = \frac{\sum_{i=1}^{m} p_i \; W_i}{\sum_{i=1}^{m} p_i} \tag{4.19}$$

Table 4.3 N_2 inelastic states, their probabilities, p, and thresholds, W, taken for electron energies above 200 eV are presented below.

State	p	W (eV)
N_2 $b^1\pi_u$	0.092	12.80
N_2 $b'^1\Sigma_u^+$	0.042	14.00
N_2 Composite	0.233	15.40
N_2^+ $X^2\Sigma_g^+$	0.289	15.58
N_2^+ $A^2\pi_u$	0.127	16.73
N_2^+ $B^2\Sigma_u^+$	0.066	18.75
N_2^+ $D^2\pi_g$	0.044	22.00
N_2^+ $C^2\Sigma_u^+$	0.044	23.60
N_2^+ 40 eV	0.063	40.00

with W_i being the threshold of the Rydberg or forbidden state.

Below 200 eV, the probabilities for excitation to the various inelastic states are changing quite rapidly. The parameters for the eight individual states are taken from Jackman et al. (1977b) and Porter et al. (1976). The composite state's properties are found in the same manner that they were above. In these lower energy regimes the probability and energy loss are changing fairly rapidly, thus Table 4.4 illustrates these probabilities and threshold values at several energies.

With the background on the inelastic cross sections and their subsequent probabilities, consider now the collision type. The R_5 random number determines the type of collision that occurs in the following manner: If

$$R_5 \le \frac{\sigma_{TE}(E)}{\sigma_T(E)} \quad \text{for all electron energies} \tag{4.20}$$

where $\sigma_{TE}(E)$ is the total elastic cross section, then the collision is elastic. If

$$\frac{\sigma_{TE}(E)}{\sigma_T(E)} < R_5 \le \frac{p_1\sigma_{TI}(E) + \sigma_{TE}(E)}{\sigma_T(E)} \quad \text{and} \quad E > 200 \text{ eV} \tag{4.21}$$

where $\sigma_{TI}(E)$ is the total inelastic cross section and p_1 is the probability for exciting the first inelastic state (in Table 4.2 the first state is the $b^1\pi_u$ thus $p_1 = 0.092$), then the inelastic collision results in the excitation of the first state.

A relation follows from Eq. (4.21) that holds true for j = 2 to 9 such that: If

Table 4.4 N_2 inelastic composite state with its characteristic probability, p, and average energy loss, W, given for several energies between 2 and 200 eV.

E (eV)	p	W (eV)
2	1.000	0.57
3	1.000	1.03
4	1.000	0.922
5	1.000	0.835
6	1.000	0.772
7	1.000	0.728
8	1.000	0.696
9	1.000	7.00
10	1.000	7.21
12	1.000	8.25
14	1.000	8.91
16	0.971	9.12
18	0.866	9.34
20	0.745	9.68
30	0.426	11.70
40	0.344	12.80
50	0.296	13.30
60	0.271	13.70
70	0.255	13.90
100	0.229	14.30
150	0.214	14.60
200	0.234	14.80

$$\frac{\sum_{i=1}^{j-1} p_i \sigma_{TI}(E) + \sigma_{TE}(E)}{\sigma_T(E)} < R_5 \leq \frac{\sum_{i=1}^{j} p_i \sigma_{TI}(E) + \sigma_{TE}(E)}{\sigma_T(E)} \quad \text{and } E > 200 \text{ eV} \qquad (4.22)$$

then the inelastic collision results in the excitation of the jth state. Thus the R_5 random number for an electron of energy E > 200 eV will determine which type of collision occurred when satisfying Eq. (4.20), (4.21), or (4.22).

For energies below 200 eV, the following relations must be considered: If

$$\frac{\sigma_{TE}(E)}{\sigma_T(E)} < R_5 \leq \frac{\sigma_1(E) + \sigma_{TE}(E)}{\sigma_T(E)} \quad \text{and } E \leq 200 \text{ eV} \qquad (4.23)$$

where $\sigma_1(E)$ is the cross section for exciting the first inelastic state, then the inelastic collision results in the excitation of this state.

A relation similar to Eq. (4.22) can now be established for j = 2 to 8 such that: If

$$\frac{\sum_{i=1}^{j-1} \sigma_i(E) + \sigma_{TE}(E)}{\sigma_T(E)} < R_5 \leq \frac{\sum_{i=1}^{j} \sigma_i(E) + \sigma_{TE}(E)}{\sigma_T(E)} \quad \text{and } E \leq 200 \text{ eV} \qquad (4.24)$$

then the jth inelastic state is excited. If

$$R_5 \geq \frac{\sum_{i=1}^{8} \sigma_i(E) + \sigma_{TE}(E)}{\sigma_T(E)} \quad \text{and } E \leq 200 \text{ eV} \qquad (4.25)$$

then the excitation of the composite state is assumed and the energy loss, W_c, in this case is found through a linear interpolation with the use of the values given in Table 4.3.

5. Sixth Random Number, R_6

The sixth random number, R_6, is computed only if the collision type is an ionization event. This R_6 determines the energy lost by the primary in creating a secondary of energy, T_s. Using the S(E,T) from Eq. (3.19) the following relationship is established:

$$R_6 = \frac{\int_0^{T_s} S(E,T)\, dT}{\sigma_{ION}(E)} \tag{4.26}$$

Integrating the numerator in Eq. (4.26) and using Eq. (3.21) to solve for T_s, Eq. (4.27) is derived.

$$T_s = \Gamma(E)[\tan\{R_6 \tan^{-1}[(T_M - T_o(E))/\Gamma(E)]$$

$$+ (R_6 - 1)\tan^{-1}[T_o(E)/\Gamma(E)]\}] + T_o(E) \tag{4.27}$$

The energy loss, W, is then found by the relation:

$$W = I_k + T_s \tag{4.28}$$

where I_k is the ionization threshold for the kth ionization state.

6. Multiple Elastic Scattering Distribution Used Below 30 eV

The MC calculation can be used to degrade an electron down to practically any energy. Even below the lowest threshold for excitation to any vibrational level, the electron will still lose energy via elastic collisions with molecules of nitrogen as well as other electrons. This energy loss to other electrons is fairly low unless a substantial fraction of the gas has been ionized (see Cravens, Victor, and Dalgarno,

1975). In this study the fraction of ionization is assumed to be negligible; therefore, this loss is ignored.

Unless there is a very large amount of money available for computer time, an electron can not be followed to its thermal energy with any practicality. This implies that a multiple elastic scattering distribution (hereafter referred to as MESD) must be used below some given energy. In this work the MESD will be used below 30 eV.

Bethe, Rose, and Smith (1938) used the Fokker-Planck differential equation, neglecting energy loss, to consider the penetration of electrons through thick plates. This, however, leads to a Gaussian solution in the small-angle approximation so that the tail of the angular distribution was omitted. The large-angle multiple scattering has been studied by Goudsmit and Saunderson (1940) [hereafter referred to as GS] who used a series of Legendre polynomials to determine the resultant angle of scattering.

Lewis (1950) studied the integro-differential diffusion equation of the multiple scattering problem in an infinite, homogeneous medium, without the usual small-angle approximation. He obtained the GS solution for the scattering angle and also derived certain moments for the longitudinal and transverse distributions.

Berger (1963) applied a MESD for condensed case history MC calculations. His application of the MESD is at the energies above 200 eV and probably is not accurate for electrons with energies less than about 100 eV. Furthermore, Berger's (1963) work contains approximations that are only good for the sharply forward peaked cross sections of higher energy electrons.

In this work a different problem exists. The MC calculation is used to degrade electrons in a collision by collision manner all the way down to 30 eV. At this energy, the elastic collisions are occurring with twice the frequency of the inelastic events, and at energies below 30 eV the number of elastic collisions between inelastic events may be up to several hundred or thousand. Keeping track of all these elastic collisions would be very costly.

Kutcher and Green (1976) [hereafter referred to as KG] studied the radial, longitudinal, and polar angle distributions for elastic scattering by H_2 in the energy range from 2 to 50 eV. An approach similar to KG's could be applied to N_2. Since such a project would require a substantial amount of time and computer money, the possibility of adapting the KG results was first considered.

With this in mind, consider the differences between N_2 and H_2. First of all, there are some dissimilarities between the differential cross sections. There is more backscatter observed experimentally in N_2 at all energies. Secondly, the total inelastic and elastic cross sections are different. The second difference is no real problem because the MESDs are given in terms of the mean free path lengths (hereafter referred to as MFPs). The first dissimilarity does pose a minor problem which is solved in a simplistic way below.

Above 5 or 6 MFPs the polar angle is approximately random. At most energies below 30 eV, the number of MFPs between inelastic collisions is above 5 or 6. Since the distribution found in KG is not easily inverted, a reasonable assumption is that the polar angle is oriented randomly.

Knowledge of the radial distribution is not crucial for our purposes. The most interesting radial distribution output from this MC calculation is that of the 3914 Å emission. Electrons below 30 eV make little contribution to this profile because the cross section for excitation to this $N_2^+ \; B^2\Sigma_u^+$ state is fairly low (see Figure 5.1). Thus knowledge of the radial distribution of these electrons multiply scattered is not extremely important.

An approximation, however, is employed in most MC computations to calculate a fairly reasonable radial distance. The average radial distance, as observed from the calculations in KG, for most energies and at the longer path lengths is approximately one-sixth of the total path lengths, thus

$$\rho_{ave} = s/6 \tag{4.29}$$

The most important spatial displacement is the longitudinal distance z. In order to calculate z, the total path length s must be known. This length s is calculated from the random number, R_1, the total elastic cross section, $\sigma_{TE}(E)$, and the total inelastic cross section, $\sigma_{TI}(E)$, by using

$$s = -\frac{\sigma_{TE}(E)}{\sigma_{TI}(E)} \ln (R_1) \tag{4.30}$$

The ratio $\sigma_{TE}(E)/\sigma_{TI}(E)$ is simply a fairly accurate approximation of the number of elastic collisions occurring per inelastic collision. The value $-\ln(R_1)$ [see Eq. (4.2)] is the path length (in units of MFPs) traveled by the electron between collisions. Thus knowing the number of elastic collisions occurring and the path length traveled between collisions allows one to write Eq. (4.30) as the expression for the

total path length s (in units of MFPs) traveled between inelastic collisions.

In KG an equation which can be easily inverted to calculate the z distance (in units of MFPs) from some random number, R_2, and path length s, is written

$$z = \ln \frac{\left\{\dfrac{[R_2^{-1/\nu} - 1]}{[F(0)^{-1/\nu} - 1]}\right\}}{-u} \tag{4.31}$$

where

$$\nu(s) = 1 - \exp[-(s/s_\nu)^D]$$

$$F(0) = K\{1 - \exp[-(s/s_f)^{0.75}]\}$$

and

$$u(s) = (H + s^I)/s^J$$

where K = 0.425.

Since there is more backscatter during N_2 elastic collisions (because of its differential backscatter contribution), it seems reasonable that the parameters for Eq. (4.31), which are useful for N_2, are different than those derived in KG. One approach to this dilemma might be to correlate the elastic differential cross section (hereafter called EDCS) from N_2 at some energy E' with the EDCS from H_2 at some energy E. This would work if the H_2 EDCSs showed more backscatter than the N_2 EDCSs; however, the opposite is observed experimentally. Thus the N_2 EDCSs from some E' (around 6-7 eV) values correlate with the H_2 EDCSs at E values less than 2 eV (where the Kutcher and Green, 1976, MESD is not defined).

Another straightforward and simplistic approach is to do the following. Calculate the approximate backscatter at three energies, the two endpoints and the middle (2 eV, 15 eV, and 30 eV), from the KG H_2 EDCS form and the experimental data on N_2 EDCSs (given in Sawada, Ganas, and Green, 1974). At these energies the backscatter with the KG H_2 EDCS form is less than that of the N_2 EDCS by the following values: 2 eV $\sim$ 5%, 15 eV $\sim$ 10%, and 30 eV $\sim$ 10%. An average of these three values is about 8%. Since the major influences of the backscatter in Eq. (4.31) is the value of K, this parameter is the only one that is changed from the KG formulation. It is, therefore, increased by $\sim$8% so that in these MC calculations K = 0.46. The other parameters in Eq. (4.31) are listed in Table 4.5.

Actually it appears that the value of K makes little difference in the MC computational results. Two MC calculations at an incident electron energy of 100 eV with K = 0.46 and with K = 0.425 were undertaken (all other parameters and inputs were the same). The yield spectra (described in Chapters II and VII) changes substantially only at fairly large longitudinal distances (where the distances are about 1.5 times the range). At these large distances there are relatively few electrons anyway, thus there is little effect on the major aspects of the spatial electron energy deposition process.

The Cartesian coordinates x_a, y_a, and z_a are found from the coordinates x_b, y_b, and z_b in the following manner. After z is calculated in units of MFPs with the use of Eq. (4.31), it can then be written in units of cm or km by multiplying by the MFP, λ (calculated from Eq. (4.1)), thus $z_a = z_b + z\lambda$.

Table 4.5 Parameters from Kutcher and Green (1976) for several energy intervals used in Eq. (4.28).

Energy Interval (eV)	H	I	J	D	s_ν	s_F
2-5	12.	1.37	1.71	1.75	5.05	8.5
5-10	9.6	1.32	1.67	2.50	4.25	8.5
10-20	15.5	1.28	1.67	2.31	6.29	10.3
20-30	23.5	1.24	1.69	1.98	9.65	13.6

As established earlier, the polar angle θ_a and azimuthal angle ϕ_a, representing the motion of the electron after the collision, can be chosen in a random way from the two random numbers, R_3 and R_4, using

$$\theta_a = \pi R_3$$

$$\phi_a = 2\pi R_4 \tag{4.32}$$

A reasonable approximation of x_a and y_a can then be made using Eqs. (4.29) and (4.32) such that

$$x_a = x_b + \rho_{ave}\,\lambda\,\cos\phi_a$$

and

$$y_a = y_b + \rho_{ave}\,\lambda\,\sin\phi_a$$

In the MESD the fifth random number, R_5, is used to determine the inelastic collision type. A method similar to that illustrated in subsection IV.C.4 is employed, the only difference is the fact that the collision is only inelastic.

7. Value of the Cutoff Energy, 2 eV

The E_c used in this work has been set at 2 eV because the lowest threshold for excitation to an inelastic state is 1.85 eV. With this cutoff energy the yield spectra can be defined down to 2 eV at all longitudinal distances. Subsequently, a reasonable calculation of the excitation to any N_2 state may be made.

D. Statistical Error in the Monte Carlo Calculation

The statistical error inherent in the MC computation can be derived by considering the following. Since the MC calculation is a probabilistic method of degrading an electron in energy, the multinomial distribution can be used to find the statistical standard deviation for each bin considered. This discussion of the statistical error employed the work of Eadie, Dryard, James, Roos, and Sadoulet (1971).

The probability of getting an excitation of a certain state j in bin k is p_{jk}. The p_{jk} is normalized such that

$$\sum_{k=1}^{m} \sum_{j=1}^{n} p_{jk} = 1 \tag{4.33}$$

In this MC study the multinomial distribution is an array of histograms containing N events distributed in n states and m bins with r_{jk} events in state j and bin k. The r_{jk} values are normalized such that

$$\sum_{k=1}^{m} \sum_{j=1}^{n} r_{jk} = N \tag{4.34}$$

Thus, the r_{jk} observations can be considered somewhat conditional on the fixed observational value of N. The variance of the calculation is represented as

$$V(r_{jk}) = N\, p_{jk}\, (1 - p_{jk}) \tag{4.35}$$

In this work the m x n variables r_{jk} can all be correlated. For the specific example of electron deposition represented in Figure 5.2, $p_{jk} << 1$. This is true because there are total almost 5×10^5 collisions (i.e., $N = 5 \times 10^5$) to consider in this degradation scheme and

at maximum $r_{jk} \gtrsim 4000$. Using this information, Eq. (4.35) can then be approximated by

$$V(r_{jk}) \sim N\, p_{jk} \sim r_{jk} \tag{4.36}$$

and the statistical standard deviation of the number of $N_2^+\ B^2\Sigma_u^+$ events in a bin becomes

$$\sigma_{jk} \sim \sqrt{r_{jk}} \tag{4.37}$$

Equation (4.37) holds true for the specific example represented in Figure 5.2 and it also holds true for all the intensity plots, energy loss plots, and yield spectra that were studied in this work. Thus, in order to obtain the approximate standard deviation for any MC generated number, the square root of this value is its standard deviation. The error bars found in the rest of this paper are determined in this manner.

Now that the MC calculational technique has been outlined, this method will be used in the next three chapters to deal with the spatial and energetic aspects of electron energy degradation.

CHAPTER V

MONTE CARLO INTENSITY PLOTS AND COMPARISON WITH EXPERIMENT

Incident electrons with energies between 0.1 and 5.0 KeV are degraded in N_2 using the MC method described in Chapter IV with the cross sections given in Chapter III. The intensity plots of the 3914 Å emission are described in this chapter.

Emission intensity plots of the 3914 Å radiation from the N_2^+ $B^2\Sigma_u^+$ state are used in describing the range (found by extrapolating the linear portion of the longitudinal 3914 Å intensity plot to the abscissa) for incident electrons. Section V.A describes the excitation of the N_2^+ $B^2\Sigma_u^+$ state. In section V.B the range of the electrons is defined more completely. Previous experimental and theoretical work on the 3914 Å emission of N_2^+ is given in section V.C. The range results from the MC calculation are then discussed in section V.D. Finally, section V.E describes the intensity plots resulting when plotted as functions of the radial direction.

A. Excitation of the $N_2^+ B\,^2\Sigma_u^+$ State

The main concern of this chapter will be the intensity plots showing the emission of the 0-0 first negative band ($B\,^2\Sigma_u^+$ state) of N_2^+ at 3914 Å. Experimentally (see Rapp and Englander-Golden, 1965; McConkey, Woolsey, and Burns, 1967; and Borst and Zipf, 1969), it has been shown that the number of photons at 3914 Å produced for each ionization of N_2 is

independent of the energy of the exciting electron for energies from 30 eV at least up to 3 KeV.

In Figure 5.1 the N_2 total ionization cross section and cross section for ionization and excitation to the B $^2\Sigma_u^+$ state of N_2^+ are presented. The curves are approximately parallel thus even if the absolute values for the two cross sections are slightly in error, the shapes of the intensity plots that result from this MC calculation should be fairly accurate.

The total ionization curve lies nicely in the middle of an array of experiments (namely, Opal, Beaty, and Peterson, 1972; Tate and Smith, 1932; Rapp and Englander-Golden, 1965; and Schram, de Heer, Wiel, and Kistenaker, 1965) but the B $^2\Sigma_u^+$ cross section values may be high when compared to experiments (see Holland, 1967; and McConkey, Woolsey, and Burns, 1967).

The threshold for excitation to this B $^2\Sigma_u^+$ state is 18.75 eV, thus any electron above that energy can excite and ionize a ground state N_2 molecule up to this level. The cross section for excitation and ionization to the B $^2\Sigma_u^+$ state is not large when compared with the total inelastic cross section. In fact, the probability for exciting this state is only 0.066 for electron energies above 200 eV. The accuracy of the MC calculation is dependent on the number of excitations in each bin (see section IV.D). In order to enhance the precision of the MC results, excitations of the X $^2\Sigma_g^+$ and A $^2\pi_u$ states of N_2^+ are added to the B $^2\Sigma_u^+$ excitations. The ionization cross sections for these two states are found to be proportional to the B $^2\Sigma_u^+$ state for electron energies above 30 eV.

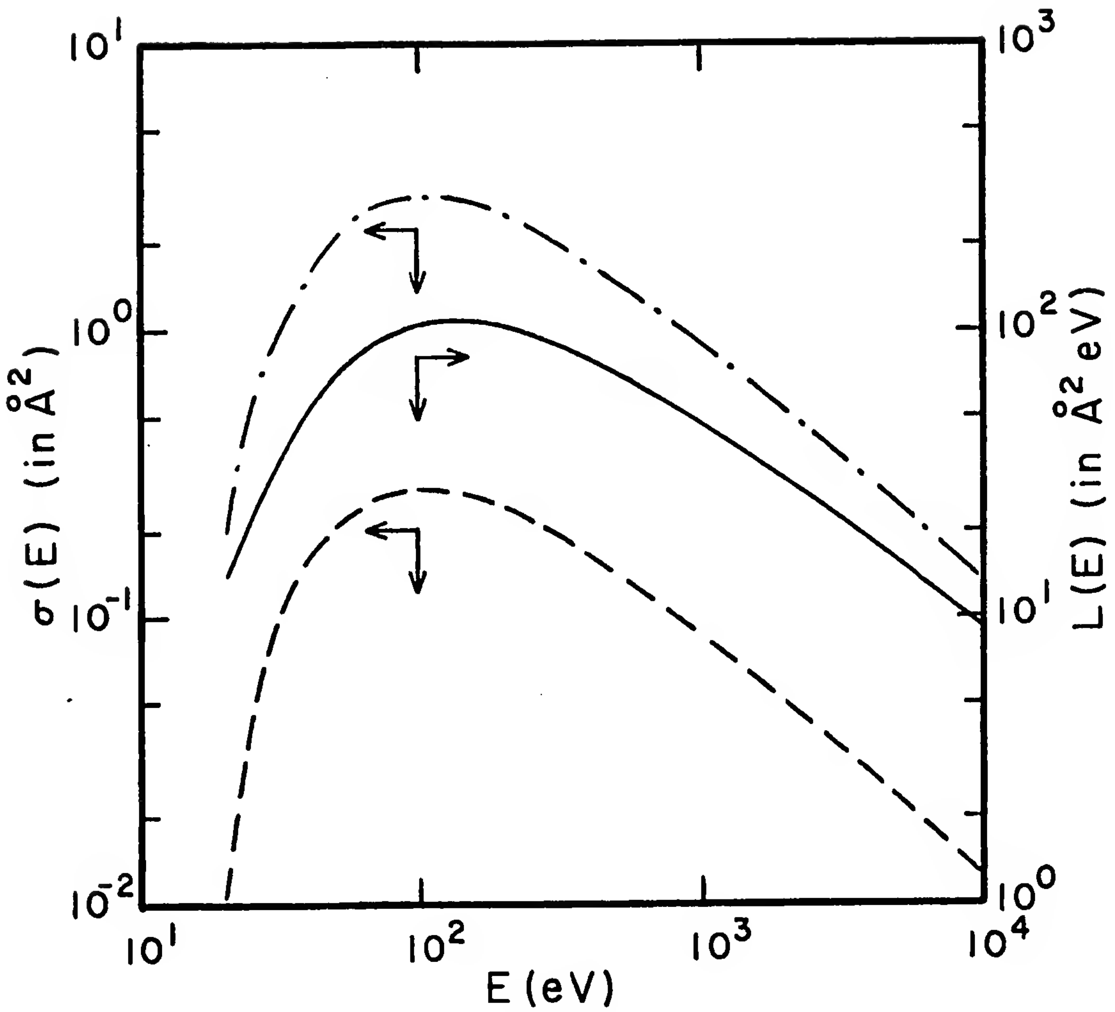

Figure 5.1 Total loss function L(E) from N_2, denoted by the solid line; total ionization cross sections for N_2, denoted by the dash-dot line; and the N_2^+ B $^2\Sigma_u^+$ cross section, denoted by the dashed line, are given as functions of energy, E.

Previous workers (Barrett and Hays, 1976; Cohn and Caledonia, 1970; and Grün, 1957) have used the 3914 Å emission as a measure of the energy deposited. In these works it is assumed that since the 3914 Å radiation is proportional to the number of ionizations in a given volume and if the number of ionizations is proportional to the energy deposited in that volume, then the 3914 Å intensity is proportional to the energy deposited in that volume. These experimenters, therefore, measured the 3914 Å radiation at several energies, extrapolated their intensity plots to find a range (to be described in section V.B), and derived an empirical expression for the range that could be used to find the energy loss function.

This idea of using the 3914 Å emission to derive the energy loss scheme is useful for energies above 2 KeV. In Figure 5.1, compare the loss function, L(E), used in this work and the N_2^+ B $^2\Sigma_u^+$ state cross section.

The two curves are not parallel below 2 KeV. This implies that the energy loss function can not be derived directly from the range results at incident energies below 2 KeV. The energy loss plots from this MC study are given in section VII.A and more will be discussed in that section about them.

B. Range of Electrons

The concept of the mean range must be defined next. For each monoenergetic primary electron impinging into a gas, a range can be calculated. In general (at least above 100 eV), the higher the electron energy the further the electron will penetrate into the medium. If an electron is incident along the z-axis, the excitations of the N_2^+ B $^2\Sigma_u^+$

state can be graphed in an intensity plot with the z-axis as the abscissa.

In Figure 5.2, the intensity plot from 5000 incident 1 KeV electrons is graphed (the model used in this MC calculation should only be taken as an illustrative example) in histogram form. Bins along the z-axis are taken to be 0.5 cm in width for these incident electrons. The linear portion of the curve may be extrapolated, as illustrated by the dashed line, to define a mean range of the beam.

All the intensity plots are normalized in this paper so that the beam starts out at z = 0 cm along the z-axis. The intensity in Figure 5.2 seen at negative values of z is brought about by backscattered electrons. The error bars given near the peak of the histogram are found simply from a method described in section IV.D.

From Figure 5.2, the range is seen to be 16 cm for these 1 KeV electrons. Range values, R_g, in units of gm/cm^2 are written

$$R_g = R_c \rho \tag{5.1}$$

where R_c is the range in cm, $\rho = n M_{N_2}$ (in gm/cm^3), n is the number density of N_2 molecules (in $\#/cm^3$), and M_{N_2} is the weight (in gms) of an N_2 molecule. In this case, $n = 8.2 \times 10^{15}$ molecules of N_2/cm^3, $M_{N_2} = 4.651 \times 10^{-23}$ gm/N_2 molecule, and $R_c = 16$ cm; therefore, $R_g = 6.06 \times 10^{-6}$ gm/cm^2.

C. Previous Experimental and Theoretical Work on the 3914 Å Emission of N_2^+

Grün (1957) measured for air the total luminosity of the 3914 Å radiation in planes perpendicular to the axis of the electron beam with

Figure 5.2 The intensity of 3914 Å radiation is given as a function of z for 5000 electrons with incident energies of 1 KeV. The range, found by extrapolating the linear portion of the histogram (illustrated by the dashed line) to the abscissa, is 16 cm. The I indicates the standard error involved in the MC calculation.

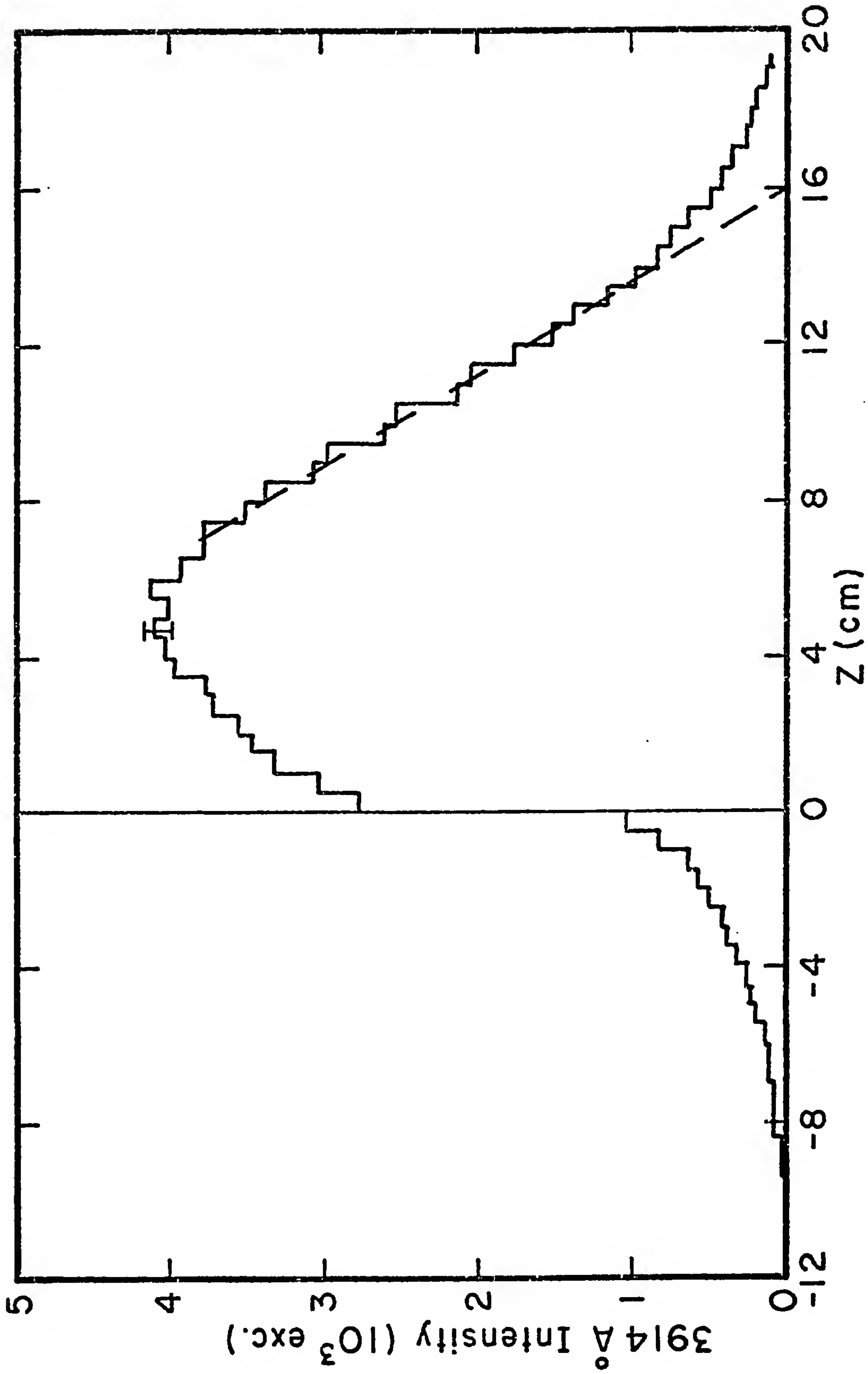

3914 Å Intensity (10^3 exc.)
0
1
2
3
4
5
Z (cm)
-12
-8
-4
0
4
8
12
16
20

an initial energy of 5 to 54 KeV. Cohn and Caledonia (1970) measured intensity profiles of electron beams with incident energies from 2 to 5 KeV impacting into N_2. Barrett and Hays (1976) then extended the incident electron range down to 300 eV by measuring the radiation profiles of 3914 Å resulting from electron beams with energies from 0.3 to 5.0 KeV impinging on N_2.

Spencer (1959) used the Spencer and Fano (1954) method of spatial energy deposition and found good agreement between his energy loss plots and the 3914 Å intensity plots of Grün (1957). The Berger, Seltzer, and Maeda (1974) [BSM] MC calculation provided energy loss plots down to 2 KeV. These plots are also in fairly good agreement with the experiments mentioned above.

Comparisons will be made in this paper between the available experimental electron energy loss data and the MC calculations done here. Since this MC calculation follows the incident electrons, as well as its secondaries and tertiaries down to 2 eV, this MC computation is one of the most detailed ever employed for electron impact energy degradation. It is, therefore, of interest to compare the results from this study with experimental results for incident electrons with energies from 300 eV up to 5 KeV.

D. Range Results and Longitudinal Intensity Plots from the Monte Carlo Calculation

Range data at several incident electron energies are calculated with the use of the screened Rutherford and the model 3 differential elastic cross sections. The screened Rutherford model is used because it is the most widely used form for elastic scattering in theoretical

studies and, also, because BSM were quite successful in using this form down to incident energies of 2 KeV. Model 3 was used because of its very close agreement with experimental differential cross section data in the range from 30 eV up to 1 KeV.

Table 5.1 presents the range data (for perpendicularly incident electrons) from three different experiments, the theoretical calculation by BSM, and two sets of theoretical computations from this study. The values in parentheses from BH (Barrett and Hays, 1976), CC (Cohn and Caledonia, 1970), and G (Grün, 1957) are simply calculated from the empirical formulae given in these works.

For the rest of this chapter, the results of this work will be compared with those of BH. This is the most recent experimental study and is probably the most reliable experimental work. They also use the same incident electron energy regime as that employed in this work. In Table 5.1 it is apparent that the BH values have the largest ranges of the experimental studies.

The two separate MC calculations in this study seem to bracket the BH results at all energies. The model 3 ranges are consistently larger than those of BH. These results are 10% higher at 5 KeV and about 19% higher at 0.3 KeV. The screened Rutherford ranges, on the other hand, are about 9% lower at 5 KeV and about 10% lower at 0.3 KeV.

If it can be assumed that the BH results are indeed the most reliable data, then the following conclusion can be made: The screened Rutherford phase function scatters the electron too much while the model 3 phase function provides too little scattering. This conclusion is made assuming that the total cross sections described in Chapter III are fairly accurate.

Table 5.1 Range data (in 10^{-6} gm/cm^2) at several energies, E (in KeV), are given below. The second column M3 (model 3), third column SR (screened Rutherford), fourth column BH (Barrett and Hays, 1976), fifth column CC (Cohn and Caledonia, 1970), sixth column G (Grün, 1957), and seventh column BSM (Berger, Seltzer, and Maeda, 1974) range values are presented.

E (KeV)	M3	SR	BH	CC	G	BSM
0.1	0.37	0.34	(0.53)	(0.07)	(0.08)	--
0.3	1.25	0.95	1.06	(0.51)	(0.56)	--
1.0	6.45	5.57	5.72	(4.17)	(4.57)	--
2.0	18.6	16.8	17.7	14.0	(15.4)	15.2
5.0	91.5	75.9	83.0	69.7	76.4	71.9

In this work model 3 is the result of a careful investigation of the detailed molecular nitrogen cross sections. Therefore no attempt will be made here to change the cross sections compiled in Chapter III. Model 3 will be used in most of the MC calculations in the rest of this chapter and also in Chapter VII (BSM have, however, chosen η_c, used in the screened Rutherford cross section, to be a constant value whose value was selected so as to obtain the best agreement between their MC calculation and the experimental results of G and CC).

In Table 5.1 the importance of the elastic phase functions is clearly illustrated. Up to a 25% change in the range is observed when comparing the screened Rutherford with the model 3 phase functions. More elaboration on the effects of various phase functions on the energy deposition process will be given in Chapter VI.

Figures 5.3 and 5.4 give intensity plots for the 3914 Å radiation resulting from 2 KeV and 0.3 KeV incident electrons, respectively. The experimental work of BH and the calculations using model 3 and the screened Rutherford are presented in these figures. The shapes appear to be somewhat similar; however, the BH results at both energies predict a range that is between the two theoretical calculations.

E. Intensity Plots in the Radial Direction

Most attention, so far in this study, has been concentrated on the intensity plots in the longitudinal direction. There is experimental data available on the intensity of the 3914 Å radiation as a function of ρ (the axis perpendicular to z). Experimentally, G, CC, and BH all present data of this type.

Figure 5.3 An intensity plot for electrons of energy 2 KeV is presented as a function of the longitudinal direction. The x's represent relative experimental values from Barrett and Hays (1976) and the histograms present the data from model 3 (heavy line) and the screened Rutherford (light line). The straight solid and the straight dashed lines represent extrapolations to find the range for the model 3 and the screened Rutherford elastic differential cross sections, respectively.

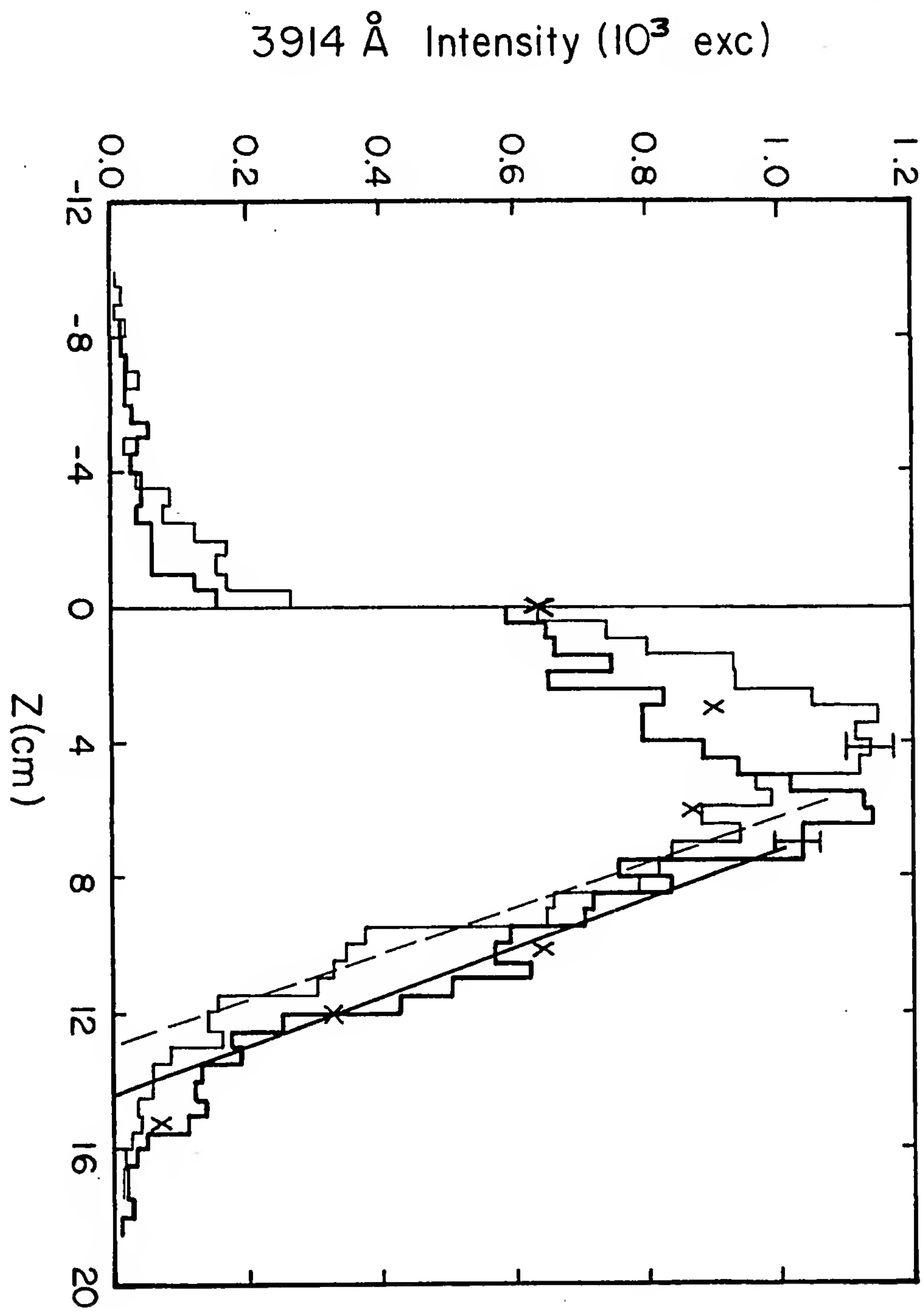
3914 Å Intensity (10^3 exc)
0.0
0.2
0.4
0.6
0.8
1.0
1.2
-12
-8
-4
0
4
8
12
16
20
Z(cm)

Figure 5.4 An intensity plot for electrons of energy 0.3 KeV is presented as a function of the longitudinal direction. The x's represent relative experimental values from Barrett and Hays (1976) and the histogram presents the data from model 3 (heavy line) and the screened Rutherford (light line). The straight lines extrapolated to the z-axis are all measures of the range. The solid line indicates the model 3 range; the dashed line indicates the screened Rutherford range; and the dash-dot line indicates the Barrett and Hays (1976) range.

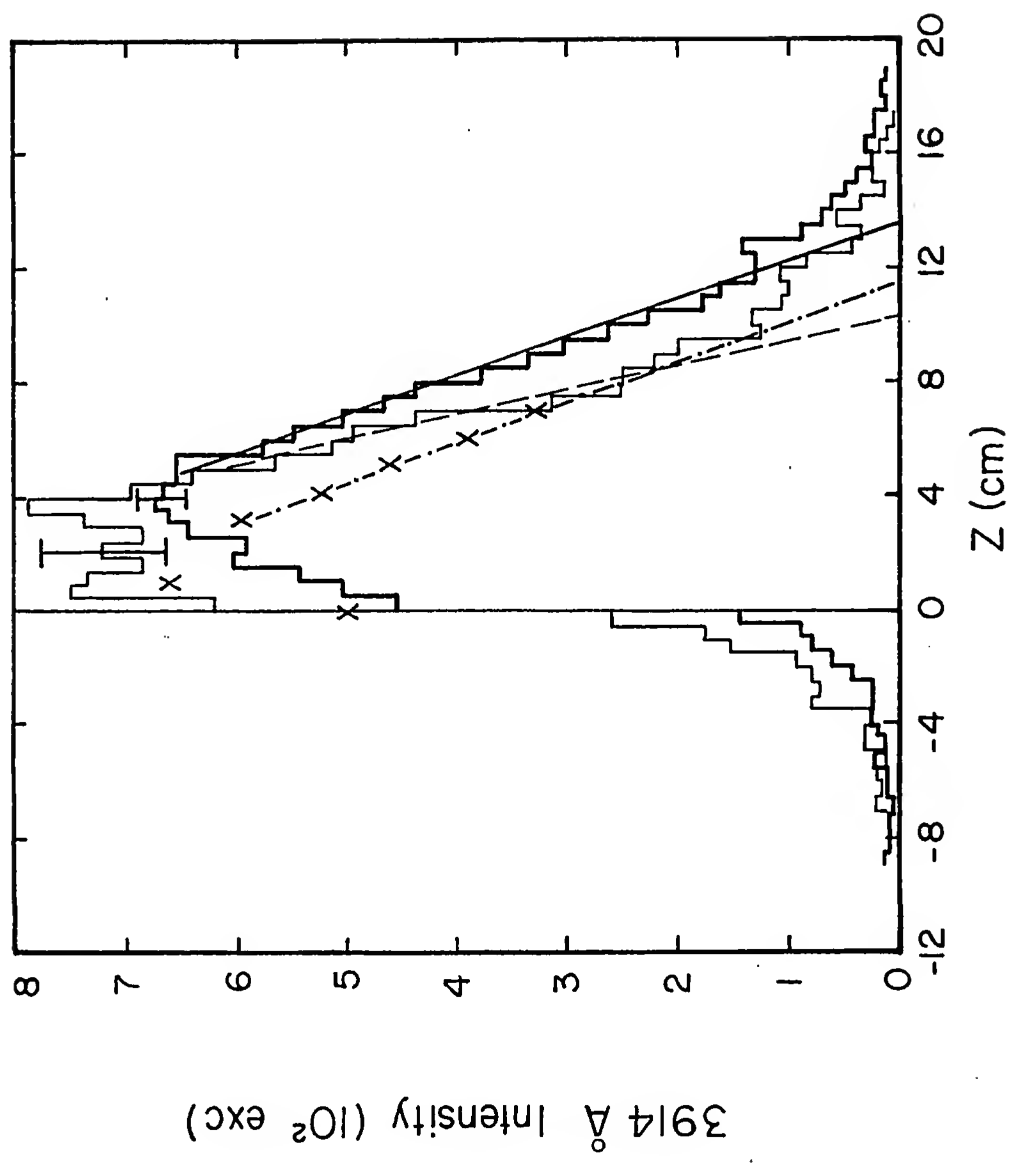
3914 Å Intensity (10² exc)
Z (cm)

This study uses the experimental data of BH as a comparison with the results of this study. The next three graphs, Figures 5.5, 5.6, and 5.7, portray sample results for incident electrons with energies 5.0, 1.0, and 0.3 KeV, respectively. The z and ρ values given in these three figures are in units of fractions of the total range.

Fairly good agreement between the MC calculation (using model 3 cross sections) and the experimental work of BH and Barrett (1975) is observed at all three incident energies. The largest differences between the two sets of data are noted at 0.3 and 1.0 KeV.

For the 1.0 KeV case, the MC calculation tends to predict more intensity at the lower values of ρ for z values of 0.3 and 0.4. A similar result is apparent for the z values of 0.36, 0.48, and 0.60 for an energy of 0.3 KeV. At a z value of 0.12, however, the experimental data tend to predict more intensity at all values of ρ.

Two conclusions can be drawn from these comparisons, if it is assumed that the experimental data of BH and Barrett (1975) are correct. First, the cross section for excitation to the $N_2^+ \; B \; ^2\Sigma_u^+$ may be underestimated in the energy regime between 0.3 and 1.0 KeV. Raising this cross section in this energy regime could bring about an increase in the intensity observed early in the electron's degradation process with a subsequent decrease in intensity later in the electron's degradation process. Second, more scattering from the elastic collisions would help to reduce the total intensity at low ρ values and raise it at the higher ρ values. The screened Rutherford differential cross section has more scattering than model 3. Use of this set of cross sections in the MC calculation did result in a little better agreement at 1.0 KeV, but only about the same type of agreement at 0.3 KeV.

Figure 5.5 Intensity plots for electrons with incident energy 5.0 KeV are presented at two z values as functions of ρ. The solid line histogram indicates the results using model 3. The x's denote the experimental data of BH and the o's denote the theoretical work of BSM.

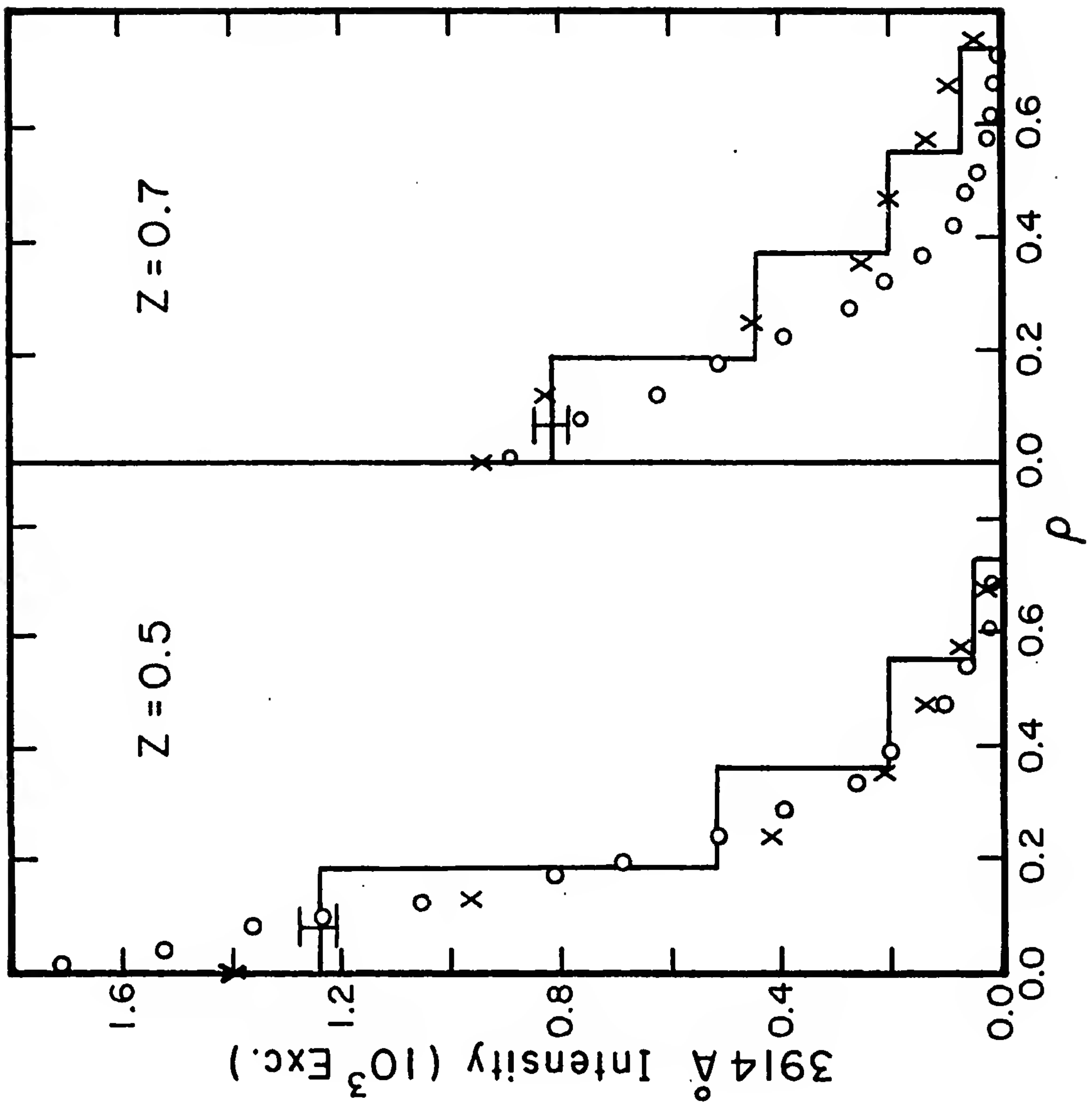
Z = 0.5
Z = 0.7
3914 Å Intensity (10³ Exc.)
ρ
0.0
0.4
0.8
1.2
1.6
0.0
0.2
0.4
0.6

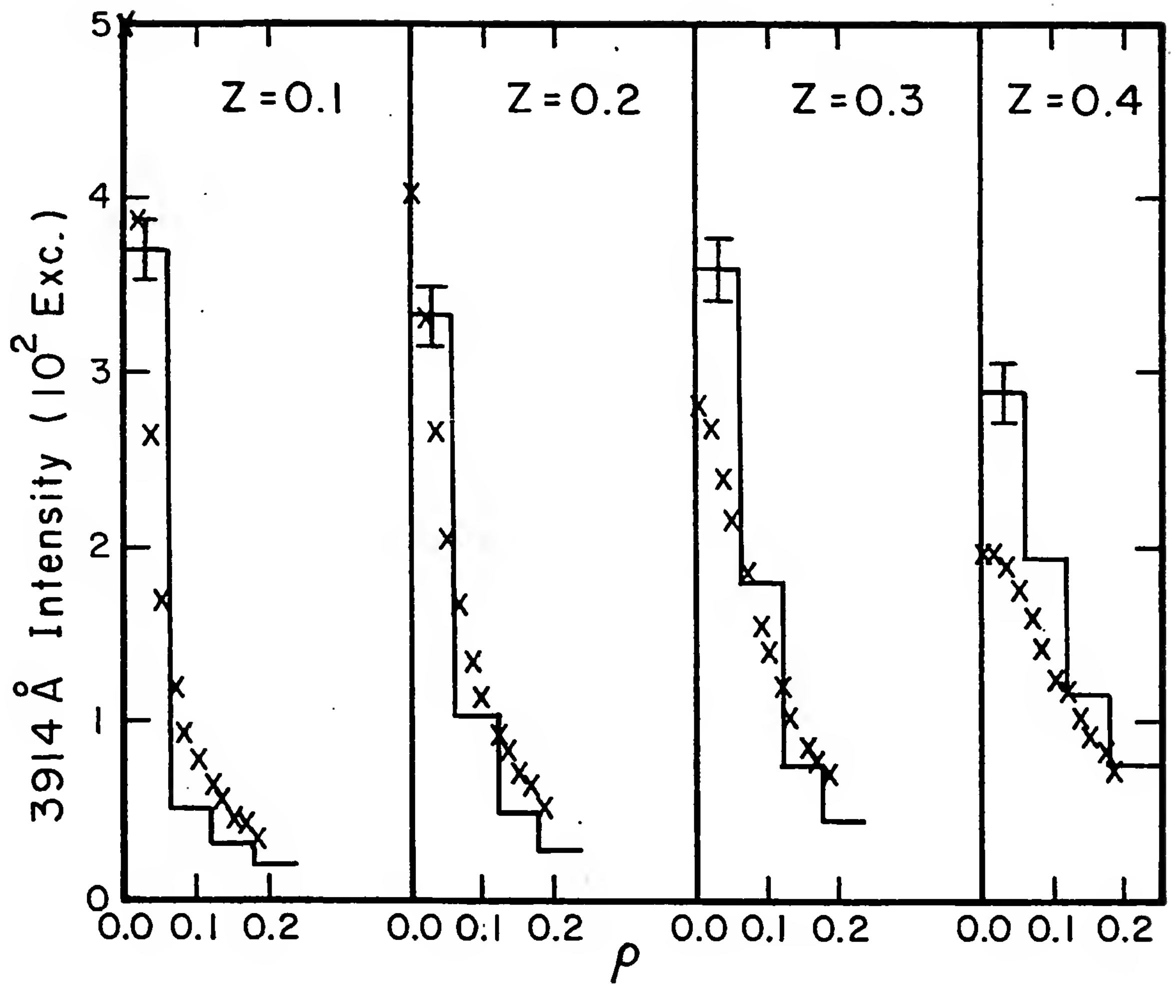

Figure 5.6 Intensity plots for electrons with incident energy 1.0 KeV are presented at four z values as functions of ρ. The solid line histogram indicates the results using model 3. The x's denote the experimental data of Barrett (1975).

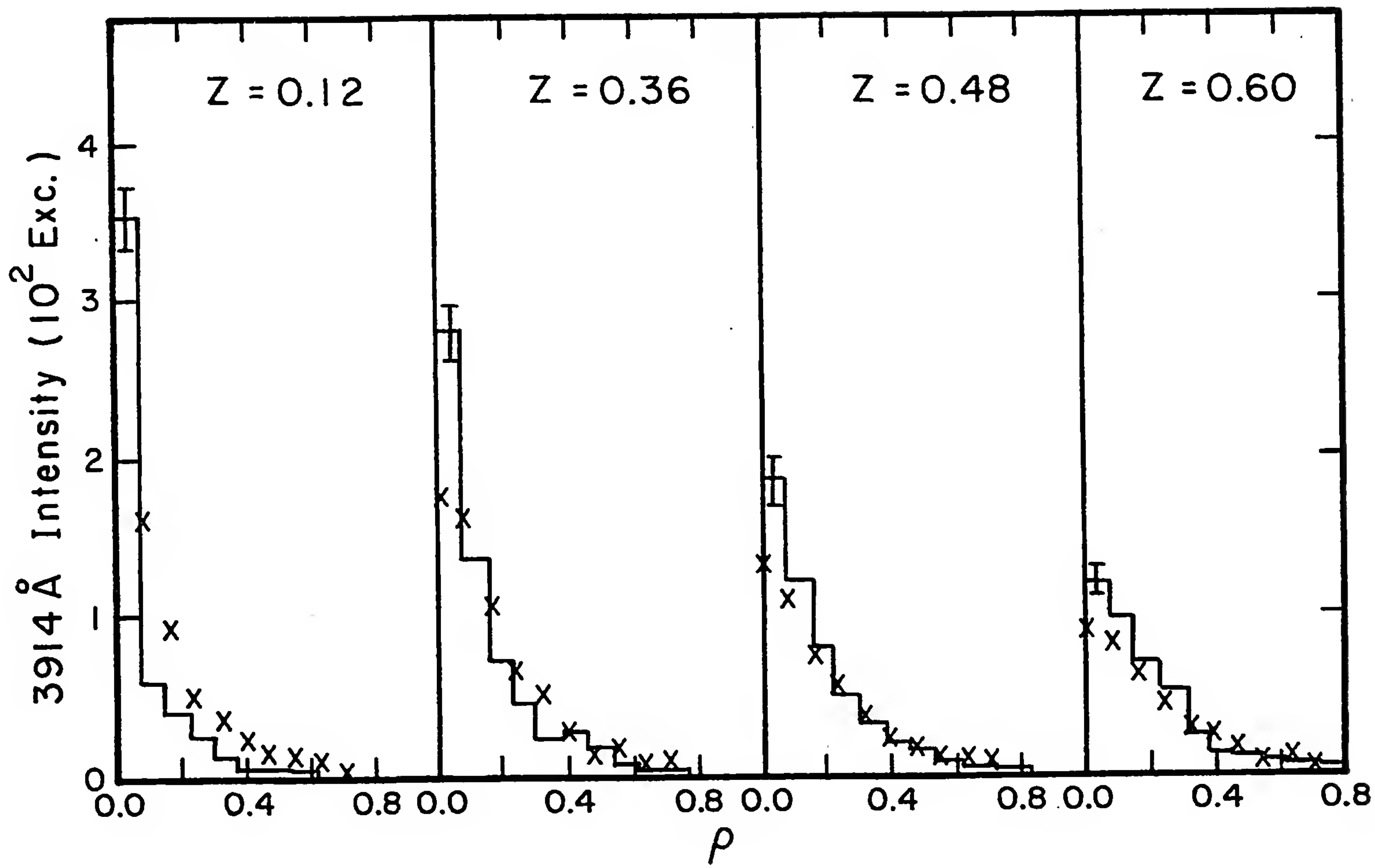

Figure 5.7 Intensity plots for electrons with incident energy 0.3 KeV are presented at four z values as functions of ρ. The solid line histogram indicates the results using model 3. The x's denote the experimental data of BH.

At 5.0 KeV a comparison is made between the theoretical calculations from this work and those of BSM. The results from this work appear to agree much better with the BH data than does the BSM work. In BSM, they follow only the primary and secondaries down to 200 eV. Since this work follows the primary, secondaries, and tertiaries down to 2 eV, it seems straightforward that the agreement should be better in this work.

CHAPTER VI

SENSITIVITY STUDY OF THE SPATIAL ELECTRON ENERGY DEGRADATION

In section V.D the ranges from two separate models of the elastic differential cross section have been compared. A sensitivity study of the influence of other differential cross sections on the electron energy deposition is the subject of this chapter. The effects of the ionization differential cross sections on the intensity distribution are considered in section VI.A. Section VI.B then discusses the influence of the inelastic differential cross sections on the intensity distribution.

In sections VI.C and VI.D, several different elastic phase functions are compared. (The elastic collisions cause more scattering than the inelastic collisions at any electron energy.) Section VI.C includes a calculation with no energy loss, while section VI.D discusses the influence of several variations of the model 1 phase function on the electron energy deposition.

As illustrated in sections VI.A through VI.D, the scattering phase functions are quite important in determining the electron energy deposition intensity or collision profiles. The total elastic cross sections are also of some significance in determining the intensity profiles and will be discussed in section VI.E.

A. Effects of Ionization Differential Cross Sections on the Intensity Distributions

The primary and secondary differential ionization forms represented in Eqs. (3.18) and (3.19) are convenient for calculating the scatter of the electrons during an ionization event. Here, the influence of these forms on the intensity plots will be considered.

Other MC calculations have computed the scattering of the electrons during an ionization event. Brinkmann and Trajmar (1970) calculated the primary scattering angle from experimental energy loss differential cross section data. They then employed an empirical simplification of the coincidence data obtained by Ehrhardt, Schulz, Tekaat, and Willmann (1969), in which half of the secondary electrons were presumed to scatter at four times the primary scattering angle and the other half at π radians plus four times the primary scattering angle.

In another MC approach, Berger, Seltzer, and Maeda (1970, 1974) used the Moller cross section for the scattering of secondary electrons as a result of an ionization collision. The angular deflection θ is given such that

$$\sin^2\theta = \frac{4\varepsilon}{\tau(1 - 2\varepsilon) + \tau + 4} \tag{6.1}$$

where ε is the energy transfer in units of E, and τ is the kinetic energy in units of the rest mass.

At the maximum incident energy of 5000 eV used in this work, $\tau \gtrsim 0.01$. Using this value of τ for primary scattering, in which $\varepsilon < 0.5$, all scatterings are between 0° and 45°. The secondary scattering turns out to be between 45° and 90°, since $0.5 \leq \varepsilon < 1.0$. This means that

most deflections of the primary electron are at small angles while most deflections of the secondary electrons are clustered near 90°.

Strickland, Book, Coffey, and Fedder (1976) used a variety of different secondary doubly differential ionization cross sections. Their solutions to the equation of transfer show little dependence on the functional form being used. Thus it is valid to ask if different primary or secondary ionization differential cross sections will have any influence on the intensity plots resulting from a MC calculation.

The primary electron is scattered the least. Therefore, for comparison, it is assumed that no scattering of the primary electron was incurred during the ionization event. The results of this comparison, using the 3914 Å intensity plots for incident electron energies of 2000 and 300 eV, were not too surprising: There was virtually no observed difference in the two intensity plots. This simply means that the scattering of the primary during an ionization event is minuscule compared to the much larger scatterings inherent in the elastic collisions. For most of the calculations following this comparison, it was assumed that no scattering of the primary electron occurred in an ionization event. This resulted in a factor of eight savings in the computer time and cost.

In Figure 6.1, the effect of the primaries and secondaries on the total 3914 Å radiation is clearly seen at the incident energy of 1 KeV. The major contribution of the secondaries is early in the history of the incident electron, when it has sufficient energy to create high energy secondaries capable of producing the 3914 Å emission. Also, the contribution by the primaries is a more sharply peaked curve than that of the secondaries. The backscatter contribution from the secondaries is

Figure 6.1 An intensity plot for electrons of energy 1 KeV is presented as a function of z. The solid line represents the primary or incident electron's contribution to the 3914 Å emission while the dashed line illustrates the contribution from the secondary electrons.

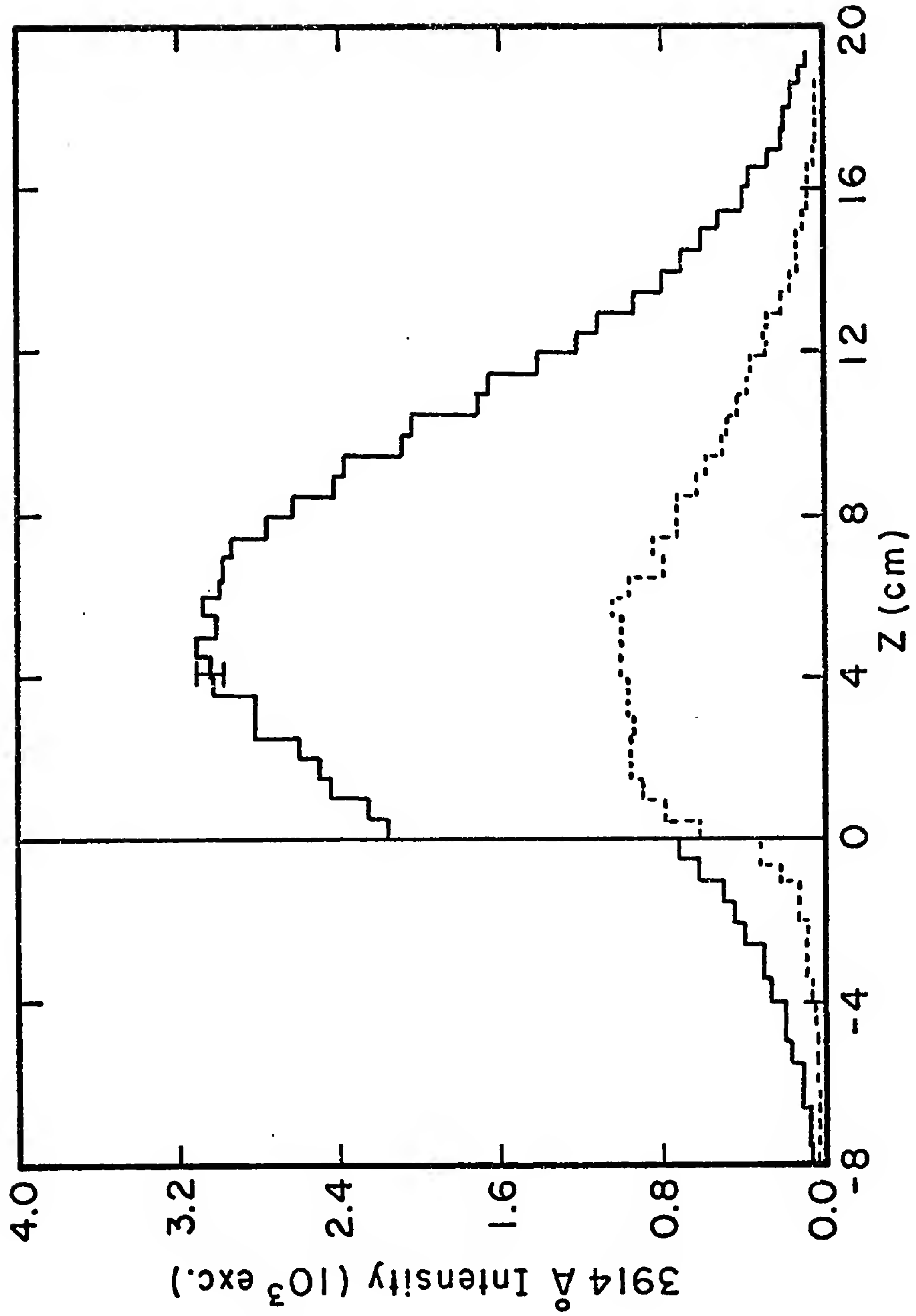
3914 Å Intensity (10^3 exc.)
0.0
0.8
1.6
2.4
3.2
4.0
Z (cm)
-8
-4
0
4
8
12
16
20

seen to be fairly high. Secondaries are at lower energies; therefore, more of them are backscattered.

In considering the secondaries, it is of interest to discover any difference in the intensity plots that may be due to the use of a different secondary scattering distribution. Consequently, a comparison was made between Eq. (3.18) and an isotropic secondary scattering function. The difference in the two resulting intensity plots was so small that they were the same within their standard deviation error bars. This result, although surprising at first glance, did not seem as surprising under careful inspection.

Consideration of Table 5.1 gives the answer. A 5 KeV electron has a range of 91.5×10^{-6} gm/cm^2 while a 0.3 KeV electron has a range of 1.25×10^{-6} gm/cm^2. Most of the secondaries contributing to the 3914 Å emission that are produced by an incident electron of energy 5 KeV have energies of only a few hundred eV or less. These electrons do not travel far, relative to the total range of the incident particle. Therefore their characteristic 3914 Å intensity profiles do not alter the total 3914 Å profile noticeably.

A 0.3 KeV electron traveling in N_2 at a density of 2×10^{15} molecules/cm^3 (which corresponds to a height in the atmosphere of roughly 70 km) has range of about 12 cm. At 150 km (where the density is about 5×10^{10} molecules/cm^3) this same electron will have a range of about 5 km. The secondary doubly differential ionization cross sections may thus have an influence on the energy deposition in applications to the upper atmosphere. As mentioned earlier, however, Strickland et al. (1976) do not observe such an effect. Inclusion of Eq. (3.19) only

increases the MC computation by 2-3%. Therefore it was left in all the calculations.

B. Influence of Inelastic Differential Cross Sections on the Intensity Distributions

Model 3 includes scattering from inelastic excitation collisions. Because of the very highly forward peaked nature of most optically allowed excitations, inelastic excitation scattering is only used below 100 eV and then only in an ad hoc manner. Below 100 eV, scattering due to inelastic excitation collisions is assumed to be the same as that due to elastic collisions (see section III.B).

The main purpose of this section is to determine whether this ad hoc excitation collision scattering makes a significant difference in the spatial energy deposition. When a MC calculation is run assuming no excitation scattering at any energy, no difference is detectable in the 3914 Å intensity plots at energies above 300 eV.

For electrons of energies 300 and 100 eV, a difference is detected. The range (in units of 10^{-6} gm/cm^2) changes from 1.25 to 1.34 for an electron energy of 300 eV and from 0.365 to 0.391 for an electron energy of 100 eV. This means that the extra scattering due to the inelastic excitation events reduces the range by about 7% at these two energies.

C. Comparison of Different Elastic Phase Functions on the Electron-N_2 Collision Profile

The large influence of the phase functions on the spatial energy deposition has been pointed out in section V.D and will be further discussed in section VI.D. These phase functions all have some type of

energy dependence. Another way to approach a sensitivity study of the elastic phase functions is the following: 1) Fix the number of collisions allowed in the MC calculations at some set number, say 25000; 2) allow only elastic collisions; and 3) assume that there can be no energy loss during a collision (the electron energy remains fixed at 300 eV).

Employing all the above assumptions, the scattering problem is very similar to the photon scattering process. The aspects of this section may, therefore, be of interest both to researchers in photon scattering as well as electron scattering.

One of the simplest ways to represent elastic scattering phase functions is with model 1 [Eq. (3.12): $P_{M3}(\theta,E) \propto \{1 - \cos\theta + a(E)\}^{-2}$]. This scattering form, as noted earlier, is very similar to the screened Rutherford cross section. Figure 6.2 illustrates five trial phase functions, designated as A1 through A5, whose properties are indicated in Table 6.1.

These five phase function trials were then run in a MC computation using the three restrictions given above. The collision plots for three of these trials are given in Figure 6.3. The input number density in all cases was 4×10^{15} molecules/cm^3 and electrons entered the N_2 gas until the total number of collisions was 25000.

From Figure 6.3 several observations can be made. Generally, the number of backscatter collisions decreased as the forward peaking of the differential cross section increased. The number of collisions occurring close to the origin of the perpendicularly incident electrons also decreased, while the number of collisions at distances forward from the origin increased.

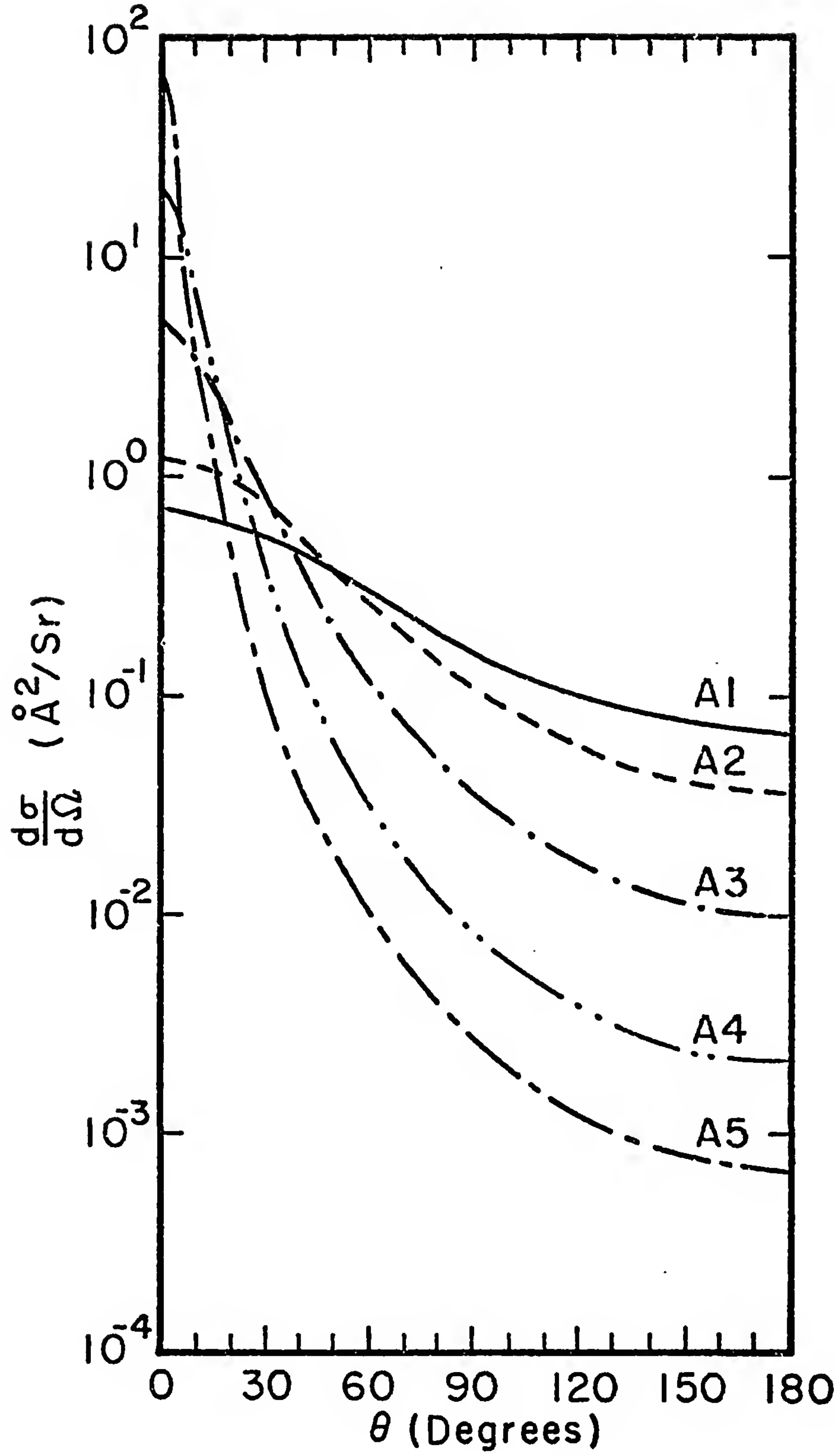

Figure 6.2 Differential cross section graph for model 1 trials: A1, A2, A3, A4, and A5.

Table 6.1 Model 1 parameter values (column labeled "a") and phase function properties for various trials. The phase function falloff (column labeled PFFO) is indicated in the number of orders of magnitude difference between the differential cross section at 0° and its value at 180°. The average angle of scattering (column labeled AAS) is found using Eq. (6.3).

Trial	a	PFFO	AAS
A1	0.9	1.0	64.5°
A2	0.4	1.5	52.2°
A3	0.095	2.5	31.6°
A4	0.02	4.0	16.3°
A5	0.0065	5.0	9.7°

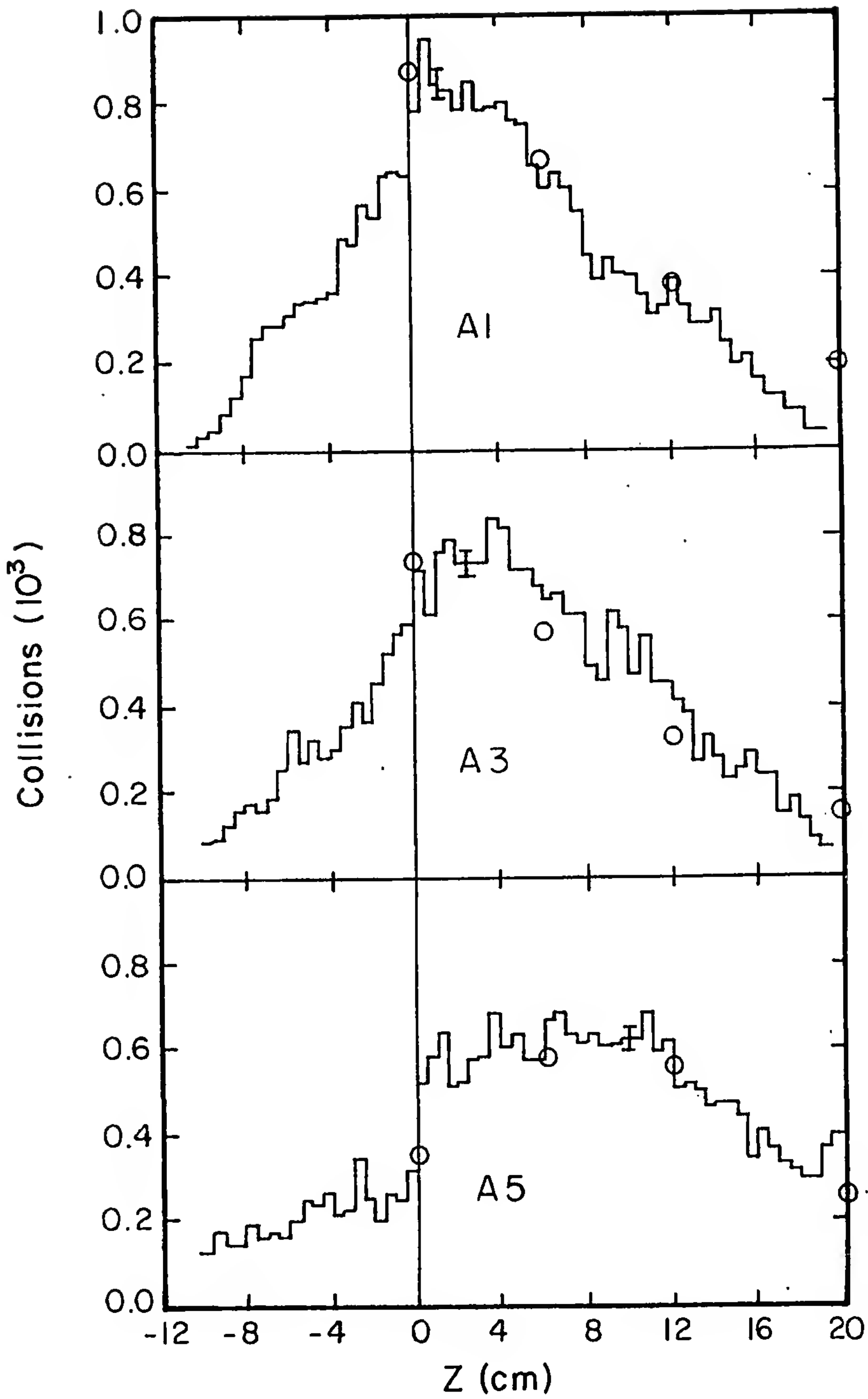

Figure 6.3 Collision plots for MC trials A1, A3, and A5. The histograms represent the MC data while the o's represent the fit using Eq. (6.2).

The shape of the collision profile at positive longitudinal distances appears to have a distribution which is dependent on the "a" parameter. This functional form for the distribution of collisions D(z) can be represented simply as

$$D(z) = \frac{1}{\alpha(z - z_0)^2 + \beta} \tag{6.2}$$

where

$$\alpha = -0.148 \ln(\frac{a}{766})$$

$$\beta = -0.09 \ln(\frac{a}{3.2 \times 10^5})$$

and

$$z_0 = 0.056/a$$

The o's in Figure 6.3 represent a visual fit to these data. Equation (6.2) does a reasonable job of indicating the gross features of the collision profile. The features illustrated with this form are the height of the peak, the width of the distribution, and the location of the peak.

The location of the peak is observed to be inversely proportional to the value of the screening parameter a. The values of α and β are directly proportional to the natural logarithm of the screening parameter a, thereby causing the peak of the collision profile to decrease in value as "a" decreases.

Model 2 [Eq. (3.13): $P_{M2}(\theta,E) \propto (-f/\{1 - \cos\theta + a\}^2) - ((1 - f)/\{1 + \cos\theta + c\}^2)$] can also be used in a MC computation of a similar nature. Figure 6.4 indicates the differential cross sections (trials B1, B2, and B3) used in this comparison and Table 6.2 lists the properties of these trials.

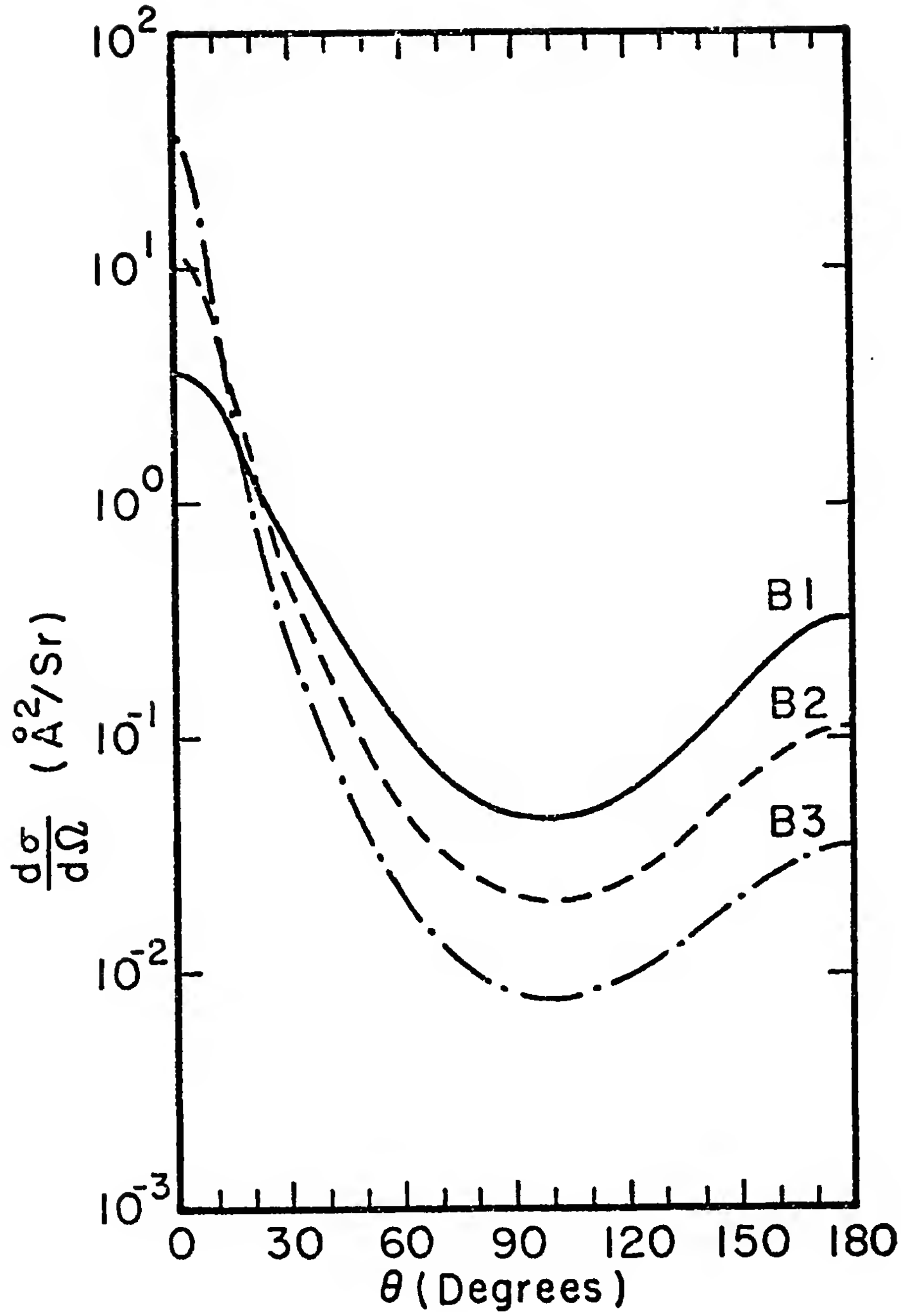

Figure 6.4 Differential cross section graph for model 2 (which contains a forward and a backward scattering contribution) trials: B1, B2, and B3.

Table 6.2 Model 2 parameter values (columns "a," "c," and "f") and phase function properties for various trials. The PFFO and AAS columns are described in Table 6.1.

Trial	a	c	f	PFFO	AAS
B1	0.1	0.3	0.8	1.0	52.3°
B2	0.033	0.38	0.92	2.0	29.0°
B3	0.012	0.46	0.97	3.0	16.3°

The results of these MC calculations are illustrated in Figure 6.5. There is no sharp discontinuity at the origin. The peak of the distribution moves along the z-axis as the forward scattering increases. The reason for this continuity in the collision distribution arises from the backscatter peak.

The average scattering angle is given by

$$\theta_{ave} = \int_0^{2\pi}\int_0^{\pi} \theta\ P(\theta)\ \sin\theta d\theta d\phi \tag{6.3}$$

where $P(\theta)$ is the phase function. The average scattering angle is nearly the same in trials A2 and B1; A3 and B2; and A4 and B3 (compare Tables 6.1 and 6.2). This means that the shape of the backward scattering part of the phase function is also very important in determining the spatial energy deposition of an electron.

D. Influence of Different Elastic Phase Functions on the Intensity Profiles

A sensitivity study involving several different, but constant, phase functions was the subject of section VI.C. The elastic scattering phase function of electrons changes with energy. Generalizing the influence of the energy dependent phase function is the subject of this section.

Section V.D includes a comparison of the screened Rutherford and the model 3 phase functions and their influence on the range values. It was learned that in the electron energy regime of interest, 2 eV to 5000 eV, the screened Rutherford causes more scattering than the model 3 phase function. The screened Rutherford range values, therefore, tend to be lower than the model 3 range values (see Table 5.1).

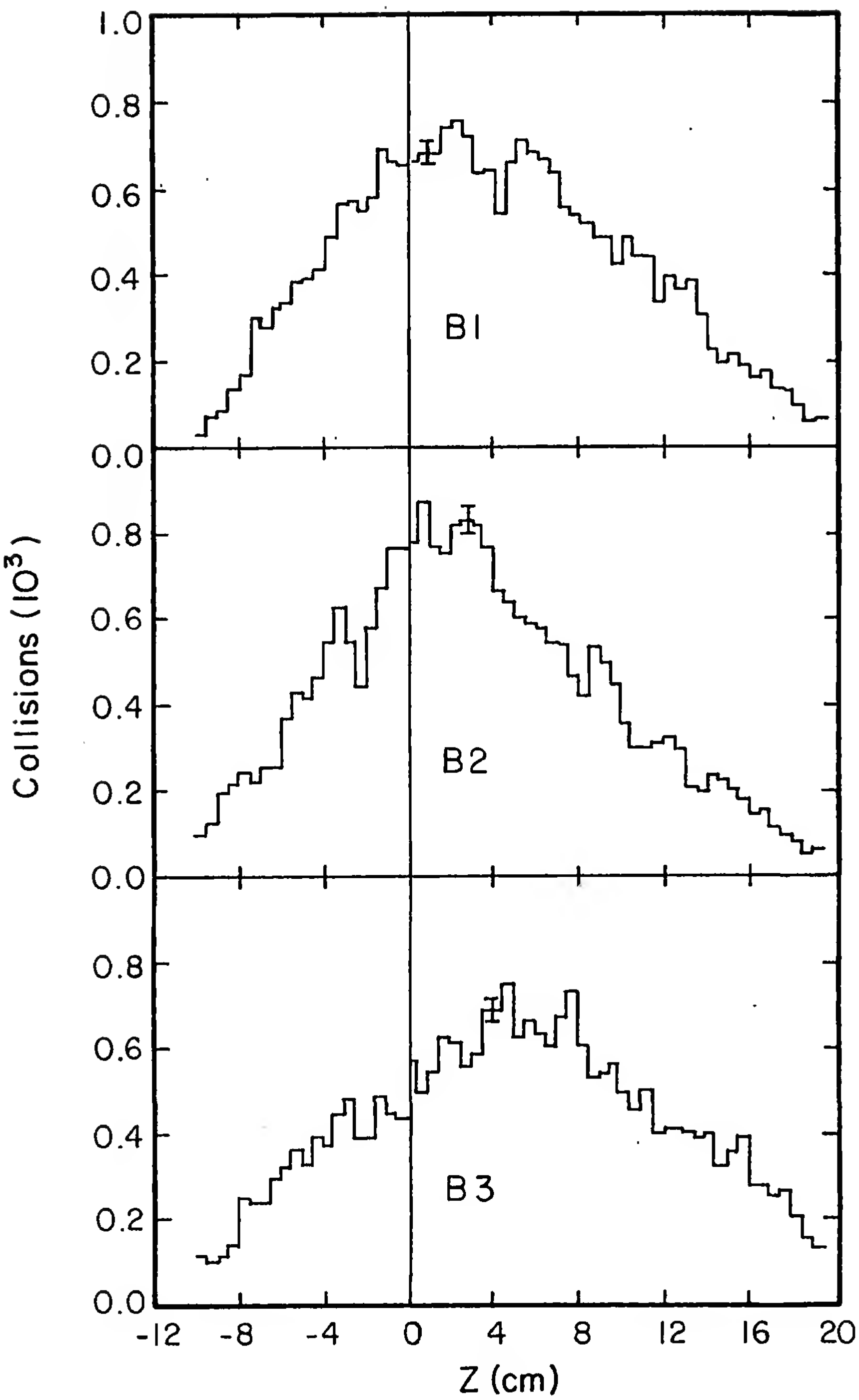

Figure 6.5 Collision plots for MC trials B1, B2, and B3. The histograms represent the MC data.

The screened Rutherford and model 3 phase functions have somewhat different forms. Thus it is difficult to compare them in ways other than the way they were compared in section V.D.

A more convenient phase function form to use for comparison is that of model 1. Model 1 depends on the one screening parameter, a, which can be written as a function of the energy such that $a(E) = a_1(E/1\ \mathrm{eV})^{a_2}$. When $a_1 = 32$ and $a_2 = -1$, this form simulates the screened Rutherford phase function and a(E) in this case is represented in Figure 6.6 by the solid line (trial C1).

Four other representations of the parameter a(E) are given in Figure 6.6. These five trials represent attempts to characterize the influence of this screening parameter on the energy deposition process. All five trials (C1, C2, C3, C4, and C5) used 1000 perpendicularly incident electrons with energies of 1 KeV and the trials and their parameters are given in Table. 6.3.

Trials C2 and C3 were attempts to detect the influence of the starting screening parameter a(1000 eV) on the energy deposition. For trial C2 a(1000 eV) [from Table 6.3] is a factor of ten lower than a(1000 eV) for trial C1. For trial C3 a(1000 eV) [from Table 6.3] is a factor of ten higher than the a(1000 eV) for trial C1. However, for trials C1, C2, and C3 the a(30 eV) values are the same.

The range and fraction of incident energy backscattered obtained from trials C1, C2, and C3 (and also trials C4 and C5) are given in Table 6.4. The range from trial C1 is 38% lower than the range from trial C2 and 38% higher than the range from trial C3. The symmetry of these results is remarkable and probably fortuitous.

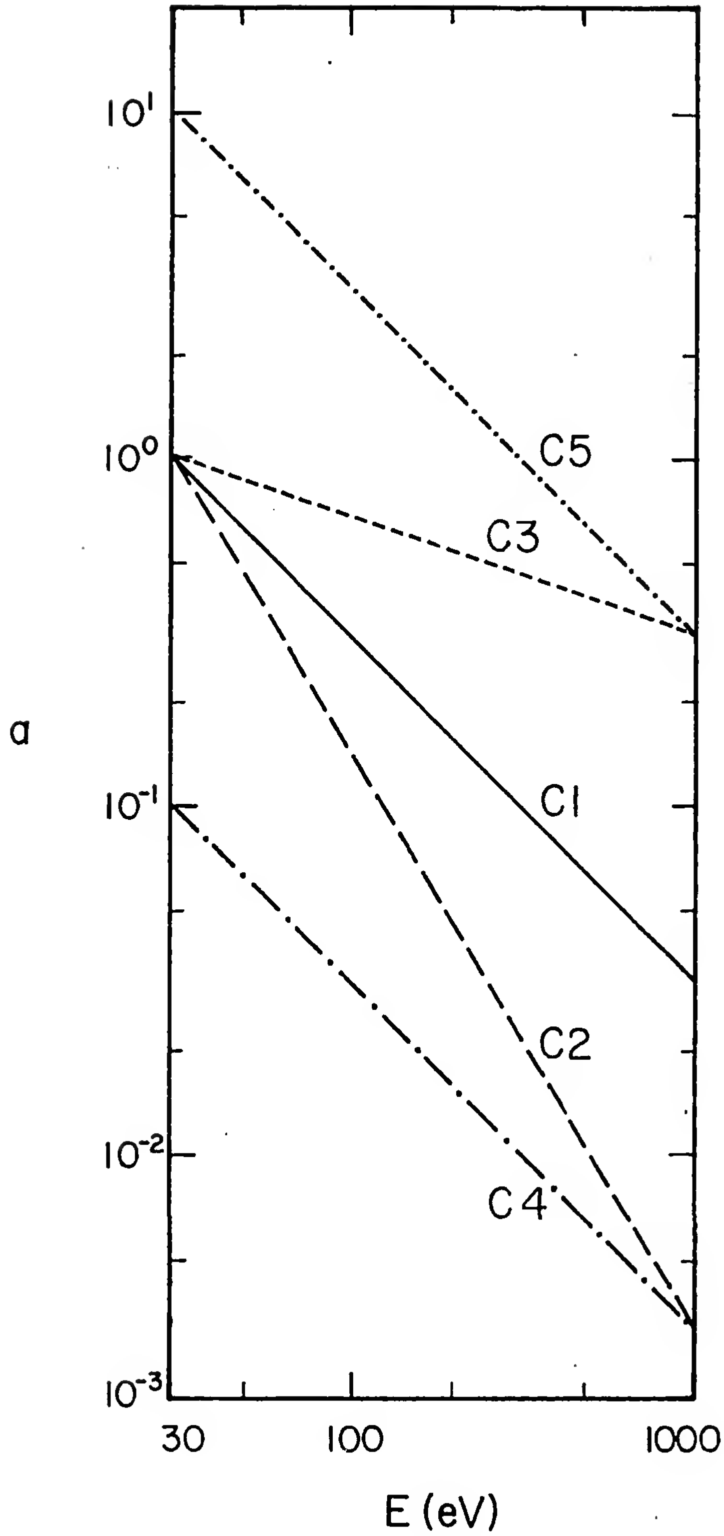

Figure 6.6 Five trials (C1, C2, C3, C4, and C5) of a(E) for use in model 1.

Table 6.3 Parameters a_1, a_2, a(1000 eV), and a(30 eV) for trials C1, C2, C3, C4, and C5.

Trial	a_1	a_2	a(1000 eV)	a(30 eV)
C1	32	-1.0	0.032	1.07
C2	303	-1.66	0.0032	1.07
C3	3.44	-0.344	0.32	1.07
C4	3.2	-1.0	0.0032	0.107
C5	320	-1.0	0.32	10.7

Table 6.4 Range, R_g (in 10^{-6} gm/cm^2), and fraction of energy backscattered, F_B, are given for trials C1, C2, C3, C4, and C5.

Trial	R_g	F_B
C1	5.57	0.078
C2	7.70	0.012
C3	3.43	0.236
C4	8.16	0.009
C5	3.32	0.211

Using only these three trials it is found that essentially

$$R_g(F_c) \approx R_{go}(1.0 + \frac{1}{\ln(F_c)}) \tag{6.4}$$

where $R_g(F_c)$ is the range of the electrons using the screening parameter $a(1000\ eV) = F_c\ a_0(1000\ eV)$. The F_c is some factor (in the case of trial C2, $F_c = 0.1$) and R_{go} is the range of the electron using the screening parameter $a_0(1000\ eV)$. Again (see Eqs. (6.2) and (6.4)) there appears to be a logarithmic type dependence on the screening parameter. In section VII.C shapes of the collision profiles were found to be proportional to ln(a). Here, the range appears to be approximately proportional to ln(a) for the three cases studied.

Next, use two more new trials, C4 and C5. The energy dependence of "a" in C1, C4, and C5 is the same and is illustrated in Figure 6.6. As seen from Table 6.4, the screening parameter for the incident energy has the most influence on the spatial energy deposition. The energy dependence of "a" influences the energy deposition such that if the parameter, a, is lower throughout the entire energy regime for a given trial than the "a" used in another trial (for example, C4 compared with C2), then the electrons will penetrate further during the course of that trial (the C4 range is greater than the C2 range).

The radial distribution of the 3914 Å intensity profile is another quantity of interest. Figure 6.7 illustrates this radial distribution for trials C1, C2, and C3 at three set distances into the medium. The sharpest forward peaked phase function (hereafter the last four words can be called FPPF) trial, C2, has an intensity distribution clustered close to the z-axis throughout the x regime. The least FPPF trial, C3, has

Figure 6.7 At three longitudinal distances (given in 10^{-6} gm/cm^2), the intensity distribution is given as a function of ρ for the three trials C1, x; C2, Δ; and C3, o.

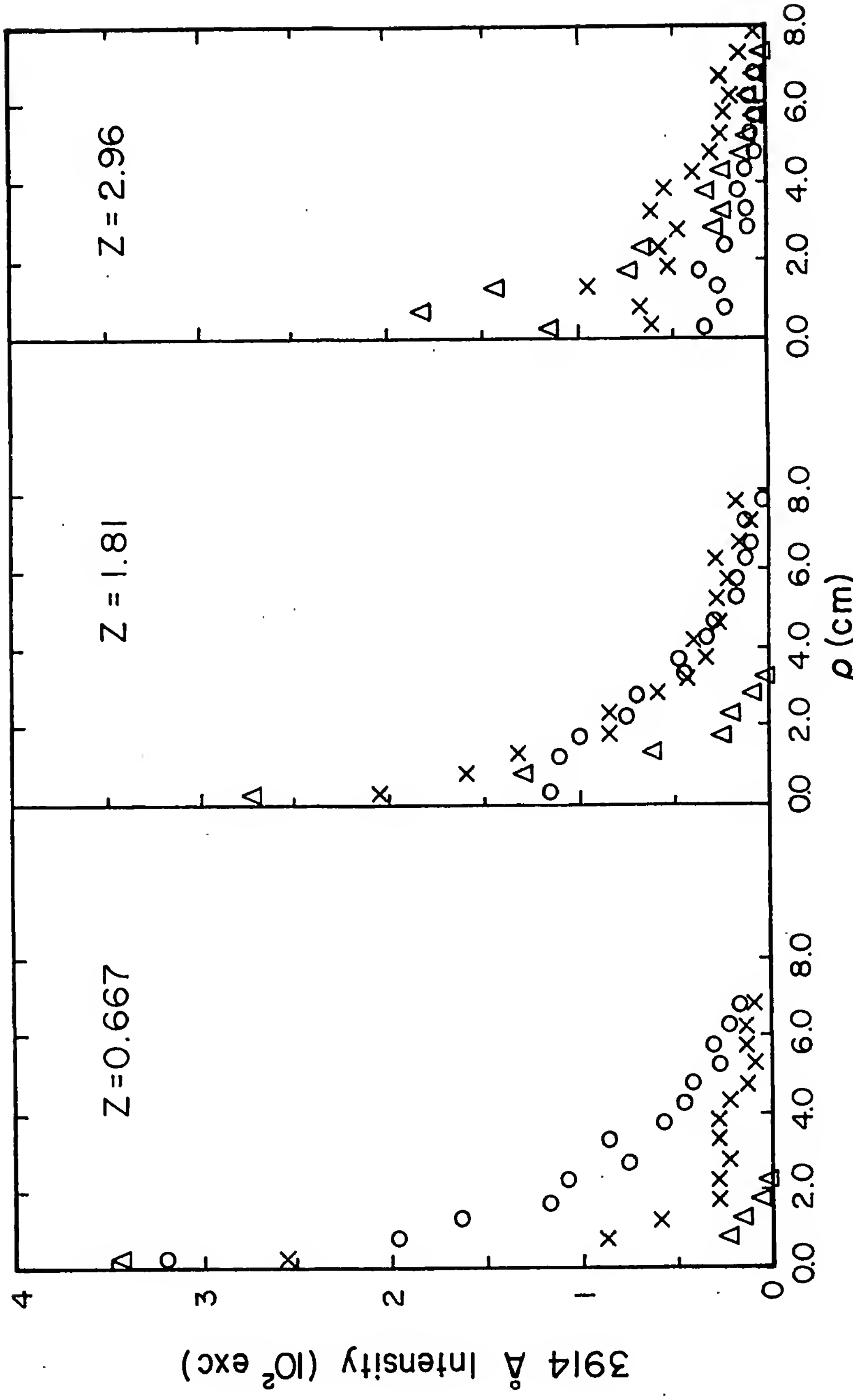
Z=0.667
Z = 1.81
Z = 2.96
ρ (cm)
3914 Å Intensity (10² exc)
0
1
2
3
4
0.0
2.0
4.0
6.0
8.0

its intensity distribution spread out the most from the z-axis throughout the z regime.

In Figure 6.8, a cut is taken through each intensity profile at the distance z = 0.3 (units are fraction of range). This type of distribution continues for all the longitudinal distances throughout the range. The 3914 Å intensity profile of the sharpest FPPF, C2, again hugs the z-axis, whereas the profile of the least FPPF, C3, again shows the greatest spread from the z-axis.

E. Effects of the Total Elastic Cross Section on the Electron Energy Degradation

As illustrated in the previous sections of this chapter, the spatial electron energy degradation is governed mainly by the elastic differential cross section. Consider the effects of the total elastic cross section on the electron energy degradation.

The total elastic cross section given by Eq. (3.9) is used in practically all the MC calculations of this study. This analytic form agrees quite well with experiment.

Berger, Seltzer, and Maeda (1970, 1974) used the integrated Rutherford cross section for their total elastic cross section. This cross section is somewhat different from the experimental data and is plotted in Figure 3.2.

If a MC calculation is made with this lower elastic cross section, it is expected that the 1 KeV electrons will penetrate further into the medium. Figure 6.9 illustrates the results of this calculation where the screened Rutherford phase function was used.

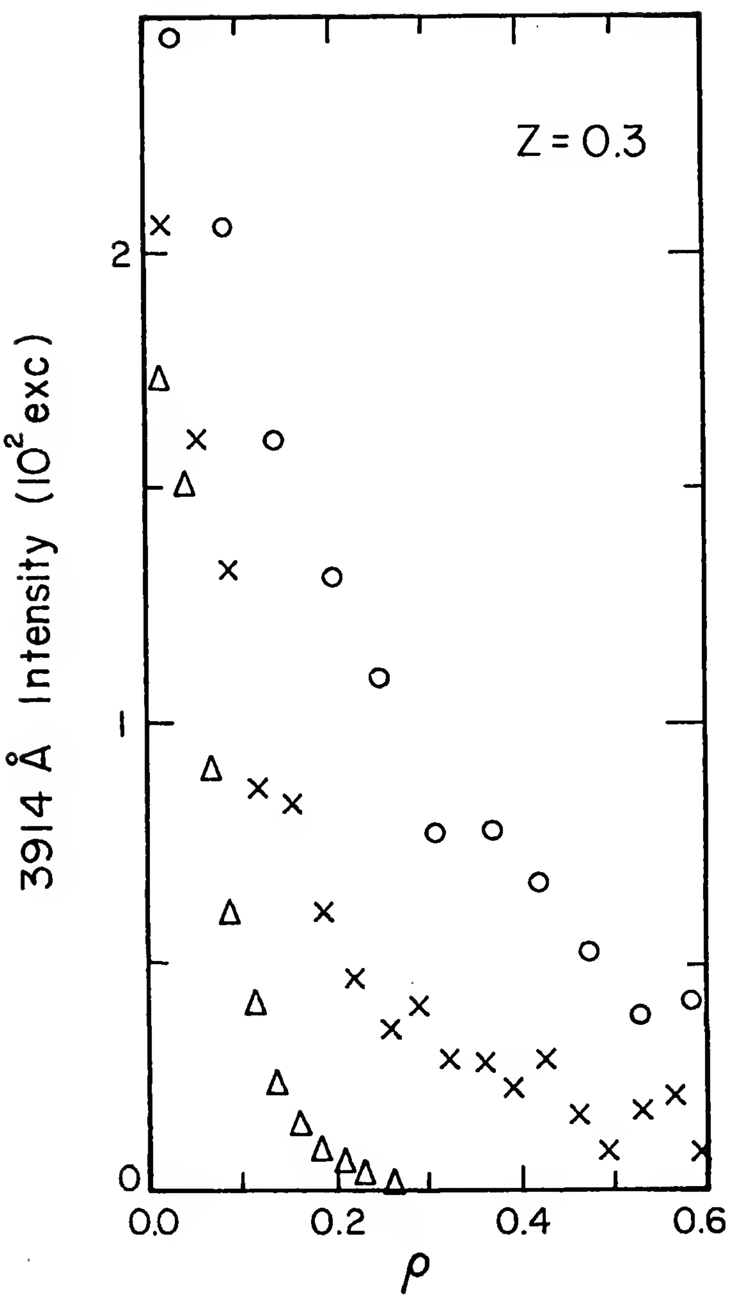

Figure 6.8 At the cut z = 0.3, the 3914 Å intensity distribution is given as a function of ρ for the three trials C1, x; C2, Δ; and C2, o.

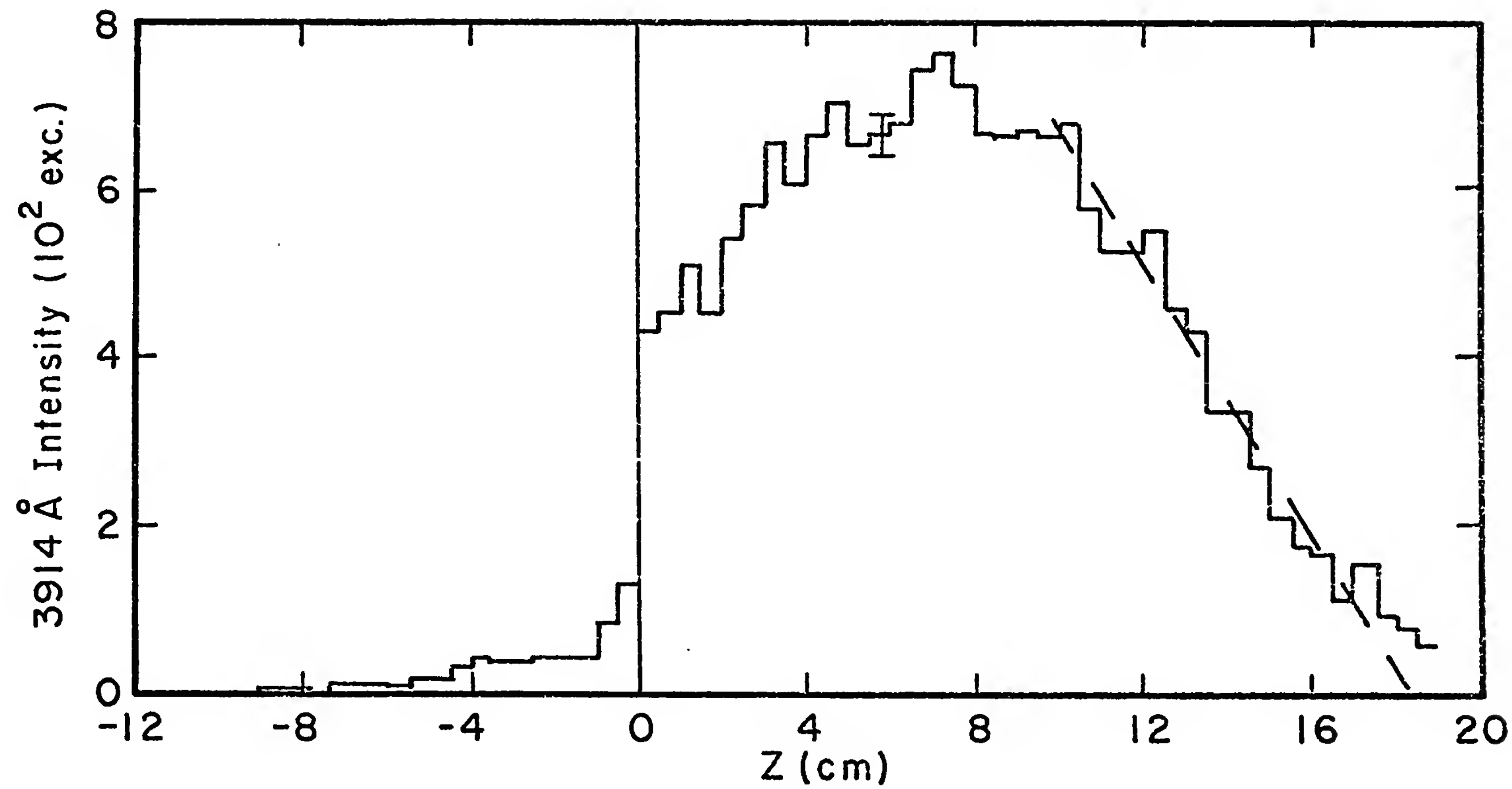

Figure 6.9 An intensity plot for electrons of energy 1 KeV is presented as a function of z. The differential and total screened Rutherford elastic cross section are used in this calculation. The range, found from the dashed line is 18.3 cm or 6.98 x 10^{-6} gm/cm^2.

The range is observed to be 6.98 x 10^{-6} gm/cm^2 as compared with 5.57 x 10^{-6} gm/cm^2 using the cross sections given by Eq. (3.9) (hereafter called MSR). The shape of the intensity profile of the 3914 Å emission is also different. The maximum of the profile is less peaked than that given by MSR.

Banks, Chappell, and Nagy (1974) used cross section values which are shown in Figure 3.2. These cross section points are somewhat different than the cross sections from MSR in the range from 100 to 500 eV. This indicates that electrons degraded with these cross sections have a range less than that of MSR.

This section completes the sensitivity study. The next chapter discusses the MC calculation, the important yield spectra, and the general energy loss scheme.

CHAPTER VII

MONTE CARLO ENERGY LOSS PLOTS AND YIELD SPECTRA

In this chapter two other very important energy degradation outputs are discussed. The rate of energy loss as the electron impinges into the medium is a very important quantity. This concept, the fraction of energy backscattered, and the correlation between the range and the loss function are discussed in section VII.A.

The most important output from the MC calculation is the spatial yield spectrum. In section VII.B, this yield spectrum is calculated at several energies and at several positions in the gas. Both the three variable spatial yield spectrum $U(E,z,E_0)$ and the four variable spatial yield spectrum $U(E,\rho,z,E_0)$ are considered in this section. Because the yield or number of excitations to any N_2 state is calculated quite easily from the spatial yield spectrum, an attempt is made to represent it analytically.

A. Energy Loss of Electrons in N_2

The rate of energy loss by electrons in a medium is a useful quantity. For higher energy electrons (above 2 KeV), the degradation of these electrons could be accomplished with the use of the loss function, L(E), and the continuous slowing down approximation (discussed in Chapter II).

This is one important reason why the range values of the electrons are under investigation. Assuming a continuous slowing down of the electron, the range $R(E_o)$ for an electron of incident energy E_o may be defined as

$$R(E_o) = \int_{E_o}^{0} \frac{dE}{dE/dx} \tag{7.1}$$

(employing Eq. (2.2)). Since $nL(E) = -\frac{dE}{dx}$ (as noted in Chapter II), then

$$R(E_o) = \frac{1}{n}\int_{0}^{E_o} \frac{dE}{L(E)} \tag{7.2}$$

In the Born-Bethe approximation L(E) is proportional to ln E/E. At the higher energies, ln E/E can approximately be written as $E^{-.75}$ (see Green and Peterson, 1968). Using this approximation in Eq. (7.2), the range is

$$R(E_o) = C\ E_o^{1.75} \tag{7.3}$$

where C is a constant.

Grün (1957) and Cohn and Caledonia (1970) have shown that such an expression is correct for electron energies from 2 to 54 KeV. Barrett and Hays (1976), on the other hand, extended this energy range down to 0.3 KeV and derived a slightly more complicated empirical formula for the electron energies from 0.3 to 5 KeV.

Much of the significance of the range is built on the idea that all the energy of the electrons is lost between z = 0.0 and z = 1.0 where z = the fraction of the range traveled. Such an approximation is quite good above 2 KeV; however, at energies below 1 KeV this is not such a good approximation.

In Figure 7.1 an energy remaining plot is given for three separate calculations with 1 KeV incident electrons. At z = 0.0, which is the point of incidence for the 1 KeV electrons, all calculations assume that no energy has been lost. Thus the amount of "energy left" is simply 1 KeV.

Stolarski (1968) integrated the universal energy loss curve derived from Grün's (1957) data to obtain the mean energy. Barrett and Hays (1976) used their empirical range formula to calculate the mean range and, subsequently, the energy remaining in the incident electron at various distances into the medium. In the MC calculation of this study only the energy lost for positive z values was employed to find the energy remaining.

The Stolarski (1968) values are closest to the MC calculation values. The major differences between Stolarski's results and this MC computation are due to three factors: First, some energy is lost by backscatter electrons to negative z values; second, some energy is lost by electrons which penetrate to z values greater than 1.0 (straggling electrons); and third, the universal energy loss curve may not be as accurate as a MC computation.

Graphing the energy loss data in Figure 7.1 is really not very informative. Figure 7.2 illustrates a more lucid way of representing the energy loss data. In Figure 7.2, the fraction of the primary energy lost is plotted as a function of z for four energies (0.1, 0.3, 1.0, and 5.0 KeV). As the incident electron's energy is reduced, the relative backscatter is increased. The most backscatter (21%) and the most energy lost in straggling (6%) is observed for the 0.1 KeV electrons.

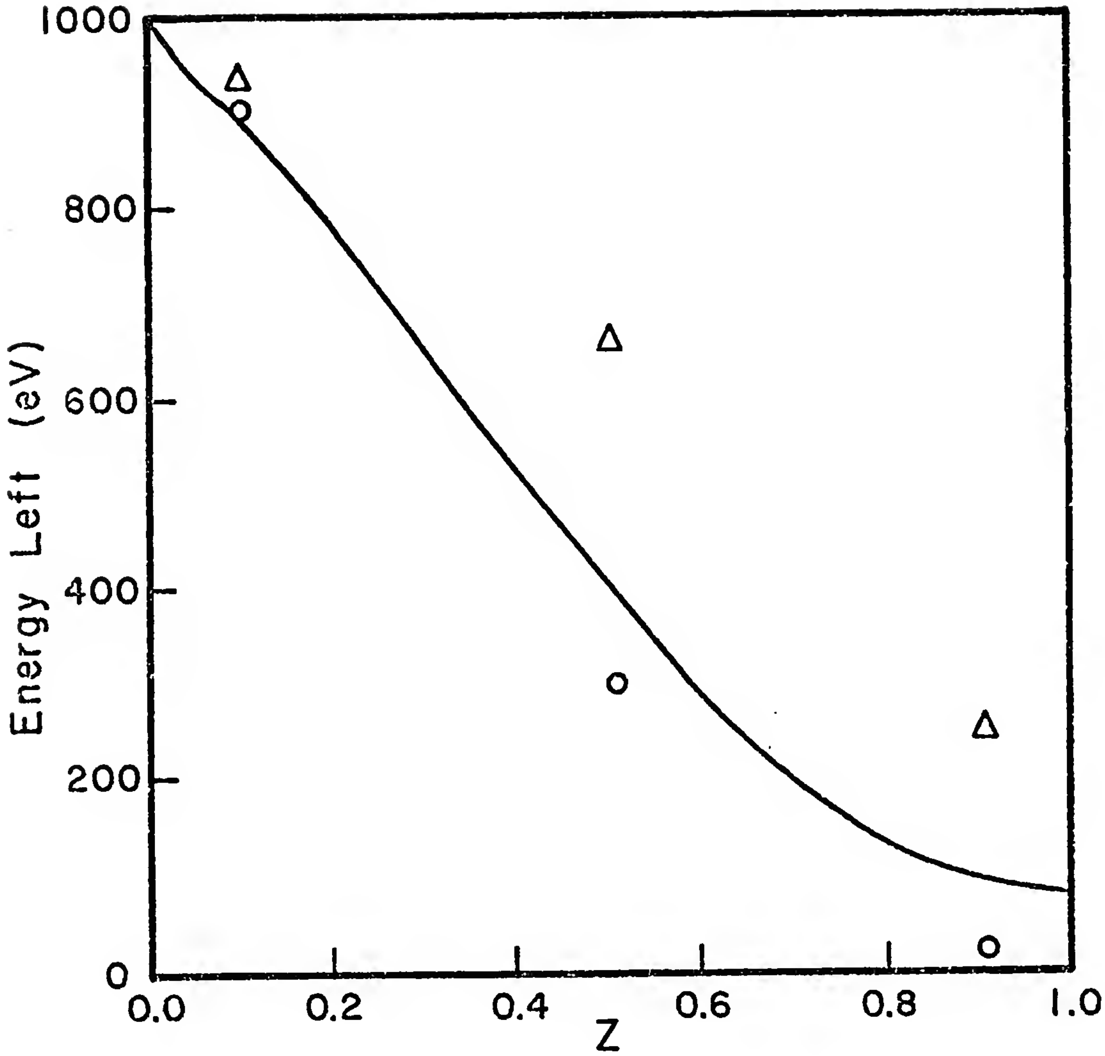

Figure 7.1 Energy remaining plot for electrons with energies incident at 1 KeV. The Δ's give the calculation of Barrett and Hays (1976), the o's give the values from Stolarski (1968), and the solid line gives the average energy left at various z values from this MC work.

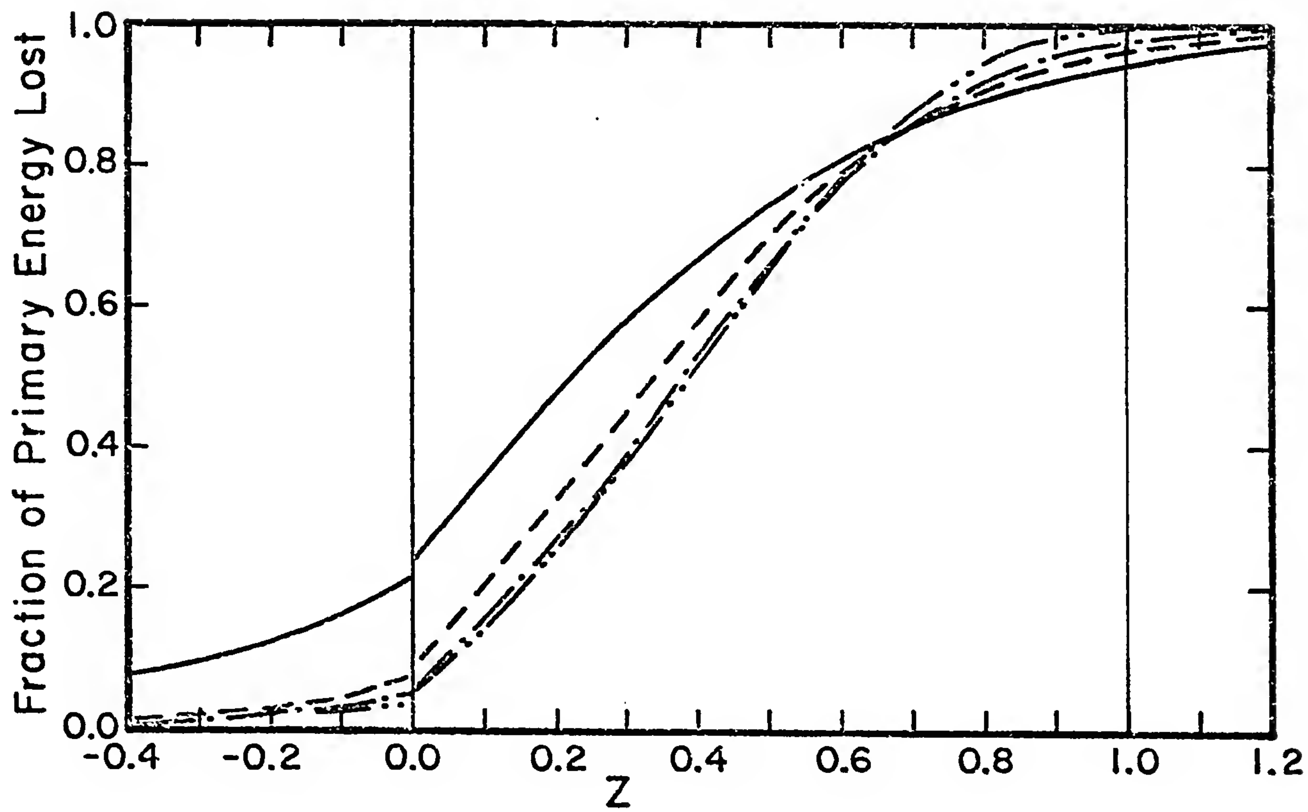

Figure 7.2 Energy loss plot for four incident electron energies: 100 eV, solid line; 300 eV, dashed line; 1000 eV, dash-dot line; and 5000 eV, dash-dot-dot line.

The fraction of energy backscattered is also of interest. The backscattering of electrons from the ionosphere has been observed in rocket experiments by McDiarmid, Rose, and Budzinski (1961) and in the Injun III satellite experiments of O'Brien (1964). Berger, Seltzer, and Maeda (1974) [BSM] have calculated backscattering coefficients for mono-energetic electrons incident on a semi-infinite air medium at energies from 10^4 KeV down to 2 KeV.

One quantity calculated by BSM is R_E, the energy albedo (computed by summing the energy backscattered). Since the incident energy range used in this work overlaps the incident energy range used by BSM from 2 to 5 KeV, a comparison of the R_E's from both calculations is of interest.

Table 7.1 presents the results from the model 3 (hereafter called M3) and the screened Rutherford (hereafter called SR) phase functions and the work of BSM. The M3 energy albedos are lower than those energy albedos resulting from the SR and the BSM calculations (at least where there are values available) down to the energy of 0.1 KeV. At this energy the M3 phase function reveals a fairly substantial backscatter with approximately one-fifth of the incident energy lost in backscatter.

Although little consideration is given to the backscattered electrons in this study, there is much information that can be derived from studying these backscattered particles in detail. This detailed spatial MC technique would be an appropriate method of studying these backscattered particles.

B. Spatial Yield Spectra for Electrons Impinging on N_2

The yield spectrum for an electron energy degradation process contains all the information necessary for computing excitations from that

Table 7.1 Energy albedos presented at five energies E_0 with the use of the model 3 (column labeled M3) and the screened Rutherford (column labeled SR) phase functions and the work of BSM.

E_o (KeV)	M3	SR	BSM
0.1	0.210	0.188	--
0.3	0.072	0.105	--
1.0	0.051	0.078	--
2.0	0.041	0.068	0.062
5.0	0.039	0.045	0.052

calculation. Green, Jackman, and Garvey (1977) [hereafter called GJG] have discussed the use of the yield spectrum $U(E,E_0)$, which was described in Chapter II of this work. This yield spectrum can be used to calculate the yield of any state by means of the equation

$$J_j(E_0) = \int_{W_j}^{E_0} U(E,E_0)p_j(E)dE \qquad (7.4)$$

where $p_j(E) = \sigma_j(E)/\sigma_{TI}(E)$ is the probability for excitation of the jth state with excitation energy W_j.

In these MC calculations information about the yield spectrum can be attained at any longitudinal and radial distance. The three variable yield spectrum $U(E,z,E_0)$, which is a function of the longitudinal distance z, as well as the incident electron energy E_0 and the energy E, is considered in subsection VII.B.1. The four variable yield spectrum $U(E,\rho,z,E_0)$, which is also a function of the radial distance ρ, is then considered in subsection VII.B.2.

1. Three Variable Spatial Yield Spectra

The three variable spatial yield spectrum $U(E,z,E_0)$ is found in the following manner. A MC calculation takes place for a certain incident energy E_0 which places all the collisions with their characteristics on a magnetic tape. The longitudinal- or z-axis is divided up into several equal intervals of Δz_{Int} gm/cm^2 each and the energy regime from 2 eV up to the incident energy E_0 is divided up into several intervals of ΔE_{Int} eV each (not all intervals being equivalent in energy).

If the spatial yield spectrum $U(E_E,z_E,E_0)$ for a certain energy value E_E and longitudinal distance z_E is desired, then the two-dimensional

rectangle with longitudinal endpoint coordinates $z_E - \Delta z_{Int}/2$ and $z_E + \Delta z_{Int}/2$ and energy width endpoint coordinates $E_E - \Delta E_{Int}/2$ and $E_E + \Delta E_{Int}/2$ is established. If the longitudinal distance to any inelastic collision (elastic collisions are excluded because of the real lack of interest in their spatial properties and also because they are not well defined at electron energies below 30 eV), z_c, is between $z_E - \Delta z_{Int}/2$ and $z_E + \Delta z_{Int}/2$ and the energy of the electron before the collision, E_{bc}, is between $E_E - \Delta E_{Int}/2$ and $E_E + \Delta E_{Int}/2$ then the number of electrons in that rectangle, $N(E_E,z_E)$, is incremented by one. This process continues until all the collisions are accounted for.

The spatial yield spectrum [in #/eV/(gm/cm^2)] is then written as

$$U(E_E,z_E,E_0) = \frac{N(E_E,z_E)}{\Delta E_{Int} \quad \Delta z_{Int}} \tag{7.5}$$

(This spatial yield spectrum is also normalized to one electron.) This process then continues for each two-dimensional rectangle across the entire plane of interest. As an example, the $U(E,z,E_0)$ for three longitudinal distances is given in Figure 7.3 for the incident energy of 1 KeV.

This $U(E,z,E_0)$ [as observed in Figure 7.3], although more complex than the $U(E,E_0)$ of GJG, has some nice general characteristics that continue throughout the entire incident energy range (from 0.1 KeV up to 5 KeV). It is, therefore, reasonable to continue the philosophy of analytic representation (see Green and Barth, 1965; Green and Dutta, 1967; Stolarski and Green, 1967; and GJG). The analytic properties of $U(E,z,E_0)$ will permit researchers to infer important spatially derived properties of N_2 with a degree of accuracy which should suffice for many atmospheric applications.

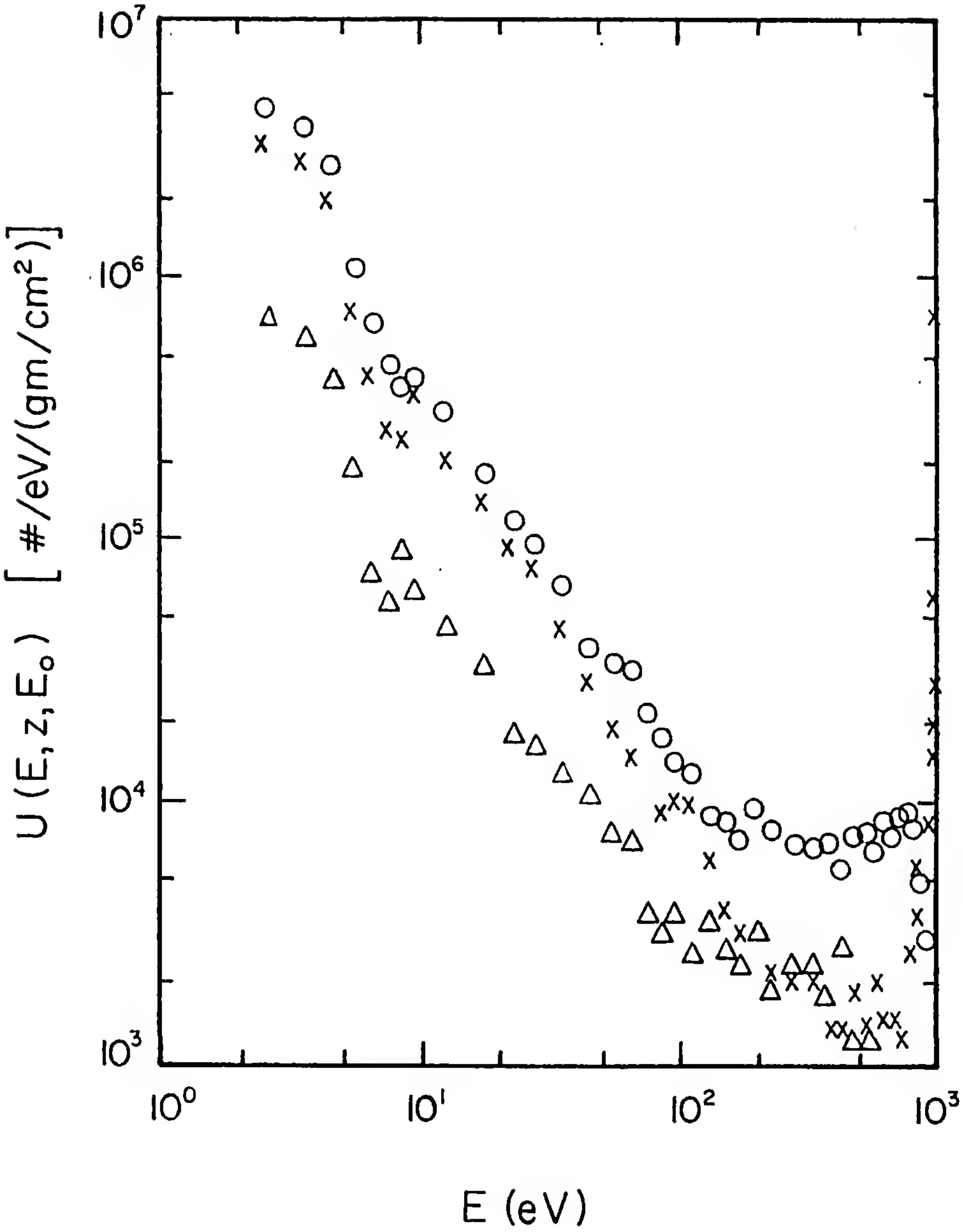

Figure 7.3 Three variable spatial yield spectrum for an incident energy of 1 KeV given at three longitudinal distances (in fractions of the range): z = 0.0739 represented by x, z = 0.429 represented by o, and z = 0.961 represented by Δ.

It should be noted that at the small longitudinal distances a fairly large "source" term persists at energies $E = E_0$. In the interval from about 4 eV to about 10 eV there is a noticeable dip in the yield spectra. In this range (see Figure 3.6), the total inelastic cross sections show a very large dip, thus many of the electrons in this range do not interact inelastically with the N_2 gas in the region of interest.

For the purposes of many applications it is useful to represent the yield spectra by

$$U(E,z,E_0) = U_a(E,z,E_0)\,\theta(E_0 - E - E_\theta) + \delta(E_0 - E)\,D(z,E_0) \tag{7.6}$$

(following the notation of GJG), where θ is the Heaviside function with E_θ, the minimum threshold of the states considered, and $\delta(E_0 - E)$ is the Dirac delta function which allows for the contribution of the source itself. The $U_a(E,z,E_0)$ is represented approximately by

$$U_a(E,z,E_0) = A(z,E_0) + B_1(z,E_0)[E_R]^{B_2} + C_1(z,E_0)[E_R]^{C_2} \tag{7.7}$$

and

$$A(z,E_0) = \frac{a_1(E_0)}{[z_R - a_2(E_0)]^2 + a_3(E_0)}$$

$$B_1(z,E_0) = \frac{b_{11}(z,E_0)}{[z_R - b_{12}(E_0)]^2 + b_{13}}$$

$$C_1(z,E_0) = \frac{c_{11}(z,E_0)}{e^{z_R/c_{12}} + 1}$$

$$D(z,E_0) = \frac{d_1(E_0)}{e^{z_R/d_2} + 1}$$

$$a_1(E_o) = a_{11}\ \xi_o^{a_{12}}$$

$$a_2(E_o) = a_{21}\ (1 - \frac{a_{22}}{\xi_o})$$

$$a_3(E_o) = a_{31} + \frac{a_{32}}{\xi_o}$$

$$b_{11}(z,E_o) = \frac{b_{111}\ \xi_o^{b_{112}}[1 + \frac{(1 - \xi_o)}{b_{113}}]}{[\exp[\{z_R - f_1(E_o)\}/f_2(E_o)] + 1]}$$

$$b_{12}(E_o) = b_{121}\ (1 - \frac{b_{122}}{\xi_o})$$

$$c_{11}(z,E_o) = c_{111}\ \xi_o^{c_{112}}\ /\ [\exp[\{z_R - f_1(E_o)\}/f_2(E_o)] + 1]$$

$$d_1(E_o) = d_{11}\xi_o^{d_{12}}$$

$$f_1(E_o) = f_{11}(1 + \frac{f_{12}}{\xi_o})$$

$$f_2(E_o) = f_{21}\ \xi_o^{f_{22}}$$

$R_g(E_o) = r_1 + r_2\ \xi_o^{r_3}$ = Range of an electron of primary energy E_o

where the parameters and their values are all given in Table 7.2. Also, $\xi_o = E_o/1000$, $E_R = E/E_o$, and $z_R = z/R_g(E_o)$.

Table 7.2 Parameters and their values are given below which are to be used in Eq. (7.7) for the molecular nitrogen spatial yield spectrum.

Parameter	Value	Parameter	Value
a_{11}	587	d_{11}	0.6×10^5
a_{12}	-1.63	d_{12}	-1.68
a_{21}	0.4	d_2	0.2
a_{22}	0.075	f_{11}	0.9
a_{31}	0.1	f_{12}	0.044
a_{32}	0.019	f_{21}	0.104
b_{111}	81	f_{22}	-0.39
b_{112}	-1.8	g_{11}	0.85
b_{113}	8.0	g_{12}	0.07
b_{121}	0.4	g_2	0.2
b_{122}	0.05	r_1	2.27×10^{-7} gm/cm^2
b_{13}	0.2	r_2	6.22×10^{-6} gm/cm^2
B_2	-1.52	r_3	1.67
c_{111}	1.30×10^4		
c_{112}	-1.5		
c_{12}	0.15		
C_2	10		

The yield of any state is then found from

$$J_j(z,E_0) = \int_{z-\frac{\Delta z}{2}}^{z+\frac{\Delta z}{2}} \int_{W_j}^{E_{ui}} U(E,z,E_0)\,dE\,dz \qquad (7.8)$$

where

$$E_{ui} = \frac{E_0}{[e^{\{z_R - g_1(E_0)\}/g_2} + 1]}$$

and

$$g_1(E_0) = \frac{g_{11}}{(1 + \frac{g_{12}}{\xi_0})}$$

The upper limit of integration in Eq. (7.8) is not E_0 but is E_{ui}. As the electrons penetrate further and further into the medium, they lose more and more of the high energy particles. The energy E_{ui} is thus a cutoff energy which must be invoked.

Equation (7.6) represents the yield spectra data fairly well in this regime of incident electron energies. The fit can be seen in Figure 7.4 for five incident energies at five longitudinal values.

A comparison is given in Table 7.3 between the yield using Eq. (7.8) and the yield using the MC calculation for several incident energies and longitudinal values for the yield of the 3914 Å emission. The two calculations are in fair agreement throughout the entire range considered. It should be noted, however, that Eq. (7.8) is not accurate at longitudinal values in the backscatter direction.

Maeda and Aikin (1968) attempted to apply an analytic degradation spectrum to problems of the atmosphere. They calculated the number of oxygen atoms resulting from the dissociation of O_2 from auroral events.

Figure 7.4 The three variable spatial yield spectrum $U(E,z,E_0)$ is plotted as function of E_R. The MC calculations are represented by symbols for each z (in fractions of the range) and E_0 (in KeV): o, z = 0.126, E_0 = 0.1; Δ, z = 0.316, E_0 = 0.3; x, z = 0.606, E_0 = 1.0; ∇, z = 0.928, E_0 = 2.0; and □, z = 1.052, E_0 = 5.0. The analytic fit using Eq. (7.6) is represented by the solid line with the source term contribution represented by ⊠.

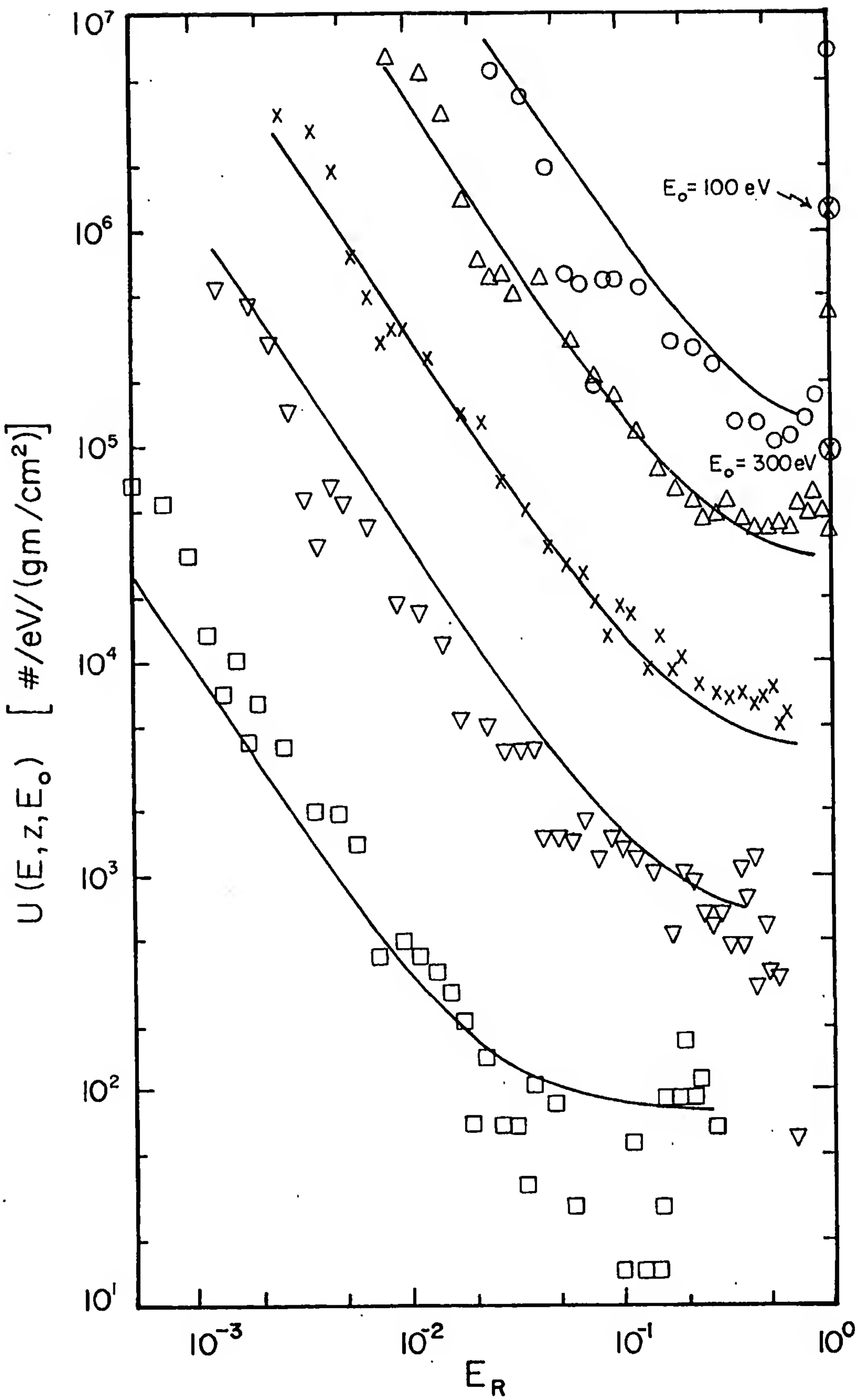

10^7
10^6
10^5
10^4
10^3
10^2
10^1
$U(E,z,E_o)$ [#/eV/(gm/cm^2)]
E_o= 100 eV
E_o= 300 eV
10^{-3}
10^{-2}
10^{-1}
10^0
E_R

Table 7.3 Comparison between the yield of the 3914 Å emission [#/(.5 cm)] from the MC calculation [column labeled MC] and with the use of Eq. (7.6) in Eq. (7.8) [column labeled AF] for several incident energies [column labeled E_0 (in KeV)] and longitudinal distances [column labeled z (in fractions of the range)].

E_0	z	MC	AF
0.1	0.01	280	287
0.1	0.2	240	272
0.1	0.5	155	168
0.1	0.8	70.0	82.3
0.1	1.0	35.2	49.7
0.3	0.01	452	406
0.3	0.2	626	523
0.3	0.5	490	429
0.3	0.8	174	177
0.3	1.0	74.2	73.2
1.0	0.01	550	556
1.0	0.2	740	797
1.0	0.4	860	908
1.0	0.7	500	456
1.0	1.0	100	91.9
2.0	0.01	600	578
2.0	0.2	780	841
2.0	0.4	1050	995
2.0	0.7	600	517
2.0	1.0	130	85.5
5.0	0.01	1300	1323
5.0	0.2	1760	1927
5.0	0.4	2100	2337
5.0	0.7	1380	1214
5.0	1.0	200	160

This yield of O atoms was then used to predict the variation of polar mesospheric oxygen and ozone during auroral events.

Shemansky, Donahue, and Zipf (1972), however, showed that Maeda's spectra are deficient in low-energy degraded primary electrons. This conclusion was also supported by BSM.

The spatial yield spectrum calculated with the use of this MC approach should be quite accurate statistically from 2 eV up to the incident energy E_0. There may be some errors inherent in the assumptions and approximations used in these MC calculations however. The analytic spatial yield spectrum given by Eq. (7.6) does represent fairly well the actual spatial yield spectrum. Thus the analytic spatial yield spectrum can be applied to some of the problems in aeronomy involving impinging electrons into the atmosphere.

Consider now the use of Eq. (7.6) with an incident electron energy flux of $\phi(E_0)$ [in units of #/cm^2/sec/eV]. A yield $J_j[z,\phi(E_0)]$ in units of #/cm^3/sec can be calculated using

$$J_j[z,\phi(E_0)] = \int_{W_j}^{\infty} \int_{W_j}^{E_{ui}} \phi(E_0)U(E,z,E_0)\rho(z)dEdE_0 \qquad (7.9)$$

where $\rho(z)$ is the density (in gm/cm^3) of the air at altitude z. Equation (7.9) is not applied by the author to any given flux $\phi(E_0)$ in this work. Future studies can make use of Eq. (7.9) in applications to aurorae and their effects on the atmosphere.

The spatial yield spectrum for N_2 can be used fairly accurately for problems dealing with the atmosphere in spite of the fact that the atmosphere is not entirely molecular nitrogen. In Green, Jackman, and Garvey (1977) the two variable yield spectrum $U(E,E_0)$ was observed to be

quite similar in all the gases considered. Thus it is expected that the spatial yield spectrum $U(E,z,E_0)$ will also be similar for electron energy degradation into the other atmospheric gases.

2. Four Variable Spatial Yield Spectra

The last subsection (VII.B.1) was only concerned with the spatial yield spectra in the longitudinal direction. This subsection deals with the four variable spatial yield spectra $U(E,\rho,z,E_0)$ which is also a function of the radial direction ρ.

The MC calculation appropriately accounts for the coordinate ρ down to the energy of 30 eV, below which the multiple elastic scattering distribution is used. In subsection IV.C.6 an approximation was made which assumed that ρ was about one-sixth of the total path length. A better approximation would be to simply assume that the ρ distribution for N_2 is similar to that of H_2.

With this assumption and inverting Eq. (8) from Kutcher and Green (1976), the expression for ρ is

$$\rho = [-\ln (1 - R)/\delta]^{1/\gamma} \tag{7.10}$$

where

$$\delta = \frac{(22 + (\frac{s}{0.3})^{1/2})}{(s + 0.3)^{1.5}}$$

$$\gamma = 2[1 - \exp(- \frac{s}{4})]$$

and R = a random number. The parameters are found by averaging those parameters in Table I of Kutcher and Green (1976).

Use of Eq. (7.10) in the MC computations resulted in the spatial yield spectra $U(E,\rho,z,E_0)$ which is fairly accurate down to 2 eV.

The $U(E,\rho,z,E_0)$ was computed in a manner similar to the way that $U(E,z,E_0)$ was computed. In subsection VII.B.1 a rectangle ΔE_{Int} by Δz_{Int} was taken as the area of interest. Here, a volume Δz_{Int} by ΔE_{Int} by ΔP_{Area} is used. The ΔP_{Area} is in units of area $[(gm/cm^2)^2]$ and is defined as

$$P_{Area} = \pi[(\rho + \frac{\Delta\rho_{Int}}{2})^2 - (\rho - \frac{\Delta\rho_{Int}}{2})^2]$$

where ρ is the mid-point of the area of interest and $\Delta\rho_{Int}$ is the radial interval of interest.

If the spatial yield spectrum $U(E_E, \rho_E, z_E, E_0)$ at a certain energy value E_E, longitudinal distance z_E, and radial distance ρ_E for an electron of incident energy E_0 is desired, then the volume with energy width endpoint coordinates $E_E - (\Delta E_{Int}/2)$ and $E_E + (\Delta E_{Int}/2)$, longitudinal endpoint coordinates $z_E - (\Delta z_{Int}/2)$ and $z_E + (\Delta z_{Int}/2)$, and radial endpoint coordinates $\rho_E - (\Delta\rho_{Int}/2)$ and $\rho_E + (\Delta\rho_{Int}/2)$ is established. If the longitudinal distance, z_c, is between $z_E - (\Delta z_{Int}/2)$ and $z_E + (\Delta z_{Int}/2)$ the radial distance, ρ_c, is between $\rho_E - (\Delta\rho_{Int}/2)$ and $\rho_E + (\Delta\rho_{Int}/2)$, and the energy before the collision, E_{bc}, is between $E_E - (\Delta E_{Int}/2)$ and $E_E + (\Delta E_{Int}/2)$, for an inelastic collision; then the number of electrons in that volume, $N(E_E,\rho_E,z_E)$ is incremented by one.

The spatial yield spectrum [in $\#/eV/(gm/cm^2)^3$] is then written as

$$U(E_E,\rho_E,z_E,E_0) = \frac{N(E_E,\rho_E,z_E)}{\Delta E_{Int}\ \Delta P_{Area}\ \Delta z_{Int}} \tag{7.11}$$

This process then continues for each small volume across the entire volume of interest. Again, it should be recognized that this yield spectrum is normalized to one electron.

The four variable spatial yield spectrum is presented in Figure 7.5 (a, b, c, and d) for an incident electron energy of 1 KeV. It is given at four radial distances at each longitudinal cut (all in units of fractions of the range). The $U(E,\rho,z,E_0)$ from other incident electron energies are not presented here but show a similar type of behavior.

The shape of $U(E,\rho,z,E_0)$ is observed to be quite similar to $U(E,z,E_0)$ [see Figure 7.3] and, indeed even to $U(E,E_0)$ [see Green, Jackman, and Garvey, 1977, Figure 1e]. The lower energy power fall-off is $\propto E_R^{-1.52}$ in all three yield spectra. All three spectra also exhibit a constant component in the middle energies with the source term feature at the incident energy ($E_R = 1.0$).

The four variable and three variable spatial yield spectra illustrate an increasing tendency at higher values of energy ($E_R \approx 0.9 \rightarrow 1.0$) and at the lower values of z and ρ. This feature is not as prominent in the non-spatial yield spectrum $U(E,E_0)$, which is calculated by integrating over the spatial component of the spatial yield spectra. In the integration process the higher energy spectra increase is averaged out by the equally important higher energy spectra decrease exhibited at the higher values of z and ρ.

Knowledge of $U(E,\rho,z,E_0)$ implies more detailed information about the entire spatial degradation process. Once the $U(E,\rho,z,E_0)$ is known then the number of excitations $J_j(\rho_{1\rightarrow 2},z)$ of the jth state can be found. This $J_j(\rho_{1\rightarrow 2},z)$ is a result of an incident electron flux $\phi(E_0)$ and is the number of excitations at altitude z in the ring between ρ_1 and ρ_2. Thus

$$J_j(\rho_{1\rightarrow 2},z) = \pi(\rho_2^2 - \rho_1^2) \int_{W_j}^{\infty} \int_{W_j}^{E_0} \phi(E_0)U(E,\rho,z,E_0)\rho(z)dEdE_0 \qquad (7.12)$$

Figure 7.5 (a, b, c, and d)	Four variable spatial yield spectra for an incident electron energy of 1 KeV given at four longitudinal distances: $z = 0.061$ (Figure 7.5a), $z = 0.305$ (Figure 7.5b), $z = 0.549$ (Figure 7.5c), and $z = 0.793$ (Figure 7.5d). At each longitudinal cut the yield spectrum is given at four radial distances: $\rho = 0.061$, o; $\rho = 0.305$, ●; $\rho = 0.549$, ■; and $\rho = 0.793$, ▲.

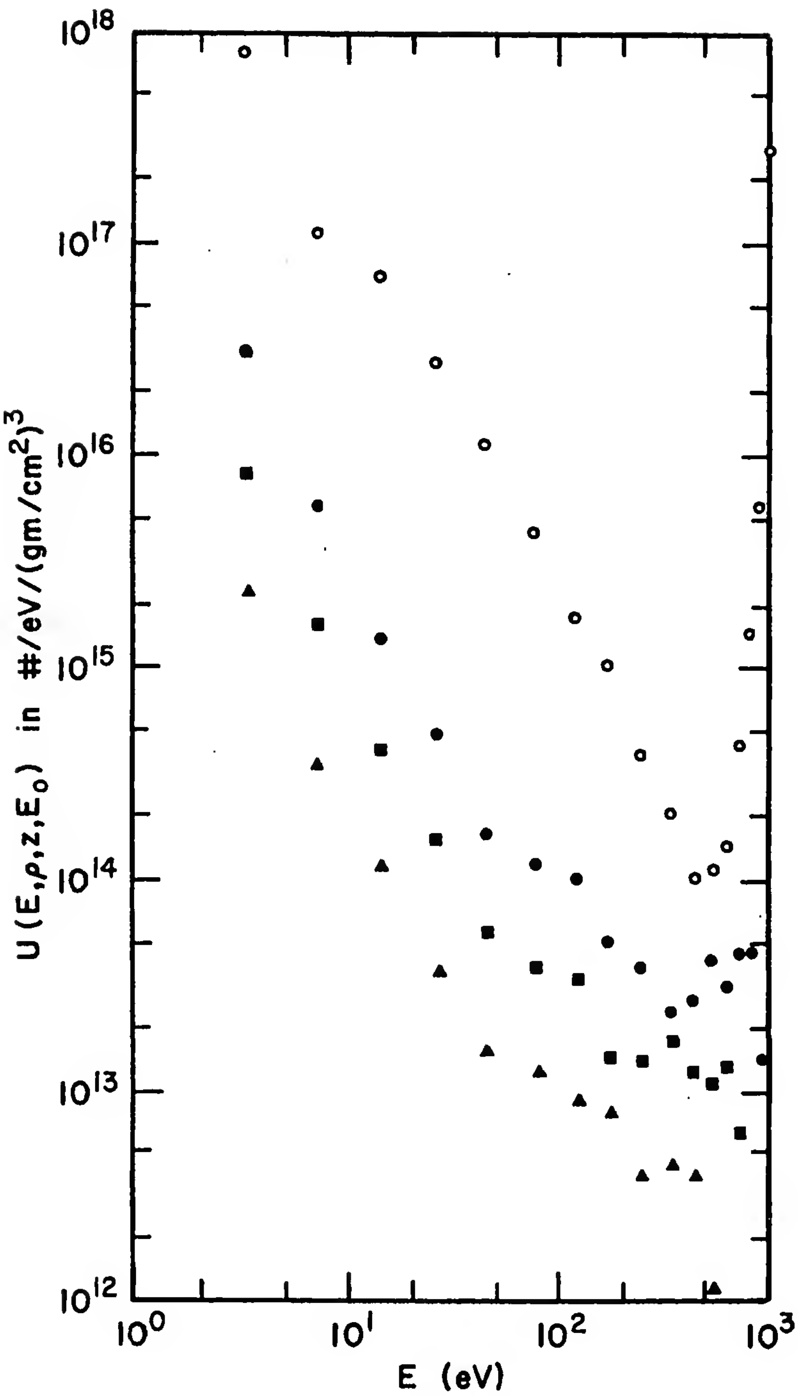

10^{18}
10^{17}
10^{16}
10^{15}
10^{14}
10^{13}
10^{12}
$U(E,\rho,z,E_o)$ in #/eV/(gm/cm^2)^3
10^0
10^1
10^2
10^3
E (eV)

Figure 7.5a

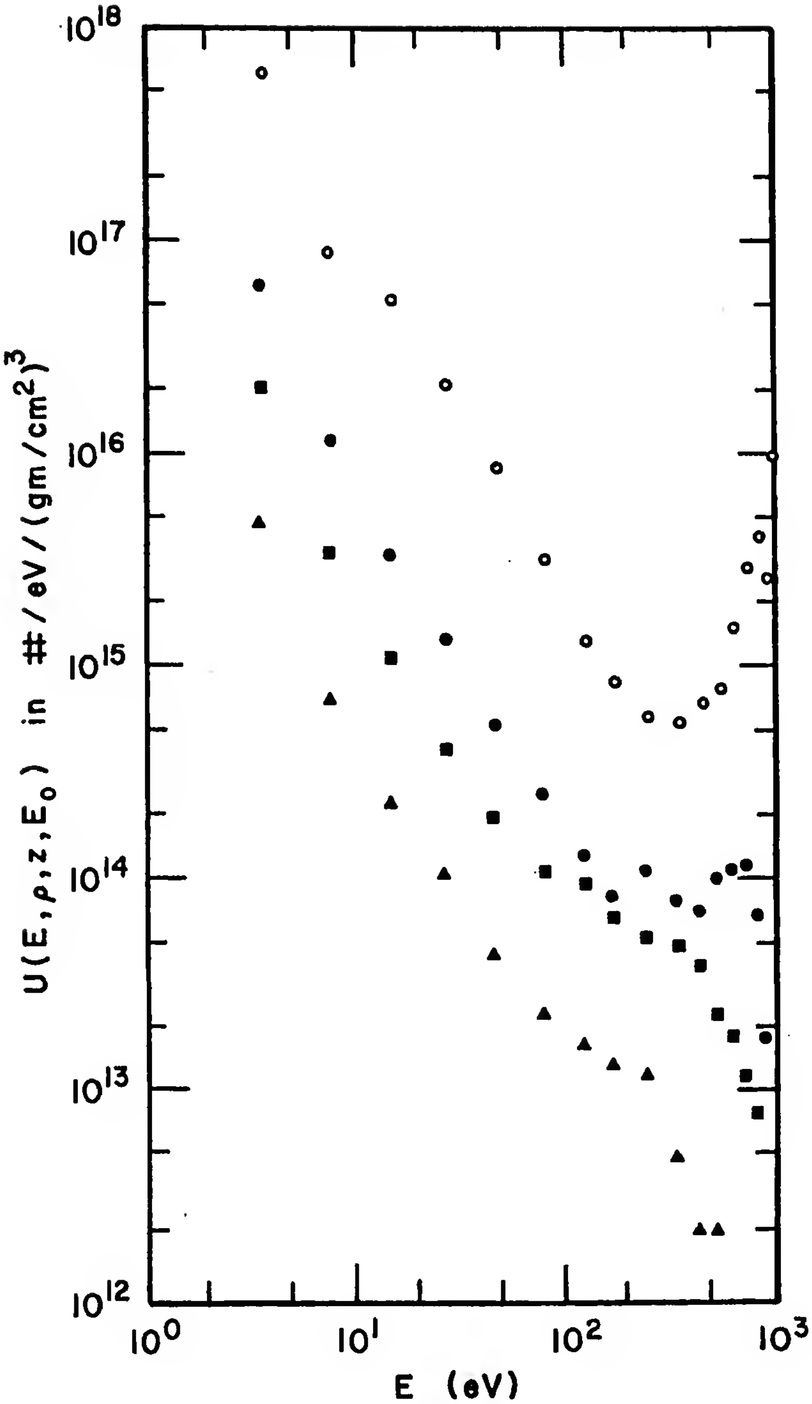
10^{18}
10^{17}
10^{16}
10^{15}
10^{14}
10^{13}
10^{12}
$U(E,\rho,z,E_o)$ in #/eV/(gm/cm^2)^3
10^0
10^1
10^2
10^3
E (eV)

Figure 7.5b

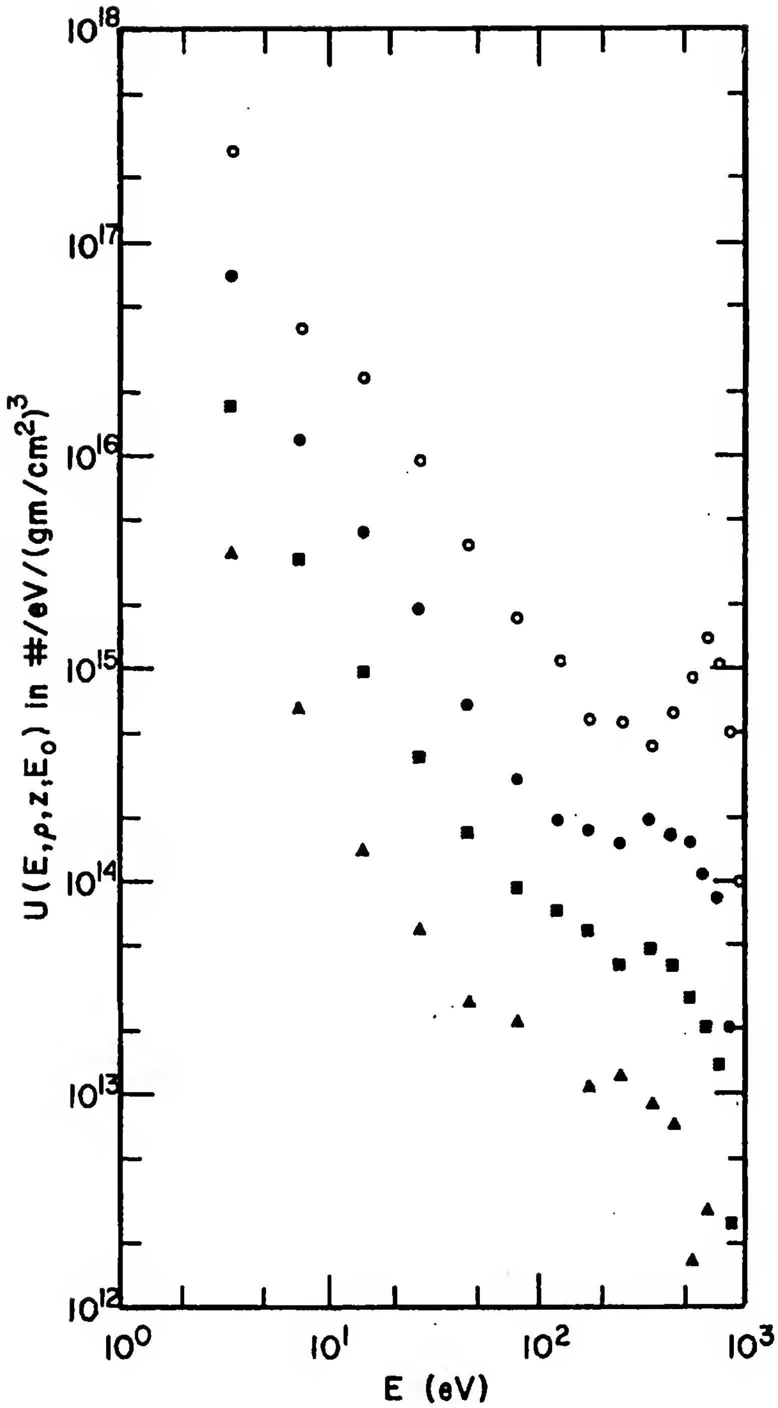
10^{18}
10^{17}
10^{16}
10^{15}
10^{14}
10^{13}
10^{12}
$U(E,\rho,z,E_o)$ in #/eV/(gm/cm^2)^3
10^0
10^1
10^2
10^3
E (eV)

Figure 7.5c

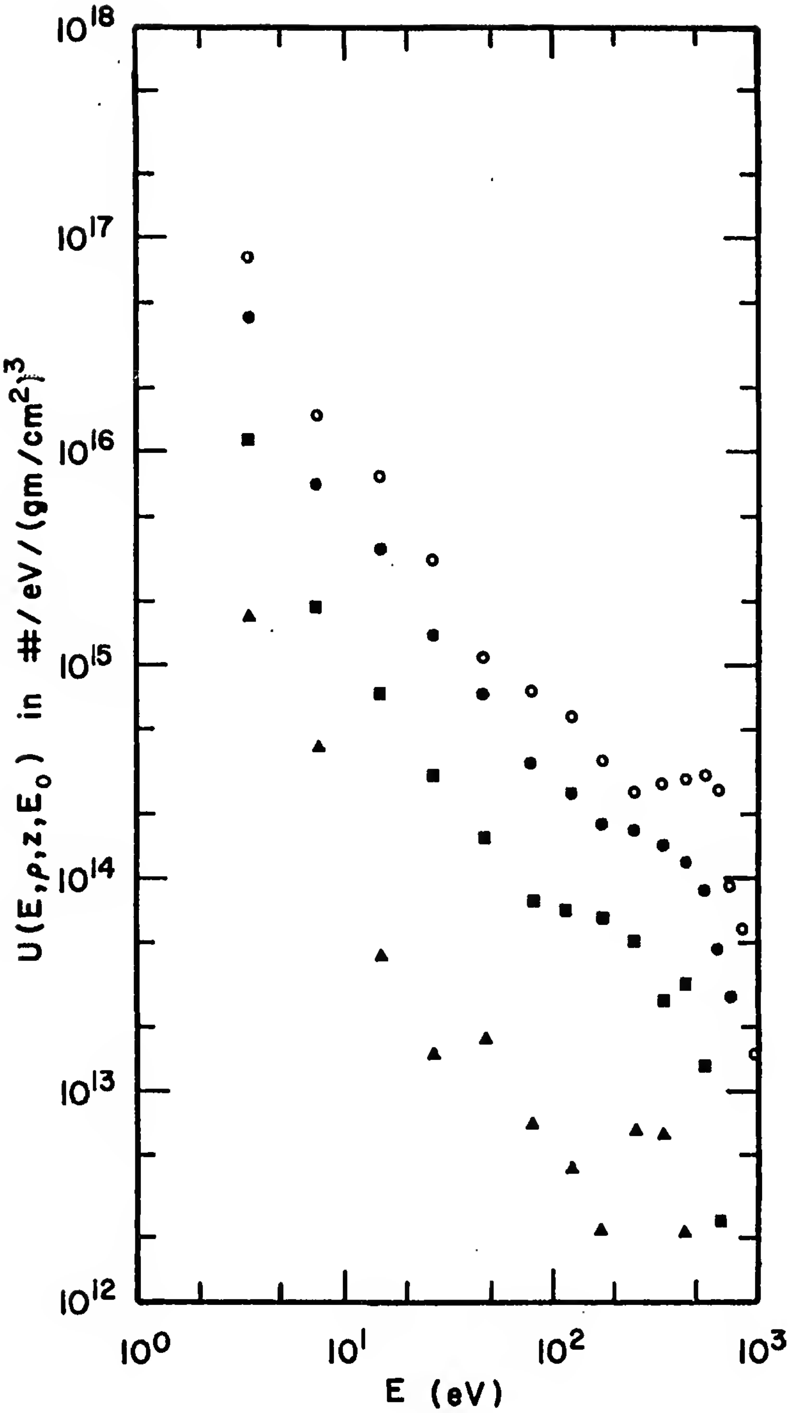

10^{18}
10^{17}
10^{16}
10^{15}
10^{14}
10^{13}
10^{12}
$U(E,\rho,z,E_0)$ in #/eV/(gm/cm^2)^3
10^0
10^1
10^2
10^3
E (eV)

Figure 7.5d

No analytic expression has been derived for $U(E,\rho,z,E_0)$; however, it does have systematics that tend to point toward some type of representation which would be useful for atmospheric scientists.

This concludes the discussion about the results from the MC calculation. The most important output from the MC computations is the spatial yield spectra because many of the other results given in Chapters V, VI, and VII can be derived easily from this spatial quantity.

CHAPTER VIII

CONCLUSIONS

There are several different theoretical approaches now being employed to study the auroral electron energy deposition problem. Researchers using these methods have concentrated for the most part on the details of the computation and on the input atmospheric parameters.

One of the concerns of this work was the cross sections, both differential and total, and their impact on the spatial and energetic aspects of the electron energy deposition. This research has shown that the input cross sections have a very large influence on the resulting electron energy deposition.

Perpendicularly incident electrons with energies from 0.1 through 5.0 KeV were degraded in molecular nitrogen using a Monte Carlo spatial energy deposition technique. This degradation method followed each electron, its secondaries, and its tertiaries in a collision by collision manner down to 30 eV. Below 30 eV, a multiple elastic scattering distribution was used to describe the energy deposition process down to the cutoff energy of 2 eV.

This Monte Carlo calculation employed new phenomenological differential elastic and doubly differential ionization cross sections which agree quite well with experimental data. Other cross sections previously developed for N_2 were also used in these computations.

To the author's knowledge, this was the first theoretical calculation resulting in three dimensional intensity profiles for incident electron energies below 2 KeV which could easily be compared to experimental work. The N_2^+ $B^2\Sigma_u^+$ intensity profiles and range values for incident energies from 0.3 to 5.0 KeV showed reasonable agreement with experimental electron energy degradation work in both the longitudinal and the radial direction.

A sensitivity study was included in this work which characterized the influence of 1) the differential ionization cross sections, 2) the differential inelastic cross sections, 3) the different shaped elastic phase functions, and 4) the total elastic cross sections on the energy deposition process. In particular, it was shown that: 1) Differential ionization cross sections have very little influence on the degradation process; 2) inelastic scattering appeared to be somewhat important for incident electrons with energies below 0.3 KeV; 3) the shape of the electron collision profiles and the range from the 3914 Å intensity profiles were functions of the screening parameter of the model 1 elastic scattering phase function; and 4) the total elastic cross section had a significant influence on the electron's spatial degradation process.

The resultant energy loss plots are used to help determine the energy albedo of the incident electrons and also the rate at which energy is lost in the medium. The spatial yield spectrum is easily employed to find the excitation profiles for any N_2 state at any position in the medium. For this reason the three variable spatial yield spectrum $U(E,z,E_0)$ is analytically characterized. The four variable spatial yield spectrum $U(E,\rho,z,E_0)$ is even more complex than $U(E,z,E_0)$; nevertheless the systematics of this quantity are described qualitatively.

This work compiled a reasonably comprehensive and realistic cross section set for N_2 in the energy range from 2 to 5000 eV. The influence of various differential and total cross sections on the spatial and energetic aspects of the electron energy deposition problem was also characterized. Finally, this study presented a spatial yield spectrum along with an analysis and analytic fit of some of its most important properties.

APPENDIX A

MONTE CARLO PROGRAM

The Monte Carlo program which is a modified version of a program used in Brinkmann and Trajmar (1970) is listed in this appendix. This program (written in Fortran IV) degrades electrons in the range from 2 to 5000 eV in a spatial manner. Each collision with its characteristics are placed on a magnetic tape.

```
C          ***MONTE CARLO PROGRAM***                                         MAIN0001
C     THIS PROGRAM IS TO BE USED IN CONJUNCTION WITH THE PROGRAM GETDAT.     MAIN0003
C     THIS PROGRAM PUTS THE DATA ON A MAGNETIC TAPE AND GETDAT COALESCES     MAIN0004
C     THE INFORMATION ON THE TAPE.                                           MAIN0005
C     THIS PARTICULAR PROGRAM IS USEFUL FOR DEGRADING ELECTRONS IN THE       MAIN0006
C     RANGE FROM 2 TO 5000 EV.                                               MAIN0007
C     RIGHT NOW THIS PROGRAM IS SET UP FOR MOLECULAR NITROGEN.               MAIN0008
C     THIS PROGRAM IS SET UP ONLY TO GIVE THE ELECTRONS ESCAPING AND         MAIN0009
C     THE TOTAL NUMBER OF COLLISIONS THAT OCCUR.  NO OTHER PRELIMINARY       MAIN0010
C     OUTPUT IS OBTAINED OF THE DEGRADATION SCHEME.                          MAIN0011
C     THERE ARE PLACES IN THE PROGRAM WHERE IT IS SET UP FOR MORE THAN       MAIN0012
C     ONE GAS.  SOME OF THESE PLACES WILL BE USEFUL IF MORE THAN ONE         MAIN0013
C     GAS IS INCLUDED IN THE MODEL ATMOSPHERE                                MAIN0014
C     THE MAIN PROGRAM IS LISTED BELOW.  THIS PROGRAM ONLY CALLS TWO         MAIN0015
C     SUBROUTINES:                                                           MAIN0016
C     1)DATA                                                                 MAIN0017
C     2)MC                                                                   MAIN0018
C                                                                            MAIN0019
C     THE COMMON BLOCK FOLLOWS.                                              MAIN0020
C     ALL VARIABLES ARE PLACED IN THIS BLOCK TO ALLOW FOR THE OPTIMIZE=2     MAIN0021
C     UNDER THE H COMPILER TO BE MOST EFFICIENT                              MAIN0022
       COMMON ALPE(6),BETE(6),CE(6),FE(6),WE(6),ALFA(15),BEFA(15),           MAIN0023
     1 CFA(15),FFA(15),WFA(15),WF(15),FACI(15),NFA,NAR,SA(3,80),             MAIN0024
     2 ZALT(80),ENR(30),PCFA(3,30),WCFA(3,30),NENR,FDG(3),PSE(3),            MAIN0025
     3 PION(3),AT(3),A(6,3),B(5,3),G(5,3),UH(10),UI(10),UJ(10),              MAIN0026
     4 UD(10),USNU(10),USF(10),UEIN(11),IUTP,IUTM1,DG(3),NSG(3),NIG(3),      MAIN0027
     5 NUMGAS,NUMST,WIS(50),NSEC,MUNIT,ISEED,ISTOP,ILAST,EIN,NPRIM,COSI,     MAIN0028
     6 H,EMIN,ZSTART,TMIN,THRESH(3),AK(2,3),AJ(3,3),GAMA(2,3),               MAIN0029
     7 TO(3,3),FAC(6),A0E(6),A1E(6),B0E(6),B1E(6),C0E(6),D0E(6),             MAIN0030
     8 D1E(6),PROB(40),W(40),NIE(40),A21(3),A22(3),A31(3),A32(3),            MAIN0031
     9 A33(3),B11(3),B12(3),B13(3),CI(3),C21(3),C22(3),C31(3),               MAIN0032
     A C32(3),D1(3),D2(3),F1(3),F2(3),THRI(16),AKI(2,15),AJI(3,16),          MAIN0033
     B GAMAI(2,16),TOI(3,16),SIGT(6),THET(40),NX,CSIE(20),EIT(20),           MAIN0034
     C IEILS,IEILM1,P,R,ZDIS,NPIN,NOP,COSPA,RT,F(40),R1,R2,R3,R4,            MAIN0035
     D R5,XV,YV,ZV,XVN,YVN,ZVN,PA,PHI,EV,WLOSS,NSTAT,NSCS,NPHF,              MAIN0036
     E IR1,IR2,NG,EVPRI,RAN,EMSD,EINEL,EXC5(50),COSPAN,T,FOVAL               MAIN0037
C                                                                            MAIN0038
C                                                                            MAIN0039
C     READ AND WRITE THE INITIAL DATA                                        MAIN0040
1        READ(5,105)NPIN,NOP,NPHF                                            MAIN0041
C     NPIN = 1 IN ALL CASES                                                  MAIN0042
C     NOP IS THE NUMBER OF PRIMARIES                                         MAIN0043
C     NPHF IS THE INDEX FOR THE ELASTIC PHASE FUNCTION BEING USED.           MAIN0044
C     IF NPHF = 0 THEN USE SUBROUTINE PHFEL.                                 MAIN0045
C     IF NPHF = 1 THEN USE SUBROUTINE PHF.                                   MAIN0046
```

```
      WRITE(6,106)NPIN,NOP,NPHF                                          MAIN0047
106      FORMAT(//,' THE NUMBER OF PRIMARY SEGMENTS=',I5,                MAIN0048
     *  /,' THE NUMBER OF PRIMARIES IN EACH SEGMENT=',I5,/,              MAIN0049
     * ' INDEX FOR PHASE FUNCTION=',I5,//)                               MAIN0050
      READ(5,105) ISEED,ILAST,ISTOP,NX,NSEC                              MAIN0051
C    ISEED IS THE INITIAL RANDOM NUMBER STARTER                          MAIN0052
C    ILAST = 0 IN ALL CASES                                              MAIN0053
C    IF ISTOP=1 THEN WE HAVE ANOTHER RUN TO MAKE                         MAIN0054
C    IF ISTOP=0 THEN THIS IS THE ONLY RUN                                MAIN0055
C    NX IS THE NUMBER OF ANGLES USED IN FINDING THE SCATTERING           MAIN0056
C    ANGLE IF NO ANALYTIC EXPRESSION CAN BE USED.                        MAIN0057
C    NSEC IS THE NUMBER OF LOWER ENERGY BIN ENDS.                        MAIN0058
C    NSEC IS USEFUL ONLY IF A LOCAL ENERGY DEGRADATION SCHEME IS         MAIN0059
C    EMPLOYED BELOW SOME ENERGY AND IF PRELIMINARY OUTPJT IS DESIRED.     MAIN0060
105   FORMAT(8I10)                                                       MAIN0061
      READ(5,550)EMIN,TMIN,EMSD,EINEL                                    MAIN0062
C    EMIN IS THE ENERGY TO WHICH THE PRIMARY ELECTRON IS DEGRADED BEFORE MAIN0063
C    LOCAL DEGRADATION IS USED                                           MAIN0064
C    TMIN IS THE ENERGY TO WHICH THE SECONDARY AND TERTIARY ELECTRONS AREMAIN0065
C    DEGRADED.                                                           MAIN0066
C    BELOW EMSD USE THE MULTIPLE SCATTERING DISTRIBUTION.                MAIN0067
C    EINEL IS THE HIGHEST ENERGY AT WHICH ELECTRONS ARE ALLOWED TO       MAIN0068
C    SCATTER INELASTICALLY,                                              MAIN0069
550   FORMAT(8E10.3)                                                     MAIN0070
      WRITE(6,620)ISEED,ILAST,ISTOP,EMIN,TMIN,EMSD,EINEL                 MAIN0071
620   FORMAT(' ISEED=',I10,/,' ILAST=',I10,/,' ISTOP=',I5,/,             MAIN0072
     A  ' EMIN=',1PE10.4,'  EV',/,' TMIN=',1PE10.4,'  EV',/,             MAIN0073
```

```
     B ' EMSD=',1PE10.4,'  EV',/,' EINEL=',1PE10.4,'  EV',//)
      NA=NX-1
      WRITE(6,250)NX
  250 FORMAT(/////,3X,'THE DISTRIBUTION FUNCTION IS EVALUATED AT ',I5,
     A' ANGLES BETWEEN ZERO AND PI',////)
      WRITE(6,622)
622   FORMAT(' INDEX OF ANGLE',5X,'ANGLE VALUE IN RADIANS',//)
      READ(5,131) (THET(I),I=1,NX)
C    THET(I) ARE THE ANGULAR BIN ENDS USEFUL IN CALCULATING THE ANGLE
C    OF SCATTER.
      DO 3 I=1,NX
      WRITE(6,624) I,THET(I)
624   FORMAT(I8,14X,1PE10.4)
    3 CONTINUE
      READ(5,105) NAR
C    NAR IS THE NUMBER OF ALTITUDE INTERVALS
      READ(5,131) (ZALT(I),I=1,NAR)
C    ZALT(I) ARE THE ARRAY OF Z VALUES.
C    THIS ARRAY IS MAINLY USEFUL IF PRELIMINARY OUTPUT IS DESIRED.
C    ZALT(1) AND ZALT(NAR) ARE THE LIMITS ON THE Z DIMENSION
C    OF THE BOX FOR DEGRADATION.
C    IF AN ELECTRON REACHES OUTSIDE THE DIMENSIONS (IN Z) OF THE BOX,
C    THEN THE ELECTRON HAS ESCAPED.
131   FORMAT(8E10.0)
      WRITE(6,632)
632   FORMAT(///,'1INDEX OF ALTITUDE RANGE',5X,'ALTITUDE IN KILOMETERS',
     * /)
      DO 10 J=1,NAR
      WRITE(6,634) J,ZALT(J)
634   FORMAT(I8,21X,1PE12.4)
10    CONTINUE
      READ(5,131)(WIS(I), I=1,NSEC)
C    WIS(I) ARE THE LOWER ELECTRON ENERGY BIN ENDS.
      NTOP=NSEC-1
      READ(5,131)(EXC5(I),I=1,NTOP)
C    EXC5(I) ARE THE NUMBER OF EXCITATIONS OF THE 3914A EMISSION STATE
C    RESULTING FROM THE LOCAL DEGRADATION OFTHE SECONDARIES IN THAT BIN.
C    THIS ARRAY IS USEFUL ONLY IF PRELIMINARY OUTPUT IS DESIRED.
      WRITE(6,640)
640      FORMAT(//,' BOUNDARIES OF BINS FOR SECONDARIES IN EV',
     *  5X,'NO. OF 3914A EMISSIONS EXCITED',/)
      DO 20 I=1,NTOP
      IP1=I+1
      WRITE(6,645)WIS(I),WIS(IP1),EXC5(I)
645      FORMAT(1PE12.3,5X,1PE12.3,14X,1PE12.3)
```

```
20       CONTINUE                                                          MAIN0119
      READ(5,120) NPRIM,COSI,EIN,H,ZSTART                                  MAIN0120
C    NPRIM IS THE NUMBER OF PRIMARIES                                      MAIN0121
C    COSI IS THE COSINE OF THE INITIAL ELECTRON                            MAIN0122
C    EIN IS THE ENERGY  OF THE PRIMARY ELECTRON                            MAIN0123
C    H IS THE MAGNETIC FIELD                                               MAIN0124
C    ZSTART IS THE ALTITUDE AT WHICH THE PRIMARY ELECTRON IMPINGES         MAIN0125
120   FORMAT(I10,F10.5,3E10.0)                                             MAIN0126
      WRITE(6,210) NPRIM,COSI,EIN,H,ZSTART                                 MAIN0127
210   FORMAT(///,'1THE BATCH OF PARTICLES HAS THE FOLLOWING ATTRIBUTES:'MAIN0128
     A  ,/,9X,'THE NUMBER OF PARTICLES=',I5,/                              MAIN0129
     B9X,'COSINE OF THE INITIAL POLAR ANGLE=',F6.3,                        MAIN0130
     C  /,9X,'INCIDENT ENERGY=',F12.3,2X,'EV',                             MAIN0131
     D  /,9X,'MAGNETIC FIELD=',F12.3,2X,'GAUSS',                           MAIN0132
     E  /,9X,'INITIAL ALTITUDE=',1PE12.3,2X,'KILOMETERS')                  MAIN0133
C                                                                          MAIN0134
C                                                                          MAIN0135
C    CALL DATA SUBROUTINE TO READ IN THE REST OF THE DATA                  MAIN0136
      CALL DATA                                                            MAIN0137
      NAR1=NAR+1                                                           MAIN0138
      NUMG=NUMST+NUMGAS                                                    MAIN0139
C                                                                          MAIN0140
C                                                                          MAIN0141
C    CALL SUBROUTINE MC WHICH DEGRADES ALL THE PRIMARIES                   MAIN0142
      CALL MC                                                              MAIN0143
      IF(ISTOP.EQ.0)GO TO 2                                                MAIN0144
      GO TO 1                                                              MAIN0145
```

```
2 CONTINUE                                                   MAIN0146
  STOP                                                       MAIN0147
  END                                                        MAIN0148
```

```
      SUBROUTINE COLTYP                                                  COLTYP01
C         SUBROUTINE COLTYP ****                                         COLTYP02
C     THIS SUBROUTINE IS ACCESSED THROUGH MC AND MESD.                   COLTYP03
C     THIS SUBROUTINE COMPUTES THE TYPE OF COLLISION THAT OCCURS.        COLTYP04
C     SOME OF THIS SUBROUTINE IS SET UP TO TAKE MORE THAN ONE GAS.       COLTYP05
      COMMON ALPE(6),BETE(6),CE(6),FE(6),WE(6),ALFA(15),BEFA(15),        COLTYP06
     1 CFA(15),FFA(15),WFA(15),WF(15),FACI(15),NFA,NAR,SA(3,80),         COLTYP07
     2 ZALT(80),ENR(30),PCFA(3,30),WCFA(3,30),NENR,FDG(3),PSE(3),        COLTYP08
     3 PION(3),AT(3),A(6,3),B(5,3),G(5,3),UH(10),UI(10),UJ(10),          COLTYP09
     4 UD(10),USNU(10),USF(10),UEIN(11),IUTP,IUTM1,DG(3),NSG(3),NIG(3),  COLTYP10
     5 NUMGAS,NUMST,WIS(50),NSEC,MUNIT,ISEED,ISTOP,ILAST,EIN,NPRIM,COSI, COLTYP11
     6 H,EMIN,ZSTART,TMIN,THRESH(3),AK(2,3),AJ(3,3),GAMA(2,3),           COLTYP12
     7 TO(3,3),FAC(6),A0E(6),A1E(6),B0E(6),B1E(6),C0E(5),D0E(6),         COLTYP13
     8 D1E(6),PROB(40),W(40),NIE(40),A21(3),A22(3),A31(3),A32(3),        COLTYP14
     9 A33(3),B11(3),B12(3),B13(3),C1(3),C21(3),C22(3),C31(3),           COLTYP15
     A C32(3),D1(3),D2(3),F1(3),F2(3),THRI(16),AKI(2,15),AJI(3,16),      COLTYP16
     B GAMAI(2,16),TOI(3,16),SIGT(6),THET(40),NX,CSIE(20),EIT(20),       COLTYP17
     C IEILS,IEILM1,P,R,ZDIS,NPIN,NOP,COSPA,RT,F(40),R1,R2,R3,R4,        COLTYP18
     D R5,XV,YV,ZV,XVN,YVN,ZVN,PA,PHI,EV,WLOSS,NSTAT,NSCS,NPHF,          COLTYP19
     E IR1,IR2,NG,EVPRI,RAN,EMSD,EINEL,EXCS(50),COSPAN,T,FOVAL           COLTYP20
C                                                                        COLTYP21
C                                                                        COLTYP22
      E=EV                                                               COLTYP23
C     EV IS THE ENERGY FROM THE MAIN PROGRAM                             COLTYP24
      DGT=0.0                                                            COLTYP25
      DO 30 I=1,NUMGAS                                                   COLTYP26
30    DGT=DGT+DG(I)                                                      COLTYP27
C     CALCULATE DGT, THE TOTAL DENSITY OF THE GASES.                     COLTYP28
      DO 20 I=1,NUMGAS                                                   COLTYP29
20    FDG(I)=DG(I)/DGT                                                   COLTYP30
C     CALCULATE FDG(I), THE FRACTION OF THE TOTAL MODEL ATMOSPHERE THAT  COLTYP31
C     IS THE ITH SPECIE.                                                 COLTYP32
      SIGEE=0.0                                                          COLTYP33
      K=0                                                                COLTYP34
      DO 1 I=1,NUMGAS                                                    COLTYP35
      DO 1 J=1,2                                                         COLTYP36
      K=K+1                                                              COLTYP37
1     SIGEE=SIGEE+SIGT(K)*FDG(I)                                         COLTYP38
C     CALCULATE SIGEE, THE TOTAL CROSS SECTION.                          COLTYP39
      PSE(1)=SIGT(2)/SIGEE                                               COLTYP40
      P=PSE(1)                                                           COLTYP41
      IF(R .LT. P) GO TO 403                                             COLTYP42
      GO TO 404                                                          COLTYP43
403   NSTAT=NUMST+1                                                      COLTYP44
      GO TO 4                                                            COLTYP45
```

```
404    IF(NUMGAS .EQ. 1) GO TO 6                                           COLTYP46
       J=2                                                                 COLTYP47
C    COME TO THIS SECTION WHEN THERE ARE MORE THAN ONE GASES.              COLTYP48
       ITOP=2*NUMGAS                                                       COLTYP49
       DO 2 I=4,ITOP,2                                                     COLTYP50
       PSE(J)=SIGT(I)/SIGEE                                                COLTYP51
       P=P+PSE(J)                                                          COLTYP52
       IF(R .LT. P) GO TO 5                                                COLTYP53
       J=J+1                                                               COLTYP54
2      CONTINUE                                                            COLTYP55
       GO TO 6                                                             COLTYP56
4      NSCS=2                                                              COLTYP57
C    ELASTIC COLLISIONS ARE SENT TO STATEMENT 4.                           COLTYP58
       GO TO 7                                                             COLTYP59
5      NSCS=J                                                              COLTYP60
       NSTAT=NUMST+J                                                       COLTYP61
7      RETURN                                                              COLTYP62
6      NSCS=-1                                                             COLTYP63
       RAN=R                                                               COLTYP64
C    RAN AND R ARE THE RANDOM NUMBERS.                                     COLTYP65
       IF(E .LT. 200.) CALL CTB200                                         COLTYP66
C    GO TO SUBROUTINE CTB200 FOR ENERGIES LESS THAN 200 EV.                COLTYP67
       IF(E .LT. 200.) GO TO 12                                            COLTYP68
       NSTAT=1                                                             COLTYP69
       JL=1                                                                COLTYP70
       DO 11 I=1,NUMGAS                                                    COLTYP71
       NSCS=NSCS+2                                                         COLTYP72
```

```
     14 JULY 1978                    NERDC --- CARD LIST UTILITY

      JU=NSG(I)                                                          COLTYP73
      DO 10 J=JL,JU                                                      COLTYP74
      P=PROB(J)*FDG(I)*(1.-PSE(I))+P                                     COLTYP75
      IF(P .GT. R) GO TO 13                                              COLTYP76
      NSTAT=NSTAT+1                                                      COLTYP77
C   NSTAT IS THE INDEX OF THE STATE.                                     COLTYP78
10    CONTINUE                                                           COLTYP79
      JL=JU+1                                                            COLTYP80
11    CONTINUE                                                           COLTYP81
13    WLOSS=W(NSTAT)                                                     COLTYP82
C   WLOSS IS THE ENERGY LOSS OF THE STATE.                               COLTYP83
12    RETURN                                                             COLTYP84
      END                                                                COLTYP85
```

```
      SUBROUTINE CRSEC                                                  CRSEC001
C        SUBROUTINE CRSEC ***                                           CRSEC002
C    THIS SUBROUTINE IS ACCESSED THROUGH MC AND ZVAL.                   CRSEC003
C    THIS SUBROUTINE CALCULATES THE TOTAL ELASTIC AND TOTAL INELASTIC   CRSEC004
C    CROSS SECTIONS.                                                    CRSEC005
      COMMON ALPE(6),BETE(6),CE(6),FE(6),WE(6),ALFA(15),BEFA(15),       CRSEC006
     1 CFA(15),FFA(15),WFA(15),WF(15),FACI(15),NFA,NAR,SA(3,80),        CRSEC007
     2 ZALT(80),ENR(30),PCFA(3,30),WCFA(3,30),NENR,FDG(3),PSE(3),       CRSEC008
     3 PION(3),AT(3),A(6,3),B(5,3),G(5,3),UH(10),UI(10),UJ(10),         CRSEC009
     4 UD(10),USNU(10),USF(10),UEIN(11),IUTP,IUTM1,DG(3),NSG(3),NIG(3), CRSEC010
     5 NUMGAS,NUMST,WIS(50),NSEC,MUNIT,ISEED,ISTOP,ILAST,EIN,NPRIM,COSI,CRSEC011
     6 H,EMIN,ZSTART,TMIN,THRESH(3),AK(2,3),AJ(3,3),GAMA(2,3),          CRSEC012
     7 TO(3,3),FAC(6),AOE(6),A1E(6),BOE(6),B1E(6),COE(5),DOE(6),        CRSEC013
     8 D1E(6),PROB(40),W(40),NIE(40),A21(3),A22(3),A31(3),A32(3),       CRSEC014
     9 A33(3),B11(3),B12(3),B13(3),C1(3),C21(3),C22(3),C31(3),          CRSEC015
     A C32(3),D1(3),D2(3),F1(3),F2(3),THRI(16),AKI(2,16),AJI(3,16),     CRSEC016
     B GAMAI(2,16),TOI(3,16),SIGT(6),THET(40),NX,CSIE(20),EIT(20),      CRSEC017
     C IEILS,IEILM1,P,R,ZDIS,NPIN,NOP,COSPA,RT,F(40),R1,R2,R3,R4,       CRSEC018
     D R5,XV,YV,ZV,XVN,YVN,ZVN,PA,PHI,EV,WLDSS,NSTAT,NSCS,NPHF,         CRSEC019
     E IR1,IR2,NG,EVPRI,RAN,EMSD,EINEL,EXCS(50),COSPAN,T,FOVAL          CRSEC020
C                                                                       CRSEC021
C                                                                       CRSEC022
      E=EV                                                              CRSEC023
      IF(E .LT. EIT(1))GO TO 1                                          CRSEC024
      Q0=651.3                                                          CRSEC025
      ST1=(1.-(WE(1)/E)**ALPE(1))**BETE(1)                              CRSEC026
      ST2=ALOG(4.*E*CE(1)/WE(1)+EXP(1.))                                CRSEC027
      SIGT(1)= Q0*FE(1)*ST1*ST2/E/WE(1)                                 CRSEC028
C    SIGT(1) IS THE TOTAL INELASTIC CROSS SECTION.                      CRSEC029
      GO TO 4                                                           CRSEC030
1     DO 2 K=1,IEILM1                                                   CRSEC031
      KP1=K+1                                                           CRSEC032
      IF(E .LE. EIT(K) .AND. E .GE. EIT(KP1))GO TO 3                    CRSEC033
2     CONTINUE                                                          CRSEC034
3     SIGT(1)=CSIE(K)+(E-EIT(K))*(CSIE(KP1)-CSIE(K))/(EIT(KP1)-EIT(K))  CRSEC035
4     CONTINUE                                                          CRSEC036
      T1=E**(.23)/1.95E-03/(475.+E**(1.23))                             CRSEC037
      T2=1.6E+03/((E-15.5)*(E-15.5)+590.5)                              CRSEC038
      T3=2.17/((E-2.47)*(E-2.47)+0.296)                                 CRSEC039
      SIGT(2)=2.5*(T1+T2+T3)                                            CRSEC040
C    SIGT(2) IS THE TOAL ELASTIC CROSS SECTION.                         CRSEC041
      RETURN                                                            CRSEC042
      END                                                               CRSEC043
```

```
      SUBROUTINE CTB200                                                 CTB20001
C         SUBROUTINE CTB200 ***                                         CTB20002
C     THIS SUBROUTINE IS ACCESSED THROUGH COLTYP.                       CTB20003
C     THIS SUBROUTINE CALCULATES THE TYPE OF COLLISION IF THE ENERGY E IS CTB20004
C     LESS THAN 200 EV.                                                 CTB20005
      COMMON ALPE(6),BETE(6),CE(6),FE(6),WE(6),ALFA(15),BEFA(15),       CTB20006
     1 CFA(15),FFA(15),WFA(15),WF(15),FACI(15),NFA,NAR,SA(3,80),        CTB20007
     2 ZALT(80),ENR(30),PCFA(3,30),WCFA(3,30),NENR,FDG(3),PSE(3),       CTB20008
     3 PION(3),AT(3),A(6,3),B(5,3),G(5,3),UH(10),UI(10),UJ(10),         CTB20009
     4 UD(10),USNU(10),USF(10),UEIN(11),IUTP,IUTM1,DG(3),NSG(3),NIG(3), CTB20010
     5 NUMGAS,NUMST,WIS(50),NSEC,MUNIT,ISEED,ISTOP,ILAST,EIN,NPRIM,COSI,CTB20011
     6 H,EMIN,ZSTART,TMIN,THRESH(3),AK(2,3),AJ(3,3),GAMA(2,3),          CTB20012
     7 TO(3,3),FAC(6),AOE(6),A1E(6),BOE(6),B1E(6),COE(6),DOE(6),        CTB20013
     8 D1E(6),PROB(40),W(40),NIE(40),A21(3),A22(3),A31(3),A32(3),       CTB20014
     9 A33(3),B11(3),B12(3),B13(3),C1(3),C21(3),C22(3),C31(3),          CTB20015
     A C32(3),D1(3),D2(3),F1(3),F2(3),THRI(16),AKI(2,16),AJI(3,16),     CTB20016
     B GAMAI(2,16),TOI(3,16),SIGT(6),THET(40),NX,CSIE(20),EIT(20),      CTB20017
     C IEILS,IEILM1,P,R,ZDIS,NPIN,NOP,COSPA,RT,F(40),RI,R2,R3,R4,       CTB20018
     D R5,XV,YV,ZV,XVN,YVN,ZVN,PA,PHI,EV,WLOSS,NSTAT,NSCS,NPHF,         CTB20019
     E IRI,IR2,NG,EVPRI,RAN,EMSD,EINEL,EXC5(50),COSPAN,T,FOVAL          CTB20020
C                                                                       CTB20021
C                                                                       CTB20022
      E=EV                                                              CTB20023
      IF(E .LT. 12.8)KADD=8                                             CTB20024
      IF(E .LT. 12.8)GO TO 30                                           CTB20025
C     12.8 EV IS THE LOWEST THRESHOLD OF THE EIGHT N2 STATES WHICH ARE  CTB20026
C     ACCOUNTED FOR INDIVIDUALLY.                                       CTB20027
      Q0=651.3                                                          CTB20028
      K=0                                                               CTB20029
      DO 3 I=1,NUMGAS                                                   CTB20030
      N=2*I-1                                                           CTB20031
      JTOP=NSG(I)-1-NIG(I)                                              CTB20032
      DO 3 J=1,JTOP                                                     CTB20033
      K=K+1                                                             CTB20034
      IF(E .LT. WF(K))GO TO 3                                           CTB20035
      ST1=(1.-(WF(K) /E)**ALFA(K))**BEFA(K)                             CTB20036
      STF2=(WF(K) /E)**CFA(K)/WF(K) *E                                  CTB20037
      ST2=ALOG(4.*E*CFA(K)/WF(K) +EXP(1.))                              CTB20038
      IF(NIE(K) .EQ. 1) ST2=STF2                                        CTB20039
      SIGFA=Q0*FFA(K)*ST1*ST2/E/WF(K)                                   CTB20040
      P=SIGFA/SIGT(N)*FDG(I)*(1.-PSE(I))+P                              CTB20041
      IF(P .GT. RAN) GO TO 12                                           CTB20042
C     INDIVIDUAL ALLOWED STATE PROBABILITIES ARE CALCULATED.            CTB20043
    3 CONTINUE                                                          CTB20044
      KIO=0                                                             CTB20045
```

```
      DO 4  I=1,NUMGAS                                                  CTB20046
      N=2*I-1                                                           CTB20047
      JTOP=NIG(I)                                                       CTB20048
      DO 4  J=1,JTOP                                                    CTB20049
      KIO=KIO+1                                                         CTB20050
      IF(E .LT. THRI(KIO))GO TO 4                                       CTB20051
      TSET=TOI(1,KIO)-TOI(2,KIO)/(E+TOI(3,KIO))                         CTB20052
      GSET=GAMAI(1,KIO)*E/(E+GAMAI(2,KIO))                              CTB20053
      TM=(E-THRI(KIO))/2.                                               CTB20054
      ASET=(AKI(1,KIO)/(E+AKI(2,KIO)))*ALOG(E/AJI(1,KIO)+AJI(2,KIO)+    CTB20055
     1  AJI(3,KIO)/E)                                                   CTB20056
      SIGI=ASET*GSET*(ATAN((TM-TSET)/GSET)+ATAN(TSET/GSET))             CTB20057
      P=SIGI/SIGT(N)*FOG(I)*(1.-PSE(I))+P                               CTB20058
      IF(P .GE. RAN) GO TO 13                                           CTB20059
C    INDIVIDUAL IONIZATION STATE PROBABILITIES ARE CALCULATED.          CTB20060
4     CONTINUE                                                          CTB20061
      KADD=K+KIO                                                        CTB20062
30    J=0                                                               CTB20063
      DO 6  I=1,NENR                                                    CTB20064
      J=J+1                                                             CTB20065
      IF(E .LT. ENR(I)) GO TO 20                                        CTB20066
6     CONTINUE                                                          CTB20067
20    JM1=J-1                                                           CTB20068
      DO 5  I=1,NUMGAS                                                  CTB20069
      N=2*I-1                                                           CTB20070
      NSTAT=KADD+I                                                      CTB20071
      EMEN=E-ENR(JM1)                                                   CTB20072
```

```
      ENME=ENR(J)-E                                                     CTB20073
      ENMEN=ENR(J)-ENR(JM1)                                             CTB20074
      WLOSS =  (WCFA(I,J)*EMEN+  WCFA(I,JM1)*ENME)/ENMEN                CTB20075
C    ENERGY LOSS FOR THE COMBINED STATE IS CALCULATED.                  CTB20076
5     CONTINUE                                                          CTB20077
      GO TO 15                                                          CTB20078
12    WLOSS=WFA(K)                                                      CTB20079
      NSTAT=K                                                           CTB20080
      GO TO 15                                                          CTB20081
13    WLOSS=THRI(KIO)                                                   CTB20082
      NSTAT=K+KIO                                                       CTB20083
15    NSCS=N                                                            CTB20084
      RETURN                                                            CTB20085
      END                                                               CTB20086
```

```
      SUBROUTINE DATA
C         SUBROUTINE DATA ***
C     THIS SUBROUTINE IS ACCESSED THROUGH THE MAIN PROGRAM,
C     ALL THE REST OF THE DATA IS READ IN HERE INCLUDING THE CROSS SECTION
C     PARAMETERS AND ALSO ALL THE OTHER PARAMETERS NEEDED.
      COMMON ALPE(6),BETE(6),CE(6),FE(6),WE(6),ALFA(15),BEFA(15),
     1 CFA(15),FFA(15),WFA(15),WF(15),FACI(15),NFA,NAR,SA(3,80),
     2 ZALT(80),ENR(30),PCFA(3,30),WCFA(3,30),NENR,FDG(3),PSE(3),
     3 PION(3),AT(3),A(6,3),B(5,3),G(5,3),UH(10),UI(10),UJ(10),
     4 UD(10),USNU(10),USF(10),UEIN(11),IUTP,IUTM1,DG(3),NSG(3),NIG(3),
     5 NUMGAS,NUMST,WIS(50),NSEC,MUNIT,ISEED,ISTOP,ILAST,EIN,NPRIM,COSI,
     6 H,EMIN,ZSTART,TMIN,THRESH(3),AK(2,3),AJ(3,3),GAMA(2,3),
     7 TO(3,3),FAC(6),AOE(6),AIE(6),BOE(6),BIE(6),COE(6),DOE(6),
     8 DIE(6),PROB(40),W(40),NIE(40),A21(3),A22(3),A31(3),A32(3),
     9 A33(3),B11(3),B12(3),B13(3),C1(3),C21(3),C22(3),C31(3),
     A C32(3),D1(3),D2(3),F1(3),F2(3),THRI(16),AKI(2,16),AJI(3,16),
     B GAMAI(2,16),TOI(3,16),SIGT(6),THET(40),NX,CSIE(20),EIT(20),
     C IEILS,IEILM1,P,R,ZDIS,NPIN,NOP,COSPA,RT,F(40),R1,R2,R3,R4,
     D R5,XV,YV,ZV,XVN,YVN,ZVN,PA,PHI,EV,WLOSS,NSTAT,NSCS,NPHF,
     E IR1,IR2,NG,EVPRI,RAN,EMSD,EINEL,EXC5(50),COSPAN,T,FOVAL
C
C
      READ(5,500) NUMGAS,NUMST,(NSG(I),I=1,NUMGAS),(NIG(I),I=1,NUMGAS)
C     NUMGAS IS THE NUMBER OF GASES.
C     NUMST IS THE TOTAL NUMBER OF STATES.
C     NSG(I) ARE THE NUMBER OF STATES IN THE ITH GAS,
C     NIG(I) ARE THE NUMBER OF IONIZATION STATES IN THE ITH GAS.
500   FORMAT(8I5)
      WRITE(6,691) NUMGAS,NUMST
691   FORMAT(/' THE NUMBER OF GASES=   ',I5,//,
     1  ' THE TOTAL NUMBER OF STATES=   ',I5,//)
      WRITE(6,695)
695   FORMAT(' NO. STATES',3X,'NO, ION STATES',3X,'GAS NUMBER',/)
      DO 22 I=1,NUMGAS
      WRITE(6,693) NSG(I),NIG(I),I
693   FORMAT(I6,7X,I6,10X,I6)
22    CONTINUE
      WRITE(6,601)
601   FORMAT(///,'  TOTAL INELASTIC CROSS SECTION PARAMETERS ARE GIVEN
     1HERE',//,6X,'GAS',15X,'ALPHA',3X,'BETA',5X,'C',7X,'F',7X,'W',/)
      NUP=2*NUMGAS
      DO 1 I=1,NUMGAS
      READ(5,502) G1,G2,G3,G4,G5,ALPE(I),BETE(I),CE(I),FE(I),WE(I)
C     READ IN THE TOTAL INELASTIC PARAMETERS.
502   FORMAT(5A4,7E8.0)
```

```
      WRITE(6,605)G1,G2,G3,G4,G5,ALPE(I),BETE(I),CE(I),FE(I),WE(I)        DATA0046
605   FORMAT(1X,5A4,9F8.3)                                                DATA0047
1     CONTINUE                                                            DATA0048
      WRITE(6,609)                                                        DATA0049
609   FORMAT(////,' THE P(E,T) PARAMETERS FOLLOW',//,6X,'GAS',14X,        DATA0050
     1  'THRESH',6X,'K',5X,'KB',7X,'J',6X,'JB',6X,'JC',7X,'GAMMAS',       DATA0051
     1  2X,'GAMMAB',6X,'TS',5X,'TA',7X,'TB',/)                            DATA0052
      DO 3 I=1,NUMGAS                                                     DATA0053
      READ(5,502) G1,G2,G3,G4,G5,THRESH(I),(AK(K,I),K=1,2),               DATA0054
     1  (AJ(J,I),J=1,3)                                                   DATA0055
      READ(5,504) (GAMA(K,I),K=1,2),(TO(K,I),K=1,3)                       DATA0056
C   READ IN THE P(E,T) PARAMETERS. THESE ARE USED TO FIND THE SECONDARY   DATA0057
C   ELECTRON ENERGY AFTER AN IONIZATION EVENT.                            DATA0058
504   FORMAT(20X,5E8.0)                                                   DATA0059
      WRITE(6,611) G1,G2,G3,G4,G5,THRESH(I),(AK(K,I),K=1,2),              DATA0060
     1  (AJ(J,I),J=1,3),(GAMA(K,I),K=1,2),(TO(K,I),K=1,3)                 DATA0061
611   FORMAT(1X,5A4,F8.3,1X,5F8.3,2X,2F8.3,F10.3,F8.1,F8.3)               DATA0062
3     CONTINUE                                                            DATA0063
      WRITE(6,613)                                                        DATA0064
613   FORMAT(////,' THE DOUBLY DIFFERENTIAL IONIZATION CROSS SECTION PARDATA0065
     1AMETERS ARE READ IN NOW',//,6X,'GAS',14X,'I/B1',7X,'AT/B2',         DATA0066
     1  7X,'A1/B3',5X,'A2/B4',6X,'A3/B5',6X,'A4/G1',6X,'A5/G2',7X,        DATA0067
     1  'A6/G3',7X,'/G4',8X,'/G5',//)                                     DATA0068
      DO 4 I=1,NUMGAS                                                     DATA0069
      READ(5,562) G1,G2,G3,G4,G5,PION(I),AT(I),(A(K,I),K=1,4)             DATA0070
C   READ IN THE DOUBLY DIFFERENTIAL IONIZATION CROSS SECTION PARAMETERS   DATA0071
C   FOR THE PRIMARY SCATTERING.                                           DATA0072
```

```
C     THIS SCATTERING IS NO LONGER INCLUDED IN THE MONTE CARLO              DATA0073
C     CALCULATION.                                                          DATA0074
C     THE SUBROUTINE DFDW AND THE FUNCTION DCS ARE INCLUDED AT THE          DATA0075
C     END OF THIS LISTING AND CAN BE MODIFIED A LITTLE TO BE PUT INTO       DATA0076
C     THE MONTE CARLO COMPUTATION.                                          DATA0077
562     FORMAT(5A4,5E10.0,E10.2)                                            DATA0078
        READ(5,522) (A(K,I),K=5,6)                                          DATA0079
        WRITE(6,615) G1,G2,G3,G4,G5,PION(I),AT(I),(A(K,I),K=1,6)            DATA0080
615     FORMAT(1X,5A4,2X,F6.2,3X,1PE10.3,2X,F8.2,3X,F7.3,3X,1PE10.3,1X,     DATA0081
      1   1PE10.3,3X,F8.2,1X,F8.2)                                          DATA0082
        READ(5,506) (B(K,I),K=1,5),(G(K,I),K=1,5)                           DATA0083
506     FORMAT(10E8.0)                                                      DATA0084
        WRITE(6,617) (B(K,I),K=1,5),(G(K,I),K=1,5)                          DATA0085
617     FORMAT(21X,F8.2,3X,F8.3,3X,F8.3,2X,1PE10.3,2X,F8.3,3X,1PE10.3       DATA0086
      1 ,2X,F8.3,3X,F8.3,2X,1PE10.3,2X,F8.3,//)                             DATA0087
4       CONTINUE                                                            DATA0088
        WRITE(6,643)                                                        DATA0089
643        FORMAT(////,' THE DOUBLY DIFFERENTIAL SECONDARY IONIZATION       DATA0090
      * CROSS SECTIONS ARE READ IN',//,6X,'GAS',14X,'F1/C1',6X,'F2/C21',    DATA0091
      *   4X,'A2/C22',3X,'A22/C31',3X,'A31/C32',3X,'A32/D1',4X,'A33/D2',    DATA0092
      *   4X,'B11/',8X,'B12/',8X,'B13/',//)                                 DATA0093
        DO 15 I=1,NUMGAS                                                    DATA0094
        READ(5,562)G1,G2,G3,G4,G5,F1(I),F2(I),B11(I),B12(I),B13(I)          DATA0095
        READ(5,564)C1(I),C21(I),C22(I),C31(I),C32(I),D1(I),D2(I)            DATA0096
C     READ IN THE DOUBLY DIFFERENTIAL SECONDARY SCATTERING PARAMETERS.      DATA0097
C     READ IN THE STATES AND THEIR THRESHOLDS.                              DATA0098
564        FORMAT(8E10.0)                                                   DATA0099
        READ(5,564)A21(I),A22(I),A31(I),A32(I),A33(I)                       DATA0100
        WRITE(6,645)G1,G2,G3,G4,G5,F1(I),F2(I),A21(I),A22(I),               DATA0101
      *   A31(I),A32(I),A33(I),B11(I),B12(I),B13(I)                         DATA0102
645        FORMAT(1X,5A4,7(F8.3,2X),F8.3,2X,F10.0,2X,F8.3)                  DATA0103
        WRITE(6,647)C1(I),C21(I),C22(I),C31(I),C32(I),D1(I),D2(I)           DATA0104
647        FORMAT(21X,7(F8.3,2X))                                           DATA0105
15        CONTINUE                                                          DATA0106
        WRITE(6,619)                                                        DATA0107
619     FORMAT(/'1THE STATES WITH THEIR PROBABILITIES AND THRESHOLDS ARE    DATA0108
      1 NOW READ IN',//,5X,'STATE',16X,'PROBABILITY',5X,'THRESHOLD',3X,     DATA0109
      1 'IONEXC NO.',3X,'INDEX NUMBER',/)                                   DATA0110
        DO 5 I=1,NUMST                                                      DATA0111
        READ(5,540) G1,G2,G3,G4,G5,PROB(I),W(I),NIE(I)                      DATA0112
C     READ IN THE PROBABILITIES AND THRESHOLDS FOR THE STATES ABOVE 200 EVDATA0113
540     FORMAT(5A4,2E8.0,I5)                                                DATA0114
        WRITE(6,621) G1,G2,G3,G4,G5,PROB(I),W(I),NIE(I),I                   DATA0115
621     FORMAT(1X,5A4,5X,F10.5,6X,F8.3,4X,I5,9X,I5)                         DATA0116
5       CONTINUE                                                            DATA0117
```

```
      NUMG=NUMST+1                                                      DATA0118
      NIE(NUMG)=4                                                       DATA0119
      WRITE(6,623)                                                      DATA0120
623   FORMAT(////,' THE STATES WITH THEIR CROSS SECTION PARAMETERS ARE  DATA0121
     1READ IN',//)                                                      DATA0122
      WRITE(6,625)                                                      DATA0123
625   FORMAT(6X,'STATE',15X,'W',7X,'ALPHA',4X,'BETA',6X,                DATA0124
     1  'WBAR',7X,'C OR O',10X,'F',9X,'FACI',/)                         DATA0125
      K=0                                                               DATA0126
      DO 7 I=1,NUMGAS                                                   DATA0127
      JTOP=NSG(I)-1-NIG(I)                                              DATA0128
      DO 7 J=1,JTOP                                                     DATA0129
      K=K+1                                                             DATA0130
      READ(5,524) G1,G2,G3,G4,G5,WF(K),WFA(K),FACI(K),ALFA(K),          DATA0131
     1  BEFA(K),CFA(K),FFA(K)                                           DATA0132
C    READ IN THE PARAMETERS USED FOR THE INDIVIDUAL CROSS SECTIONS BELOW DATA0133
C    200 EV.                                                            DATA0134
524   FORMAT(5A4,6E6.0,E8.0)                                            DATA0135
      WF(K)=ABS(WF(K))                                                  DATA0136
      WRITE(6,627) G1,G2,G3,G4,G5,WF(K),ALFA(K),BEFA(K),WFA(K),         DATA0137
     1  CFA(K),FFA(K),FACI(K)                                           DATA0138
627   FORMAT(1X,5A4,3F9.3,F10.3,F11.3,F15.6,2F10.3)                     DATA0139
7     CONTINUE                                                          DATA0140
      NFA=K                                                             DATA0141
      JL=1                                                              DATA0142
      WRITE(6,629)                                                      DATA0143
629   FORMAT(////' THE S(E,T) PARAMETERS FOLLOW',//,6X,'ION. STATES',7X,DATA0144
```

```
     1   'THRI',6X,'KI',6X,'KBI',5X,'JI',5X,'JBI',5X,'JCI',6X,'GAMSI',3X,DATA0145
     1   'GAMBI',7X,'TSI',4X,'TAI',5X,'TBI',/)                           DATA0146
      DO 10 I=1,NUMGAS                                                    DATA0147
      JU=NIG(I)                                                           DATA0148
      DO 9 J=JL,JU                                                        DATA0149
      READ(5,502) G1,G2,G3,G4,G5,THRI(J),(AKI(K,J),K=1,2),(AJI(K,J),     DATA0150
     1  K=1,3)                                                            DATA0151
      READ(5,504)(GAMAI(K,J),K=1,2),(TOI(K,J),K=1,3)                      DATA0152
C    READ IN THE S(E,T) PARAMETERS FOR THE INDIVIDUAL IONIZATION CROSS    DATA0153
C    SECTIONS.                                                            DATA0154
      WRITE(6,611) G1,G2,G3,G4,G5,THRI(J),(AKI(K,J),K=1,2),(AJI(K,J),    DATA0155
     1  K=1,3),(GAMAI(K,J),K=1,2),(TOI(K,J),K=1,3)                        DATA0156
9     CONTINUE                                                            DATA0157
      JL=JU+1                                                             DATA0158
10    CONTINUE                                                            DATA0159
      READ(5,500) NENR                                                    DATA0160
      READ(5,522) (ENR(I),I=1,NENR)                                       DATA0161
      DO 8 I=1,NUMGAS                                                     DATA0162
      READ(5,522) (PCFA(I,J),J=1,NENR)                                    DATA0163
      READ(5,522) (WCFA(I,J),J=1,NENR)                                    DATA0164
C    READ IN THE COMPOSITE STATE PARAMETERS OR ITS PROBABILITY AND        DATA0165
C    THRESHOLD VALUES FOR ENERGIES LESS THAN 200 EV.                      DATA0166
8     CONTINUE                                                            DATA0167
      WRITE(6,633)                                                        DATA0168
633   FORMAT(////,' THE COMPOSITE LEFT-OVER STATES ARE NOW READ IN',//,  DATA0169
     1  4X,'ENERGY',6X,'PROBABILITY',5X,'AVE,ENERGY LOSS',3X,             DATA0170
     1  'GAS INDEX',/)                                                    DATA0171
      DO 11 I=1,NUMGAS                                                    DATA0172
      DO 11 J=1,NENR                                                      DATA0173
      WRITE(6,635) ENR(J),PCFA(I,J),WCFA(I,J),I                           DATA0174
635   FORMAT(3G15.7,3X,I7)                                                DATA0175
11    CONTINUE                                                            DATA0176
522   FORMAT(8E10.0)                                                      DATA0177
      READ(5,500)IEILS                                                    DATA0178
      IEILM1=IEILS-1                                                      DATA0179
      DO 24 I=1,NUMGAS                                                    DATA0180
      READ(5,522)(EIT(J),J=1,IEILS)                                       DATA0181
      READ(5,522)(CSIE(J),J=1,IEILS)                                      DATA0182
C    READ IN THE TOTAL INELASTIC CROSS SECTION AT ENERGIES BELOW 30 EV.   DATA0183
24    CONTINUE                                                            DATA0184
      WRITE(6,671)                                                        DATA0185
671   FORMAT(/////,'1THE TOTAL INELASTIC CROSS SECTION IS READ IN FOR     DATA0186
     *ENERGIES BELOW 30 EV.  THE UNITS ARE 10**(-16) CM**2',//,           DATA0187
     *  4X,'ENERGY',6X,'CROSS SECTION',/)                                 DATA0188
      DO 26 I=1,NUMGAS                                                    DATA0189
```

```
      DO 26 J=1,IEILS                                                   DATA0190
      WRITE(6,673)EIT(J),CSIE(J)                                        DATA0191
673   FORMAT(2G15.7)                                                    DATA0192
26    CONTINUE                                                          DATA0193
      READ(5,572)IUTP,FOVAL                                             DATA0194
572   FORMAT(I5,4E10.0)                                                 DATA0195
      IUTM1=IUTP-1                                                      DATA0196
      READ(5,522)(UEIN(I),I=1,IUTP)                                     DATA0197
      READ(5,522)(UH(I),I=1,IUTM1)                                      DATA0198
      READ(5,522)(UI(I),I=1,IUTM1)                                      DATA0199
      READ(5,522)(UJ(I),I=1,IUTM1)                                      DATA0200
      READ(5,522)(UD(I),I=1,IUTM1)                                      DATA0201
      READ(5,522)(USNU(I),I=1,IUTM1)                                    DATA0202
      READ(5,522)(USF(I),I=1,IUTM1)                                     DATA0203
C   READ IN THE MULTIPLE ELASTIC SCATTERING PARAMETERS FOR THE LONGITU- DATA0204
C   DINAL DISTRIBUTION.                                                 DATA0205
      WRITE(6,651)                                                      DATA0206
651   FORMAT('1PARAMETERS FOR THE LONGITUDINAL OR Z CHARACTERIZATION OF DATA0207
     *THE ELECTRONS WITH ENERGIES BELOW 30 EV ARE NOW PRESENTED',//,    DATA0208
     *4X,'E MIN',4X,'E MAX',6X,'H',8X,'I',8X,'J',8X,'D',5X,'S SUB NU',  DATA0209
     *2X,'S SUB F',3X,'FOVAL',/)                                        DATA0210
      DO 30 I=1,IUTM1                                                   DATA0211
      IP1=I+1                                                           DATA0212
      WRITE(6,653)UEIN(I),UEIN(IP1),UH(I),UI(I),UJ(I),UD(I),USNU(I),    DATA0213
     *USF(I),FOVAL                                                      DATA0214
653   FORMAT(9F9.2)                                                     DATA0215
30    CONTINUE                                                          DATA0216
```

14 JULY 1978 NERDC --- CARD LIST UTILITY

```
      DO 6 I=1,NUMGAS                                                   DATA0217
      READ(5,522)SA(1,1)                                                DATA0218
C     READ IN THE MODEL ATMOSPHERE.                                     DATA0219
C     RIGHT NOW THIS IS SET UP FOR ONLY ONE DENSITY AND ONLY ONE GAS BUT DATA0220
C     IT CAN BE EASILY MODIFIED.                                        DATA0221
6     CONTINUE                                                          DATA0222
      WRITE(6,637)                                                      DATA0223
637   FORMAT(////,' THE STANDARD ATMOSPHERE IS NOW PRINTED',            DATA0224
     1 ' WITH DENSITIES IN 1/CM**3',//,3X,                              DATA0225
     1  'ALTITUDE',10X,'GAS 1',10X,'GAS 2',10X,'GAS 3',/)               DATA0226
      WRITE(6,639)ZALT(1),SA(1,1)                                       DATA0227
639   FORMAT(4G15.7)                                                    DATA0228
      RETURN                                                            DATA0229
      END                                                               DATA0230
```

```
      SUBROUTINE MC
C         SUBROUTINE MC ***
C     THIS IS THE MAJOR SUBROUTINE
C     THIS SUBROUTINE IS ACCESSED THROUGH THE MAIN PROGRAM.
C     IN THIS SUBROUTINE THE ELECTRON IS DEGRADED IN ENERGY IN A COLLISION
C     BY COLLISION MANNER DOWN TO THE CUTOFF ENERGY EMIN.
C     THE FOLLOWING SUBROUTINES ARE CALLED FROM THIS SUBROUTINE:
C     1)RANDU
C     2)ZVAL
C     3)PHF
C     4)PHFEL
C     5)PETI
C     6)SDIFM
C     7)CRSEC
C     8)COLTYP
C     9)MESD
      COMMON ALPE(6),BETE(6),CE(6),FE(6),WE(6),ALFA(15),BEFA(15),
     1 CFA(15),FFA(15),WFA(15),WF(15),FACI(15),NFA,NAR,SA(3,80),
     2 ZALT(80),ENR(30),PCFA(3,30),WCFA(3,30),NENR,FDG(3),PSE(3),
     3 PION(3),AT(3),A(6,3),B(5,3),G(5,3),UH(10),UI(10),UJ(10),
     4 UD(10),USNU(10),USF(10),UEIN(11),IUTP,IUTM1,DG(3),NSG(3),NIG(3),
     5 NUMGAS,NUMST,WIS(50),NSEC,MUNIT,ISEED,ISTOP,ILAST,EIN,NPRIM,COSI,
     6 H,EMIN,ZSTART,TMIN,THRESH(3),AK(2,3),AJ(3,3),GAMA(2,3),
     7 TO(3,3),FAC(6),AOE(6),A1E(6),B0E(6),B1E(6),C0E(6),D0E(6),
     8 D1E(6),PROB(40),W(40),NIE(40),A21(3),A22(3),A31(3),A32(3),
     9 A33(3),B11(3),B12(3),B13(3),C1(3),C21(3),C22(3),C31(3),
     A C32(3),D1(3),D2(3),F1(3),F2(3),THRI(16),AKI(2,16),AJI(3,16),
     B GAMAI(2,16),TOI(3,16),SIGT(6),THET(40),NX,CSIE(20),EIT(20),
     C IEILS,IEILM1,P,R,ZDIS,NPIN,NOP,COSPA,RT,F(40),R1,R2,R3,R4,
     D R5,XV,YV,ZV,XVN,YVN,ZVN,PA,PHI,EV,WLOSS,NSTAT,NSCS,NPHF,
     E IR1,IR2,NG,EVPRI,RAN,EMSD,EINEL,EXC5(50),COSPAN,T,FOVAL
C
C
      WRITE(6,9002)
9002  FORMAT('1')
C     HEADING FOR ELECTRON COUNT CAN BE PUT HERE
C
C     INITIALIZE SOME INTEGERS
      NA=NX-1
      IR1=ISEED
      NI2=0
      NSPA=0
      NG200=0
      IEL=0
      M=9
```

```
C     M IS THE UNIT NUMBER FOR THE TAPE.
C
         DO 8 M1=1,NPIN
C     NPIN = 1 IN OUR CASE.  IT CAN BE VARIED HOWEVER TO ALLOW FOR DIFFER-
C     ENT GROUPS OF ELECTRONS TO BE DEGRADED.
         N=0
C     N KEEPS TRACK OF THE NUMBER OF COLLISIONS
         DO 18 IPRI=1,NOP
C     NOP= THE NUMBER OF PRIMARIES
         IEL=IEL+1
C     IEL KEEPS TRACK OF THE NUMBER OF PRIMARY ELECTRONS THAT HAVE
C     ALREADY BEEN DEGRADED.
C     WRITE OUT IEL IF DESIRED
C
C
C     STARTING PARAMETERS
         ZV=ZSTART
         XV=0.0
         YV=0.0
         COSPA=COSI
         PHI=0.0
         PA=ARCOS(COSI)
         S=0.
         EV=EIN
16       IF(EV .LE. EMIN)GO TO 27
C     EMIN IS THE CUTOFF ENERGY.
         IESCP=0
```

```
      T=0.0                                                             MC000073
C     THIS T=0.0 IS INITIALIZED HERE SO THAT THE STATEMENT              MC000074
C     IF(T .LT. TMIN)GO TO 27 CAN WORK, OTHERWISE THE T WOULD BE        MC000075
C     GREATER THAN TMIN FOR MORE CASES THAN DESIRED                     MC000076
      WRITE(M)NI2                                                       MC000077
C     WRITE(M)NI2                                                       MC000078
      ARGC=1.-COSPA*COSPA                                               MC000079
      IF(ARGC .LT. 0.0E0)GO TO 8989                                     MC000080
      SINPA=SQRT(ARGC)                                                  MC000081
      GO TO 8980                                                        MC000082
8989      SINPA=0.0E0                                                   MC000083
8980      CONTINUE                                                      MC000084
      SINPHI=SIN(PHI)                                                   MC000085
      COSPHI=COS(PHI)                                                   MC000086
C                                                                       MC000087
C                                                                       MC000088
C                                                                       MC000089
C                                                                       MC000090
      IF(EV .GE. EMSD)GO TO 7139                                        MC000091
C     WE GO HERE WHEN THE ELECTRON ENERGY IS LESS THAN EMSD             MC000092
      CALL RANDU                                                        MC000093
      IR1=IR2                                                           MC000094
      R1=R                                                              MC000095
      CALL RANDU                                                        MC000096
      IR1=IR2                                                           MC000097
      R2=R                                                              MC000098
      CALL RANDU                                                        MC000099
      IR1=IR2                                                           MC000100
      R3=R                                                              MC000101
      CALL RANDU                                                        MC000102
      IR1=IR2                                                           MC000103
      R4=R                                                              MC000104
      CALL RANDU                                                        MC000105
      IR1=IR2                                                           MC000106
      R5=R                                                              MC000107
      CALL MESD                                                         MC000108
      GO TO 2213                                                        MC000109
7139  CONTINUE                                                          MC000110
C                                                                       MC000111
C                                                                       MC000112
C     CALCULATE PATHLENGTH RT HERE                                      MC000113
      CALL RANDU                                                        MC000114
      IR1=IR2                                                           MC000115
       CALL ZVAL                                                        MC000116
C     ZVN IS CALCULATED IN ZVAL.                                        MC000117
```

```
      S=S+RT
      XVN=RT*SINPA*COSPHI+XV
      YVN=RT*SINPA*SINPHI+YV
C
C
C   CALCULATE THE COLLISION TYPE
      CALL RANDU
      IR1=IR2
      CALL COLTYP
      NCHE=(NSCS/2)*2
C
C
C   CALCULATE THE AZIMUTH ANGLE HERE
      CALL RANDU
      IR1=IR2
      AZAV=6.283185*R
C   AZAV IS THE AZIMUTHAL SCATTERING ANGLE
      SINAZA=SIN(AZAV)
      COSAZA=COS(AZAV)
C
C
      IF(NIE(NSTAT) .NE. 2) GO TO 700
C
C
C   CALCULATE THE SECONDARY ELECTRON ENERGY T
      CALL RANDU
      IR1=IR2
```

```
      NG=(NSCS+1)/2
      CALL PETI
      EVPRI=EV
      WL=T+WLOSS
      WED=WL/EV
      IF(EV .LE. WL) GO TO 2213
700   CONTINUE
      IF(NCHE .EQ. NSCS)GO TO 751
C    IF NCHE = NSCS THEN THE COLLISION WAS ELASTIC.
      IF(NIE(NSTAT) .EQ. 2)GO TO 2213
      IF(EV.GT. EINEL)GO TO 2213
C    IF THE ENERGY EV IS LESS THAN EINEL AND THE COLLISION IS INELASTIC
C    AND ONLY AN EXCITATION THEN ALLOW IT TO SCATTER BY THE ELASTIC
C    PHASE FUNCTION.
C    THE PRIMARY SCATTERING ANGLE IS NOT COMPUTED AND THE SUBROUTINE
C    THAT IS USEFUL FOR THIS IS NOT INCLUDED IN THIS PROGRAM.  THE
C    SCATTERING FROM THE IONIZATION EVENTS IS MINISCULE FOR THE
C    PRIMARY ELECTRONS.
C
C
C    CALCULATE THE SCATTERING ANGLE AFTER AN ELASTIC COLLISION
751   CONTINUE
      CALL RANDU
      IR1=IR2
C
C    CALCULATE THE SCATTERING ANGLE
      IF(NPHF .EQ. 0)GO TO 771
      CALL PHF
      RR=R
      DO 5 J=1,NA
      J2=J+1
      IF(RR-F(J2 ))4,6,5
    5 CONTINUE
      WRITE(6,500)
  500 FORMAT('1','******-COSINE CELL NOT FOUND-ERROR-*******')
    6 COSPAN=COS(THET(J2))
      GO TO 761
    4 J1=J2-1
      FJ2=F(J2)
      FJ1=F(J1)
      CJ2=THET(J2)
      CJ1=THET(J1)
      PAN=(CJ1*(FJ2-RR)+CJ2*(RR-FJ1))/(FJ2-FJ1)
C    PAN IS THE POLAR SCATTERING ANGLE
      COSPAN=COS(PAN)
```

```
      GO TO 761                                                         MC000190
771   CALL PHFEL                                                        MC000191
761   SINPAN=SQRT(1.-COSPAN*COSPAN)                                     MC000192
      COSPLF=COSPA*COSPAN-SINPA*SINPAN*COSAZA                           MC000193
      IF(COSPLF .GT. 0.999) COSPLF=0.999                                MC000194
      IF(COSPLF .LT. -0.999) COSPLF=-0.999                              MC000195
      ARGC=1.-COSPLF*COSPLF                                             MC000196
      IF(ARGC .LT. 0.0E0)GO TO 8979                                     MC000197
      SINPLF=SQRT(ARGC)                                                 MC000198
      GO TO 8970                                                        MC000199
8979      SINPLF=1.0E-6                                                 MC000200
8970      CONTINUE                                                      MC000201
      PLF=ARCOS(COSPLF)                                                 MC000202
      IF(COSPLF .LE. 0.99) GO TO 20                                     MC000203
      ALF=0.0                                                           MC000204
      GO TO 21                                                          MC000205
20    COSALF=(COSPA*COSPHI*SINPAN*COSAZA-SINPHI*SINPAN*SINAZA+          MC000206
     1   SINPA*COSPHI*COSPAN)/SINPLF                                    MC000207
      SINALF=(COSPA*SINPHI*SINPAN*COSAZA+COSPHI*SINPAN*SINAZA           MC000208
     1  +SINPA*SINPHI*COSPAN)/SINPLF                                    MC000209
      IF(COSALF .LT. -0.999)COSALF=-0.999                               MC000210
      IF(COSALF .GT. 0.999)COSALF=0.999                                 MC000211
      ALF=ARCOS(COSALF)                                                 MC000212
      IF(SINALF .LT. 0.0) ALF=6.28318 5-ALF                             MC000213
   21 CONTINUE                                                          MC000214
      COSPA=COSPLF                                                      MC000215
      PHI=ALF                                                           MC000216
```

```
      PA=PLF                                                            MC000217
 2213 CONTINUE                                                          MC000218
      IF(NCHE .EQ. NSCS)WLOSS=EV*(1.-COSPA)*7.776E-5                    MC000219
C  COMPUTE ENERGY LOSS DURING AN ELASTIC COLLISION.                     MC000220
      WRITE(M)NSTAT,WLOSS                                               MC000221
C     WRITE(M)NSTAT,WLOSS                                               MC000222
      IF(NIE(NSTAT) .EQ. 2)WRITE(M)T                                    MC000223
C     WRITE(M)T                                                         MC000224
      EVN=EV-WLOSS                                                      MC000225
      IF(NIE(NSTAT) .EQ. 2) EVN=EVN-T                                   MC000226
      ZV=ZVN                                                            MC000227
      XV=XVN                                                            MC000228
      YV=YVN                                                            MC000229
      WRITE(M)XV,YV,ZV,EVN,PA,PHI,NG200,EV                              MC000230
C     WRITE(M)XV,YV,ZV,EVN,PA,PHI,NG200,EV                              MC000231
      N=N+1                                                             MC000232
      EV=EVN                                                            MC000233
      IF(ZV .GT. ZALT(1)) GO TO 801                                     MC000234
      IF(ZV .LT. ZALT(NAR))GO TO 801                                    MC000235
      IF(NG200.EQ.2)GO TO 27                                            MC000236
      IF(NG200.EQ.1)GO TO 31                                            MC000237
C   IF NG200=0 THEN THERE IS A PRIMARY COLLISION                        MC000238
C   IF NG200=1 THEN THERE IS A SECONDARY COLLISION                      MC000239
C   IF NG200=2 THEN THERE IS A TERTIARY COLLISION                       MC000240
      IF(T .LT. TMIN) GO TO 27                                          MC000241
C   TMIN IS THE CUTOFF FOR THE SECONDARIES                              MC000242
C   IF T IS GREATER THAN TMIN THEN WE DEGRADE IT  OTHERWISE WE DO NOT.  MC000243
      NG200=1                                                           MC000244
C                                                                       MC000245
C                                                                       MC000246
C   SAVE THE PRIMARY PARAMETERS                                         MC000247
      EVSAV=EV                                                          MC000248
      EV=T                                                              MC000249
      CPSAV=COSPA                                                       MC000250
      PASAV=PA                                                          MC000251
      PHISV=PHI                                                         MC000252
      XVSV=XV                                                           MC000253
      YVSV=YV                                                           MC000254
      ZVSV=ZV                                                           MC000255
C                                                                       MC000256
C                                                                       MC000257
C   CALCULATE THE SECONDARY ELECTRON SCATTERING                         MC000258
      CALL RANDU                                                        MC000259
      IR1=IR2                                                           MC000260
      CALL SDIFM                                                        MC000261
```

```
      COSPLF=COSPA*COSPAN-SINPA*SINPAN*COSAZA                           MC000262
      IF(COSPLF .GT. 0.999) COSPLF=0.999                                MC000263
      IF(COSPLF .LT. -0.999) COSPLF=-0.999                              MC000264
      ARGC=1.-COSPLF*COSPLF                                             MC000265
      IF(ARGC .LT. 0.0E0)GO TO 6979                                     MC000266
      SINPLF=SQRT(ARGC)                                                 MC000267
      GO TO 6970                                                        MC000268
6979      SINPLF=1.0E-6                                                 MC000269
6970      CONTINUE                                                      MC000270
      PLF=ARCOS(COSPLF)                                                 MC000271
      IF(COSPLF .LE. 0.99) GO TO 60                                     MC000272
      ALF=0.0                                                           MC000273
      GO TO 61                                                          MC000274
60    COSALF=(COSPA*COSPHI*SINPAN*COSAZA-SINPHI*SINPAN*SINAZA+          MC000275
     1   SINPA*COSPHI*COSPAN)/SINPLF                                    MC000276
      SINALF=(COSPA*SINPHI*SINPAN*COSAZA+COSPHI*SINPAN*SINAZA           MC000277
     1  +SINPA*SINPHI*COSPAN)/SINPLF                                    MC000278
      IF(COSALF .LT. -0.999)COSALF=-0.999                               MC000279
      IF(COSALF .GT. 0.999)COSALF=0.999                                 MC000280
      ALF=ARCOS(COSALF)                                                 MC000281
      IF(SINALF .LT. 0.0) ALF=6.28318 5-ALF                             MC000282
   61 CONTINUE                                                          MC000283
      COSPA=COSPLF                                                      MC000284
      PHI=ALF                                                           MC000285
      PA=PLF                                                            MC000286
      GO TO 27                                                          MC000287
C                                                                       MC000288
```

```
C
C
31    IF(T .LT. TMIN)GO TO 27
C   TMIN IS CUTOFF OF THE TERTIARIES
      NG200=2
C   SAVE THE SECONDARY PARAMETERS
      EVSAVS=EV
      EV=T
      CPSAVS=COSPA
      PASAVS=PA
      PHISVS=PHI
      XVSVS=XV
      YVSVS=YV
      ZVSVS=ZV
C   CALCULATE THE TERTIARY ELECTRON SCATTERING
      CALL RANDU
      IR1=IR2
      CALL SDIFM
      COSPLF=COSPA*COSPAN-SINPA*SINPAN*COSAZA
      IF(COSPLF .GT. 0.999) COSPLF=0.999
      IF(COSPLF .LT. -0.999) COSPLF=-0.999
      ARGC=1.-COSPLF*COSPLF
      IF(ARGC .LT. 0.0E0)GO TO 5979
      SINPLF=SQRT(ARGC)
      GO TO 5970
5979      SINPLF=1.0E-6
5970      CONTINUE
      PLF=ARCOS(COSPLF)
      IF(COSPLF .LE. 0.99) GO TO 70
      ALF=0.0
      GO TO 71
70    COSALF=(COSPA*COSPHI*SINPAN*COSAZA-SINPHI*SINPAN*SINAZA+
     1    SINPA*COSPHI*COSPAN)/SINPLF
      SINALF=(COSPA*SINPHI*SINPAN*COSAZA+COSPHI*SINPAN*SINAZA
     1  +SINPA*SINPHI*COSPAN)/SINPLF
      IF(COSALF .LT. -0.999)COSALF=-0.999
      IF(COSALF .GT. 0.999)COSALF=0.999
      ALF=ARCOS(COSALF)
      IF(SINALF .LT. 0.0) ALF=6.283185-ALF
   71 CONTINUE
      COSPA=COSPLF
      PHI=ALF
      PA=PLF
C
C
```

```
C
27       IF(EV .GT. EMIN)GO TO 16
      IF(NG200 .EQ. 0)GO TO 29
      EVD=EV
      ZVD=ZV
C
C
C
39    IF(NG200.EQ.1)GO TO 33
C   NOW DEGRADE THE SECONDARY
      EV=EVSAVS
      COSPA=CPSAVS
      PA=PASAVS
      PHI=PHISVS
      XV=XVSVS
      YV=YVSVS
      ZV=ZVSVS
      NG200=1
      IF(IESCP .EQ. 1)GO TO 16
      NI2=1
      WRITE(M)NI2
      WRITE(M)EVD,ZVD
      N=N+1
      NI2=0
      GO TO 16
C
C
```

```
C                                                                         MC000361
33     IF(NG200 .EQ. 0)GO TO 29                                           MC000362
C                                                                         MC000363
C                                                                         MC000364
C    NOW DEGRADE THE PRIMARY                                              MC000365
       EV=EVSAV                                                           MC000366
       COSPA=CPSAV                                                        MC000367
       PA=PASAV                                                           MC000368
       PHI=PHISV                                                          MC000369
       XV=XVSV                                                            MC000370
       YV=YVSV                                                            MC000371
       ZV=ZVSV                                                            MC000372
       IF(IESCP .EQ. 1)GO TO 37                                           MC000373
29       NI2=1                                                            MC000374
C      WRITE(M)NI2                                                        MC000375
       WRITE(M)NI2                                                        MC000376
C    IF NI2=1 THEN THE PRIMARY OR SECONDARY HAS SLIPPED BELOW EMIN AND    MC000377
C    NEEDS TO BE ACCOUNTED FOR                                            MC000378
C    IF NI2=0 THEN THE PRIMARY OR SECONDARY BEING DEGRADED IS ABOVE EMIN  MC000379
C      WRITE(M)EVD,ZVD                                                    MC000380
       WRITE(M)EVD,ZVD                                                    MC000381
       N=N+1                                                              MC000382
       NI2=0                                                              MC000383
37     IF(NG200 .EQ. 0)GO TO 18                                           MC000384
       NG200=0                                                            MC000385
       GO TO 16                                                           MC000386
C                                                                         MC000387
C                                                                         MC000388
C    THE PRIMARY OR SCONDARY HAS ESCAPED IF WE REACH HERE                 MC000389
801    WRITE(6,650) ZV,EV                                                 MC000390
650    FORMAT(' THE ELECTRON HAS ESCAPED AT ALTITUDE=',1PE12.3,           MC000391
     1  4X,'WITH AN ENERGY=',1PE14.6)                                     MC000392
       IESCP=1                                                            MC000393
C    IESCP = 1 MEANS THE ELECTRON HAS ESCAPED.                            MC000394
       IF(NG200 .NE. 0)GO TO 39                                           MC000395
18       CONTINUE                                                         MC000396
       WRITE(6,655)N                                                      MC000397
655    FORMAT(' THE TOTAL NUMBER OF COLLISIONS FOR ALL ELECTRONS=',I12)   MC000398
8      CONTINUE                                                           MC000399
       WRITE(6,483)IR1,IR2                                                MC000400
483    FORMAT(' IR1=',I15,' IR2=',I15)                                    MC000401
       RETURN                                                             MC000402
       END                                                                MC000403
```

```
      SUBROUTINE MESD
C         SUBROUTINE MESD ***
C     THIS SUBROUTINE IS ACCESSED THROUGH MC.
C     THIS SUBROUTINE CALCULATES THE COORDINATES RESULTING FROM THE
C     MULTIPLE ELASTIC SCATTERING OF AN ELECTRON BETWEEN INELASTIC
C     COLLISIONS.
C     THE FOLLOWING SUBROUTINE IS CALLED HERE:
C     1)COLTYP
      COMMON ALPE(6),BETE(6),CE(6),FE(6),WE(6),ALFA(15),BEFA(15),
     1 CFA(15),FFA(15),WFA(15),WF(15),FACI(15),NFA,NAR,SA(3,80),
     2 ZALT(80),ENR(30),PCFA(3,30),WCFA(3,30),NENR,FDG(3),PSE(3),
     3 PION(3),AT(3),A(6,3),B(5,3),G(5,3),UH(10),UI(10),UJ(10),
     4 UD(10),USNU(10),USF(10),UEIN(11),IUTP,IUTM1,DG(3),NSG(3),NIG(3),
     5 NUMGAS,NUMST,WIS(50),NSEC,MUNIT,ISEED,ISTOP,ILAST,EIN,NPRIM,COSI,
     6 H,EMIN,ZSTART,TMIN,THRESH(3),AK(2,3),AJ(3,3),GAMA(2,3),
     7 TD(3,3),FAC(6),A0E(6),A1E(6),B0E(6),B1E(6),C0E(6),D0E(6),
     8 D1E(6),PROB(40),W(40),NIE(40),A21(3),A22(3),A31(3),A32(3),
     9 A33(3),B11(3),B12(3),B13(3),C1(3),C21(3),C22(3),C31(3),
     A C32(3),D1(3),D2(3),F1(3),F2(3),THRI(16),AKI(2,16),AJI(3,16),
     B GAMAI(2,16),TOI(3,16),SIGT(6),THET(40),NX,CSIE(20),EIT(20),
     C IEILS,IEILM1,P,R,ZDIS,NPIN,NOP,COSPA,RT,F(40),R1,R2,R3,R4,
     D RS,XV,YV,ZV,XVN,YVN,ZVN,PA,PHI,EV,WLOSS,NSTAT,NSCS,NPHF,
     E IR1,IR2,NG,EVPRI,RAN,EMSD,EINEL,EXC5(50),COSPAN,T,FOVAL
      CALL CRSEC
      RT=SIGT(2)/SIGT(1)
      PL=-ALOG(R1)*RT
C     PL IS THE PATH LENGTH IN MEAN FREE PATH LENGTHS
      J=0
      DO 1 I=1,IUTM1
      J=J+1
      IP1=I+1
      IF(EV.GE. UEIN(I) .AND. EV.LE. UEIN(IP1))GO TO 2
1     CONTINUE
2     UMU=(UH(J)+PL**UI(J))/PL**UJ(J)
      FO=FOVAL
      IF(PL .LT. 500.0)FO=FOVAL*(1.-EXP(-(PL/USF(J))**0.75))
      UNU=1.
      CH3=(PL/USNU(J))**UD(J)
      IF(CH3 .LT. 1.E-5)GO TO 3
      IF(PL .LT. 25.0)UNU=1.-EXP(-(PL/USNU(J))**UD(J))
      GO TO 4
3     UNU=1.E-5
4     UNUIN=1./UNU
      CH1=UNUIN*ALOG(R2)
      CH2=UNUIN*ALOG(F0)
```

```
      ANUM=-1.                                                          MESD0046
      ADEN=-1.                                                          MESD0047
      IF(CH1 .GT.-55.0)ANUM=R2**UNUIN-1.                                MESD0048
      IF(CH2 .GT.-55.0)ADEN=F0**UNUIN-1.                                MESD0049
      Z=-ALOG(ANUM/ADEN)/UMU                                            MESD0050
C   Z IS IN MEAN FREE PATHS                                             MESD0051
      SIGEE=SIGT(1)+SIGT(2)                                             MESD0052
      FMFP=1./SIGEE/SA(1,1)/1.E-16                                      MESD0053
C   FMFP IS IN CM.                                                      MESD0054
      ZADD=Z*FMFP*1.E-5                                                 MESD0055
C   ZADD IS IN KM.                                                      MESD0056
      ZVN=ZV+ZADD                                                       MESD0057
C   CALCULATE THE Z COORDINATE                                          MESD0058
      PA=3.141592*R4                                                    MESD0059
      PHI=6.283185*R5                                                   MESD0060
      GAM=2.                                                            MESD0061
      IF(PL .LT. 400.)GAM=2.*(1.-EXP(-PL/4.))                           MESD0062
      DEL=(22.+SQRT(PL/0.3))/(PL+0.3)**1.5                              MESD0063
      RHO=0.0                                                           MESD0064
      IF(GAM .GT. 0.2)RHO=(-ALOG(1.-R4)/DEL)**(1./GAM)                  MESD0065
      XADD=COS(PHI)*RHO*FMFP*1.E-5                                      MESD0066
      YADD=SIN(PHI)*RHO*FMFP*1.E-5                                      MESD0067
      XVN=XV+XADD                                                       MESD0068
      YVN=YV+YADD                                                       MESD0069
C   CALCULATE THE X AND Y COORDINATES.                                  MESD0070
      P=0.0                                                             MESD0071
      PSE(1)=0.0                                                        MESD0072
```

```
      RAN=R3                                                            MESD0073
      CALL CTB200                                                       MESD0074
      WLOSS=WLOSS+RT*EV*7.776E-5                                        MESD0075
C     CALCULATE THE ENERGY LOSS DUE TO THE INELASTIC COLLISION AS WELL  MESD0076
C     AS THE ENERGY LOSS DUE TO THE ELASTIC COLLISIONS.                 MESD0077
      RETURN                                                            MESD0078
      END                                                               MESD0079
```

14 JULY 1978 NERDC --- CARD LIST UTILITY

```
      SUBROUTINE PETI                                                   PETI0001
C        SUBROUTINE PETI ***                                            PETI0002
C    THIS SUBROUTINE IS ACCESSED THROUGH MC.                            PETI0003
C    THIS SUBROUTINE CALCULATES THE ENERGY OF THE SECONDARY ELECTRON   PETI0004
C    AFTER AN IONIZATION EVENT.                                         PETI0005
      COMMON ALPE(6),BETE(6),CE(6),FE(6),WE(6),ALFA(15),BEFA(15),       PETI0006
     1 CFA(15),FFA(15),WFA(15),WF(15),FACI(15),NFA,NAR,SA(3,80),        PETI0007
     2 ZALT(80),ENR(30),PCFA(3,30),WCFA(3,30),NENR,FDG(3),PSE(3),       PETI0008
     3 PION(3),AT(3),A(6,3),B(5,3),G(5,3),UH(10),UI(10),UJ(10),         PETI0009
     4 UD(10),USNU(10),USF(10),UEIN(11), IUTP,IUTM1,DG(3),NSG(3),NIG(3), PETI0010
     5 NUMGAS,NUMST,WIS(50),NSEC,MUNIT,ISEED,ISTOP,ILAST,EIN,NPRIM,COSI,PETI0011
     6 H,EMIN,ZSTART,TMIN,THRESH(3),AK(2,3),AJ(3,3),GAMA(2,3),          PETI0012
     7 TO(3,3),FAC(6),A0E(6),A1E(6),B0E(6),B1E(6),C0E(6),D0E(6),        PETI0013
     8 D1E(6),PROB(40),W(40),NIE(40),A21(3),A22(3),A31(3),A32(3),       PETI0014
     9 A33(3),B11(3),B12(3),B13(3),C1(3),C21(3),C22(3),C31(3),          PETI0015
     A C32(3),D1(3),D2(3),F1(3),F2(3),THRI(16),AKI(2,15),AJI(3,16),     PETI0016
     B GAMAI(2,16),TDI(3,16),SIGT(6),THET(40),NX,CSIE(20),EIT(20),      PETI0017
     C IEILS,IEILM1,P,R,ZDIS,NPIN,NOP,COSPA,RT,F(40),R1,R2,R3,R4,       PETI0018
     D R5,XV,YV,ZV,XVN,YVN,ZVN,PA,PHI,EV,WLOSS,NSTAT,NSCS,NPHF,         PETI0019
     E IR1,IR2,NG,EVPRI,RAN,EMSD,EINEL,EXC5(50),COSPAN,T,FOVAL          PETI0020
C                                                                       PETI0021
C                                                                       PETI0022
      E=EV                                                              PETI0023
      RN=R                                                              PETI0024
      N=NG                                                              PETI0025
      TSET=TO(1,N)-TO(2,N)/(E+TO(3,N))                                  PETI0026
      GSET=GAMA(1,N)*E/(E+GAMA(2,N))                                    PETI0027
      TM=(E-THRESH(N))/2.                                               PETI0028
      TN1P=ATAN2((TM-TSET),GSET)                                        PETI0029
      TN2P=ATAN2(TSET,GSET)                                             PETI0030
      TN1=TAN(RN*TN1P+(RN-1.)*TN2P)                                     PETI0031
      T=GSET*TN1   +   TSET                                             PETI0032
C    T IS THE KINETIC ENERGY OF THE SECONDARY ELECTRON.                 PETI0033
      RETURN                                                            PETI0034
      END                                                               PETI0035
```

```
      SUBROUTINE PHF                                                    PHF00001
C         SUBROUTINE PHF ***                                            PHF00002
C     THIS SUBROUTINE IS ACCESSED THROUGH MC.                           PHF00003
C     THIS SUBROUTINE HELPS CALCULATE THE POLAR ANGLE OF SCATTERING     PHF00004
C     AS A RESULT OF AN ELASTIC COLLISION.                              PHF00005
C     ANY PHASE FUNCTION FORM MAY BE PLACED HERE.                       PHF00006
C     RIGHT NOW MODEL 3 IS EXPRESSED HERE.                              PHF00007
C     THIS SUBROUTINE IS MAINLY FOR PHASE FUNCTIONS WHICH ARE NOT       PHF00008
C     EASILY INTEGRATED AND SOLVED FOR THE POLAR ANGLE OF SCATTERING.   PHF00009
      COMMON ALPE(6),BETE(6),CE(6),FE(6),WE(6),ALFA(15),BEFA(15),       PHF00010
     1 CFA(15),FFA(15),WFA(15),WF(15),FACI(15),NFA,NAR,SA(3,80),        PHF00011
     2 ZALT(80),ENR(30),PCFA(3,30),WCFA(3,30),NENR,FDG(3),PSE(3),       PHF00012
     3 PION(3),AT(3),A(6,3),B(5,3),G(5,3),UH(10),UI(10),UJ(10),         PHF00013
     4 UD(10),USNU(10),USF(10),UEIN(11),IUTP,IUTM1,DG(3),NSG(3),NIG(3), PHF00014
     5 NUMGAS,NUMST,WIS(50),NSEC,MUNIT,ISEED,ISTOP,ILAST,EIN,NPRIM,COSI,PHF00015
     6 H,EMIN,ZSTART,TMIN,THRESH(3),AK(2,3),AJ(3,3),GAMA(2,3),          PHF00016
     7 TO(3,3),FAC(6),A0E(6),A1E(6),B0E(6),B1E(6),C0E(6),D0E(6),        PHF00017
     8 D1E(6),PROB(40),W(40),NIE(40),A21(3),A22(3),A31(3),A32(3),       PHF00018
     9 A33(3),B11(3),B12(3),B13(3),C1(3),C21(3),C22(3),C31(3),          PHF00019
     A C32(3),D1(3),D2(3),F1(3),F2(3),THRI(16),AKI(2,16),AJI(3,16),     PHF00020
     B GAMAI(2,16),TOI(3,16),SIGT(6),THET(40),NX,CSIE(20),EIT(20),      PHF00021
     C IEILS,IEILM1,P,R,ZDIS,NPIN,NOP,COSPA,RT,F(40),R1,R2,R3,R4,       PHF00022
     D R5,XV,YV,ZV,XVN,YVN,ZVN,PA,PHI,EV,WLOSS,NSTAT,NSCS,NPHF,         PHF00023
     E IR1,IR2,NG,EVPRI,RAN,EMSD,EINEL,EXC5(50),COSPAN,T,FOVAL          PHF00024
C                                                                       PHF00025
C                                                                       PHF00026
      E=EV                                                              PHF00027
      FT=(E/10.)**(.5)                                                  PHF00028
      FM=FT/(FT+0.87)                                                   PHF00029
      C=1.27*(1.-(12./E)**0.27)                                         PHF00030
      Q2=0.43*E**(-0.29)                                                PHF00031
      QT=(E/100.)**(.84)                                                PHF00032
      Q1=QT/(QT+1.92)                                                   PHF00033
      AA=0.11                                                           PHF00034
      FC=1.-Q1                                                          PHF00035
      FCP=0.0E0                                                         PHF00036
      IF(E .LT. 200.)FC=FC*FM                                           PHF00037
      IF(E .LT. 200.)FCP=1.-Q1-FC                                       PHF00038
      FF1=FC/(1./(2.+AA)-1./AA)                                         PHF00039
      FF2=FCP/(1./(2.+C)-1./C)                                          PHF00040
      AL=1./AA                                                          PHF00041
      CL=1./(C+2.)                                                      PHF00042
      NXM1=NX-1                                                         PHF00043
      DO 1 I=2,NXM1                                                     PHF00044
      TU=COS(THET(I))                                                   PHF00045
```

```
      AU=1./(1.+AA-TU)                                                    PHF00046
      CU=1./(1.+C+TU)                                                     PHF00047
      RLU=1.-EXP(-THET(I)/Q2)*(SIN(THET(I))/Q2+COS(THET(I)))              PHF00048
      F3=Q1/(1.+EXP(-3.1416/Q2))                                          PHF00049
      F3R=F3*RLU                                                          PHF00050
      F(I)=FF1*(AU-AL)-FF2*(CU-CL)+F3R                                    PHF00051
1     CONTINUE                                                            PHF00052
      F(1)=0.0                                                            PHF00053
      F(NX)=1.0                                                           PHF00054
C    THE ARRAY F(I) OF PROBABILITIES FOR SCATTERING IN CERTAIN ANGULAR   PHF00055
C    REGIMES HAS BEEN SET.                                               PHF00056
      RETURN                                                              PHF00057
      END                                                                 PHF00058
```

```
      SUBROUTINE PHFEL
C        SUBROUTINE PHFEL ***
C     THIS SUBROUTINE IS ACCESSED THROUGH MC.
C     THIS SUBROUTINE CALCULATES THE SCATTERING POLAR ANGLE FROM AN
C     ELASTIC COLLISION WHICH IS EXPRESSED ANALYTICALLY.
C     RIGHT NOW THE SCREENED RUTHERFORD DIFFERENTIAL CROSS SECTION
C     IS EXPRESSED ANALYTICALLY.
      COMMON ALPE(6),BETE(6),CE(6),FE(6),WE(6),ALFA(15),BEFA(15),
     1 CFA(15),FFA(15),WFA(15),WF(15),FACI(15),NFA,NAR,SA(3,80),
     2 ZALT(80),ENR(30),PCFA(3,30),WCFA(3,30),NENR,FDG(3),PSE(3),
     3 PION(3),AT(3),A(6,3),B(5,3),G(5,3),UH(10),UI(10),UJ(10),
     4 UD(10),USNU(10),USF(10),UEIN(11),IUTP,IUTM1,DG(3),NSG(3),NIG(3),
     5 NUMGAS,NUMST,WIS(50),NSEC,MUNIT,ISEED,ISTOP,ILAST,EIN,NPRIM,COSI,
     6 H,EMIN,ZSTART,TMIN,THRESH(3),AK(2,3),AJ(3,3),GAMA(2,3),
     7 TO(3,3),FAC(6),AOE(6),A1E(6),BOE(6),B1E(6),COE(6),DOE(6),
     8 D1E(6),PROB(40),W(40),NIE(40),A21(3),A22(3),A31(3),A32(3),
     9 A33(3),B11(3),B12(3),B13(3),C1(3),C21(3),C22(3),C31(3),
     A C32(3),D1(3),D2(3),F1(3),F2(3),THRI(16),AKI(2,16),AJI(3,16),
     B GAMAI(2,16),TOI(3,16),SIGT(6),THET(40),NX,CSIE(20),EIT(20),
     C IEILS,IEILM1,P,R,ZDIS,NPIN,NOP,COSPA,RT,F(40),R1,R2,R3,R4,
     D R5,XV,YV,ZV,XVN,YVN,ZVN,PA,PHI,EV,WLOSS,NSTAT,NSCS,NPHF,
     E IR1,IR2,NG,EVPRI,RAN,EMSD,EINEL,EXC5(50),COSPAN,T,FOVAL
C
C
      E=EV
      ETA=16./E
      COSPAN=1.+2.*ETA-2.*ETA*(1.+ETA)/(1.+ETA-R)
      PAN=ARCOS(COSPAN)
C     PAN IS THE POLAR SCATTERING ANGLE.
      RETURN
      END
```

```
      SUBROUTINE RANDU                                                  RANDU001
C         SUBROUTINE RANDU ***                                          RANDU002
C     THIS SUBROUTINE IS ACCESSED THROUGH MC.                           RANDU003
C     THIS SUBROUTINE CALCULATES THE RANDOM NUMBERS WHOSE VALUES ARE    RANDU004
C     BETWEEN 0.0 AND 1.0.                                              RANDU005
C     RANDOM NUMBER GENERATOR (SEE IBM 360 SSP DESCRIPTION)             RANDU006
      COMMON ALPE(6),BETE(6),CE(6),FE(6),WE(6),ALFA(15),BEFA(15),       RANDU007
     1 CFA(15),FFA(15),WFA(15),WF(15),FACI(15),NFA,NAR,SA(3,80),        RANDU008
     2 ZALT(80),ENR(30),PCFA(3,30),WCFA(3,30),NENR,FDG(3),PSE(3),       RANDU009
     3 PION(3),AT(3),A(6,3),B(5,3),G(5,3),UH(10),UI(10),UJ(10),         RANDU010
     4 UD(10),USNU(10),USF(10),UEIN(11),IUTP,IUTM1,DG(3),NSG(3),NIG(3), RANDU011
     5 NUMGAS,NUMST,WIS(50),NSEC,MUNIT,ISEED,ISTOP,ILAST,EIN,NPRIM,COSI,RANDU012
     6 H,EMIN,ZSTART,TMIN,THRESH(3),AK(2,3),AJ(3,3),GAMA(2,3),          RANDU013
     7 TO(3,3),FAC(6),A0E(6),A1E(6),B0E(6),B1E(6),C0E(6),D0E(6),        RANDU014
     8 D1E(6),PROB(40),W(40),NIE(40),A21(3),A22(3),A31(3),A32(3),       RANDU015
     9 A33(3),B11(3),B12(3),B13(3),C1(3),C21(3),C22(3),C31(3),          RANDU016
     A C32(3),D1(3),D2(3),F1(3),F2(3),THRI(16),AKI(2,16),AJI(3,16),     RANDU017
     B GAMAI(2,16),TOI(3,16),SIGT(6),THET(40),NX,CSIE(20),EIT(20),      RANDU018
     C IEILS,IEILM1,P,R,ZDIS,NPIN,NOP,COSPA,RT,F(40),R1,R2,R3,R4,       RANDU019
     D R5,XV,YV,ZV,XVN,YVN,ZVN,PA,PHI,EV,WLOSS,NSTAT,NSCS,NPHF,         RANDU020
     E IR1,IR2,NG,EVPRI,RAN,EMSD,EINEL,EXC5(50),COSPAN,T,FOVAL          RANDU021
C                                                                       RANDU022
C                                                                       RANDU023
C     YFL AND R ARE THE RANDOM NUMBERS.                                 RANDU024
      IX=IR1                                                            RANDU025
      IY=IX*65539                                                       RANDU026
      IF(IY) 5,6,6                                                      RANDU027
    5 IY=IY+2147483647+1                                                RANDU028
    6 YFL=IY                                                            RANDU029
      YFL=YFL*.4656613E-9                                               RANDU030
      IR2=IY                                                            RANDU031
      R=YFL                                                             RANDU032
      RETURN                                                            RANDU033
      END                                                               RANDU034
```

```
      SUBROUTINE SDIFM
C         SUBROUTINE SDIFM ***
C     THIS SUBROUTINE IS ACCESSED THROUGH MC.
C     THIS SUBROUTINE CALCULATES THE POLAR ANGLE OF SCATTERING OF THE
C     SECONDARY ELECTRON.
      COMMON ALPE(6),BETE(6),CE(6),FE(6),WE(6),ALFA(15),BEFA(15),
     1 CFA(15),FFA(15),WFA(15),WF(15),FACI(15),NFA,NAR,SA(3,80),
     2 ZALT(80),ENR(30),PCFA(3,30),WCFA(3,30),NENR,FDG(3),PSE(3),
     3 PION(3),AT(3),A(6,3),B(5,3),G(5,3),UH(10),UI(10),UJ(10),
     4 UD(10),USNU(10),USF(10),UEIN(11),IUTP,IUTM1,DG(3),NSG(3),NIG(3),
     5 NUMGAS,NUMST,WIS(50),NSEC,MUNIT,ISEED,ISTOP,ILAST,EIN,NPRIM,COSI,
     6 H,EMIN,ZSTART,TMIN,THRESH(3),AK(2,3),AJ(3,3),GAMA(2,3),
     7 TO(3,3),FAC(6),AOE(6),A1E(6),BOE(6),B1E(6),COE(6),DOE(6),
     8 D1E(6),PROB(40),W(40),NIE(40),A21(3),A22(3),A31(3),A32(3),
     9 A33(3),B11(3),B12(3),B13(3),C1(3),C21(3),C22(3),C31(3),
     A C32(3),D1(3),D2(3),F1(3),F2(3),THRI(16),AKI(2,16),AJI(3,16),
     B GAMAI(2,16),TOI(3,16),SIGT(6),THET(40),NX,CSIE(20),EIT(20),
     C IEILS,IEILM1,P,R,ZDIS,NPIN,NDP,COSPA,RT,F(40),R1,R2,R3,R4,
     D R5,XV,YV,ZV,XVN,YVN,ZVN,PA,PHI,EV,WLOSS,NSTAT,NSCS,NPHF,
     E IR1,IR2,NG,EVPRI,RAN,EMSD,EINEL,EXCS(50),COSPAN,T,FOVAL
C
C
      E=EVPRI
      D=D1(NG)/(T+D2(NG))
C     D IS THE C(T) IN THE SEC. DIF. FORM.
      BB=B11(NG)+(E/B12(NG))**B13(NG)
C     B IS THE B(E) IN THE SEC. DIF. FORM.
      C2=C21(NG)+C22(NG)*E
C     C2 IS THE THETA SUBSCRIPT A (E)
      C3=C31(NG)+C32(NG)*E
C     C3 IS THE THETA SUBSCRIPT B (E)
      SQB=SQRT(BB)
      THO=C1(NG)+C2/(T+C3)
      CST=COS(THO)
      FTN=SQB*(-1.-CST)
      STN=SQB*(1.-CST)
      TMNM=ATAN2(FTN,D)-ATAN2(STN,D)
      SLI=ATAN2(STN,D)
      RATAN=R*TMNM+SLI
      TM1=D*TAN(RATAN)/SQB
      COSPAN=TM1+CST
C     PAN IS THE POLAR SCATTERING ANGLE.
      PAN=ARCOS(COSPAN)
      IF(PAN .GT. 3.1416)PAN=PAN-3.1416
      RETURN
```

SDIFM046

END

```
      SUBROUTINE ZVAL
C         SUBROUTINE ZVAL ***
C     THIS SUBROUTINE IS ACCESSED THROUGH MC.
C     THIS SUBROUTINE CALCULATES THE PATH LENGTH TO THE COLLISION AND
C     THE LONGITUDINAL DISTANCE TO THE COLLISION.
C     THE FOLLOWING SUBROUTINE IS CALLED HERE:
C     1)CRSEC
      COMMON ALPE(6),BETE(6),CE(6),FE(6),WE(6),ALFA(15),BEFA(15),
     1 CFA(15),FFA(15),WFA(15),WF(15),FACI(15),NFA,NAR,SA(3,80),
     2 ZALT(80),ENR(30),PCFA(3,30),WCFA(3,30),NENR,FDG(3),PSE(3),
     3 PION(3),AT(3),A(6,3),B(5,3),G(5,3),UH(10),UI(10),UJ(10),
     4 UD(10),USNU(10),USF(10),UEIN(11),IUTP,IUTM1,DG(3),NSG(3),NIG(3),
     5 NUMGAS,NUMST,WIS(50),NSEC,MUNIT,ISEED,ISTOP,ILAST,EIN,NPRIM,COSI,
     6 H,EMIN,ZSTART,TMIN,THRESH(3),AK(2,3),AJ(3,3),GAMA(2,3),
     7 TD(3,3),FAC(6),A0E(6),A1E(6),B0E(6),B1E(6),C0E(6),D0E(6),
     8 D1E(6),PROB(40),W(40),NIE(40),A21(3),A22(3),A31(3),A32(3),
     9 A33(3),B11(3),B12(3),B13(3),C1(3),C21(3),C22(3),C31(3),
     A C32(3),D1(3),D2(3),F1(3),F2(3),THRI(16),AKI(2,16),AJI(3,16),
     B GAMAI(2,16),TOI(3,16),SIGT(6),THET(40),NX,CSIE(20),EIT(20),
     C IEILS,IEILM1,P,R,ZDIS,NPIN,NOP,COSPA,RT,F(40),R1,R2,R3,R4,
     D R5,XV,YV,ZV,XVN,YVN,ZVN,PA,PHI,EV,WLOSS,NSTAT,NSCS,NPHF,
     E IR1,IR2,NG,EVPRI,RAN,FMSD,EINEL,EXCS(50),COSPAN,T,FOVAL
C
C
      R=1.-R
      AC=ABS(COSPA)
      STUN=1.E-16
      FRAC=0.0
      ZCHE=ZV
      ZADD=ZCHE*1.E-5
      ZCHE=ZCHE-ZADD
      J=1
      IF(PA .GT. 1.5708) J=NAR
      ZDIS=0.0
      DG(1)=SA(1,1)
      CALL CRSEC
      DO 45 IDS=1,NUMGAS
      JU=2*IDS
      JL=JU-1
      SUM=0.0
      DO 45 JDS=JL,JU
      SUM=SUM + DG(IDS)*SIGT(JDS)*STUN
   45 CONTINUE
      RMFP=1./SUM
C     RMFP IS THE MEAN FREE PATH OF THE ELECTRON IN THE MODEL ATMOSPHERE.
```

```
      RMFP=RMFP*1.E-5                                                   ZVAL0046
      RV=-ALOG(R)*RMFP                                                  ZVAL0047
      RT=RV                                                             ZVAL0048
C    RV AND RT ARE THE PATH LENGTHS TO THE COLLISION.                   ZVAL0049
      RVCOS=RV*AC                                                       ZVAL0050
      IF(PA .GT. 1.5708) GO TO 7                                        ZVAL0051
      ZVN=ZV-RVCOS                                                      ZVAL0052
C    ZVN IS THE NEW Z COORDINATE OF THE ELECTRON.                       ZVAL0053
      RETURN                                                            ZVAL0054
7     ZVN=ZV+RVCOS                                                      ZVAL0055
      RETURN                                                            ZVAL0056
      END                                                               ZVAL0057
```

```
      SUBROUTINE DFDW(W,E,F,NSCS)                                       DFDW0001
C         SUBROUTINE DFDW ***                                           DFDW0002
C   THIS SUBROUTINE CAN BE USED TO HELP CALCULATE THE POLAR SCATTERING  DFDW0003
C   ANGLE OF THE PRIMARY ELECTRON IN AN IONIZATION EVENT.               DFDW0004
C   THIS SUBROUTINE IS NOT ACCESSED BY MC AND IS INCLUDED ONLY          DFDW0005
C   BECAUSE IT CAN BE EASILY ADAPTED TO BE ACCESSED BY MC.              DFDW0006
C   THIS SUBROUTINE CALLS THE FOLLOWING FUNCTION:                       DFDW0007
C   1)DCS                                                               DFDW0008
      NG=NSCS*2 - 1                                                     DFDW0009
      SUM2=0.0                                                          DFDW0010
      NA=NX-1                                                           DFDW0011
      IF(NX-1)44,33,11                                                  DFDW0012
   11 DO 22 I=2,NX                                                      DFDW0013
      SUM1=SUM2                                                         DFDW0014
      XL=THET(I-1)                                                      DFDW0015
      XU=THET(I)                                                        DFDW0016
      AA=.5*(XU+XL)                                                     DFDW0017
      BB=XU-XL                                                          DFDW0018
      CC=.4305682*BB                                                    DFDW0019
      Z=AA+CC                                                           DFDW0020
      G1=DCS(E,W,NG,Z)                                                  DFDW0021
      Z=AA-CC                                                           DFDW0022
      G2=DCS(E,W,NG,Z)                                                  DFDW0023
      Y=.1739274*(G1+G2)                                                DFDW0024
      CC=.1699905*BB                                                    DFDW0025
      Z=AA+CC                                                           DFDW0026
      G1=DCS(E,W,NG,Z)                                                  DFDW0027
      Z=AA-CC                                                           DFDW0028
      G2=DCS(E,W,NG,Z)                                                  DFDW0029
      Y=BB*(Y+.3260726*(G1+G2))                                         DFDW0030
      SUM2=SUM2+Y                                                       DFDW0031
   22 F(I-1)=SUM1                                                       DFDW0032
   33 F(NX)=SUM2                                                        DFDW0033
   44 CONTINUE                                                          DFDW0034
      DO 4 J=1,NX                                                       DFDW0035
      F(J)=F(J)/F(NX)                                                   DFDW0036
4     CONTINUE                                                          DFDW0037
      F(1)=0.0                                                          DFDW0038
      F(NX)=1.0                                                         DFDW0039
C   THE ARRAY F(I) OF SCATTERING PROBABILITIES WITHIN CERTAIN           DFDW0040
C   ANGULAR BINS IS ESTABLISHED.                                        DFDW0041
      RETURN                                                            DFDW0042
      END                                                               DFDW0043
```

```
      FUNCTION DCS(E,W,NG,Z)
C         FUNCTION DCS ***
C     THIS FUNCTION IS ACCESSED BY DFDW.
C     THIS FUNCTION AIDS IN THE CALCULATION OF THE PLLAR ANGLE OF
C     SCATTERING OF THE PRIMARY ELECTRON IN AN IONIZATION EVENT.
C     THIS FUNCTION CALCULATES THE DIFFERENTIAL CROSS SECTION DCS.
C     THIS FUNCTION MUST BE CHANGED SOME TO BE USEFUL FOR IMPLEMENT
C     WITH THE MONTE CARLO PROGRAM.
      RE=13.6
      A0=.5292E-8
      PI=PION(NG)
      WP=W/PI
      ARG=WP-1.E0
      IF(ARG .LT. 0.0E0)GO TO 20
      T=W-PI
      ALPH2=SQRT(ARG)
      GO TO 21
20    ALPH2=0.0E0
      T=1.0E-8
21    CONTINUE
      AT1=(T+0.1)**A(3,NG)/(T**A(2,NG) + A(1,NG)**A(2,NG))
      AT2=A(4,NG)/(A(5,NG)**A(6,NG) + T**A(6,NG))
      ATS=AT(NG)*(AT1+AT2)
      BETA1=B(1,NG)*(T+0.1)**B(4,NG)/(T**B(3,NG) + B(2,NG)**B(3,NG))
      GAM=G(1,NG)*(T+0.1)**G(4,NG)/(T**G(3,NG) + G(2,NG)**G(3,NG))
      BETA1=BETA1+B(5,NG)
      GAM=GAM+G(5,NG)
      X=2.0*E*(1.0-COS(Z)*SQRT(1.0-W/E)-W/2.0/E)/RE
      FN1=ATS*GAM**3*WP*(X+WP/3.0)
      FD1=((X-BETA1*WP)**2+4.0*GAM*X)**3
      FN2=EXP(-1.0)
      IF(ALPH2 .GT. 1.E-6)FN2=EXP(-2.*ATAN2(ALPH2,2.)/ALPH2)
      FD2=1.0
      IF(ALPH2 .GT. .1)FD2=1.0-EXP(-6.2832/ALPH2)
      FOX=FN1*FN2/FD1/FD2
      DEN=4.0*A0*A0*SQRT(1.0-W/E)/W/X
      DCS=DEN*FOX*1.E+16*SIN(Z)
C     DCS IS THE DIFFERENTIAL CROSS SECTION FOR AN ELECTRON OF ENERGY
C     E LOSING ENERGY W WITH A SCATTERING OF Z (POLAR ANGLE).
      RETURN
      END
```

APPENDIX B

GETDAT PROGRAM

The Getdat program is listed in this appendix. This program was written entirely by the author. This program (written in Fortran IV) collects the collision data from the magnetic tape and coalesces and systematizes it.

```
C          ***GETDAT PROGRAM***                                          MAIN0001
C     THIS PROGRAM TAKES THE COLLISION DATA FROM THE MAGNETIC TAPE       MAIN0003
C     AND COALESCES AND SYSTEMATIZES IT.                                 MAIN0004
C     THIS PROGRAM IS RUN IN CLASS = L                                   MAIN0005
C     THE FOLLOWING PROGRAMS ARE CALLED IN THIS MAIN PROGRAM:            MAIN0006
C     1)RDCARD                                                           MAIN0007
C     2)MATIN                                                            MAIN0008
C     3)RDTAPE                                                           MAIN0009
C     4)WRTDAT                                                           MAIN0010
C                                                                        MAIN0011
C     THIS COMMON BLOCK CONTAINS ALL THE VARIABLES OF USE BY THE         MAIN0012
C     SUBROUTINES.  IT IS SO LONG TO PERMIT THE OPTIMIZE=2 IN THE        MAIN0013
C     H COMPILER TO BE USED FOR MOST EFFICIENCY.                         MAIN0014
      COMMON ALAB(20),ANEI(5,20,100),ALT(20),EAVE(3),EIP(100),           MAIN0015
     1 EXC5(50),JES(50),JIS(50),JZE(3,50,80),JSEC(50,80),KREX(10,40,40),MAIN0016
     2 NIE(40),NZX(20),NOFE(3,80),NCRO(10),RHO(40),SA(3,80),SIG(100),    MAIN0017
     3 TOTE(3,80),TN1(3,80),TN5(3,80),TN10(3,80),WIE(50),WIS(50),        MAIN0018
     4 YSPEC(100),ZNUM(10),ZALT(80),NUMGAS,NAR1,NVR,NJMST,NUMG,NRM,      MAIN0019
     5 NSEC,NSPZ,NEIP,NEXC,NTOP,NAR,NSPEC,NRHO,NAVEE,NPRIM,EIN,          MAIN0020
     6 ZVAL,EMIN,DENGS,M,NSPUN,NSPR,ANER(1,10,20,100),RYS(10),NSPRO      MAIN0021
C                                                                        MAIN0022
C                                                                        MAIN0023
       CALL RDCARD                                                       MAIN0024
       CALL MATIN                                                        MAIN0025
       CALL RDTAPE                                                       MAIN0026
       CALL WRTDAT                                                       MAIN0027
       STOP                                                              MAIN0028
       END                                                               MAIN0029
```

```
      SUBROUTINE RDCARD                                                 RDCARD01
C        SUBROUTINE RDCARD ***                                          RDCARD02
C     THIS SUBROUTINE IS ACCESSED BY THE MAIN PROGRAM.                  RDCARD03
C     THIS PROGRAM READS IN THE DATA FROM THE CARDS AND SETS UP ALL     RDCARD04
C     THE NECESSARY INFORMATION.                                        RDCARD05
      COMMON ALAB(20),ANEI(5,20,100),ALT(20),EAVE(3),EIP(100),          RDCARD06
     1 EXC5(50),JES(50),JIS(50),JZE(3,50,80),JSEC(50,80),KREX(10,40,40),RDCARD07
     2 NIE(40),NZX(20),NOFE(3,80),NCRO(10),RHO(40),SA(3,80),SIG(100),   RDCARD08
     3 TOTE(3,80),TN1(3,80),TN5(3,80),TN10(3,80),WIE(50),WIS(50),       RDCARD09
     4 YSPEC(100),ZNUM(10),ZALT(80),NUMGAS,NAR1,NVR,NUMST,NUMG,NRM,     RDCARD10
     5 NSEC,NSPZ,NEIP,NEXC,NTOP,NAR,NSPEC,NRHO,NAVEE,NPRIM,EIN,         RDCARD11
     6 ZVAL,EMIN,DENGS,M,NSPUN,NSPR,ANER(1,10,20,100),RYS(10),NSPRO     RDCARD12
C                                                                       RDCARD13
C                                                                       RDCARD14
C     READ IN THE NECESSARY DATA CARDS                                  RDCARD15
      M=9                                                               RDCARD16
C     M IS THE LOGICAL UNIT NUMBER FOR THE TAPE.                        RDCARD17
7     READ(5,2248)(ALAB(I),I=1,20)                                      RDCARD18
C     FIRST CARD IS THE TITLE CARD.                                     RDCARD19
2248  FORMAT(20A4)                                                      RDCARD20
      WRITE(6,2249)(ALAB(I),I=1,20)                                     RDCARD21
2249  FORMAT('1',20A4,///)                                              RDCARD22
      READ(5,2244)NAVEE,NRHO,NVR,NRM,NSPEC,NSPUN,NSPRO                  RDCARD23
C     IF NAVEE=1 THEN WE WANT TO CALCULATE THE AVERAGE ENERGY OF THE    RDCARD24
C     PRIMARY AT A GIVEN DISTANCE                                       RDCARD25
C     IF NRHO=1 THEN WE WANT TO CALCULATE THE DISTRIBUTION OF THE       RDCARD26
C     EXCITATIONS AS A FUNCTION OF RHO FOR A GIVEN NVR NO. OF Z VALUES. RDCARD27
C     NVR IS THE NO. OF Z VALUES AT WHICH YOU WANT THE DISTRIBUTION     RDCARD28
C     NRM IS THE NUMBER OF RHO VALUES IN THE MATRIX IN WHICH THE        RDCARD29
C     EXCITATIONS WILL BE INPUT                                         RDCARD30
C     IF NSPEC=1 THEN WE WANT TO GET OUT THE SPECTRUM OF ELECTRONS      RDCARD31
C     IF NSPUN = 1 THEN WE WANT TO PUNCH OUT THE YIELD SPECTRUM OF THE  RDCARD32
C     ELECTRONS.                                                        RDCARD33
C     IF NSPRO = 1 THEN WE WANT THE YIELD SPECTRUM AS A FUNCTION OF RHO RDCARD34
      IF(NVR .EQ. 0)NVR=1                                               RDCARD35
C     NVR=1 FOR DEFAULT                                                 RDCARD36
      WRITE(6,710) NAVEE,NRHO,NVR,NRM,NSPEC,NSPUN,NSPRO                 RDCARD37
710   FORMAT(' NAVEE=',I5,/,' NRHO=',I5,/,' NVR=',I5,/,' NRM=',I5,/,    RDCARD38
     * ' NSPEC=',I5,/,' NSPUN=',I5,/   ,' NSPRO=',I5,///)               RDCARD39
      READ(5,2246)NEXC,NPRIM,NAR,NSEC,NUMST,NUMGAS,NEIP,NSPZ,NSPR       RDCARD40
2246  FORMAT(I10,14I5)                                                  RDCARD41
C     NEXC IS THE TOTAL NUMBER OF COLLISIONS                            RDCARD42
C     NPRIM IS THE NUMBER OF PRIMARY ELECTRONS                          RDCARD43
C     NAR IS THE NUMBER OF ALTITUDE INTERVALS                           RDCARD44
C     NSEC IS THE NUMBER OF LOWER ELECTRON ENERGY BIN ENDS.             RDCARD45
```

```
C     NUMST IS THE NUMBER OF STATES                                         RDCARD46
C     NUMGAS IS THE NUMBER OF GASES                                         RDCARD47
C     NEIP IS THE NUMBER OF ENERGY INTERVALS FOR THE SPECTRUM               RDCARD48
C     NSPZ ARE THE NUMBER OF Z VALUES AT WHICH WE WANT THE SPECTRUM         RDCARD49
C     NSPR IS THE NUMBER OF RHO VALUES FOR EACH Z VALUE AT WHICH WE         RDCARD50
C     WANT THE YIELD SPECTRUM.                                              RDCARD51
2244  FORMAT(16I5)                                                          RDCARD52
      WRITE(6,701) NEXC,NPRIM,NAR,NSEC,NUMST,NUMGAS,NEIP,NSPZ               RDCARD53
701   FORMAT(' TOTAL NUMBER OF COLLISIONS=',I10,/,                          RDCARD54
     *  ' NUMBER OF PRIMARIES=',I10,/,' NUMBER OF ALT. INTERVALS=',I10,     RDCARD55
     *  /,' NUMBER OF SECONDARY ENERGY ENDS=',I10,/,                        RDCARD56
     *  ' NUMBER OF INELASTIC STATES=',I10,/,' NUMBER OF GASES=',I10,       RDCARD57
     * /,' NUMBER OF ENERGY INTERVALS FOR SPECTRUM=',I10,/,                 RDCARD58
     *  ' NUMBER OF Z VALUES AT WHICH WE WANT A SPECTRUM=',I10)             RDCARD59
      READ(5,2255)ZVAL,EIN,EMIN,DENGS                                       RDCARD60
C     ZVAL IS THE STARTING ALTITUDE                                         RDCARD61
C     EIN IS THE INITIAL ELECTRON ENERGY                                    RDCARD62
C     EMIN IS THE LOWEST ENERGY THE ELECTRONS ARE ALLOWED TO DEGRADE TO     RDCARD63
C     DENGS IS THE DENSITY OF THE GAS IN 1./CM**3                           RDCARD64
      WRITE(6,703)EIN,ZVAL,EMIN,DENGS                                       RDCARD65
703   FORMAT(////,' INC. ENERGY=',G15.7,' EV',/,' INC. ALT.=',G15.7,        RDCARD66
     *  ' KM.',/,' EMIN=',G15.7,' EV',/,' GAS DENSITY=',G15.7,              RDCARD67
     *  ' CM**(-3)')                                                        RDCARD68
      IF(NSPEC .NE. 1)GO TO 1142                                            RDCARD69
      READ(5,2244)(NZX(I),I=1,NSPZ)                                         RDCARD70
C     NZX(I) ARE THE INDEX VALUES ON THE Z VALUES AT WHICH THE YIELD        RDCARD71
C     SPECTRUM IS CALCULATED.                                               RDCARD72
```

```
      READ(5,2255)(ALT(I),I=1,NSPZ)                                     RDCARD73
C    ALT(I) ARE THE Z VALUES AT WHICH THE YIELD SPECTRUM IS CALCULATED. RDCARD74
      READ(5,2255)(RYS(I),I=1,NSPR)                                     RDCARD75
C    RYS(I) ARE THE RHO VALUES AT WHICH THE YIELD SPECTRUM IS CALCULATED.RDCARD76
      READ( 5,2255)(EIP(I),I=1,NEIP)                                    RDCARD77
C    EIP(I) ARE THE ENERGY VALUES AT WHICH THE YIELD SPECTRUM IS CALCU- RDCARD78
C    LATED.                                                             RDCARD79
      NEIP1=NEIP-1                                                      RDCARD80
      WRITE(6,3499)                                                     RDCARD81
3499  FORMAT(     '1ALTITUDES WHERE SPECTRUM WILL BE CALCULATED',//,    RDCARD82
     *  ' INDEX',5X,'ALT. IN KM.',/)                                    RDCARD83
      DO 3497 I=1,NSPZ                                                  RDCARD84
      WRITE(6,3504)NZX(I),ALT(I)                                        RDCARD85
3497  CONTINUE                                                          RDCARD86
      WRITE(6,3599)                                                     RDCARD87
3599  FORMAT('1RHO VALUES WHERE SPECTRUM WILL BE CALCULATED',//,        RDCARD88
     *    ' RHO (IN KM.)',/)                                            RDCARD89
      DO 3597 I=1,NSPR                                                  RDCARD90
      WRITE(6,3604)RYS(I)                                               RDCARD91
3604  FORMAT(1PE11.3)                                                   RDCARD92
3597  CONTINUE                                                          RDCARD93
      WRITE(6,3515)                                                     RDCARD94
3515  FORMAT(///,' SPECTRA INDEX',8X,'ENERGY INTERVAL ENDS',///)        RDCARD95
      DO 4515 I=2,NEIP                                                  RDCARD96
      IM1=I-1                                                           RDCARD97
      WRITE(6,3517)IM1,EIP(IM1),EIP(I)                                  RDCARD98
3517  FORMAT(I7,12X,1PE11.3,3X,1PE11.3)                                 RDCARD99
4515  CONTINUE                                                          RDCAR100
1142  CONTINUE                                                          RDCAR101
      NAR1=NAR+1                                                        RDCAR102
      NUMG=NUMST+NUMGAS                                                 RDCAR103
      NTOP=NSEC-1                                                       RDCAR104
      IF(NRHO .NE. 1) GO TO 1141                                        RDCAR105
      READ(5,2244)(NCRO(J),J=1,NVR)                                     RDCAR106
C    NCRO(J) ARE THE INDEX VALUES OF THE Z DISTANCES AT WHICH A RHO     RDCAR107
C    INTENSITY PLOT IS DESIRED.                                         RDCAR108
      READ(5,2255)(ZNUM(J),J=1,NVR)                                     RDCAR109
C    ZNUM(J) ARE THE Z VALUES AT WHICH A RHO INTENSITY PLOT IS DESIRED. RDCAR110
      WRITE(6,3503)                                                     RDCAR111
3503  FORMAT(///,'1ALTITUDES WHERE RHO EXC. WILL BE CALCULATED',//,     RDCAR112
     * ' INDEX',5X,'ALT. IN KM.',/)                                     RDCAR113
      DO 4503 J=1,NVR                                                   RDCAR114
4503  WRITE(6,3504)NCRO(J),ZNUM(J)                                      RDCAR115
3504  FORMAT(I5,5X,1PE11.3)                                             RDCAR116
      READ(5,2255)(RHO(I),I=1,NRM)                                      RDCAR117
```

```
C     RHO(I) ARE THE RHO VALUES AT WHICH THE RHO INTENSITY PLOT IS          RDCAR118
C     CALCULATED,                                                           RDCAR119
      WRITE(6,3505)                                                         RDCAR120
3505  FORMAT(////,' RHO INTERVAL',10X,'RHO BIN ENDS',/)                     RDCAR121
      DO 4505 I=2,NRM                                                       RDCAR122
      IM1=I-1                                                               RDCAR123
4505  WRITE(6,3506)IM1,RHO(IM1),RHO(I)                                      RDCAR124
3506  FORMAT(I5,11X,1PE11.3,5X,1PE11.3)                                     RDCAR125
1141  CONTINUE                                                              RDCAR126
      READ(5,2255)(ZALT(I),I=1,NAR)                                         RDCAR127
C     ZALT(I) ARE THE Z INTERVALS INTO WHICH THE LONGITUDINAL REGIME        RDCAR128
C     IS DIVIDED.                                                           RDCAR129
C     ZALT(1) AND ZALT(NAR) MUST CORRESPOND TO THE Z BOUNDS SET IN THE      RDCAR130
C     MONTE CARLO PROGRAM.                                                  RDCAR131
C     THE OTHER VALUES IN BETWEEN ARE VARIABLE.                             RDCAR132
      WRITE(6,3507)                                                         RDCAR133
3507  FORMAT('1ALT. INDEX',8X,'ALT. ENDS',/)                                RDCAR134
      DO 4507 I=1,NAR                                                       RDCAR135
4507  WRITE(6,3508)I,ZALT(I)                                                RDCAR136
3508  FORMAT(I8,9X,1PE11.3)                                                 RDCAR137
C                                                                           RDCAR138
C                                                                           RDCAR139
C     WIS(I) AND EXC5(I) ARE MAINLY USEFUL WHEN LOCAL ENERGY DEGRADA-       RDCAR140
C     TION IS USED BELOW EMIN.                                              RDCAR141
      READ(5,2255)(WIS(I),I=1,NSEC)                                         RDCAR142
C     WIS(I) ARE THE ENERGY BIN ENDS FOR THE LOW ENERGY ELECTRONS.          RDCAR143
      READ(5,2255)(EXC5(I),I=1,NTOP)                                        RDCAR144
```

```
C    EXC5(I) ARE THE NUMBER OF EXCITATIONS THAT CAUSE THE 3914 A         RDCAR145
C    EMISSION THAT ARE EXCITED BY EACH ELECTRON IN THESE LOWER ENERGY    RDCAR146
C    BINS.                                                               RDCAR147
2255  FORMAT(8E10.0)                                                     RDCAR148
      WRITE(6,3509)                                                      RDCAR149
3509  FORMAT('1EXC. OF 3914A BY SECONDARIES',5X,'ENERGY BIN ENDS',/)     RDCAR150
      DO 4509 I=1,NTOP                                                   RDCAR151
      IP1=I+1                                                            RDCAR152
4509  WRITE(6,3510)EXC5(I),WIS(I),WIS(IP1)                               RDCAR153
3510  FORMAT(G15.7,16X,G15.7,5X,G15.7)                                   RDCAR154
      READ(5,2266)(NIE(I),I=1,NUMG)                                      RDCAR155
C    NIE(I) INDICES INDICATE WHICH STATES ARE IONIZATION AND WHICH       RDCAR156
C    ARE ELASTIC.                                                        RDCAR157
2266  FORMAT(16I5)                                                       RDCAR158
      WRITE(6,3511)                                                      RDCAR159
3511  FORMAT(///,' STATE NO.',5X,'NIE VALUE',/)                          RDCAR160
      DO 4511 I=1,NUMG                                                   RDCAR161
4511  WRITE(6,3512)I,NIE(I)                                              RDCAR162
3512  FORMAT(I7,I12)                                                     RDCAR163
      RETURN                                                             RDCAR164
      END                                                                RDCAR165
```

```
      SUBROUTINE MATIN                                                  MATIN001
C         SUBROUTINE MATIN ***                                          MATIN002
C     THIS SUBROUTINE IS ACCESSED BY THE MAIN PROGRAM.                  MATIN003
C     THIS SUBROUTINE INITIALIZES ALL THE MATRICES.                     MATIN004
      COMMON ALAB(20),ANEI(5,20,100),ALT(20),EAVE(3),EIP(100),          MATIN005
     1 EXC5(50),JES(50),JIS(50),JZE(3,50,80),JSEC(50,80),KREX(10,40,40),MATIN006
     2 NIE(40),NZX(20),NOFE(3,80),NCRD(10),RHO(40),SA(3,80),SIG(100),   MATIN007
     3 TOTE(3,80),TN1(3,80),TN5(3,80),TN10(3,80),WIE(50),WIS(50),       MATIN008
     4 YSPEC(100),ZNUM(10),ZALT(80),NUMGAS,NAR1,NVR,NUMST,NUMG,NRM,     MATIN009
     5 NSEC,NSPZ,NEIP,NEXC,NTOP,NAR,NSPEC,NRHO,NAVEE,NPRIM,EIN,         MATIN010
     6 ZVAL,EMIN,DENGS,M,NSPUN,NSPR,ANER(1,10,20,100),RYS(10),NSPRO     MATIN011
C                                                                       MATIN012
C                                                                       MATIN013
C     INITIALIZE THE MATRICES                                           MATIN014
      DO 26 K=1,3                                                       MATIN015
      DO 26 I=1,NAR1                                                    MATIN016
      TOTE(K,I)=0.0E0                                                   MATIN017
      NOFE(K,I)=0                                                       MATIN018
      TN10(K,I)=0.0E0                                                   MATIN019
26    TN5(K,I)=0.0E0                                                    MATIN020
      DO 139 I=1,NVR                                                    MATIN021
      DO 139 J=1,NUMG                                                   MATIN022
      DO 139 K=1,NRM                                                    MATIN023
139   KREX(I,J,K)=0                                                     MATIN024
      DO 140 K=1,3                                                      MATIN025
      DO 140 I=1,NUMG                                                   MATIN026
      DO 140 J=1,NAR1                                                   MATIN027
140   JZE(K,I,J)=0                                                      MATIN028
      DO 142 I=1,NSEC                                                   MATIN029
      DO 142 J=1,NAR1                                                   MATIN030
142   JSEC(I,J)=0                                                       MATIN031
      DO 143 J=1,NSEC                                                   MATIN032
143   JIS(J)=0                                                          MATIN033
      DO 144 J=1,NUMG                                                   MATIN034
      WIE(J)=0.0E0                                                      MATIN035
144   JES(J)=0                                                          MATIN036
      DO 145 K=1,1                                                      MATIN037
      DO 145 I=1,NSPZ                                                   MATIN038
      DO 145 J=1,NEIP                                                   MATIN039
      ANEI(K,I,J)=0.0E0                                                 MATIN040
      DO 145 L=1,NSPR                                                   MATIN041
145   ANER(K,L,I,J)=0.0E0                                               MATIN042
      RETURN                                                            MATIN043
      END                                                               MATIN044
```

```
      SUBROUTINE RDTAPE                                                 RDTAPE01
C         SUBROUTINE RDTAPE ***                                         RDTAPE02
C     THIS SUBROUTINE IS ACCESSED BY THE MAIN PROGRAM.                  RDTAPE03
C     THIS SUBROUTINE READS OFF OF THE TAPE AND PLACES THE EVENTS INTO  RDTAPE04
C     THEIR PROPER INTERVALS AND BOXES.                                 RDTAPE05
      COMMON ALAB(20),ANEI(5,20,100),ALT(20),EAVE(3),EIP(100),          RDTAPE06
     1 EXC5(50),JES(50),JIS(50),JZE(3,50,80),JSEC(50,80),KREX(10,40,40),RDTAPE07
     2 NIE(40),NZX(20),NOFE(3,80),NCRO(10),RHO(40),SA(3,80),SIG(100),   RDTAPE08
     3 TOTE(3,80),TN1(3,80),TN5(3,80),TN10(3,80),WIE(50),WIS(50),       RDTAPE09
     4 YSPEC(100),ZNUM(10),ZALT(80),NUMGAS,NAR1,NVR,NUMST,NUMG,NRM,     RDTAPE10
     5 NSEC,NSPZ,NEIP,NEXC,NTOP,NAR,NSPEC,NRHO,NAVEE,NPRIM,EIN,         RDTAPE11
     6 ZVAL,EMIN,DENGS,M,NSPUN,NSPR,ANER(1,10,20,100),RYS(10),NSPRD     RDTAPE12
C                                                                       RDTAPE13
C                                                                       RDTAPE14
      CONST=DENGS*DENGS*2.163E-35                                       RDTAPE15
C     CONST IS USED IN FINDING THE RADIAL YIELD SPECTRA WHICH MUST      RDTAPE16
C     BE DIVIDED BY AN AREA.                                            RDTAPE17
C     (4.651E-23 GM/MOLECULE)**2 * (1.E+5 CM/KM)**2  =  2.163E-35       RDTAPE18
      N1Z=0                                                             RDTAPE19
      DO 30  I=1,NEXC                                                   RDTAPE20
      ISAV=I                                                            RDTAPE21
      ELOSS=0.0E0                                                       RDTAPE22
C     ELOSS IS THE ENERGY LOSS BY EACH ELECTRON                         RDTAPE23
      READ(M,END=333)NCHE                                               RDTAPE24
      IF(NCHE .EQ. 0) GO TO 1131                                        RDTAPE25
C     THIS IF STATEMENT DETERMINES IF THE ELECTRON HAS DROPPED BELOW THE RDTAPE26
C     ENERGY CUTOFF.                                                    RDTAPE27
C     IF NCHE=1, THEN WE KNOW THERE IS AN ELECTRON TO BE PUT INTO ITS   RDTAPE28
C     PROPER BIN BELOW THE ENERGY CUTOFF.                               RDTAPE29
      READ(M)WLS,Z                                                      RDTAPE30
      ELOSS=ELOSS+WLS                                                   RDTAPE31
C     WLS=ENERGY OF THE ELECTRON                                        RDTAPE32
C     Z=ALTITUDE IN KM.                                                 RDTAPE33
      DO 83  I1=1,NTOP                                                  RDTAPE34
      I1P1=I1+1                                                         RDTAPE35
      IF(WLS .GT. WIS(I1) .AND. WLS .LT. WIS(I1P1))II=I1                RDTAPE36
83       CONTINUE                                                       RDTAPE37
      IF(Z .GT. ZALT(1))JSEC(II,1)=JSEC(II,1)+1                         RDTAPE38
      IF(Z .LT. ZALT(NAR))JSEC(II,NAR1)=JSEC(II,NAR1)+1                 RDTAPE39
      DO 84  I2=2,NAR                                                   RDTAPE40
      I2M1=I2-1                                                         RDTAPE41
      IF(Z .GT. ZALT(I2) .AND. Z .LT. ZALT(I2M1))JSEC(II,I2)=           RDTAPE42
     *  JSEC(II,I2)+1                                                   RDTAPE43
84       CONTINUE                                                       RDTAPE44
      JIS(II)=JIS(II)+1                                                 RDTAPE45
```

```
      IF(NAVEE .EQ. 1)GO TO 6611                                        RDTAPE46
      GO TO 30                                                          RDTAPE47
1131       CONTINUE                                                     RDTAPE48
      READ(M)N,WL                                                       RDTAPE49
      ELOSS=ELOSS+WL                                                    RDTAPE50
C    N=NUMBER OF THE STATE                                              RDTAPE51
C    WL=ENERGY LOSS OF THE PRIMARY ELECTRON IN EXCITING STATE N         RDTAPE52
      WIE(N)=WL                                                         RDTAPE53
      JES(N)=JES(N)+1                                                   RDTAPE54
      IF(NIE(N) .EQ. 2) GO TO 3                                         RDTAPE55
      GO TO 20                                                          RDTAPE56
3      READ(M)WL                                                        RDTAPE57
4466  II=NSEC                                                           RDTAPE58
C    WE PUT THE SECCNDARY AND TERTIARY HERE INITIALLY.  IF THE ELECTRON'SRDTAPE59
C    ENERGY IS ABOVE THE TMIN THEN THE ELECTRON STAYS HERE.             RDTAPE60
20    READ(M)X,Y,Z,E,PA,PHI,NG200,EBEF                                  RDTAPE61
C    X= THE X COORDINATE                                                RDTAPE62
C    Y= THE Y COORDINATE                                                RDTAPE63
C    Z= THE Z COORDINATE                                                RDTAPE64
C    E= THE ENERGY OF THE PRIMARY OR SECONDARY AT THIS POINT IN ITS     RDTAPE65
C    DEGRADATION.                                                       RDTAPE66
C    PA = THE POLAR ANGLE OF THE ELECTRON.                              RDTAPE67
C    PHI = THE AZIMUTHAL ANGLE                                          RDTAPE68
C    IF NG200=0 THEN WE HAVE A PRIMARY HERE                             RDTAPE69
C    IF NG200=1 THEN WE HAVE A SECONDARY HERE.                          RDTAPE70
C    IF NG200=2 THEN WE HAVE A TERTIARY HERE                            RDTAPE71
C    EBEF IS THE ENERGY OF THE ELECTRON BEFORE THE COLLISION.           RDTAPE72
```

```
      IF(NIE(N) .NE. 2)GO TO 5577                                       RDTAPE73
      IF(NG230 .EQ. 2)GO TO 5588                                        RDTAPE74
      IF(WL .GT. WIS(NSEC))GO TO 5577                                   RDTAPE75
5588  ELOSS=ELOSS+WL                                                    RDTAPE76
5577  IF(Z .GT. ZALT(1) .OR. Z .LT. ZALT(NAR))ELOSS=ELOSS+E             RDTAPE77
C                                                                       RDTAPE78
C                                                                       RDTAPE79
C                                                                       RDTAPE80
      IF(ELOSS .LT. 0.4)GO TO 1143                                      RDTAPE81
C    DO NOT COUNT ELASTIC COLLISIONS IN YIELD SPECTRA                   RDTAPE82
C    SOMETIMES ELOSS MAY BE GREATER THAN 0.4 AND STILL BE AN ELASTIC COL.RDTAPE83
C    THE ELOSS IS GREATER ONLY IN THE CASE WHERE THE ELECTRON HAS AN    RDTAPE84
C    ELASTIC COLLISION OUTSIDE THE BOX AND ESCAPES.                     RDTAPE85
      IF(NSPEC .NE. 1)GO TO 1143                                        RDTAPE86
      DO 2203 IL=1,NSPZ                                                 RDTAPE87
      INIE=IL                                                           RDTAPE88
      N1=NZX(IL)                                                        RDTAPE89
      N1M1=N1-1                                                         RDTAPE90
      IF(Z .GT. ZALT(N1) .AND. Z .LT. ZALT(N1M1))GO TO 2204             RDTAPE91
2203  CONTINUE                                                          RDTAPE92
      GO TO 1143                                                        RDTAPE93
2204  DO 69 IM=2,NEIP                                                   RDTAPE94
      IMM1=IM-1                                                         RDTAPE95
      IF(EBEF .GT. EIP(IMM1) .AND. EBEF .LT. EIP(IM))JNIE=IMM1          RDTAPE96
69    CONTINUE                                                          RDTAPE97
      ANEI(1,INIE,JNIE)=ANEI(1,INIE,JNIE)+1.0                           RDTAPE98
      IF(NSPRO .NE. 1)GO TO 1143                                        RDTAPE99
      RHOV=SQRT(X*X+Y*Y)                                                RDTAP100
      DO 2205 IN=2,NSPR                                                 RDTAP101
      IN1=IN-1                                                          RDTAP102
      IF(RHOV .GT. RYS(IN1) .AND. RHOV .LT. RYS(IN)) GO TO 2207         RDTAP103
2205  CONTINUE                                                          RDTAP104
      GO TO 1143                                                        RDTAP105
2207  AREA=3.14159*(RYS(IN)*RYS(IN)-RYS(IN1)*RYS(IN1))*CONST            RDTAP106
      ANER(1,IN1,INIE,JNIE)=ANER(1,IN1,INIE,JNIE)+1.0/AREA              RDTAP107
1143  CONTINUE                                                          RDTAP108
C                                                                       RDTAP109
C                                                                       RDTAP110
C                                                                       RDTAP111
      IF(NRHO .EQ. 1)GO TO 151                                          RDTAP112
1161  IF(NAVEE .EQ. 1)GO TO 6611                                        RDTAP113
6622  IF(NIE(N) .NE. 2)GO TO 702                                        RDTAP114
      DO 63 I1=1,NTOP                                                   RDTAP115
      I1P1=I1+1                                                         RDTAP116
      IF(WL .GT. WIS(I1) .AND. WL .LT. WIS(I1P1))II=I1                  RDTAP117
```

```
63        CONTINUE                                                         RDTAP118
      IF(Z .GT. ZALT(1))JSEC(II,1)=JSEC(II,1)+1                            RDTAP119
      IF(Z .LT. ZALT(NAR))JSEC(II,NAR1)=JSEC(II,NAR1)+1                    RDTAP120
      DO 64 I2=2,NAR                                                       RDTAP121
      I2M1=I2-1                                                            RDTAP122
      IF(Z .GT. ZALT(I2) .AND. Z .LT. ZALT(I2M1))JSEC(II,I2)=              RDTAP123
     * JSEC(II,I2)+1                                                       RDTAP124
64        CONTINUE                                                         RDTAP125
      JIS(II)=JIS(II)+1                                                    RDTAP126
702         CONTINUE                                                       RDTAP127
      IF(EBEF .LT. WIS(NSEC))GO TO 30                                      RDTAP128
      IF(Z .GT. ZALT(1))JZE(3,N,1)=JZE(3,N,1)+1                            RDTAP129
      IF(Z .LT. ZALT(NAR)) JZE(3,N,NAR)=JZE(3,N,NAR)+1                     RDTAP130
      DO 31 IA=2,NAR                                                       RDTAP131
      IAM1=IA-1                                                            RDTAP132
      IASET=IA                                                             RDTAP133
      IF(Z .GT. ZALT(IA) .AND. Z .LT. ZALT(IAM1))GO TO 555                 RDTAP134
31    CONTINUE                                                             RDTAP135
      GO TO 30                                                             RDTAP136
555   DO 560 KA=1,3                                                        RDTAP137
560   JZE(KA,N,IASET)=JZE(KA,N,IASET)+1                                    RDTAP138
      IF(NG200 .EQ. 1)JZE(1,N,IASET)=JZE(1,N,IASET)-1                      RDTAP139
      IF(NG200 .EQ. 0)JZE(2,N,IASET)=JZE(2,N,IASET)-1                      RDTAP140
      GO TO 30                                                             RDTAP141
C                                                                          RDTAP142
C                                                                          RDTAP143
C    THIS PART OF THE PROGRAM CALCULATES THE DISTRIBUTION OF EXCITATIONS RDTAP144
```

```
C     AT A GIVEN ALTITUDE AS A FUNCTION OF RHO.                                RDTAP145
151     DO 6149 IZV=1,NVR                                                      RDTAP146
        IC=IZV                                                                 RDTAP147
        NC=NCRO(IZV)                                                           RDTAP148
        NCRM1=NCRO(IZV)-1                                                      RDTAP149
        IF(Z .GT. ZALT(NC) .AND. Z .LT. ZALT(NCRM1))GO TO 155                  RDTAP150
6149    CONTINUE                                                               RDTAP151
        GO TO 1161                                                             RDTAP152
155     RHOV=ABS(X)                                                            RDTAP153
        DO 159 I3=2,NRM                                                        RDTAP154
        I3M1=I3-1                                                              RDTAP155
        IF(RHOV .LT. RHO(I3) .AND. RHOV .GT. RHO(I3M1))                        RDTAP156
       *  KREX(IC,N,I3)=KREX(IC,N,I3)+1                                        RDTAP157
159     CONTINUE                                                               RDTAP158
        GO TO 1161                                                             RDTAP159
C                                                                              RDTAP160
C                                                                              RDTAP161
C     THIS PART OF THE PROGRAM CALCULATES THE AVERAGE ENERGY AT A GIVEN        RDTAP162
C     ALTITUDE.                                                                RDTAP163
6611    CONTINUE                                                               RDTAP164
        IF(Z .LT. ZALT(1))GO TO 6767                                           RDTAP165
        NOFE(1,1)=NOFE(1,1)+1                                                  RDTAP166
        TOTE(1,1)=TOTE(1,1)+ELOSS                                              RDTAP167
        IF(PA .LE. 1.57)NOFE(2,1)=NOFE(2,1)+1                                  RDTAP168
        IF(PA .LE. 1.57)TOTE(2,1)=TOTE(2,1)+ELOSS                              RDTAP169
        IF(PA .GT. 1.57)NOFE(3,1)=NOFE(3,1)+1                                  RDTAP170
        IF(PA .GT. 1.57)TOTE(3,1)=TOTE(3,1)+ELOSS                              RDTAP171
        GO TO 6769                                                             RDTAP172
6767    IF(Z .GT. ZALT(NAR))GO TO 6768                                         RDTAP173
        NOFE(1,NAR1)=NOFE(1,NAR1)+1                                            RDTAP174
        TOTE(1,NAR1)=TOTE(1,NAR1)+ELOSS                                        RDTAP175
        IF(PA .LE. 1.57)NOFE(2,NAR1)=NOFE(2,NAR1)+1                            RDTAP176
        IF(PA .LE. 1.57) TOTE(2,NAR1)=TOTE(2,NAR1)+ELOSS                       RDTAP177
        IF(PA .GT. 1.57)NOFE(3,1)=NOFE(3,1)+1                                  RDTAP178
        IF(PA .GT. 1.57)TOTE(3,1)=TOTE(3,1)+ELOSS                              RDTAP179
        GO TO 6769                                                             RDTAP180
6768    DO 13 I4=2,NAR                                                         RDTAP181
        I4M1=I4-1                                                              RDTAP182
        IF(Z .GT. ZALT(I4) .AND. Z .LT. ZALT(I4M1))N1Z=1                       RDTAP183
        IF(N1Z .EQ. 1)NOFE(1,I4)=NOFE(1,I4)+1                                  RDTAP184
        IF(N1Z .EQ. 1)TOTE(1,I4)=TOTE(1,I4)+ELOSS                              RDTAP185
        IF(N1Z .EQ. 1 .AND. PA .LE. 1.57)NOFE(2,I4)=NOFE(2,I4)+1               RDTAP186
        IF(N1Z .EQ. 1 .AND. PA .LE. 1.57)TOTE(2,I4)=TOTE(2,I4)+ELOSS           RDTAP187
        IF(N1Z .EQ. 1 .AND. PA .GT. 1.57) NOFE(3,I4)=NOFE(3,I4)+1              RDTAP188
        IF(N1Z .EQ. 1 .AND. PA .GT. 1.57) TOTE(3,I4)=TOTE(3,I4)+ELOSS          RDTAP189
```

```
      N1Z=0                                                             RDTAP190
13    CONTINUE                                                          RDTAP191
6769  CONTINUE                                                          RDTAP192
      IF(NCHE .EQ. 1)GO TO 30                                           RDTAP193
      GO TO 6622                                                        RDTAP194
30      CONTINUE                                                        RDTAP195
333   CONTINUE                                                          RDTAP196
      WRITE(6,334)ISAV                                                  RDTAP197
334   FORMAT(' ISAV=',I9)                                               RDTAP198
      RETURN                                                            RDTAP199
      END                                                               RDTAP200
```

```
      SUBROUTINE WRTDAT                                                 WRTDAT01
C         SUBROUTINE WRTDAT ***                                         WRTDAT02
C   THIS SUBROUTINE WRITES OUT THE MATRICES THAT HAVE BEEN FILLED      WRTDAT03
C   WITH INFORMATION ABOUT THE DEGRADATION PROCESS.                    WRTDAT04
C   THIS SUBROUTINE IS ACCESSED BY THE MAIN PROGRAM.                   WRTDAT05
      COMMON ALAB(20),ANEI(5,20,100),ALT(20),EAVE(3),EIP(100),          WRTDAT06
     1 EXC5(50),JES(50),JIS(50),JZE(3,50,80),JSEC(50,80),KREX(10,40,40),WRTDAT07
     2 NIE(40),NZX(20),NOFE(3,80),NCRO(10),RHO(40),SA(3,80),SIG(100),   WRTDAT08
     3 TOTE(3,80),TN1(3,80),TN5(3,80),TN10(3,80),WIE(50),WIS(50),       WRTDAT09
     4 YSPEC(100),ZNUM(10),ZALT(80),NUMGAS,NARI,NVR,NUMST,NUMG,NRM,     WRTDAT10
     5 NSEC,NSPZ,NEIP,NEXC,NTOP,NAR,NSPEC,NRHO,NAVEE,NPRIM,EIN,         WRTDAT11
     6 ZVAL,EMIN,DENGS,M,NSPUN,NSPR,ANER(1,10,20,100),RYS(10),NSPRO     WRTDAT12
C                                                                       WRTDAT13
C                                                                       WRTDAT14
C   WRITE OUT ALL THE STATISTICS YOU NEED HERE                          WRTDAT15
      DO 1 K=1,3                                                        WRTDAT16
      DO 1  I=1,NAR1                                                    WRTDAT17
      DO 1  J=1,NUMG                                                    WRTDAT18
C   WE HAVE SUPPLEMENTED THE 3914A EMISSION WITH 3RD AND 4TH STATES     WRTDAT19
      IF(J .EQ. 3)GO TO 6655                                            WRTDAT20
      IF(J .EQ. 4)GO TO 6655                                            WRTDAT21
      IF(J .EQ. 5)GO TO 6655                                            WRTDAT22
      GO TO 767                                                         WRTDAT23
6655  TN5(K,I)=TN5(K,I)+JZE(K,J,I)                                      WRTDAT24
757   IF(J .NE. 10)GO TO 1                                              WRTDAT25
      TN10(K,I)=TN10(K,I)+JZE(K,J,I)                                    WRTDAT26
1     CONTINUE                                                          WRTDAT27
      DO 4 K=2,3                                                        WRTDAT28
      DO 4 I=1,NAR1                                                     WRTDAT29
      DO 4 J=1,NTOP                                                     WRTDAT30
      TN5(K,I)=TN5(K,I)+  JSEC(J,I)*EXC5(J)                             WRTDAT31
4     CONTINUE                                                          WRTDAT32
      DO 46 K=1,3                                                       WRTDAT33
      IF(K .EQ. 1)WRITE(6,780)                                          WRTDAT34
      IF(K .EQ. 2)WRITE(6,781)                                          WRTDAT35
      IF(K .EQ. 3)WRITE(6,782)                                          WRTDAT36
780   FORMAT('1PRIMARY COLLISIONS',/)                                   WRTDAT37
781   FORMAT('1SECONDARY COLLISIONS',/)                                 WRTDAT38
782   FORMAT('1PRIMARY PLUS SECONDARY COLLISIONS',/)                    WRTDAT39
      WRITE(6,755)                                                      WRTDAT40
755   FORMAT(     ' ALT. INTERVAL',8X,'ALT. VALUE',9X,'3914A EXC.',8X,  WRTDAT41
     *   'ELASTIC EXC.',/)                                              WRTDAT42
      DO 46 I=2,NAR                                                     WRTDAT43
      IM1=I-1                                                           WRTDAT44
      ZMV=(ZALT(I)+ZALT(IM1))/2.                                        WRTDAT45
```

```
      ZMV=ZVAL-ZMV                                                      WRTDAT46
      WRITE(6,32) I,ZMV,TN5(K,I),TN10(K,I)                              WRTDAT47
32    FORMAT(I10,11X,1PE12.4,6X,G15.7,4X,G15.7)                         WRTDAT48
46    CONTINUE                                                          WRTDAT49
C                                                                       WRTDAT50
C                                                                       WRTDAT51
C                                                                       WRTDAT52
C    WRITE OUT THE YIELD SPECTRA INFORMATION.                           WRTDAT53
      IF(NSPEC .NE. 1)GO TO 1144                                        WRTDAT54
      ZDEL=(ZALT(1)-ZALT(2))*1.E+05*DENGS*4.651E-23                     WRTDAT55
      DO 790 I=1,NSPZ                                                   WRTDAT56
      N1=NZX(I)                                                         WRTDAT57
      N1M1=N1-1                                                         WRTDAT58
      ZMV=(ZALT(N1)+ZALT(N1M1))/2.                                      WRTDAT59
      ZMV=(ZVAL-ZMV)*1.E+05                                             WRTDAT60
      ZRNG=ZMV*DENGS*4.651E-23                                          WRTDAT61
C    ZRNG IS THE PATH LENGTH IN GM/CM**2                                WRTDAT62
C    THERE ARE 4.651E-23 GM/MOLECULE                                    WRTDAT63
      WRITE(6,791)ZMV,ZRNG                                              WRTDAT64
791   FORMAT('1AT AN ALTITUDE=',1PE11.3,' CM.   WITH A VALUE OF',       WRTDAT65
     1 1PE11.3,' GM/CM**2',/,' WE HAVE THE FOLLOWING ELECTRON SPECTRA,',WRTDAT66
     2 4X,'YIELD SPECTRA = U(E) IN #/EV/(GM/CM**2)',//,                 WRTDAT67
     3  ' MID-ENERGY',8X,'U(E)'//)                                      WRTDAT68
      NEIP1=NEIP-1                                                      WRTDAT69
      DO 795 J=2,NEIP                                                   WRTDAT70
      JM1=J-1                                                           WRTDAT71
      EMID=(EIP(JM1)+EIP(J))/2.                                         WRTDAT72
```

```
      EDEL=EIP(J)-EIP(JM1)                                              WRTDAT73
C     THIS IS FOR THE LONGITUDINAL YIELD SPECTRA.                       WRTDAT74
      YSPEC(JM1)=ANEI(1,I,JM1)/EDEL/NPRIM/ZDEL                          WRTDAT75
C     NORMALIZE THE YIELD SPECTRA TO ONE ELECTRON                       WRTDAT76
C     YSPEC(JM1) IS IN UNITS OF #/EV/(GM/CM**2).                        WRTDAT77
C     ANEI(1,I,JM1) HAS THE EXTRA DIMENSION OF THE MATRIX IN CASE A     WRTDAT78
C     DEGRADATION SPECTRA OR SOME OTHER FLUX IS DESIRED.                WRTDAT79
      IF(J .EQ. NEIP) YSPEC(JM1)=YSPEC(JM1)*EDEL                        WRTDAT80
C     THIS EXPRESSION TAKES CARE OF THOSE ELECTRONS IN THE SOURCE TERM. WRTDAT81
      WRITE(6,793)EMID,YSPEC(JM1)                                       WRTDAT82
793   FORMAT(1PE11.3,5X,1PE11.3)                                        WRTDAT83
      IF(YSPEC(JM1) .LT. 1.E-30)GO TO 795                               WRTDAT84
      IF(NSPUN .EQ. 1)WRITE(7,850)EMID,ZRNG,EIN,YSPEC(JM1)              WRTDAT85
850   FORMAT(2X,4E12.5)                                                 WRTDAT86
795   CONTINUE                                                          WRTDAT87
      IF(NSPRO .NE. 1)GO TO 790                                         WRTDAT88
      DO 803 IR=2,NSPR                                                  WRTDAT89
      IR1=IR-1                                                          WRTDAT90
      RMID=(RYS(IR)+RYS(IR1))/2.*1.E+5                                  WRTDAT91
      WRITE(6,800)ZMV,RMID                                              WRTDAT92
800   FORMAT('1AT A Z VALUE=',1PE11.3,' CM.',                           WRTDAT93
     *2X,'AND  AT A RHO VALUE=',1PE11.3,' CM. WE HAVE THE FOLLOWING ',  WRTDAT94
     * /,' ELECTRON SPECTRA, YIELD SPECTRA = U(E) IN #/EV/(GM/CM**2)**3'WRTDAT95
     *,//,' MID-ENERGY',8X,'U(E)',//)                                   WRTDAT96
      DO 803 JR=2,NEIP                                                  WRTDAT97
      JRM1=JR-1                                                         WRTDAT98
      EMID=(EIP(JRM1)+EIP(JR))/2.                                       WRTDAT99
      EDEL=EIP(JR)-EIP(JRM1)                                            WRTDA100
C     THIS IS FOR THE RADIAL YIELD SPECTRA.                             WRTDA101
      YSRHO=ANER(1,IR1,I,JRM1)/EDEL/NPRIM/ZDEL                          WRTDA102
C     YSRHO HAS THE DIMENSIONS OF #/EV/(GM/CM**2)**3.                   WRTDA103
      IF(JR .EQ. NEIP)YSRHO=YSRHO*EDEL                                  WRTDA104
C     THIS EXPRESSION TAKES CARE OF THE SOURCE TERM.                    WRTDA105
      WRITE(6,793)EMID,YSRHO                                            WRTDA106
803   CONTINUE                                                          WRTDA107
790   CONTINUE                                                          WRTDA108
1144  CONTINUE                                                          WRTDA109
C                                                                       WRTDA110
C                                                                       WRTDA111
C                                                                       WRTDA112
C     WRITE OUT A QUICK AND DIRTY ENERGY CONSERVATION COMPARISON.       WRTDA113
C     THIS IS NOT ACCURATE FOR REASONS GIVEN BELOW.                     WRTDA114
      ESI=NPRIM*EIN                                                     WRTDA115
C     ESI IS THE INCIDENT ENERGY.                                       WRTDA116
      ESF=0.0E0                                                         WRTDA117
```

```
      WRITE(6,100)
100      FORMAT('1INDEX OF STATE',6X,' NO. OF EXCITATIONS',6X,
     *   'ENERGY LOSS',//)
      DO 51  IC=1,NUMG
      WRITE(6,111) IC,JES(IC),WIE(IC)
111      FORMAT(7X,I5,10X,I7,12X,F12.3)
51    ESF=ESF+JES(IC)*WIE(IC)
      WRITE(6,200)
200   FORMAT(///,' LOWER EN. INTERVAL',7X,'MID ENERGY',7X,
     *   'NO. OF EXCITATIONS',//)
      DO 52 ID=1,NTOP
      IDP1=ID+1
      WMID=(WIS(ID)+WIS(IDP1))/2.
      WRITE(6,201)ID,WMID,JIS(ID)
201   FORMAT(I10,11X,F12.3,5X,I10)
52    ESF=ESF+JIS(ID)*WMID
C    ESF IS THE ENERGY DEPOSITED.
C    THE ENERGIES ESI AND ESF WILL NOT BE EQUAL BECAUSE OF THE COMBINED
C    STATE.  THE THRESHOLD OF THE COMBINED STATE IS CHANGING BELOW
C    200 EV THUS YOU WOULD NOT EXPECT THIS MODE OF COMPARISON TO WORK.
      WRITE(6,511)ESI,ESF
511   FORMAT(////,' INITIAL ENERGY=',G15.7,/,' ENERGY DEPOSITED=',G15.7)
C
C
C
C    WRITE OUT THE INTENSITY INFORMATION AS A FUNCTION OF RHO.
      IF(NRHO .NE. 1)GO TO 3311
```

```
      DO 160 I=1,NVR                                                    WRTDA145
      ZMZV=(ZVAL-ZNUM(I))*1.E+05                                        WRTDA146
      WRITE(6,730)ZMZV,NCRO(I)                                          WRTDA147
730   FORMAT('1AT A Z VALUE OF',1PE11.3,' CM. AND NCRO=',I5,/,          WRTDA148
     *  ' WE HAVE THE FOLLOWING EXCITATION DISTRIBUTION',///,           WRTDA149
     *  ' RHO VALUE',6X,'3914A EXC.',8X,'ELASTIC EXC.',/)               WRTDA150
      DO 160 J=2,NRM                                                    WRTDA151
      JM1=J-1                                                           WRTDA152
      RMV=(RHO(J)+RHO(JM1))/2.                                          WRTDA153
      K345=KREX(I,3,J)+KREX(I,4,J)+KREX(I,5,J)                          WRTDA154
      WRITE(6,705)RMV,K345,KREX(I,10,J)                                 WRTDA155
705   FORMAT(2X,1PE10.4,2X,I9,9X,I10)                                   WRTDA156
150   CONTINUE                                                          WRTDA157
C                                                                       WRTDA158
C                                                                       WRTDA159
C                                                                       WRTDA160
C    WRITE OUT THE ENERGY LOST INFORMATION.                             WRTDA161
3311  IF(NAVEE .NE. 1) GO TO 6633                                       WRTDA162
      DO 4477 I=1,3                                                     WRTDA163
4477  EAVE(I)=0.0D0                                                     WRTDA164
      WRITE(6,712)                                                      WRTDA165
712   FORMAT('1THE AVE. ENERGY LOST IN EACH Z VALUE IS PRINTED OUT NOW',WRTDA166
     *  //,' ALT. INTERVAL',8X,'ALT. VALUE',4X,'MEAN ENERGY(ALL)',      WRTDA167
     *  5X,'MEAN ENERGY(PA<PI/2)',5X,'MEAN ENERGY(PA>PI/2)',/)          WRTDA168
      DO 15 I=1,NAR1                                                    WRTDA169
      IF(I .EQ. 1)GO TO 2965                                            WRTDA170
      IF(I .EQ. NAR1)GO TO 2966                                         WRTDA171
      IM1=I-1                                                           WRTDA172
      ZMV=(ZALT(I)+ZALT(IM1))/2.                                        WRTDA173
      ZMV=ZVAL-ZMV                                                      WRTDA174
      GO TO 2967                                                        WRTDA175
2965  ZMV=ZVAL-ZALT(1)                                                  WRTDA176
      GO TO 2967                                                        WRTDA177
2966  ZMV=ZVAL-ZALT(NAR)                                                WRTDA178
2967  DO 2961 J=1,3                                                     WRTDA179
      EAVE(J)=EAVE(J)+TOTE(J,I)                                         WRTDA180
2961  CONTINUE                                                          WRTDA181
      EV1=EAVE(1)/NPRIM                                                 WRTDA182
      EV2=EAVE(2)/NPRIM                                                 WRTDA183
      EV3=EAVE(3)/NPRIM                                                 WRTDA184
      WRITE(6,714)I,ZMV,EV1,EV2,EV3                                     WRTDA185
714   FORMAT(I10,10X,1PE12.4,7X,G15.7,6X,G15.7,10X,G15.7)               WRTDA186
15    CONTINUE                                                          WRTDA187
6633  CONTINUE                                                          WRTDA188
      RETURN                                                            WRTDA189
```

```
END                                                     WRTDA190
```

REFERENCES

Banks, P.M., C.R. Chappell, and A.F. Nagy, A new model for the interaction of auroral electrons with the atmospheres: Spectral degradation, backscatter, optical emission, and ionization, J. Geophys. Res., 79, 1459, 1974.

Barrett, J.L., Energy loss of electrons in nitrogen, Ph.D. thesis, University of Michigan, Ann Arbor, Michigan, 1975.

Barrett, J.L., and P.B. Hays, Spatial distribution of energy deposited in nitrogen by electrons, J. Chem. Phys., 64, 743, 1976.

Berger, M.J., Monte Carlo calculation of the penetration and diffusion of fast charged particles, Methods in Computational Physics, 1, 135, 1963.

Berger, M.J., S.M. Seltzer, and K. Maeda, Energy deposition by auroral electrons in the atmosphere, J. Atmos. Terr. Phys., 32, 1015, 1970.

Berger, M.J., S.M. Seltzer, and K. Maeda, Some new results on electron transport in the atmosphere, J. Atmos. Terr. Phys., 36, 591, 1974.

Bethe, H., Zur theorie des durchgangs schneller korpuskularstrahler durch materie, Ann. Phys., 5, 325, 1930.

Bethe, H.A., M.E. Rose, and L.P. Smith, The multiple scattering of electrons, Proc. Amer. Phil. Soc., 78, 573, 1938.

Blaauw, H.J., F.J. de Heer, R.W. Wagenaar, and D.H. Barends, Total cross sections for electron scattering from N_2 and He, J. Phys. B: Atom. Molec. Phys., 10, L299, 1977.

Bohr, N., On the theory of the decrease of velocity of moving electrified particles on passing through matter, Phil. Mag., 25, 10, 1913.

Bohr, N., On the decrease of velocity of swiftly moving electrified particles in passing through matter, Phil. Mag., 30, 581, 1915.

Borst, W.L. and E.C. Zipf, Cross section for electron impact excitation of the (0,0) first negative band of N_2^+ from threshold to 3 KeV, Phys. Rev. A, 1, 834, 1969.

Brinkmann, R.T. and S. Trajmar, Electron impact excitation of N_2, Ann. Geophys., 26, 201, 1970.

Cartwright, D.C., A. Chutjian, S. Trajmar, and W. Williams, Electron impact excitation of the electronic states of N_2. I. Differential cross sections at incident energies from 10 to 50 eV, Phys. Rev. A, 16, 1013, 1977.

Chutjian, A., D.C. Cartwright, and S. Trajmar, Electron impact excitation of the electronic states of N_2. III. Transitions in the 12.5-14.2 eV energy-loss region at incident energies of 40 and 60 eV, Phys. Rev. A, 16, 1052, 1977.

Cicerone, R.J. and S.A. Bowhill, Photoelectron escape fluxes obtained by a Monte Carlo technique, Radio Sci., 5, 49, 1970.

Cicerone, R.J. and S.A. Bowhill, Photoelectron fluxes in the ionosphere computed by a Monte Carlo method, J. Geophys. Res., 76, 8299, 1971.

Cohn, A. and G. Caledonia, Spatial distribution of the fluorescent radiation emission caused by an electron beam, J. Appl. Phys., 41, 3767, 1970.

Cravens, T.E., G.A. Victor, and A. Dalgarno, The absorption of energetic electrons by molecular hydrogen gas, Planet. Space Sci., 23, 1059, 1975.

Dalgarno, A., 15. Range and energy loss, Atomic and Molecular Processes: 13, pp. 622-662, edited by D.R. Bates, Academic Press, New York, 1962.

Dalgarno, A. and G. Lejeune, The absorption of electrons in atomic oxygen, Planet. Space Sci., 19, 1653, 1971.

Douthat, D.A., Energy deposition by electrons and degradation spectra, Radiat. Res., 64, 141, 1975.

DuBois, R.D. and M.E. Rudd, Absolute doubly differential cross sections for ejection of secondary electrons from gases by electron impact. II. 100-500-eV electrons on neon, argon, molecular hydrogen, and molecular nitrogen, Phys. Rev. A, 17, 843, 1978.

Eadie, W.T., D. Dryard, F.E. James, M. Roos, and B. Sadoulet, Statistical Methods in Experimental Physics, pp. 44-47, North-Holland Publishing Company, Amsterdam, 1971.

Ehrhardt, H., M. Schulz, T. Tekaat, and K. Willmann, Ionization of helium: Angular correlation of the scattered and ejected electrons, Phys. Rev. Lett., 22, 89, 1969.

Fowler, R.H., Theory of motion of α-particles through matter, Proc. Camb. Philos. Soc., 121, 521, 1922-23.

Garvey, R.H., H.S. Porter, and A.E.S. Green, An analytic degradation spectrum for H_2, J. Appl. Phys., 48, 190, 1977.

Goudsmit, S. and J.L. Saunderson, Multiple scattering of electrons, Phys. Rev., 57, 24, 1940.

Green, A.E.S. and C.A. Barth, Calculations of ultraviolet molecular nitrogen emissions from the aurora, J. Geophys. Res., 70, 1083, 1965.

Green, A.E.S. and C.A. Barth, Calculations of the photoelectron excitation of the dayglow, J. Geophys. Res., 72, 3975, 1967.

Green, A.E.S. and S.K. Dutta, Semi-empirical cross sections for electron impacts, J. Geophys. Res., 72, 3933, 1967.

Green, A.E.S., C.H. Jackman, and R.H. Garvey, Electron impact on atmospheric gases. 2. Yield spectra, J. Geophys. Res., 82, 5104, 1977.

Green, A.E.S. and L.R. Peterson, Energy loss functions for electrons and protons in planetary gases, J. Geophys. Res., 73, 233, 1968.

Green, A.E.S. and T. Sawada, Ionization cross sections and secondary electron distributions, J. Atmos. Terr. Phys., 34, 1719, 1972.

Green, A.E.S. and P.J. Wyatt, Atomic and Space Physics, p. 170, Addison-Wesley Publishing Company, Inc., Reading, Mass., 1965.

Grün, A.E., Lumineszenz-photometrische messungen der energieabsorption in strahlungsfeld von elektronenquellen eindimensionalor fall in luft, Z. Naturforschg., 12a, 89, 1957.

Heaps, M.G. and A.E.S. Green, Monte Carlo approach to the spatial deposition of energy by electrons in molecular hydrogen, J. Appl. Phys., 45, 3183, 1974.

Herrmann, D., K. Jost, and J. Kessler, Differential cross sections for elastic electron scattering. II. Charge cloud polarization in N_2, J. Chem. Phys., 64, 1, 1976.

Holland, R.F., Cross sections for electron excitation of the 3914-Å (0,0) band of the N_2^+ first negative system, Tech. Rep. LA-3783, Los Alamos Scientific Laboratory of the University of California, Los Alamos, New Mexico, 1967.

Inokuti, M., D.A. Douthat, and A.R.P. Rau, Degradation spectra and ionization yields of electrons in gases, Proceedings of the Fifth Symposium on Microdosimetry, pp. 977-1006, Varbania-Pallanza, Italy, Sept. 22-26, 1975.

Irvine, W.M., Multiple scattering by large particles, Astrophys. J., 142, 1563, 1965.

Jackman, C.H., R.H. Garvey, and A.E.S. Green, Yield spectra and the continuous-slowing-down approximation, J. Phys. B: Atom Molec. Phys., 10, 2873, 1977a.

Jackman, C.H., R.H. Garvey, and A.E.S. Green, Electron impact on atmospheric gases. 1. Updated cross sections, J. Geophys. Res., 82, 5081, 1977b.

Jasperse, J.R., Boltzmann-Fokker-Planck model for the electron distribution function in the earth's ionosphere, Planet. Space Sci., 24, 33, 1976.

Jasperse, J.R., Electron distribution function and ion concentrations in the earth's lower ionosphere from Boltzmann-Fokker-Planck theory, Planet. Space Sci., 25, 743, 1977.

Jung, K., E. Schubert, D.A.L. Paul, and H. Ehrhardt, Angular correlation of outgoing electrons following ionization of H_2 and N_2 by electron impact, J. Phys. B: Atom. Molec. Phys., 8, 1330, 1975.

Jura, M., Models of the interstellar gas, Ph.D. thesis, Harvard Univ., Cambridge, Mass., 1971.

Jusick, A.T., C.E. Watson, L.R. Peterson, and A.E.S. Green, Electron impact cross sections for atmospheric species. 1. Helium, J. Geophys. Res., 72, 3943, 1967.

Kamiyami, H., The electron density distribution in the lower ionosphere produced through impact ionization by precipitating electrons and through photoionization by the associated bremsstrahlung x-rays, J. Geomag. and Geoelec., 19, 27, 1967.

Kieffer, L.J., Low-energy electron-collision cross-section data, part III: Total scattering; differential elastic scattering, Atomic Data, 2, 293, 1971.

Kutcher, G.J. and A.E.S. Green, Multiple elastic scattering of slow electrons: Parametric study for H_2, J. Appl. Phys., 47, 2175, 1976.

Lewis, H.W., Multiple scattering in an infinite medium, Phys. Rev., 78, 526, 1950.

Maeda, K. and A.C. Aikin, Variations of polar mesospheric oxygen and ozone during auroral events, Planet. Space Sci., 16, 371, 1968.

Mantas, G.P., Theory of photoelectron thermalization and transport in the ionosphere, Planet. Space Sci., 23, 337, 1975.

McConkey, J.W., J.M. Woolsey, and D.J. Burns, Absolute cross section for electron impact excitation of 3914 Å N_2^+, Planet. Space Sci., 15, 1332, 1967.

McDiarmid, J.B., D.C. Rose, and E. Budzinski, Direct measurement of charged particles associated with auroral zone radio absorption, Can. J. Phys., 39, 1888, 1961.

Moliere, G., Theory of scattering of fast charged particles. I. Single scattering in a screened Coulomb field, Z. Naturf., 2a, 133, 1947.

Moliere, G., Theory of scattering of fast charged particles. II. Plural and multiple scattering, Z. Naturf., 3a, 78, 1948.

Mott, N.F. and H.S.W. Massey, The Theory of Atomic Collisions, Clarendon Press, Third Edition, Oxford, England, 1965.

Mumma, M.J. and E.C. Zipf, Dissociative excitation of vacuum-ultraviolet emission features by electron impact on molecular gases. II. N_2, J. Chem. Phys., 55, 5582, 1971.

O'Brien, D.J., High-latitude geophysical studies with satellite Injun 3. 3. Precipitation of electrons into the atmosphere, J. Geophys. Res., 69, 13, 1964.

Opal, C.B., E.C. Beaty, and W.K. Peterson, Tables of secondary-electron-production cross sections, Atomic Data, 4, 209, 1972.

Peterson, L.R., Discrete deposition of energy by electrons in gases, Phys. Rev., 187, 105, 1969.

Polak, L.S., D.I. Slovetskii, and A.S. Sokolov, Dissociation of nitrogen molecules from excited electronic states. I. Predissociation efficiency, High Energy Chemistry, 6, 350, 1972.

Porter, H.S. and A.E.S. Green, Comparison of Monte Carlo and continuous slowing-down approximation treatments of 1-KeV proton energy deposition in N_2, J. Appl. Phys., 46, 5030, 1975.

Porter, H.S., C.H. Jackman, and A.E.S. Green, Efficiencies for production of atomic nitrogen and oxygen by relativistic proton impact in air, J. Chem. Phys., 65, 154, 1976.

Porter, H.S. and F.W. Jump, Jr., Analytic total and angular elastic electron impact cross sections for planetary atmospheres, Tech. Rep. CSC/TM-78/6017, prepared for Goddard Space Flight Center by Computer Sciences Corporation, Greenbelt, Maryland, 1978.

Rapp, D. and P. Englander-Golden, Total cross sections for ionization and attachment in gases by electron impact. I. Positive ionization, J. Chem. Phys., 43, 1464, 1965.

Rapp, D., P. Englander-Golden, and D. Briglia, Cross sections for dissociative ionization of molecules by electron impact, J. Chem. Phys., 42, 4081, 1965.

Rees, M.H., A.I. Stewart, and J.C.G. Walker, Secondary electrons in aurora, Planet. Space Sci., 17, 1997, 1969.

Riewe, F. and A.E.S. Green, Ultraviolet aureole around a source at a finite distance, to be published in Appl. Optics, 1978.

Rohrlich, F. and B.C. Carlson, Positron-electron differences in energy loss and multiple scattering, Phys. Rev., 93, 38, 1954.

Sawada, T., P.S. Ganas, and A.E.S. Green, Elastic scattering of electrons from N_2, Phys. Rev. A, 9, 1130, 1974.

Schram, B.L., F.J. de Heer, M.J. Van der Wiel, and J. Kistemaker, Ionization cross sections for electrons (0.6-20 KeV) in noble and diatomic gases, Physica, 31, 94, 1965.

Shemansky, D.E., T.M. Donahue, and E.C. Zipf, Jr., N_2 positive and N_2^+ band systems and the energy spectra of auroral electrons, Planet. Space Sci., 20, 905, 1972.

Shyn, T.W., R.S. Stolarski, and G.R. Carignan, Angular distribution of electrons elastically scattered from N_2, Phys. Rev. A, 6, 1002, 1972.

Silverman, S.M. and E.N. Lassettre, Generalized oscillator strengths and electronic collision cross sections for nitrogen at excitation energies above 10 eV, J. Chem. Phys., 42, 3420, 1965.

Spencer, L.V., Energy dissipation by fast electrons, National Bureau of Stand. Monogr., 1, 1959.

Spencer, L.V. and U. Fano, Energy spectrum resulting from electron slowing down, Phys. Rev., 93, 1172, 1954.

Stolarski, R.S., Calculation of auroral emission rates and heating effects, Planet. Space Sci., 16, 1265, 1968.

Stolarski, R.S., V.A. Dulock, Jr., C.E. Watson, and A.E.S. Green, Electron impact cross sections for atmospheric species. 2. Molecular nitrogen, J. Geophys. Res., 72, 3953, 1967.

Stolarski, R.S. and A.E.S. Green, Calculations of auroral intensities from electron impact, J. Geophys. Res., 72, 3067, 1967.

Strickland, D.J., D.L. Book, T.P. Coffey, and J.A. Fedder, Transport equation techniques for the deposition of auroral electrons, J. Geophys. Res., 81, 2755, 1976.

Tate, J.T. and P.T. Smith, The efficiencies of ionization and ionization potentials of various gases under electron impact, Phys. Rev., 39, 270, 1932.

Walt, M., W.M. MacDonald, and W.E. Francis, Penetration of auroral electrons into the atmosphere, Physics of the Magnetosphere, p. 534, edited by R.L. Carovillano, J.F. McClays, and H.R. Radoski, D. Reidel, Dordrecht, Netherlands, 1967.

Watson, C.E., V.A. Dulock, Jr., R.S. Stolarski, and A.E.S. Green, Electron impact cross sections for atmospheric species. 3. Molecular oxygen, J. Geophys. Res., 72, 3961, 1967.

Wedde, T., Scattering cross sections. A compilation of O, O_2, and N_2 data between 1 and 1000 eV. I. Elastic scattering, Center for Research in Aeronomy, Tech. Rep. CRA 76-1, Utah State University, Logan, Utah, 1976.

Wedde, T. and T.G. Strand, Scattering cross sections for 40 eV to 1 KeV electrons colliding elastically with nitrogen and oxygen, J. Phys. B: Atom. Molec. Phys., 7, 1091, 1974.

Winters, H.F., Ionic adsorption and dissociation cross section for nitrogen, J. Chem. Phys., 44, 1472, 1966.

BIOGRAPHICAL SKETCH

Charles Herbert Jackman was born on September 9, 1950, at David City, Nebraska. He graduated as salutatorian of his class from O'Neill Public High School of O'Neill, Nebraska, in May, 1968. In May, 1972, he received the degree of Bachelor of Science with highest distinction in physics and mathematics from Nebraska Wesleyan University in Lincoln, Nebraska. From September, 1972, until the present time he has pursued his work toward the degree of Doctor of Philosophy in the Department of Physics and Astronomy at the University of Florida. During this time he has held a graduate teaching and research assistantship.

His publications to date include:

Green, A.E.S., R.H. Garvey, and C.H. Jackman, A Thomas-Fermi-like analytic independent particle model for atoms and ions, Int. J. Quantum Chem. Symp., 9, 43-50, 1975.

Garvey, R.H., C.H. Jackman, and A.E.S. Green, Independent-particle-model potentials for atoms and ions with $36 < Z \leq 54$ and a modified Thomas-Fermi atomic energy formula, Phys. Rev. A, 12, 1144-52, 1975.

Porter, H.S., C.H. Jackman, and A.E.S. Green, Efficiencies for production of atomic nitrogen and oxygen by relativistic proton impact in air, J. Chem. Phys., 65, 154-67, 1976.

Green, A.E.S., R.H. Garvey, and C.H. Jackman, Analytic yield spectra for electrons on H_2, Int. J. Quantum Chem. Symp., 11, 97-103, 1977.

Jackman, C.H., R.H. Garvey, and A.E.S. Green, Yield spectra and the continuous-slowing-down approximation, J. Phys. B: Atom. Molec. Phys., 10, 2873-82, 1977.

Jackman, C.H., R.H. Garvey, and A.E.S. Green, Electron impact on atmospheric gases, 1, Updated cross sections, J. Geophys. Res., 82, 5081-90, 1977.

Green, A.E.S., C.H. Jackman, and R.H. Garvey, Electron impact on atmospheric gases, 2, Yield spectra, J. Geophys. Res., 82, 5104-11, 1977.

I certify that I have read this study and that in my opinion it conforms to acceptable standards of scholarly presentation and is fully adequate, in scope and quality, as a dissertation for the degree of Doctor of Philosophy.

Alex E. S. Green

Alex E.S. Green, Chairman
Graduate Research Professor of Physics and Astronomy

I certify that I have read this study and that in my opinion it conforms to acceptable standards of scholarly presentation and is fully adequate, in scope and quality, as a dissertation for the degree of Doctor of Philosophy.

Thomas L. Bailey

Thomas L. Bailey
Professor of Physics and Electrical Engineering

I certify that I have read this study and that in my opinion it conforms to acceptable standards of scholarly presentation and is fully adequate, in scope and quality, as a dissertation for the degree of Doctor of Philosophy.

Stephen T. Gottesman

Stephen T. Gottesman
Associate Professor of Astronomy

I certify that I have read this study and that in my opinion it conforms to acceptable standards of scholarly presentation and is fully adequate, in scope and quality, as a dissertation for the degree of Doctor of Philosophy.

Lennart R. Peterson

Lennart R. Peterson
Professor of Physics

I certify that I have read this study and that in my opinion it conforms to acceptable standards of scholarly presentation and is fully adequate, in scope and quality, as a dissertation for the degree of Doctor of Philosophy.

George R Lebo

George R. Lebo
Assistant Professor of Physics and Astronomy

This dissertation was submitted to the Graduate Faculty of the Department of Physics and Astronomy in the College of Arts and Sciences and to the Graduate Council, and was accepted as partial fulfillment of the requirements for the degree of Doctor of Philosophy.

August 1978

H H Sisler

Dean, Graduate School